1-1-1988

Modal analysis of a computer disk drive

Michael G. Thurston

MODAL ANALYSIS OF A COMPUTER DISK DRIVE

by

Michael G. Thurston

A Thesis Submitted
in
Partial Fulfillment
of the
Requirements for the Degree of
MASTER OF SCIENCE
in
Mechanical Engineering

Approved by:

Prof. Richard S. Budynas
(Thesis Advisor)

Prof. _____

Prof. _____

Prof. P. Marletcar
(Department Head)

DEPARTMENT OF MECHANICAL ENGINEERING
COLLEGE OF ENGINEERING
ROCHESTER INSTITUTE OF TECHNOLOGY
ROCHESTER, NEW YORK
JANUARY, 1988

Modal Analysis of a Computer Disk Drive.

I Michael G. Thurston hereby grant permission to the Wallace Memorial Library, of R.I.T., to reproduce my thesis in whole or in part. Any reproduction will not be for commercial use or profit.

19 January, 1988

ACKNOWLEDGEMENT

This work is dedicated to my family, and in particular my mom. You were always behind me for support and encouragement through all of the difficult times and challenges; THANK YOU.

To Dr. Richard Budynas, my thanks for your guidance in selecting a thesis topic, and for your assistance in accumulating the necessary resources.

To Dan Foley and Bruel and Kjaer, and to Les Goldberg and Structural Measurement Systems, my thanks for technical support and for the use of your hardware and software products which made the experimental analysis possible.

To all of my friends, who provided constant diversions to my work, but also constant encouragement; I'm finally finished and it wouldn't have been as much fun without you.

And finally, to the members of my thesis defense committee, thank you for the hours spent reading and reviewing my work.

ABSTRACT

The normal (real) modes of an Winchester type hard disk drive were determined in the frequency range 0-2200hz. Two methods of analysis were used in order to allow cross-correlation of the results. Experimental modal analysis was performed using Structural Measurement Systems' (SMS) Modal 3.0 analysis system and the requisite experimental hardware. A finite element analysis was also performed using MSC/NASTRAN; the NASTRAN model was created using the PATRAN pre-processing program. In order to alleviate the complications associated with matching the structural mounting conditions, a free-free analysis was performed using NASTRAN, and a light string was used to free mount the test specimen for the experimental work. The two analyses showed a one-to-one correspondence of modes; both showed 15 modes in the frequency range. Deviations of the NASTRAN natural frequencies from the experimentally determined natural frequencies ranged from -22 percent to +11.7 percent. Of the 15 modes, 10 showed deviation magnitudes of 10 percent or less, and 6 of the 15 were below 5 percent. Mode shape correlation was performed solely by observation. Errant DOFs in the experimental mode shapes made correlation difficult for several of the modes. In particular, the modes which showed higher frequency deviation (in excess of 10 percent) did not yield exact mode shape correlation although the primary deflection patterns were similar.

TABLE OF CONTENTS

LIST OF TABLES

LIST OF FIGURES

List of Symbols

$[A_k]$, $[A_k^*]$	Residue and conjugate residue matrices for the k_{th} mode
$A_k(i,j)$, $A_k^*(i,j)$	ij_{th} (i_{th} row, j_{th} column) element of the residue matrix for the k_{th} mode
$[B(s)]$	System matrix
$[C]$	Damping matrix
$[\lambda c]$	Modal damping matrix
$[D(s)]$	Adjunct of the system matrix
$\underset{\sim}{d}_j$	J_{th} column of $[D]$
$\{d_j\}$	J_{th} row of $[D]$
$\underset{\sim}{f}(t)$	Applied force vector
$\underset{\sim}{F}(s)$	Applied force in the Laplace domain
$[H(s)]$	Transfer function
H_{ij}	ij_{th} element of the transfer function
$(H_{ij}(s))_k$, $(H_{ij})_k$	Contribution of the k_{th} mode to the ij_{th} element of the transfer function
$[h(i\omega)]$	Frequency response function
$h_{ij}(j\omega)$	ij_{th} element of the frequency response function
$(h_{ij}(i\omega))_k$, $(h_{ij})_k$	Contribution of the k_{th} mode to the ij_{th} element of the frequency response function
$[\lambda I]$	Identity matrix
i	$\sqrt{-1}$
$[K]$	Stiffness matrix
$[\lambda k]$	Modal stiffness matrix
$[M]$	Mass matrix
$[\lambda m]$	Modal mass matrix
p_k, p_k^*	Pole and conjugate pole of the system
$q(t)$	Generalized modal coordinates
$Q(s)$	Generalized modal coordinates in the Laplace domain
s	Laplace variable
$\underset{\sim}{u}_k$, $\underset{\sim}{u}_k^*$	Eigenvector for the k_{th} mode
u_k^i, $u_k(i)$	i_{th} element of the k_{th} eigenvector
$\underset{\sim}{x}(t)$	Response vector
$\underset{\sim}{X}(s)$	Response vector in the Laplace domain
α	Real part of the Laplace variable
σ_k	Damping coefficient for the k_{th} mode
ω	Imaginary part of the Laplace variable
ω_k	Damped natural frequency for the k_{th} mode
Ω_k	Undamped natural frequency for the k_{th} mode
ζ_k	Damping factor for the k_{th} mode
$[\lambda\Lambda_k]$	General diagonal matrix
$[\Phi]$	Modal, mode shape matrix

Symbols (cont)

$[\ ]^T$	Matrix transpose
$[\ ]^{-1}$	Matrix inverse
$\lvert[\ ]\rvert$	Determinant of the matrix
$[\searrow\ ]$	Diagonal matrix
$\ddot{}$	Designates second time derivative
$\dot{}$	Designates first time derivative
DOF	Degree of freedom
FFT	Fast Fourier transform
FRF	Frequency response function
MDOF	Multiple degree of freedom
SDOF	Single degree of freedom
SMS	Structural Measurement Systems Corp.

CHAPTER 1. Introduction

1.1 Description of Vibration Problem and its Practical Importance

Mechanical design has evolved from the method of trial and error to a point where many hours of engineering analysis are often performed before the first prototype is turned out. This evolution was prompted, in part, by the need to produce a more competitive (lighter, stronger, cheaper, quieter) product, and by the increase in technical complexity of the products being produced. This change in the conventional design process was made possible by the evolution of the digital computer. The aerospace industry can largely be credited with driving the computer advances, as well as the development of efficient mathematical methods and software implementation.

Dynamic analysis is necessary to predict structural response to real life vibratory excitations. Very low level excitations may cause catastrophic failure if they happen to be of a certain frequency. A well known example is the failure of the Tacoma Narrows Bridge. A strong wind produced oscillatory aerodynamic forces which excited a bridge resonance, causing catastrophic failure.

In today's high-tech industrial environment, small dynamic oscillations may cause part failure or malfunction. Another problem in consumer, office, and industrial goods is high operational noise levels. A properly functioning part, which happens to be very noisy in operation, will not be accepted by the consumer. These problems may be prevented during the design process if the vibration response of the structure is known.

This thesis concerns the analysis of a Winchester type computer hard disk drive. The design of a disk drive unit must take into account both noise and structural vibration considerations. High levels of structural vibration may cause the loss of stored data, or physical damage to the disk or read head. Disk drive noise is also an important consideration because many of these units are used in office environments.

There are many different questions that can be asked regarding the dynamic response of the disk drive unit. What excitation frequencies are going to produce high response vibration levels? What is the response of the structure to the drive motor vibration? What happens in a shock loading situation, for example if the host computer is dropped? Are there any other system vibrations which will adversely affect the disk drive? In order to begin to answer these questions either an experimental, or analytical analysis must be performed. In the pre-prototype stage, analytical analysis is the only option. Analytical analyses might include: modal analysis to determine

the natural frequencies and associated mode shapes, or transient response analysis to find structural response to an arbitrary input. Once a prototype is available, the following experimental analyses could be performed: experimental modal analysis, transient response using a shaker to excite an instrumented test unit, measurement of vibration levels in standard operation, noise level measurements, etc.

Modal analysis is very often the starting point in the analysis of the dynamic characteristics of a structure. Modal analysis will directly answer some of the questions and it may be used as a starting point for further analyses. The critical frequencies (natural frequencies) and the associated mode shapes at these frequencies are determined. It is useful to know these frequencies because excitation of the structure at one of these frequencies will yield the undesired result of high vibration levels. If all of the mode shapes of a structure are known (in a frequency range) the transient response of the structure may be determined from a superposition of these mode shapes. This is a secondary advantage to performing modal analysis.

In the subsequent disk drive analysis, the objective was the determination of the resonant frequencies and associated mode shapes. In this case, the interest in the mode shapes and resonant frequencies of the disk drive is purely academic. However, resonant frequency and mode shape information is useful in addressing vibration, noise, durability, performance, and

mounting problems. Through structural modification the resonant frequencies of the disk drive may be shifted so as not to coincide with system excitation frequencies. Or conversely, the excitation frequencies may be tailored such that they do not correspond to disk drive resonances. In addition, performance and mounting configurations may be optimized from knowledge of the system mode shapes. In general, this information may also be used as the corner stone of a more thorough dynamic analysis.

Experimental and analytical modal analyses were performed on the disk drive. Experimental modal analysis requires a significant amount of testing to determine structural response patterns and a software package to analyze the test data. Structural Measurement Systems' Modal 3.0 software was used for this analysis. The primary analytical technique for modal analysis of a complex structure is the finite element method. A geometric preprocessor, PATRAN was used to generate the 796 element geometric model of the disk drive. PATRAN includes a translation program by which the geometric model may be output in formats directly usable by several different finite element codes. The PATRAN geometric model was translated into MSC/NASTRAN bulk data format for subsequent analysis. NASTRAN has many analysis capabilities, one of which is modal analysis. NASTRAN was used here to generate the mode shapes, but also has the capability to perform transient analyses using mode superposition.

1.2 Modal Approach to Vibration Analysis

The dynamic behavior of structures is often modeled by a set of second order differential equations. System response is related to force input by the dynamic properties of the structure: the mass, damping and stiffness distributions. Equation (1) is an example of such a set of equations, written as a single matrix equation:

$$[M]\,\ddot{\underset{\sim}{x}}(t) + [C]\,\dot{\underset{\sim}{x}}(t) + [K]\,x(t) = \underset{\sim}{f}(t) \qquad [1]$$

where [M] is the mass matrix, [C] is the damping matrix, [K] is the stiffness matrix, $\underset{\sim}{x}(t)$ is the displacement vector, and $\underset{\sim}{f}(t)$ is the applied load vector. If the structure is to be modeled in this fashion, the mass, damping and stiffness matrices must first be determined, then the system of equations may be solved.

If the three property matrices are diagonal matrices, the system equations are uncoupled. Assuming that these equations are also linear, the property matrices are constant and the forcing function is an independent function of time, the solution to the system is straight forward. A structure modeled using lumped parameter techniques yields a system of equations that may be uncoupled, but most "real" structures cannot be accurately modeled in this way. Therefore, more complex solution methods are required to solve the coupled systems of equations used in dynamic modeling.

Two solution methods are possible. One method is a direct iterative approach to solving the coupled equations. The other is the modal approach which allows the solution of an alternate set of uncoupled equations. The modal approach requires more work up front, uncoupling the equations, but it allows for a simpler final solution process. In the long run, the modal approach will save computation time if response to a number of different forcing functions is required.

The modal problem is formulated in terms of a set of generalized (modal) coordinates, $\underset{\sim}{q}(t)$, rather than the physical coordinates, $\underset{\sim}{x}(t)$. The physical and generalized coordinates are related by the modal matrix, $[\Phi]$, in the following fashion:

$$\underset{\sim}{q}(t) = [\Phi]^{-1}\,\underset{\sim}{x}(t) \quad \text{or} \quad \underset{\sim}{x}(t) = [\Phi]\,\underset{\sim}{q}(t) \qquad [2]$$

The columns of the modal matrix are the normal (principal) modes of the system, the mode shapes. Substituting the relation of equation (2) into equation (1) yields the system equations of motion in terms of the generalized coordinates:

$$[M][\Phi]\,\ddot{\underset{\sim}{q}}(t) + [C][\Phi]\,\dot{\underset{\sim}{q}}(t) + [K][\Phi]\,\underset{\sim}{q}(t) = \underset{\sim}{f}(t) \qquad [3]$$

Premultiplication of equation (3) by the transpose of the modal matrix yields equation (4), the uncoupled modal equations of motion:

$$[\Phi]^T[M][\Phi]\ddot{\underset{\sim}{q}}(t) + [\Phi]^T[C][\Phi]\dot{\underset{\sim}{q}}(t) + [\Phi]^T[K][\Phi]\underset{\sim}{q}(t) = [\Phi]^T\underset{\sim}{f}(t) \qquad [4]$$

This uncoupling phenomenon is due to the orthogonality of the modal matrix.

The modal mass, damping, and stiffness matrices, [m], [c], and [k] respectively, are defined as follows:

$$[m] = [\Phi]^T[M][\Phi] \quad [5]$$

$$[c] = [\Phi]^T[C][\Phi] \quad [6]$$

$$[k] = [\Phi]^T[K][\Phi] \quad [7]$$

For the modal equations of motion to be uncoupled, each of the modal matrices must be diagonal. In general, damping is not correctly modeled by a diagonal modal damping matrix, however, this assumption must be made in order to uncouple the system of equations. In formulation of the damping matrix, proportional damping is assumed. This means that the damping matrix is proportional to the mass and/or stiffness matrices. Under this assumption, the modal damping matrix is guaranteed to be diagonal, and equation (4) will be uncoupled.

The objective of the disk drive analysis has been stated to be the determination of the modal matrix. After the modal matrix has been determined, the vibration problem of equation (1) may be solved in its uncoupled form, equation (4). The solution of equation (4) is motion in terms of the generalized coordinates, $\underset{\sim}{q}(t)$. The physical motion, $\underset{\sim}{x}(t)$, may be determined from the generalized coordinates using equation (2).

1.3 Modal Matrix Theory

Once the structural property matrices have been defined, the mode shapes and natural frequencies may determined using straight forward mathematical procedures. Laplace transformation of equation (1) (after rearranging terms) yields:

$$\left[[M]s^2 + [C]s + [K]\right] \underset{\sim}{X}(s) = \underset{\sim}{F}(s) + s[M]\underset{\sim}{x}(t=0) + [M]\dot{\underset{\sim}{x}}(t=0) + [C]\underset{\sim}{x}(t=0) \quad [8]$$

where $\underset{\sim}{X}(s)$ and $\underset{\sim}{F}(s)$ are respectively, the response and forcing function vectors in the Laplace plane. If the initial condition vectors (displacement and velocity) are null, the system equations of motion in the Laplace domain may be written:

$$[B(s)]\ \underset{\sim}{X}(s) = \underset{\sim}{F}(s) \ ; \quad [B(s)] = \left[[M]s^2 + [C]s + [K]\right] \quad [9]$$

where [B(s)] is called the system matrix.

The forcing function vector and response vector may also be related, in the Laplace domain, by the transfer function matrix, [H(s)]. The forcing function vector premultiplied by the transfer function matrix yields the response vector:

$$[H(s)]\ \underset{\sim}{F}(s) = \underset{\sim}{X}(s) \quad [10]$$

Comparison of equations (9) and (10) with the initial conditions set to zero shows:

$$[H(s)] = [B(s)]^{-1} \quad [11]$$

The unforced case of equation (9) yields the homogeneous equation:

$$[B(s)]\,\underset{\sim}{X}(s) = \underset{\sim}{0} \qquad [12]$$

The solution of equation (12) is, in general, trivial. It is, however, non-trivial for a specific set of values of the Laplace variable, s. These values are the characteristic values (eigenvalues) of the system. In order for equation (12) to have a non-trivial solution, the system matrix must be singular[1].* This implies that the determinant of the system matrix is zero:

$$\left|[B(s)]\right| = 0 \qquad [13]$$

Equation (13) defines a characteristic equation in (s), the roots of this equation are the system eigenvalues. Based on equation (11) and the definition of the inverse of a matrix the transfer function matrix may be written:

$$[H(s)] = [B(s)]^{-1} = \frac{[D(s)]}{|[B(s)]|} \qquad [14]$$

where [D(s)] is the adjoint matrix (matrix of cofactors) of [B(s)]. Because the eigenvalues of the system defined in equation (12) are the roots of the determinant of the system matrix, they are poles (cause singularity) of the transfer function matrix.

* Numbers in square brackets refer to references at the end of this thesis

Substitution of the modal matrices of equations (5,6, and 7) into equation (4) yields:

$$[\lambda m]\,\ddot{\underset{\sim}{q}}(t) + [\lambda c]\,\dot{\underset{\sim}{q}}(t) + [\lambda k]\,\underset{\sim}{q}(t) = [\Phi]^T\,\underset{\sim}{f}(t) \qquad [15]$$

The time domain modal equations of motion may be transformed into the Laplace domain, as were the physical equations (reference equation (8)). If the initial conditions are zero the modal equations of motion may be written:

$$\left[[\lambda m]s^2 + [\lambda c]s + [\lambda k]\right]\,\underset{\sim}{Q}(s) = [\Phi]^T\,\underset{\sim}{F}(s) \qquad [16]$$

where $\underset{\sim}{Q}(s)$ is the generalized coordinate vector in the Laplace domain. The unforced modal problem yields a homogeneous system with the same eigenvalues as equation (12). Generally, the modal matrix will be scaled such that the modal mass matrix is the identity matrix. If this is the case, the modal mass, damping, and stiffness matrices may be defined as follows:

$$[\lambda m] = [\Phi]^T[M][\Phi] = [\lambda I] \qquad [17]$$

$$[\lambda c] = [\Phi]^T[C][\Phi] = [\lambda\ 2\sigma_k] = [\lambda\ 2\zeta_k\Omega_k] \qquad [18]$$

$$[\lambda k] = [\Phi]^T[K][\Phi] = [\lambda\ \sigma_k^2+\omega_k^2] = [\lambda\ \Omega_k^2] \qquad [19]$$

The modal parameters are defined by equations (17 to 19), σ_k is the damping coefficient, ω_k is the damped natural frequency, Ω_k is the undamped natural frequency, and ζ_k the damping factor (percent critical damping). The eigen-problem may now be expressed in equation (20), in terms of the modal parameters:

$$\left[[\lambda I]s^2 + [\lambda\ 2\sigma_k]s + [\lambda\ \sigma_k^2+\omega_k^2]\right] \underset{\sim}{Q}(s) = \underset{\sim}{0} \qquad [20]$$

Since the modal mass, damping, and stiffness matrices are diagonal, the eigenvalues of the system, λ_k , may be determined, from the quadratic formula, to be:

$$p_k = -\sigma_k \pm i\omega_k \qquad [21]$$

The poles, p_k, and conjugate poles, p_k^*, of the transfer function matrix are then given by:

$$p_k = -\sigma_k + i\omega_k \ , \qquad p_k^* = -\sigma_k - i\omega_k \qquad [22]$$

Figure (1) shows the pole and conjugate pole plotted on the Laplace plane and explains the relationships between the modal parameters.

Each unique eigenvalue has an associated eigenvector which is the solution vector to equation (12) or (20) when the eigenvalue is substituted for s. The eigenvector, $\underset{\sim}{U}_k$, and conjugate eigenvector, $\underset{\sim}{U}_k^*$, may therefore be defined by equations (23) and (24):

$$[B(p_k)]\ \underset{\sim}{X}(p_k) = \underset{\sim}{0} \Rightarrow \underset{\sim}{U}_k = \underset{\sim}{X}(p_k) \qquad [23]$$

$$[B(p_k^*)]\ \underset{\sim}{X}(p_k^*) = \underset{\sim}{0} \Rightarrow \underset{\sim}{U}_k^* = \underset{\sim}{X}(p_k^*) \qquad [24]$$

All other values for (s) yield a trivial solution (null vector). The eigenvectors are also called the mode shapes of the system;

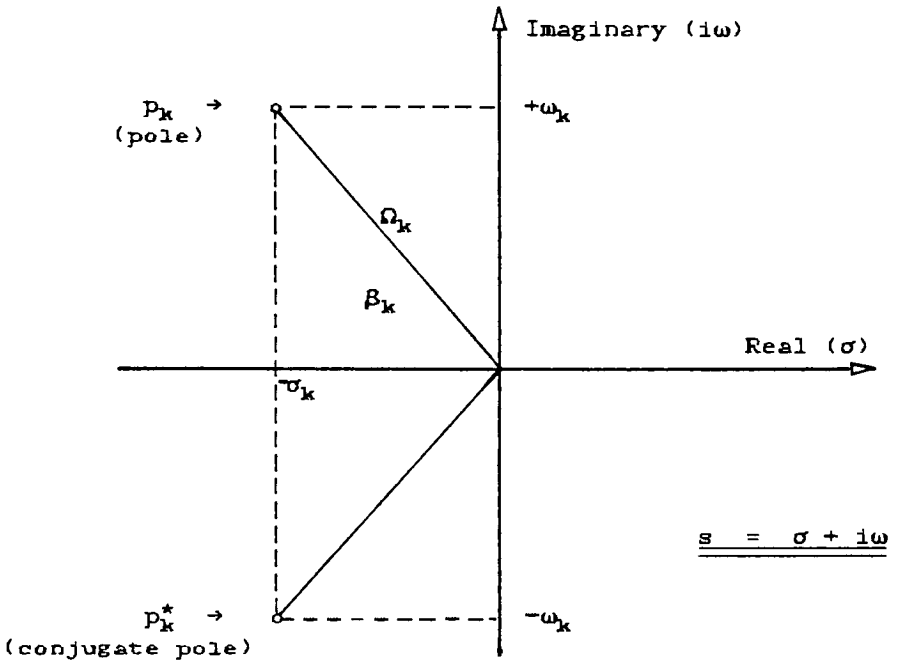

FIGURE 1: Pole Location in the LaPlace Plane

σ_k - Damping Coefficient
ω_k - Damped Natural Frequency
Ω_k - $(\sqrt{\sigma_k^2+\omega_k^2})$ - Undamped Natural Frequency
ζ_k - Cos β_k - Damping Factor (percent critical damping)

they are the mode shapes that compose the modal matrix as expressed in equation (25).

$$[\Phi]_{nxn} = \left[\underset{\sim}{U}_1 \quad \underset{\sim}{U}_2 \quad \underset{\sim}{U}_3 \quad \cdots \quad \underset{\sim}{U}_n \right] \qquad [25]$$

The transformation from equation (16) to equation (20) requires that the modal matrix be orthogonal as well as mass normalized. Orthogonality is satisfied if each eigenvector is orthogonal to every other eigenvector. Mathematically this requirement may be stated:

$$\underset{\sim}{U}_i^T \underset{\sim}{U}_j = 0 \; ; \qquad i \neq j \qquad [26]$$

Systems with symmetric system matrices necessarily yield linearly independent orthogonal eigenvectors. In general, however, the modal matrix will not be mass normalized as initially determined. Premultiplying the mass matrix by the transpose of the modal matrix, and postmultiplying by the modal matrix yields equation (27):

$$[\Phi]_{init}^T [M] [\Phi]_{init} = [\searrow \Lambda_k] \qquad [27]$$

where $[\searrow \Lambda_k]$ is a general diagonal matrix. A simple matrix multiplication, using the results of equation (27), may be used to transform the original modal matrix into mass normalized form:

$$[\Phi_{\substack{mass \\ norm}}] = [\searrow \sqrt{\Lambda_K}\,]^{-1} [\Phi]_{init} \qquad [28]$$

1.4 Finite Element Method in Modal Analysis

The analytical approach using finite element analysis is a direct approach to solving equation (12). The system matrix is generated using the finite element method, and the resulting eigen-problem is solved numerically. The finite element method is used to determine the property matrices [M], [C], and [K], and therefore the system matrix of the structure. The structure is modeled as an assembly of small pieces (elements), each of which has its own geometry and material properties, and its own second order matrix equation governing the dynamic behavior of the element. The individual element equations are combined to form a global equation, equation (1), from which the eigenvalue problem, equation (12) may be defined.

In general, the global equation will have a very large number of degrees of freedom (DOFs). The DOFs of the problem are independent coordinates that are used to describe the motion of the structure. There are several methods available to reduce the number of DOFs that are used in the solution procedure. In general, these methods eliminate certain DOFs, while not excluding the static properties associated with those DOFs. After the solution to the reduced problem is determined, the motion of the eliminated DOFs is calculated from the DOFs that were used in the solution process.

In practice, the finite element method is applied through use of a commercial program. There are programs available for both mainframe and personal computers. The mainframe programs are, of course, much more powerful with respect to problem size, solution speed, and the advanced capabilities available. All finite element codes, however, have the capability to generate and numerically solve the global equations for static problems, and most also have modal and dynamic analysis capabilities. NASTRAN is one of the most popular and powerful of the mainframe programs and was used exclusively for the finite element modeling of the disk drive.

1.5 Experimental Modal Analysis

Experimental modal analysis may also be used to solve for the modal matrix of a system but the approach is entirely different from the analytical finite element method. Experimental modal analysis requires a physical prototype to characterize. An input force, f(t), at a single point on a structure will produce a displacement response, x(t), at another point on the structure:

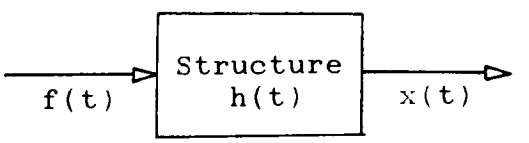

Figure 2: Structural Time Response

In the time domain, the input and the response are related by a second order differential operator, h(t). Looking at the same problem in the Laplace domain, the input, F(s), produces a response, X(s). Where F(s) and X(s) are defined by equations (29) and (30).

$$F(s) = \mathcal{L}\{f(t)\} \qquad [29]$$

$$X(s) = \mathcal{L}\{x(t)\} \qquad [30]$$

The structural vibration problem in the Laplace domain may be illustrated by figure (3).

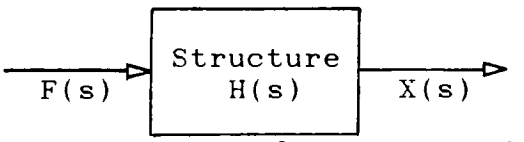

Figure 3: Structural Frequency Response

In this case, F(s) and X(s) are related by an algebraic operator, H(s), called the transfer function.

$$F(s) \cdot H(s) = X(s) \qquad [31]$$

This concept may be illustrated with a simple example. Consider the cantilever beam of figure (4). The vibration of the beam is to be characterized by the motion of the 4 points shown.

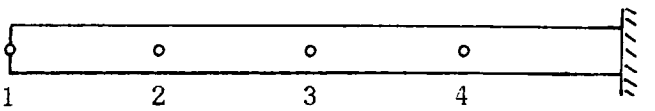

Figure 4: Four DOF Cantilever Beam Model

For this four DOF beam, the relation between a force input vector and the vibration response vector is given by the matrix equation:

$$\begin{bmatrix} H_{11}(s) & H_{12}(s) & H_{13}(s) & H_{14}(s) \\ H_{21}(s) & H_{22}(s) & H_{23}(s) & H_{24}(s) \\ H_{31}(s) & H_{32}(s) & H_{33}(s) & H_{34}(s) \\ H_{41}(s) & H_{42}(s) & H_{43}(s) & H_{44}(s) \end{bmatrix} \begin{Bmatrix} F_1(s) \\ F_2(s) \\ F_3(s) \\ F_4(s) \end{Bmatrix} = \begin{Bmatrix} X_1(s) \\ X_2(s) \\ X_3(s) \\ X_4(s) \end{Bmatrix} \qquad [32]$$

If the transfer function matrix could be determined with ease experimentally, it could be used in experimental modal analysis to find the modal matrix and modal frequencies. This, however, is not the case. Therefore, in place of the transfer function matrix, experimental modal analysis makes use of the frequency response function matrix.

A special case of the Laplace transform is the Fourier transform. The Laplace variable, s, is given by:

$$s = \sigma + i\omega \qquad [33]$$

where α is the real part, and ω the imaginary part. If the real part is zero, the Laplace transform reduces to the Fourier transform and the transfer function matrix becomes the frequency response function (FRF) matrix. In terms of the FRF matrix, the relation between the forcing function and the response of the cantilever beam becomes:

$$\begin{bmatrix} H_{11}(i\omega) & H_{12}(i\omega) & H_{13}(i\omega) & H_{14}(i\omega) \\ H_{21}(i\omega) & H_{22}(i\omega) & H_{23}(i\omega) & H_{24}(i\omega) \\ H_{31}(i\omega) & H_{32}(i\omega) & H_{33}(i\omega) & H_{34}(i\omega) \\ H_{41}(i\omega) & H_{42}(i\omega) & H_{43}(i\omega) & H_{44}(i\omega) \end{bmatrix} \begin{Bmatrix} F_1(i\omega) \\ F_2(i\omega) \\ F_3(i\omega) \\ F_4(i\omega) \end{Bmatrix} = \begin{Bmatrix} X_1(i\omega) \\ X_2(i\omega) \\ X_3(i\omega) \\ X_4(i\omega) \end{Bmatrix} \qquad [34]$$

The frequency response function matrix may be experimentally determined using the Fast Fourier Transform (FFT) algorithm and digital instrumentation. The simplest way of measuring an element of the frequency response function matrix is as a ratio of the FFT of a single response to the FFT of a single force input, for example:

$$Hnm(i\omega) = \frac{Xn(i\omega)}{Fm(i\omega)} \qquad [35]$$

where n is the response DOF, and m the excitation DOF.

The frequency response function matrix will be an (n x n) matrix, where n is the number structural test DOFs. Experimental modal analysis requires the determination of only a single row or column of the FRF matrix. Impact testing, which was used exclusively for the disk drive problem, uses a fixed response DOF and varies the excitation DOF in order to obtain a row of the FRF matrix. Conversely, random testing varies the response DOF while exciting the structure at a fixed DOF. This yields a single column of the FRF matrix. By measuring only (n) FRFs, the modal properties of the entire structure may be determined.

CHAPTER 2. Experimental Modal Analysis

2.1 System Requirements for Experimental Modal Analysis

The principal requirements of an experimental modal analysis system are signal processing capability and modal parameter estimation. Accomplishment of either of these tasks requires both software and its host hardware. Although many different systems (and types of systems) are available, this discussion will be limited to the system that was used for the disk drive analysis.

Some systems host signal processing and modal parameter estimation software on a single dedicated piece of hardware. The system that was used for this study consisted of a dedicated signal processing unit (B&K 2032 dual channel signal analyzer), and Structural Measurement Systems' (SMS) modal 3.0 software on a HP 9816 host computer.

The structure was excited with a force hammer, B&K model 8202, equipped with a B&K 8200 model force transducer. This force transducer is a piezo-electric transducer with a compressive force limit of 5000N. Although the transducer is good up to 10kHz, the magnitude and frequency content of the impact force are dependent on the type of tip used for the hammer. Rubber, plastic, and Steel tips are available. In

general, a softer tip will provide a lower force magnitude and frequency range and would be preferable for low frequency measurements. The opposite would be true of a harder tip.

Structural response acceleration was measured with a piezo-electric accelerometer (B&K model 4374). There are many criteria that must be taken into account in accelerometer selection. An ideal choice would have high sensitivity, wide frequency range, and low weight. However, high sensitivity generally implies more weight and less frequency range. For modal testing, as long as the accelerometer will cover the frequency range of interest, low relative weight is the most important selection criterion. The weight of the accelerometer should be insignificant relative to the weight of the test specimen to prevent the accelerometer mass from altering the dynamic properties of the structure. The accelerometer model that was used for this modal study has a mass of only 0.65 grams. This was negligible relative to the mass of the test structure. The accelerometer was mounted to the structure using bee's wax, which has been shown to be an accurate mounting method even at frequencies above 10kHz.

The excitation and response signals were amplified by conditioning amplifiers (B&K 2626) before being fed into the dual channel analyzer. This analyzer is a dedicated piece of hardware which is preprogrammed with fast Fourier transform algorithms, as well as special time domain weighting functions.

The FRFs generated on the analyzer are transferred over a GPIB bus to the HP 9816 computer where they can be stored for later analysis. A schematic of the entire experimental setup is shown in figure (5).

2.2 Procedure for Experimental Modal Analysis

The first step of any modal test is the identification of the structural degrees of freedom to be tested. A DOF has both location and direction associated with it, therefore a single point on a structure may yield up to three orthogonal translational testing DOFs. Too few, or poorly chosen DOFs should not affect the accuracy of the modal parameter estimation but will yield poor characterization of the structure's deflection pattern. On the other hand, too many unnecessary DOFs will result in lengthy, inefficient testing.

The analysis program needs to know the location and the label for each of the test points. Modal 3.0 utilizes a Coordinates file, which includes point numbers and the points location in rectangular, cylindrical, or spherical coordinates. For graphical purposes only, Modal 3.0 requires a Display Sequence file. This file determines how the test points are to be connected by graphical line segments during display.

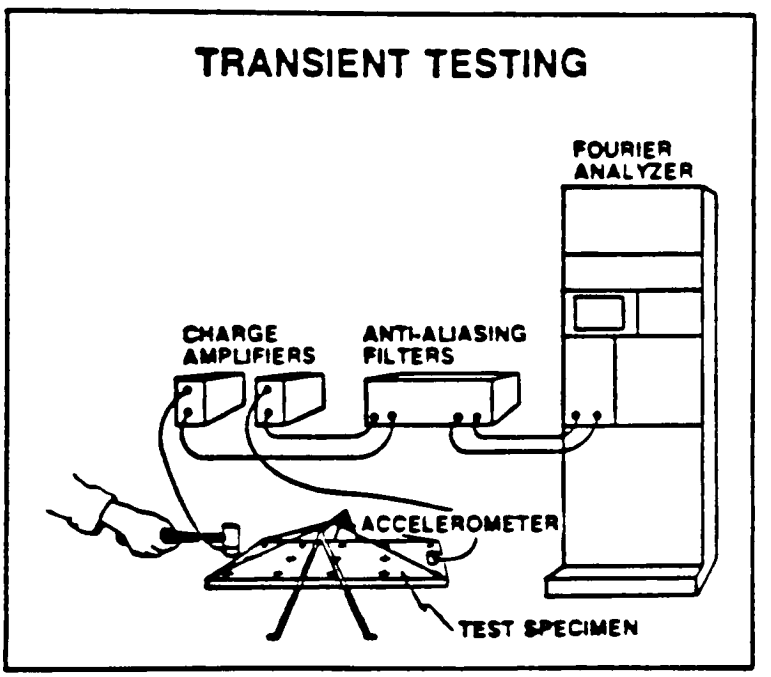

Figure 5: Test Set-up for Experimental Modal Analysis [2]

The next step is to obtain the necessary FRFs, and store them (in digital form) on floppy disk. The type of analysis that was performed on the disk drive was single reference impact testing. For this type of modal test, a single response accelerometer is fixed at a single DOF and the impact hammer is used to provide an input force at each of the DOFs of the structure independently. An FRF between the hammer input force and the acceleration response is obtained for each DOF. In this manner (n) FRFs are obtained for an (n) DOF structure.

The FRFs which were finally accepted and stored were the average of 5 to 10 trials. The FRF averaging procedure is useful in averaging out the effect of errant, or inconsistent FRFs. The coherence function, which is programmed into the FFT analyzer, was used as an indicator of whether or not the averaged FRF was acceptable. The coherence function is a magnitude versus frequency function which is indicative of the cause and effect relationship of the input force and response acceleration. For example, the coherence between hammer input force and random noise should be close to zero (no coherence) over the entire frequency range. However, the coherence between hammer input and acceleration response on the structure should be close to one if the measurement is to be accepted. Two problems with the FRF which may be indicated by poor coherence are noise, and nonlinear behavior. When an acceptable measurement has been obtained,

transfer to the computer and data storage is controlled by the Modal 3.0 software. When measurements have been stored for every DOF the experimental work is complete.

The remaining steps are computational processes which determine the modal parameters from the stored FRFs. The first and most important of the analysis steps is curve fitting. The experimentally determined FRF is a digitized representation of a magnitude versus frequency curve and is stored on disk as a set of magnitude, frequency data points. Frequency domain curve fitting fits these data points to an analytical expression from which the modal parameters may be obtained.

The important modal parameters, natural frequencies and modal residues (see section 2.3), are obtained directly from the curve fitting process. From the modal residue matrices, the modal (mode shape) matrix, the objective, may be determined. The process by which Modal 3.0 extracts mode shapes from the residue matrices is called modal sorting. Modal 3.0 has three mode shape scaling options that may be used in the sorting process. The modal matrix may be scaled to modal masses, actual displacement units, or it may be left unscaled.

2.3 Representation of the Transfer Function in Terms of Modal Vectors

The purpose of this section is to define the modal residue, to show how the residue matrix may be defined from the transfer function or FRF matrix, and to show how the mode shape may be determined from the residue matrix. The key to experimental modal analysis is that the modal matrix may be accurately estimated after determination of a single row or column of the FRF matrix. The significance of this is that only (n) FRFs need be determined for an (n) DOF structure, rather than all of the (n^2) FRFs which make up the FRF matrix.

Equation (14) shows that the transfer function matrix may be expressed as a ratio of the adjoint of the system matrix by the determinant of the system matrix. The adjoint of the system matrix will have polynomial members of order (2n-1), while the determinant of the system matrix will be a polynomial of order (2n). Because the system poles are roots of the determinant of the system matrix, it may be factored as shown in equation (36):

$$\left|[B(s)]\right| = a\,(s-p_1)(s-p_1^*)(s-p_2)(s-p_2^*)\ \ldots\ (s-p_k)(s-p_k^*) \qquad [36]$$

where (a) is a constant.

A rational function (quotient of two polynomials) may be expanded in partial fraction form about the poles of the function.[3] If equation (36) contains no repeated roots, the poles of the transfer function will all be first order poles, and [H(s)] may be expressed from equations (14 and 36) as:

$$[H(s)] = \sum_{k=1}^{n} \frac{[Ak]}{s - p_k} + \frac{[A_k^*]}{s - p_k^*} \qquad [37]$$

where the numerator of the first term is the matrix of residues corresponding to the pole, and the numerator of the second term is the matrix of residues corresponding to the conjugate pole. The residue of a function (f(z)), corresponding to a first order pole (c) is given by equation (38):[4]

$$\text{Residue} = (z - c)\, f(z)\Big|_{z=c} \qquad [38]$$

Similarly, the residue matrices, $[A_k]$ and $[A_k^*]$, of equation (37) may be defined by equation (39):

$$[A_k] = (s-p_k)\, \frac{[D(s)]}{|[B(s)]|}\Big|_{s=p_k} \quad ; \quad [A_k^*] = (s-p_k^*)\, \frac{[D(s)]}{|[B(s)]|}\Big|_{s=p_k^*} \qquad [39]$$

Substituting into equation (39) from equation (36) and evaluating equation (39) at the poles, the residue matrices may be defined as given in equation (40):

$$[A_k] = \frac{[D(p_k)]}{\prod_{i=1}^{k-1}(p_k-p_i)\prod_{i=k+1}^{n}(p_k-p_i)\prod_{i=1}^{n}(p_k-p_i^*)} \quad ;$$

$$[A_k^*] = \frac{[D(p_k^*)]}{\prod_{i=1}^{n}(p_k^*-p_i)\prod_{i=1}^{k-1}(p_k^*-p_i^*)\prod_{i=k-1}^{n}(p_k^*-p_i^*)} \qquad [40]$$

It can now be shown that the system matrix adjoint, [D(s)], when evaluated at a pole, is related to the mode shape corresponding to that particular pole. From the definition of the matrix inverse:

$$[B(s)]\,[B(s)]^{-1} = [\searrow I] \qquad [41]$$

Substituting from equation (14) for the inverse of the system matrix into equation (41):

$$\frac{[B(s)][D(s)]}{|[B(s)]|} - [\searrow I] \Rightarrow [B(s)][D(s)] - |[B(s)]|\,[\searrow I] \qquad [42]$$

The determinant of [B(s)] is, by definition of the poles of the transfer function matrix, zero when evaluated at the poles. Therefore, from equation (42):

$$[B(p_k)][D(p_k)] = |[B(p_k)]|\,[\searrow I] = [0] \;;$$
$$[B(p_k^*)][D(p_k^*)] = |[B(p_k^*)]|\,[\searrow I] = [0] \qquad [43]$$

If the column vectors of [D(s)] are indicated by a lower case (d), then from equation (43):

$$[B(p_k)]\,\underset{\sim}{d}_j(p_k) = \underset{\sim}{0} \;;\quad [B(p_k^*)]\,\underset{\sim}{d}_j(p_k^*) = \underset{\sim}{0} \qquad [44]$$
$$(\text{for } j = 1,2, \ldots n)$$

Comparison of equation (44) with equations (23 and 24) shows that all of the columns of the adjoint matrix (defined for a given pole) are proportional to the mode shape for that pole.

$$\underset{\sim}{v}_k = \alpha_k \underset{\sim}{d}_j(p_k) \;;\quad \underset{\sim}{v}_k^* = \alpha_k^* \underset{\sim}{d}_j(p_k^*) \qquad [45]$$
$$(\text{for } j = 1,2, \ldots n)$$

where α_k and α_k^* are proportionality constants.

Mass, stiffness, and damping matrices were assumed to be symmetric, therefore the system matrix and corresponding adjoint matrix are also symmetric. Because [D(s)] is symmetric, the rows of $[D(p_k)]$ are also proportional to the mode shapes.

$$\underset{\sim}{u}_k^T = \alpha_k[d_j(p_k)] \quad ; \quad \underset{\sim}{u}_k^{*T} = \alpha_k^*[d_j(p_k^*)} \qquad [46]$$

where $[d_j]$ is the j_{th} row of [D]

In order that both the rows and columns of $[D(p_k)]$ be proportional to the mode shape, $[D(p_k)]$ must be of the form:

$$[D(p_k)] = q_k \underset{\sim}{u}_k \underset{\sim}{u}_k^T = q_k \begin{bmatrix} u_k^1 u_k^1 & u_k^1 u_k^2 & \cdots & u_k^1 u_k^n \\ u_k^1 u_k^2 & u_k^2 u_k^2 & \cdots & u_k^2 u_k^n \\ \vdots & \vdots & & \vdots \\ u_k^1 u_k^n & u_k^2 u_k^n & \cdots & u_k^n u_k^n \end{bmatrix} \qquad [47]$$

and

$$[D(p_k^*)] = q_k^* \underset{\sim}{u}_k^* \underset{\sim}{u}_k^{*T} = q_k^* \begin{bmatrix} u_k^{*1} u_k^{*1} & u_k^{*1} u_k^{*2} & \cdots & u_k^{*1} u_k^{*n} \\ u_k^{*1} u_k^{*2} & u_k^{*2} u_k^{*2} & \cdots & u_k^{*2} u_k^{*n} \\ \vdots & \vdots & & \vdots \\ u_k^{*1} u_k^{*n} & u_k^{*2} u_k^{*n} & \cdots & u_k^{*n} u_k^{*n} \end{bmatrix} \qquad [48]$$

where q_k and q_k^* are constants

Combining equations (47 and 48) with equation (40), and lumping all of the constants into a single term, Q_k, the residual matrix may now be written in terms of the associated eigenvector and a scaling constant.

$$[A_k] = Q_k \underset{\sim}{u}_k^T \underset{\sim}{u}_k \quad ; \quad [A_k] = Q_k^* \underset{\sim}{u}_k^{*T} \underset{\sim}{u}_k^* \qquad [49]$$

where:

$$[A_k] = \frac{q_k}{a\sum_{i=1}^{k-1}(p_k - p_i)\sum_{i=k+1}^{n}(p_k - p_i)\sum_{i=1}^{n}(p_k - p_i^*)} \; ;$$

$$[A_k^*] = \frac{q_k^*}{a\sum_{i=1}^{n}(p_k^* - p_i)\sum_{i=1}^{k-1}(p_k^* - p_i^*)\sum_{i=k-1}^{n}(p_k^* - p_i^*)} \qquad [50]$$

Substituting the relations of equation (49 and 50) into equation (37) yields equation (51), which expresses the transfer function matrix in terms of the eigenvectors, poles, and scaling constants.

$$[H(s)] = \sum_{k=1}^{n} \frac{Q_k u_k^T u_k}{s - p_k} + \frac{Q_k^* u_k^{*T} u_k^*}{s - p_k^*} \qquad [51]$$

Given the transfer function matrix and the pole location, the mode shape may be determined to within a scaling constant by solving equation (51). Similarly, equation (51) could be re-written by substituting the Fourier variable for the Laplace variable ($s=i\omega$). The new equation would relate the mode shapes to the frequency response function matrix rather than the transfer function matrix. The curve fitting process, which is discussed in the next section, fits different representations of equation (51) to the experimental FRF in order to determine the pole location, p_k, and the residue matrix, $[A_k]$. The mode shapes are then extracted from the residue matrix as discussed in section 2.5.

2.4 Curve Fitting

Frequency domain curve fitting is a process in which the experimental data, the FRF, is fit to an analytical expression. The residue and conjugate residue matrices may then be defined in terms of the curve fit parameters. One division between

different methods is Single Degree Of Freedom (SDOF) versus Multiple Degree of Freedom (MDOF). SDOF methods fit each mode of a measurement singly. They are computationally simpler and therefore require much less solution time than the MDOF methods. Lightly coupled modes may be curve fit using the quicker SDOF methods, while MDOF methods must be used for closely coupled modes. Figures (6a and 6b) show the difference between light and heavy modal coupling. Figure (6b) shows an example of a heavily coupled system, indicated by the close spacing (overlapping) of the modal peaks. Figure (6a), however, shows light coupling; each peak is well defined and spaced out from the others.

2.4.1 Peak Picking from the Quadrature Response

The simplest method of determining the residue of a lightly coupled system does not require that a curve fit be performed on the experimental FRF. The residue is determined by picking the peak value of the quadrature (imaginary) response near the modal frequency.

Figures (7a) and (7b) show the real and imaginary part of the frequency response for a single lightly damped mode. At resonance, the real part of the FRF is close to zero, and the imaginary part is nearly maximum. Figure (7c) shows the representation of a single DOF transfer function in the Laplace domain, the transfer function is represented by the shaded

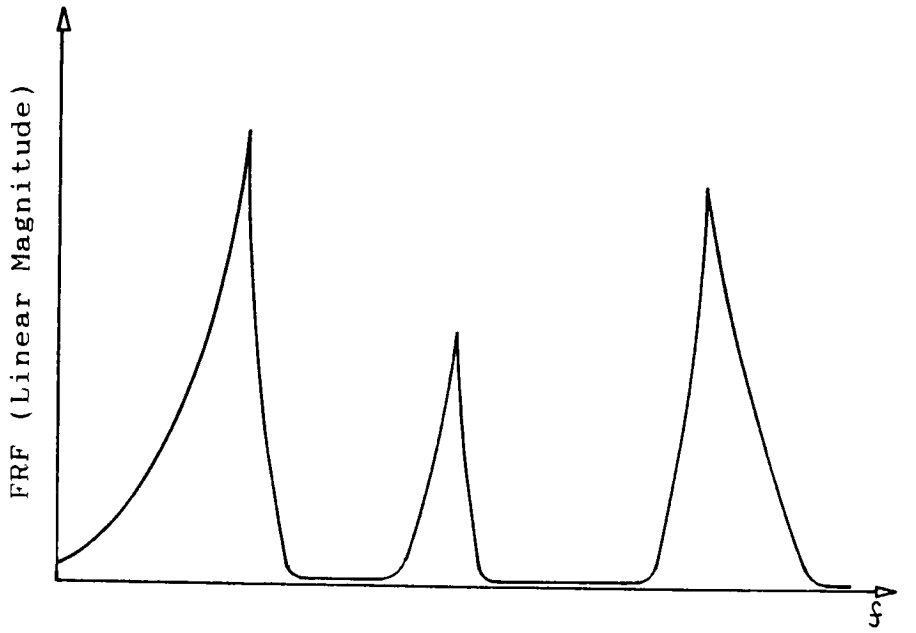

Figure 6a: FRF with Light Damping and Coupling

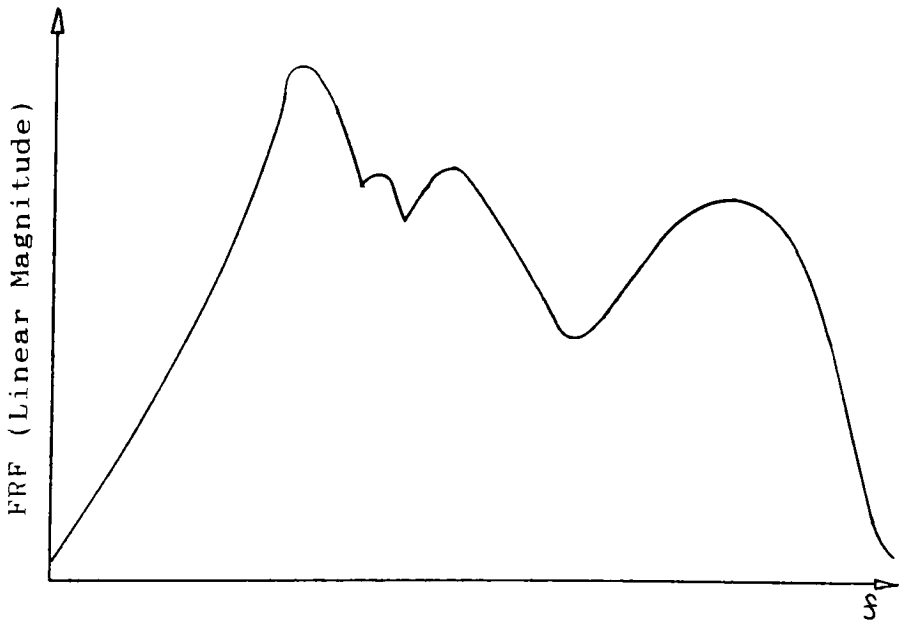

Figure 6b: FRF with Heavy Damping and Coupling

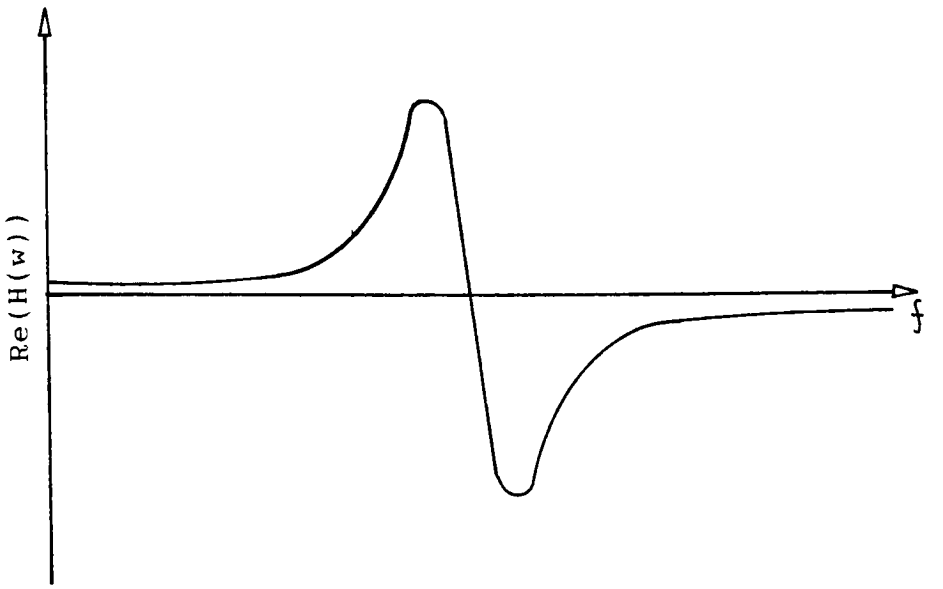

Figure 7a: Real Component of the Frequency Response Function

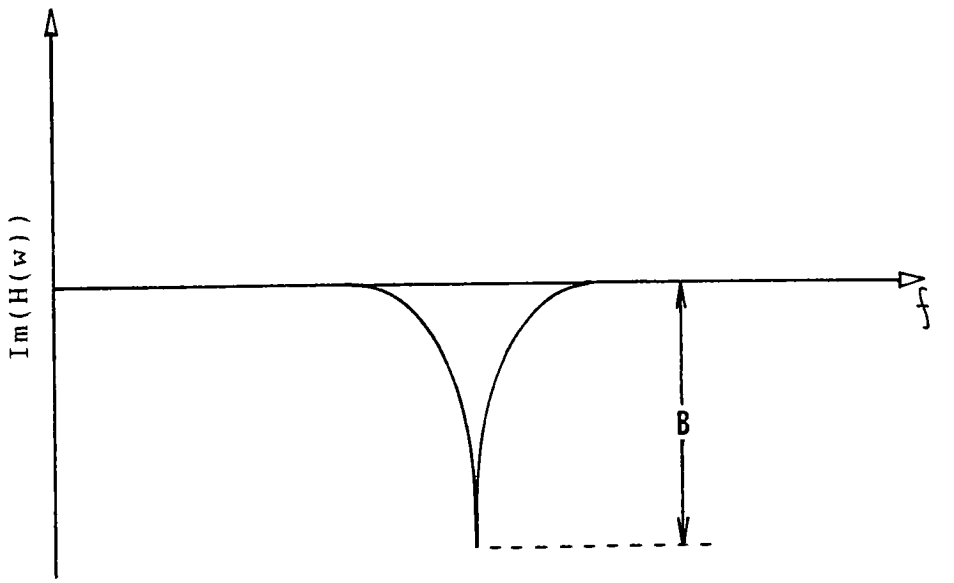

Figure 7b: Imaginary Component of the Frequency Response Function

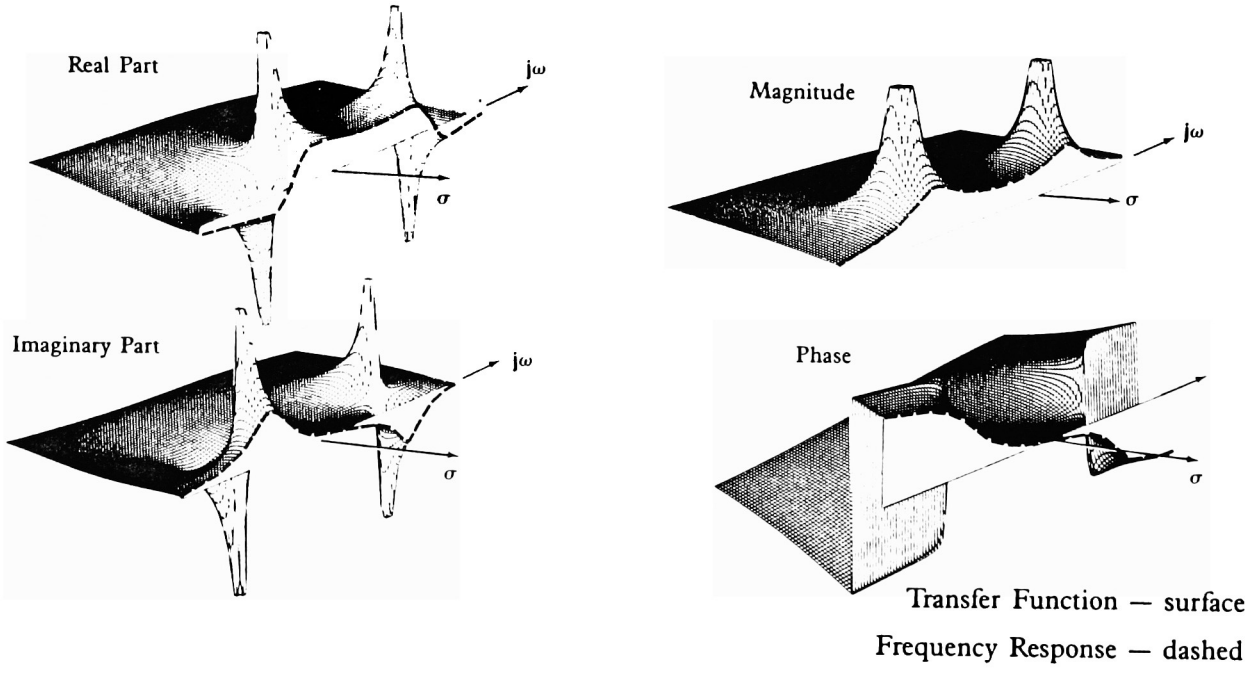

Figure 7c: Plots of the Transfer Function in the Laplace Plane [5]

surface, and is sectioned along the real axis. The FRF is represented by a dashed line along the section. At the pole location in the Laplace plane, the real part of the transfer function is zero valued. As the modal damping decreases, the pole location approaches the real axis of the Laplace plane, and the real part of the FRF at the resonant frequency approaches zero. Because the real part of the FRF is nearly zero for lightly damped modes, the real part of the residue is also close to zero and the residue may be estimated from the imaginary part of the FRF only.

An expression for a single element of the transfer function matrix, equation (52), may be written from equation (37):

$$H_{ij}(s) = \sum_{k=1}^{n} \frac{A_k(i,j)}{s - p_k} + \frac{A_k^*(i,j)}{s - p_k^*} \qquad [52]$$

Looking at the contribution of a single mode (the k_{th} mode) to the transfer function element, equation (55) follows:

$$(H_{ij}(s))_k = \frac{A_k(i,j)}{s - p_k} + \frac{A_k^*(i,j)}{s - p_k^*} \qquad [53]$$

$$\text{let } A_k(i,j) = a_1 + a_2 i \text{ , then } A_k^*(i,j) = a_1 - a_2 i \qquad [54]$$

$$\text{and: } (H_{ij})_k = \frac{(a_1 + a_2 i)}{s - (-\sigma_k + i\omega_k)} + \frac{(a_1 - a_2 i)}{s - (-\sigma_k - i\omega_k)} \qquad [55]$$

When the real part of the LaPlace variable goes to zero, the transfer function becomes the frequency response function and equations (56) to (60) follow from equation (55):

$$(h_{ij}(i\omega))_k = \frac{(a_1 + a_2 i)}{i\omega - (-\sigma_k + i\omega_k)} + \frac{(a_1 - a_2 i)}{i\omega - (-\sigma_k - i\omega_k)} \qquad [56]$$

$$\mathrm{Re}((h_{ij})_k) = \frac{a_1\sigma_k + a_2(\omega-\omega_k)}{\sigma_k^2 + (\omega-\omega_k)^2} + \frac{a_1\sigma_k - a_2(\omega-\omega_k)}{\sigma_k^2 + (\omega-\omega_k)^2} \quad [57]$$

$$\mathrm{Im}((h_{ij})_k) = \frac{a_2\sigma_k - a_1(\omega-\omega_k)}{\sigma_k^2 + (\omega-\omega_k)^2} - \frac{a_2\sigma_k - a_1(\omega-\omega_k)}{\sigma_k^2 + (\omega-\omega_k)^2} \quad [58]$$

$$\lim_{\substack{\omega \to \omega_k \\ \omega_k >> \sigma_k}} \left(\mathrm{Re}((h_{ij})_k)\right) = \frac{a_1}{\sigma_k} \quad [59]$$

$$\lim_{\substack{\omega \to \omega_k \\ \omega_k >> \sigma_k}} \left(\mathrm{Im}((h_{ij})_k)\right) = \frac{a_2}{\sigma_k} \quad [60]$$

Based on the previous discussion, it will be assumed that the real part of the FRF is zero, and therefore the real part of the residue, a_1 is also zero. The residue is therefore determined from the magnitude of the imaginary part of the FRF, B, as shown graphically in figure (7b). The residue and conjugate residue for the k_{th} mode are therefore given by equations (61) and (62):

$$A_k(i,j) = a_{2i} = \sigma_k B_i \quad [61]$$

$$A_k^*(i,j) = -a_{2i} = -\sigma_k B_i \quad [62]$$

As indicated by equations (61) and (62), correct scaling of the residues requires that both the magnitude of the imaginary response, B, and the damping coefficient σ_k are known. The peak pick method does not determine the damping coefficient. Therefore, if correct scaling of the residue is required, the

damping must be determined by some other means. A method of damping coefficient estimation is discussed at the end of section 2.4.2.

2.4.2 Circle Fitting

A second method of characterizing the FRFs fits a circle to the data points in the Nyquist (real -versus- imaginary) plane. Dropping the conjugate contribution to the transfer function, the contribution of a single mode to a single element of the transfer function matrix may be written (from equation 53):

$$(H_{ij}(s))_k = \frac{A_k(i,j)}{s - p_k} \qquad [63]$$

Substituting an expression for $[A_k]$ from equation (54), and substituting for p_k, equation (63) becomes:

$$(H_{ij}(s))_k = \frac{a_1 + a_2 i}{s - (-\sigma_k + i\omega_k)} \qquad [64]$$

Changing from the Laplace to the Fourier variable, the contribution of the k_{th} mode to the ij_{th} element of the FRF matrix may be written:

$$(h_{ij}(i\omega))_k = \frac{a_1 + a_2 i}{i\omega - (-\sigma_k + i\omega_k)} \qquad [65]$$

Equations (66) and (67) follow:

$$Re((h_{ij})_k) = \frac{a_1\sigma_k + a_2(\omega - \omega_k)}{\sigma_k^2 + (\omega - \omega_k)^2} \qquad [66]$$

$$\mathrm{Im}((h_{ij})_k) = \frac{a_2\sigma_k - a_1(\omega-\omega_k)}{\sigma_k^2 + (\omega-\omega_k)^2} \qquad [67]$$

When plotted in the Nyquist plane, equations (66) and (67) will form a circle with a center and diameter that can be expressed in terms of the modal parameters (see figure 8).

Multi-Degree of Freedom (MDOF) systems show only a portion of a circle for each mode due to the interactions between adjacent modes. For example, the Nyquist plot of a three-DOF system might look like figure (9). As the modes are more distantly spaced in the frequency domain, the circles become more clearly defined. In figure (9), the second mode would not be accurately curve fit by a SDOF circle fit because it is not a complete enough circle. This effect is again due to the degree of coupling of the system; a lightly coupled system would yield more completely defined circles, and therefore, more accurate SDOF circle fits. The natural frequency associated with each mode coincides with the maximum pseudo-vector on the Nyquist plot for that mode.

The first step in the curve fitting process is to identify the frequency range of the data points to be included in the curve fit. The data points chosen are then fit to equation (68):

$$(\mathrm{Im} - A)^2 + (\mathrm{Re} - B)^2 = C^2 \qquad [68]$$

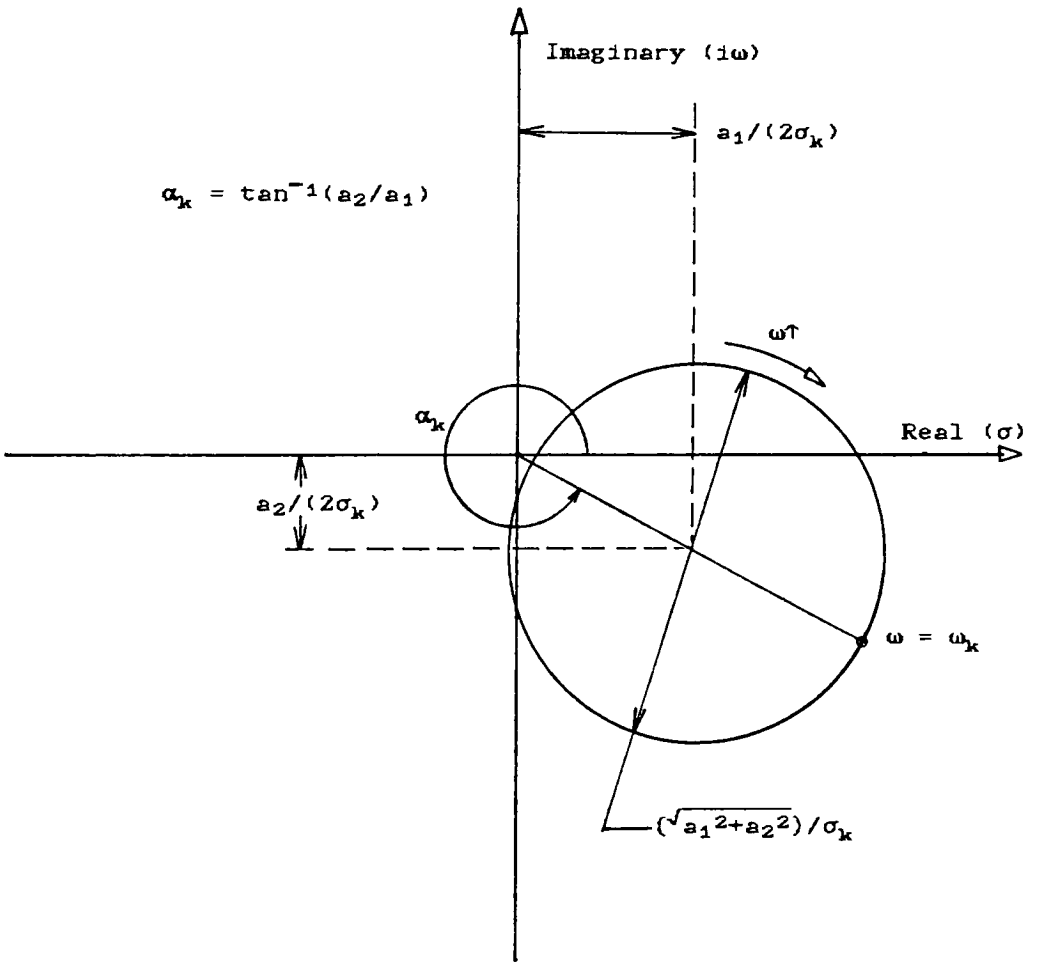

Figure 8: Nyquist Plot of Single DOF Frequency Response Function

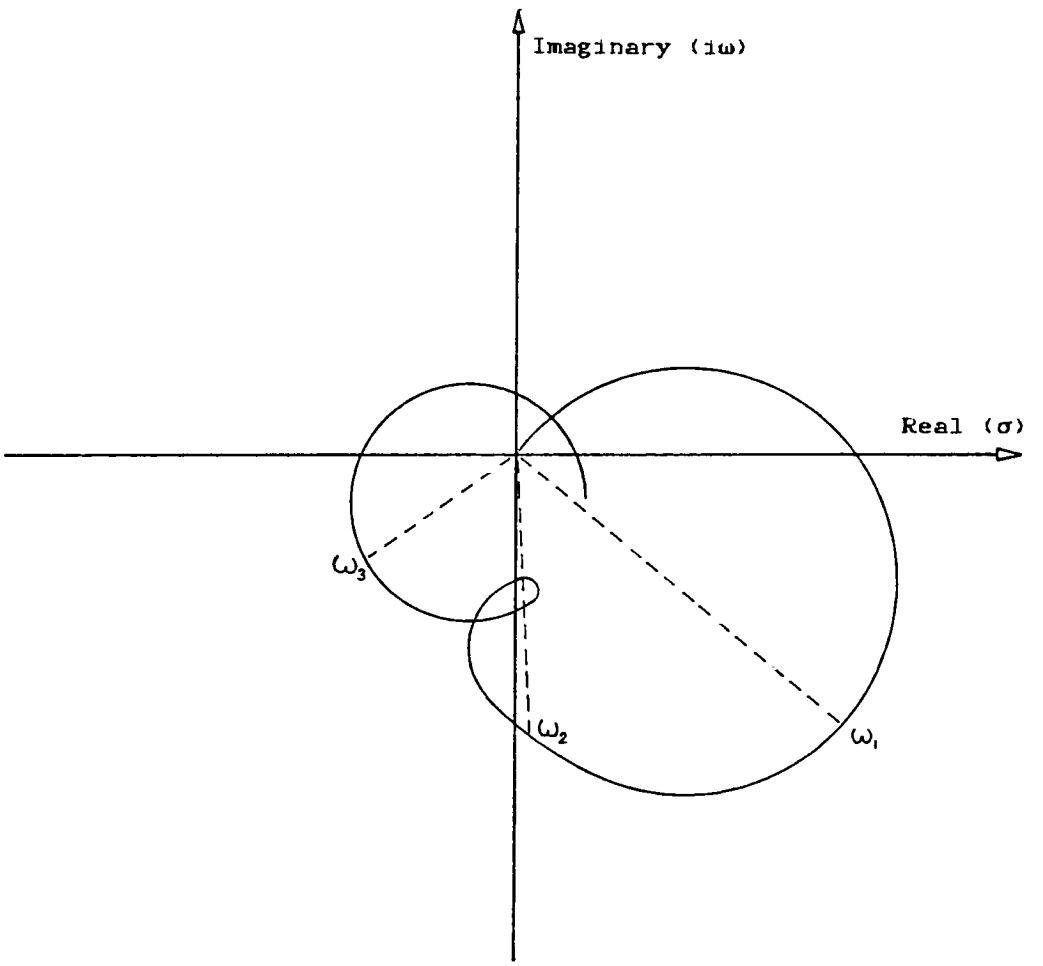

Figure 9: Nyquist Plot of 3 DOF Frequency Response Function

The SMS Modal 3.0 procedure uses a least squares error minimization technique to identify A, B, and C. Based on equation (68) and figure (8), the curve fit coefficients (A,B, and C) may be related to the modal residue and damping coefficient, as shown in equations (69) to (71):

$$A = -\frac{a_2}{2\sigma_k} \qquad [69]$$

$$B = -\frac{a_1}{2\sigma_k} \qquad [70]$$

$$C = \frac{\sqrt{a_1^2+a_2^2}}{\sigma_k} \qquad [71]$$

If the damping coefficient were known a priori, the complex residue could be determined and correctly scaled. The circle fit method is incapable of determining the damping coefficient, therefore determination of the scaled complex residue is not possible. The Modal 3.0 circle fit uses the circle diameter, which is proportional to the residue magnitude, to characterize the imaginary part of the modal residue. If the system is lightly damped, it has been shown that the real part of the pole, and therefore, the real part of the residue, a_1, approaches zero. From equation (71), the limit of C as a_1 approaches zero is proportional to a_2:

$$\lim_{a_1 \to 0} (C) = \frac{a_2}{\sigma_k} \qquad [72]$$

Therefore, the unscaled imaginary part of the residue, a_2, is set equal to the circle diameter C, and the real part of the residue, a_1, is assumed to be zero. If the damping coefficient is

determined by some other method, the residue, a_2, may be correctly scaled. The Modal 3.0 algorithm will not, however, determine the complex residue.

One method of damping estimation based on the Nyquist representation of the FRF is given by Kennedy and Pancu[6]. This method is roughly equivalent to the half power band width method. The damping coefficient is estimated as shown in equation (73):

$$\frac{\sigma_k}{\omega_k} = \xi_k = \frac{1}{2}\left(\frac{\omega_2 - \omega_1}{\omega_k}\right) \qquad [73]$$

The frequencies ω_1 and ω_2 are the frequencies located at plus/minus 90 degrees on the Nyquist circle. This method could be used to determine damping coefficients to be manually input into the circle fit routine.

2.4.3 Single and Multi DOF Polynomial Fits

The rational function polynomial fit fits a polynomial to the magnitude versus frequency form of the FRF. If the system consists of lightly coupled modes, each mode may be fit independently with a SDOF polynomial curve fit. However, for closely coupled modes, an MDOF polynomial fit must be used. It is more costly (computationally) to fit a group of modes simultaneously with the MDOF method than it would be to fit each singly with the SDOF method. Therefore, the SDOF method is preferable except in cases of closely coupled modes.

The contribution of the k_{th} mode to an element of the transfer function matrix may be repeated from equation (55). For the ij_{th} element of the transfer function matrix, the contribution due to the k_{th} mode is given by:

$$(H_{ij}(s))_k = \frac{(a_1 + a_2 i)}{((s+\sigma_k) - i\omega_k)} + \frac{(a_1 - a_2 i)}{((s+\sigma_k) + i\omega_k)} \qquad [74]$$

Equations (75 and 76) follow:

$$(H_{ij}(s))_k = \frac{(a_1+a_2 i)((s+\sigma_k)+i\omega_k)}{(s+\sigma_k)^2 + \omega_k^2} + \frac{(a_1-a_2 i)((s+\sigma_k)-i\omega_k)}{(s+\sigma_k)^2 + \omega_k^2} \qquad [75]$$

$$(H_{ij}(s))_k = 2\left[\frac{a_1 s + a_1\sigma_k - a_2\omega_k}{s^2 + 2\sigma_k s + \sigma_k^2 + \omega_k^2}\right] \qquad [76]$$

Equation (76) is a theoretical form of the transfer function. The Modal 3.0 SDOF polyfit method fits equation (77), which is based on equation (76), to the range of experimental FRF data points using a least squares error minimization technique.

$$h_k(i\omega) = \frac{C_1 s + C_2}{C_3 s^2 + C_4 s + C_5} + C_6 + C_7 s + C_8 s^2 \Big|_{s=i\omega} \qquad [77]$$

The first term of equation (77), in terms of constants C_1, C_2, C_3, C_4, and C_5, accounts for the contribution of the k_{th} mode to the experimental data. This term corresponds directly to equation (76). The last three terms account for the contribution of modes other than the k_{th}. When choosing the curve fit range for an SDOF fit, the ideal choice is a range of data points which are affected by only the k_{th} mode. In practice, this is

impossible; there will always be at least a small effect due to neighboring modes. The constants C_6, C_7, and C_8, (residual function constants) are used to compensate for these nearby modes.

After equation (77) has been fit to the experimental FRF, the modal parameters (modal frequency and damping) are determined by solving for the roots of the polynomial defined by the coefficients C_3, C_4, and C_5. Partial fraction expansion is then used to determine the components of the modal residue, a_1 and a_2. The constants may be substituted back into equation (77) to synthesize a FRF which can be compared with the experimental FRF. This comparison gives an idea of the accuracy of the curve fit procedure. The residual function constants are not saved for subsequent analysis; they are used only for this comparison.

The MDOF polyfit formulation is similar to the SDOF method. The difference is that the contributions of several modes are estimated simultaneously. From equations (76) and (77) an MDOF polyfit function could be written:

$$(h_{ij}(i\omega))_{k=P}^{P+n} = \sum_{k=P}^{P+n} \frac{C_1^k s + C_2^k}{C_3^k s^2 + C_4^k s + C_5^k} + \sum_{i=1}^{m} C_i \, s^i \Big|_{s=i\omega} \qquad [78]$$

where: p is the first mode in the frequency range, n is the number of consecutive modes to be fit simultaneously, m is the number of out-of-band modes to be accounted for, and C_i are the out-of-band residual coefficients. A set of constants, $C_1{}^k$ to $C_5{}^k$, would be identified for each mode. From these sets of

constants the modal residue could be calculated for each mode in the frequency range. Up to 10 modes may be simultaneously fit using the Modal 3.0 MDOF algorithm.

2.4.4 Autofitting

Every mode must be curve fit for every FRF measurement. For an n DOF modal model with m modes in the frequency range of interest, (n x m) modal residues must be determined. This could be accomplished with (n x m) SDOF curve fits if the modes were not closely coupled. If it was necessary to perform each of these curve fits manually, it would take a very long time. Modal 3.0 uses an AUTOmatic FIT (autofit) to fit the bulk of the measurements.

Each mode must be fit manually for a single measurement; the remainder of the curve fits are then done using the autofit procedure. The first step of the entire curve fit procedure is a visual survey of a number of the FRFs. The objective of this survey is to determine the number of modes and their nature, lightly or heavily coupled. An initial curve fit must be performed on each mode. This is done by choosing a frequency range which encloses the mode or modes, and choosing a curve fit procedure (SDOF or MDOF). This process causes the creation of an AUTOFIT table which records the frequency band and type of curve

fit used for each mode. An AUTOFIT command then fits every mode for every measurement using the frequency bands and curve fit methods defined in the autofit table.

2.5 Residue Sorting

The last step is modal sorting. This procedure converts the residue matrix into the modal matrix. For single reference modal analysis, curvefitting transforms a single column or row of the FRF matrix into a single column or row of the residue matrices, $[A_k]$; k=1,2,...n. A residue matrix will exist for each pole p_k, and each residue matrix will generate a modal vector (column of the modal matrix). From equation (49):

$$[A_k] = q_k \, \underset{\sim}{u}_k^T \underset{\sim}{u}_k \qquad [79]$$

A diagonal element of the residual matrix may therefore be defined as follows:

$$A_k(i,i) = q_k \, u_k(i) \, u_k(i) \qquad [80]$$

and a single element of the modal vector may be defined:

$$u_k(i) = \sqrt{A_k(i,i)/q_k} \qquad [81]$$

Any diagonal element, $A_k(i,i)$, of the residual matrix may be used as a starting point (driving point) for mode shape determination. All of the other elements of the modal vector are defined in terms of the driving point element. From equation (79) a general element of the residual matrix is given in index notation by:

$$A_k(i,j) = q_k \, u_k(i) \, u_k(j) \qquad [82]$$

A general element of the mode shape is therefore given by:

$$u_k(j) = \frac{A_k(j,i)}{\sqrt{A_k(i,i) \, q_k}} \qquad [83]$$

Using equation (83) and varying j from 1 to n, the k_{th} mode shape is determined from a single column of the k_{th} residual matrix $[A_k]$.

The equations developed above hold for an impact modal test. In order to determine the entire modal matrix a single column of the residual matrix corresponding to each mode must be known. The sorting of a random modal test will yield slightly different equations, however, the procedure is analogous.

The modal matrix, in terms of the modal vectors, the mode shapes, is given by:

$$[\Phi] = [\, \underset{\sim}{u}_1 \;\; \underset{\sim}{u}_2 \;\; \underset{\sim}{u}_3 \;\; \cdots \;\; \underset{\sim}{u}_n \,]_{n \times m} \qquad [84]$$

From equation (83) each modal vector is given by:

$$\underset{\sim}{u}_k = \frac{1}{\sqrt{q_k}} \begin{Bmatrix} A_k(1,i)/\sqrt{A_k(i,i)} \\ A_k(2,i)/\sqrt{A_k(i,i)} \\ \vdots \\ A_k(n,i)/\sqrt{A_k(i,i)} \end{Bmatrix} \qquad [85]$$

Index n is the number of DOFs of the system, and i is the DOF at which the system was excited.

The scaling coefficient (q_k) is determined based on the type of scaling desired; the scaling procedure uniquely defines the modal matrix. Modal 3.0 allows several scaling options which are chosen with the sort command. The most common scaling procedure is scaling to modal masses. Reiterating equations (27 and 28), the modal mass criterion requires that:

$$[\Phi]^T[M][\Phi] = [\searrow I] \qquad [86]$$

Equation (86) is satisfied if the scaling constant is defined as:

$$q_k = \frac{1}{\omega_k} \qquad [87]$$

Equation (88) is derived from equations (85) and (87), and defines the general equation of the mass normalized mode shape:

$$\underset{\sim}{u}_k = \sqrt{\omega_k} \begin{Bmatrix} A_k(1,i)/\sqrt{A_k(i,i)} \\ A_k(2,i)/\sqrt{A_k(i,i)} \\ \vdots \\ A_k(n,i)/\sqrt{A_k(i,i)} \end{Bmatrix} \qquad [88]$$

3. Modal Analysis Using NASTRAN

As discussed briefly in chapter 1, the Finite Element Method may be used to model the dynamic characteristics of complex structures. One of the most popular commercial codes (MSC/NASTRAN) has many dynamic analysis capabilities. The modal analysis capability was used to determine the real modes of a Winchester hard disk drive.

The NASTRAN program consists of several 100 thousand lines of FORTRAN code. The user accesses the power of NASTRAN through the user written data set. The data set is used to define the structure, and to choose from the many analysis options available within NASTRAN.

3.1 NASTRAN Data Set Structure

The data set is broken into functionally separate blocks called "decks". The term deck has survived from the days of the old computer systems which required computer card input. Similarly, each line of the data deck is referred to as a "card". The three decks are the Executive Control Deck, the Case Control Deck, and the Bulk Data Deck. They have a prescribed order, as referenced above, and the transition between decks is indicated by specific cards. The data set features which are required for

modal analysis will be described here. For further information on NASTRAN, see the NASTRAN Handbooks published by the MacNeal Schwendler Corporation.

3.1.1 Executive Control Deck

The first deck is the Executive Control Deck. It controls some interactions with the host computer system, and also controls the outline of the analysis procedure. The first card in every Exec Deck is the ID card. This card allows for an identifying title for the particular analysis run.

ex: ID MGThurston, Disk Drive

NASTRAN is essentially a matrix manipulating program, consisting of many subroutines. In the early days, much of the subroutine control was performed manually from the Exec Deck. Now, rigid formats exist to control the entire analysis procedure for nearly any type of problem. Therefore, instead of being required to know all of the subroutines necessary to solve a problem and listing them in the Exec Deck, a rigid solution format may be chosen with a single card.

Modal analysis is performed by rigid formats SOL 3, and SOL 29. SOL 3 is a normal modes solution format, while SOL 29 may be used for complex modes. The rigid format is indicated by the SOL card:

ex: SOL 3 or SOL MODES

An optional card which is recommended, especially for beginning users, is the TIME card. This card limits the maximum number of CPU minutes allotted to the solution process. This prevents inefficient models from wasting large amounts of CPU time and is also a check for data set errors which might cause the job to run for a very long time if not aborted. The format of the time card is:

TIME 10

where 10 is the number of CPU minutes allotted to the solution procedure. The last card in every Exec Deck is the CEND card. This card signifies the transition between Exec and Case Control Decks.

3.1.2 Case Control Deck

The Case Control is used to select items from the Bulk Data Deck by set ID, thereby defining solution subcases. If several different analyses falling under the same solution sequence are required of the same structure, a large number of the required calculations are repetitive. The Case Control may be used to define multiple subcases such that the repetitive calculations need be made only once. For large problems this may result in a significant time savings.

MSC/NASTRAN also has plot routines which may be accessed by cards placed at the end of the Case Control deck. An external post processing program was used in the disk drive analysis instead of NASTRAN, therefore this feature will not be discussed.

The cards that are likely to show up in the case control deck for a modal solution sequence are: SPC, DYNRED, METHOD, and DISPLACEMENT. The SPC card identifies single point constraint sets which are generally structural displacement boundary conditions. The set IDs (SIDs) referenced on the SPC card are from Bulk data SPC or SPC1 cards. The format is:

SPC=SID#1,SID#2,...

The DYNRED card chooses a dynamic reduction method from the Bulk Data DYNRED cards.

DYNRED=SID

The METHOD card chooses from the real eigenvalue extraction methods defined on Bulk Data EIGR cards.

METHOD=SID

The DISPLACEMENT card chooses the output option for displacement output, and the set of grids for which displacement results will be output.

$$\text{DISPL(options)} = \begin{matrix} \text{ALL} \\ n \\ \text{NONE} \end{matrix}$$

Three possibilities exist for the displacement grid set: all of the grids, none of the grids, or the set (n) of grids. The (n) set is defined on the Case Control SET card:

ex: SET n=1 THRU 10,20,30,40 THRU 60

The subcase card (SUBCASE n) is used to define the different problem subcases. Each subcase may have one SPC, DYNRED, METHOD, and DISPL card. If that card is not included, the subcase will use a previously defined default if available. The TITLE and SUBTITLE cards give titles for the solution run (they are the same for all subcases). A LABEL card may be included within the subcase for a unique subcase label.

3.1.3 Bulk Data Deck

The BEGIN BULK card signifies the end of the Case Control Deck, and and the beginning of the Bulk Data Deck. The ENDDATA card follows the Bulk Data, and is the last card in the data set.

The Bulk Data Deck contains the meat of the NASTRAN model; structural geometry, element and material properties, boundary conditions, applied loads, and processing options are defined in this deck. For modal analysis, the Bulk Data also defines dynamic reduction techniques, eigenvalue extraction methods, and partitioning of DOFs. These features will be discussed in detail later.

A special type of card found in the Bulk Data is the PARAM card. There are a large number of different PARAM cards which allow the request of special processing features. Three PARAM cards which are useful for modal analysis are: COUPMASS, GRDPNT, and AUTOSPC.

The AUTOSPC parameter is used to automatically constrain degrees of freedom with very low or zero stiffness. A very low stiffness term may cause ill-conditioning and therefore inaccurate solutions, while a zero stiffness term will cause solution failure due to matrix singularity. AUTOSPC causes these DOFs to be searched out, and single point constraints are applied to the offending DOFs. Care must be taken in using AUTOSPC, such a low stiffness may indicate a modeling error which should be corrected. The AUTOSPC feature may be turned on by the following card:

```
PARAM,AUTOSPC,YES
```

The COUPMASS parameter may be used to create coupled element mass matrices. The default option creates diagonal (lumped) mass matrices by lumping the element mass evenly at the element grid points. COUPMASS creates a much more realistic mass distribution resulting in non-diagonal mass matrices which couple the grid points of the element. The COUPMASS option is invoked by the following card:

```
PARAM,COUPMASS,1
```

The effect of using COUPMASS is a more accurate solution, but at a higher computer time cost. The cost will be particularly higher if the generalized dynamic reduction method is also used.

The third parameter, GRDPNT, may be used to invoke the grid point weight generator. The GRDPNT card is applied as follows:

PARAM,GRDPNT,n (n >= 0)

where n is the number of the grid point to be used as a reference point. If n is zero, or an undefined grid point, the basic (global) coordinate system is used as the reference. The following information will be calculated: the rigid body mass matrix, the transformation matrix from basic coordinates to principal mass axes, mass and center of gravity relative to the mass axes, the inertia matrix about the center of gravity (relative to the principal mass axes), the same inertia matrix (relative to the principal inertia axes), and the transformation matrix from principal mass to principal inertia axes.

3.2 NASTRAN Model Building Blocks

The geometric model is the most important part of the data set. The challenge is to accurately represent the properties of a continuous physical structure with a combination of finite elements. The elements are the most important model building blocks, however all elements are built around grids (the most basic building blocks).

3.2.1 Grid Points

A grid point in NASTRAN is a point in space with 6 independent degrees of freedom; 3 orthogonal translational and 3 orthogonal rotational DOFs. The only property of a grid is its location in space. In order for that location to be defined a coordinate system must first be defined.

The NASTRAN default coordinate system is the rectangular Basic Coordinate System. A grid point is located in the Basic Coordinate System by its X, Y, and Z coordinates. Alternate coordinate systems may be defined relative to the Basic System. Rectangular systems are defined using the CORD1R or CORD2R cards. Similarly, cylindrical systems may be defined with the CORD1C or CORD2C cards, and spherical systems with CORD1S or CORD2S. The two different card formats for each type of coordinate system allow different methods of definition. Each coordinate system has a unique CID (coordinate system ID), and each coordinate system is defined relative to a uniquely defined system which trees back to the Basic System (Basic CID=0).

Grid points are defined with the GRID card (see A-1)*. Each grid has a unique GID (grid ID) which is defined on the grid card. In addition to the GID, the following information is required on the GRID card: CID of defining coordinate system,

* A-1 refers to page 1 of Appendix A located at the end of this thesis

three coordinates to define the grid location, CID for grid displacement output, and any permanent grid point constraints.

3.2.2 Grid Point Constraints

Grid DOFs may have to be constrained for several reasons, one reason being the physical constraint of the structure. Structural boundary conditions arise due to physical mounting or symmetric simplification of a structure. A second factor which may necessitate the constraint of a DOF is the characteristic of an element which is connected to the DOF. Some elements have no stiffness associated with certain DOFs, they will not support a load which acts on that DOF. If these DOFs are not constrained a singular stiffness matrix will result. A third reason for DOF constraint is problem simplification. The dimensions of a problem may be reduced by constraining a certain DOF (or DOF set) at all of the grid points of the structure. A one or two dimensional model may often be used as an accurate estimation of a structure's properties.

There are many ways to constrain a DOF, a single point constraint method constrains a DOF relative to the Basic Coordinate System. The following Bulk Data cards may be used for

single point constraint: SPC, SPC1, GRDSET, GRID, and PARAM,AUTOSPC. The AUTOSPC method has already been discussed, and is an after the fact safety measure in case one of the other methods was mistakenly omitted.

The GRDSET card is used for eliminating a single DOF (or DOF set) from all grids at the same time. This is useful in reducing the dimensions of the problem. The DOFs of a grid may also be eliminated using the eighth field of the GRID card. If one of these two methods are used, the constraint forces will not be output.

The SPC card (see A-2) may be used to enforce a fixed displacement, or to enforce zero displacement for up to 12 DOFs (the DOFs of two grid points). The SPC1 card (see A-3) can enforce zero displacement of a DOF set for many grid points. The SPC, and SPC1 constraints have a SPC ID (SID) which must be referenced on a SPC card in the case control. Constraint forces are calculated for both of these constraint methods.

3.2.3 Elements

In finite elements, an element is a matrix equation which defines the connectivity of grid points and approximates the behavior of a geometric element. NASTRAN has three primary

families of elements: line elements, surface elements, and solid elements. In addition to the three main families, there are some additional specialty elements.

3.2.3.1 Line Elements

The family of line elements includes: rod, conrod, tube, bar, beam, and bend elements. The rod and conrod elements are pin ended elements with axial and torsional stiffness only. Their properties are constant over the length of the element. The tube is a rod element with the provision for a tubular cross section. The bend element may be used to represent a curved section of pipe, or a curved beam of arbitrary cross section. This element has extensional, bending, and torsional stiffness, and shear flexibility in two directions.

The Beam element is a sophisticated element which includes most of the advanced capabilities of beam analysis: variable cross section, offset shear center, torsional and transverse shear stiffness variations with warping, offset non-structural mass axis, and distributed torsional mass moment of inertia. The bar element is a simplification of the beam element for basic applications. The limitations of the bar element are as follows: element properties are constant over the element length, the shear center coincides with the neutral axis, and torsional stiffening due to warping is neglected.

The bar element was used in modeling the disk drive and will therefore be described in detail. The bar element is defined with the CBAR card (see A-4). Each element of the NASTRAN model has a unique EID (element ID number), and an associated property card (PBAR for the bar element). The PBAR card has a unique PID (property ID), which may be referenced on any number of bar elements.

The following input is required in order to describe the geometric characteristics of the bar element. GA and GB are the grids that define the bar end points. The vector $\underset{\sim}{V}$ must be identified in order to differentiate between planes 1 and 2 of the element (see figure 10). This is done by specifying one point on a vector through point A, and non colinear with AB. PA and PB are pin flags used for disconnecting the bar from the indicated DOFs at ends A and B respectively. Using WA and WB vectors, the neutral axis of the bar may be offset from grids GA and GB. This is particularly useful for attaching ribs to a surface or solid element, the bar may use the grids of the surface (or solid) element and have an offset neutral axis.

The structural properties of the bar are defined on the PBAR card (see A-6). The following element property input is required: material property ID number (MID), the cross sectional area (A), the area moments of inertia (I1, I2, I12 defined per figure 10), the torsional moment of inertia (J), and the non-structural mass per unit length (NSM). Stresses are computed

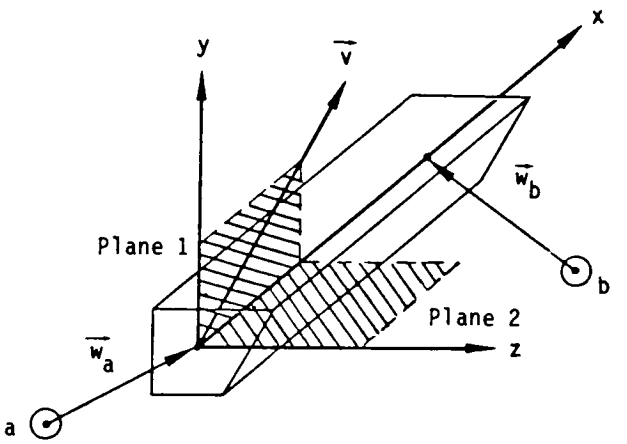

Figure 10: Bar Element Coordinate System Definition [7]

at each end of the bar, and the stress recovery coefficients allow the user to define at which point on the cross section stresses will be calculated.

3.2.3.2 Surface Elements

The family of surface elements includes the following elements: quad4, quad8, tria3, tria6, and shear. The shear element, as implied by its name, is primarily a planar shear bearing element. It supports planar shear stresses, and extensional force between adjacent grid points. For this reason it is not a general purpose shell element, it is used primarily in the analysis of thin reinforced plates or shells. In this application the reinforcing element takes the bending and extensional load, and the shear element takes the in-plane shear.

The other four elements are general purpose elements for membrane, plate and shell analyses. The quad4 and tria3 elements have only corner grids, while the quad8 and tria6 have both corner and mid-side grids (see figure 11). In general, the quad elements have better accuracy than the tria elements. The main problem with the tria elements, particularly the tria3, is that they give poor results for membrane problems. This is due to excessive stiffness in that deformation mode. Their primary purpose is for filling in voids left between quad elements due to irregular part geometries.

Name	Shape	No. of Grid Points	Connected Components(1)	Applications
SURFACE ELEMENTS				
QUAD4	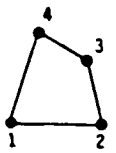	4	T,R	Membrane; plate; shell.
QUAD8	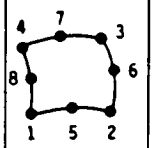	8(3)	T,R	Membrane; plate; shell.
TRIA3	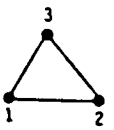	3	T,R	Membrane; plate; shell; prefer QUAD4 when practical.
TRIA6	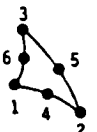	6(3)	T,R	Membrane; plate; shell; prefer QUAD8 when practical.
SHEAR	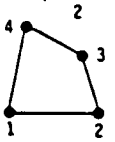	4	T	Shear panel; thin reinforced shell.

(1) T = translational components of motion; R = rotational components of motion

(3) Any or all edge points may be deleted.

Figure 11: Surface Element Table [8]

The quad8 element will yield better results than the quad4 for most problems, at nearly the same cost. For flat membranes, plates, and singly curved shells (i.e. cylinders) the quad8 has better accuracy, however for doubly curved surfaces (spheres) the quad4 is preferable.

The quad4 was used almost exclusively for modeling the computer disk drive. The NASTRAN Static Handbook has the following assessment of the quad4 element:

> The quad4 behaves well when its shape is irregular. There is no aspect ratio limit. Good results have been obtained with skew angles up to 45 degrees. The corner points are not required to lie in the same plane.[9]

The Data Deck card for the quad4 is the CQUAD4 card (see A-7). Required input on the CQUAD4 card is: EID, PID, the four grid points, the material orientation angle, and the thicknesses of the element at the grid points (if it varies). The property card for all of the quad and tria elements is the PSHELL card (see A-9). There are four surface element analysis options which may be turned on or off with the PSHELL card. Membrane effects, bending effects, transverse shear, and membrane/bending coupling are controlled by the MID1, MID2, MID3, and MID4 fields respectively. The option will be turned on if a material ID (MID) is entered in the appropriate field. If the element's cross section is symmetric (i.e. constant thickness) then MID4 should be left blank, dropping membrane/bending coupling. For

best accuracy, all of the other fields should be used. However, if the material has uniform properties in the thickness direction, the first three fields should use the same material ID. Also, in that case, the $12I/T^3$ and TS/T fields may be left blank.

The tria3 element was also used in modeling the disk drive, primarily to fill in gaps. The CTRIA3 card is the Bulk Data card for the tria3 element (see A-11). The data required for the CTRIA3 card is directly analogous to the CQUAD4, and the two elements (if the same material and thickness) can use the same PSHELL card.

3.2.3.3 Solid Elements

The third family of elements is the solid element family. The five solid elements (hexa, penta, tetra, hex20, and triax6) are shown in figure (12). No solid elements were used in modeling the disk drive, therefore they will be covered very briefly.

The hexa and penta are the best general purpose solid elements, they can even be used as "near" shell elements with good accuracy. The element property card which is used for these two is the PSOLID card. The hex20 is similar to the hexa, but isn't as useful for general purpose problems. The primary applications of the hex20 element are for crack-tip elements in

Name	Shape	No. of Grid Points	Connected Components(1)	Applications
SOLID ELEMENTS				
HEXA	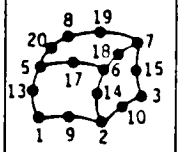	20(3)	T	Solid; thick shell.
PENTA	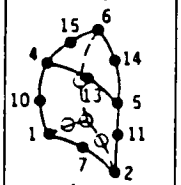	15(3)	T	Solid; thick shell; prefer HEXA when practical.
TETRA	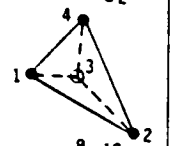	4	T	Solid; prefer HEXA or PENTA when practical.
HEX20	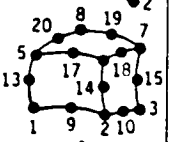	20(3)	T	Solid, crack tip element; prefer for nearly incompressible materials; isotropic material only; prefer HEXA for thick shells.
TRIAX6	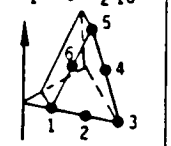	6	T	Solid of Revolution with axisymmetric loading; including orthotropic material.

(1) T = translational components of motion; R = rotational components of motion

(3) Any or all edge points may be deleted.

Figure 12: Solid Element Table [10]

fracture mechanics, or for very incompressible materials (poissons ratio approaching 0.5). The tetra solid element functions as the tria elements in plate/shell problems. It is a four grid, constant strain element which is used primarily to fill voids left between hexa and penta elements. The triax6 element models a solid of revolution using six grid points at a single cross section. This element is only good for problems with axisymmetric loading. For non-axisymmetric loading hexa or penta elements would have to be used.

3.2.3.4 Special Elements

The CONM2, RBE2 and RBE3 elements were used in modeling the disk drive. The CONM2 element was used to model the mass and inertia of rigid parts of the system, while the RBE3 element was used to distribute the effects of that mass and inertia to several grid points. "The RBE2 element defines a rigid body whose independent degrees of freedom are specified at a single grid point, and whose dependent degrees of freedom are specified at an arbitrary number of grid points."[11]

The CONM2 element allows mass and inertia to be applied at a grid point. This allows the properties of a rigid part of the structure to be added to the dynamics of the overall structure without a large amount of modeling. The CONM2 card (see A-12)

requires the following input: unique EID, GID that mass is applied to, coordinate ID for center of gravity input, center of gravity offset from GID, and mass and inertia terms.

The RBE3 element defines a constraint relation in which the motion at a single dependent grid point is the least square weighted average of the motions at a set of other independent grid points. The main use of the RBE3 is to distribute loads, masses, and inertias from a single grid point to a collection of grid points. The RBE3 card (see A-14) requires the following input: EID, the ID of the dependent grid (REFGRID), the DOFs of REFGRID which are to have their values computed (REFC), and the grid IDs, DOFs, and weighting factors for the independent grids.

The RBE2 card defines a constraint relation in which the motion of a dependent set of grid points is equivalent to the motion of a single independent grid point. One use of the RBE2 element is connection of an elastic structure to a single grid point of a rigid structure. The RBE2 card (see A-16) requires the following input: EID, the ID and DOFs of the independent grid, and the IDs of the dependent grids.

3.2.4 Material Properties

Element property cards define the structural characteristics of elements. The properties of the material, of which the elements are composed, are defined on MAT cards. Each element

property card references a MAT card by material ID (MID). The element mass matrices depend on the material density which is defined here, the element damping matrices depend on the structural damping coefficient, and the element stiffness matrices depend on the elastic moduli.

Five material types are available with NASTRAN: isotropic material, two-dimensional anisotropic material, axisymmetric solid orthotropic material, and three-dimensional anisotropic material. The material types are defined with the MAT1, MAT2, MAT3, MAT8, and MAT9 cards respectively. The difference between the different material types is the complexity of the definition of the elastic moduli. Any of the material properties defined on the material card may be made into functions of temperature using the MATTi cards (where "i" is the trailing integer from the associated MAT card).

All of the materials used in modeling the computer disk drive were assumed to be isotropic. Therefore, the only material card that was used is the MAT1 card (see A-17). For an isotropic material, the properties do not vary in any direction. Assuming no temperature dependence, the shear moduli are constant. The MAT1 card requires input of 2 of the following properties: modulus of elasticity (E), poissons ratio (ν), and the shear modulus (G). The third property is calculated from the following formula:

$$G = E/2(1+\nu) \qquad [89]$$

For line elements, E is used as the modulus for extension and bending, and G is used as the modulus for torsion and transverse shear.

In addition to the material properties listed above, the following input is required for the MAT1 card: a unique MID, material mass density, thermal expansion coefficient, thermal expansion reference temperature, structural element damping coefficient, tension, compression, and shear stress limits (for factor of safety calculation), and material coordinate system ID (if required).

3.3 NASTRAN Model Generation

A NASTRAN model can be generated piece by piece using the bulk data cards defined in the last chapter. For very simple models which can be easily sketched out by hand this is practical. As the number of grids and elements increases this becomes increasingly more difficult. Keeping track of grid IDs, element IDs, element attachment, and other important parameters becomes very cumbersome.

There are many programs available which offer simplified model creation (pre-processing), and analysis of results (post-processing). MSC/NASTRAN offers a pre-processing program, MSG MESH, which is integrated into the NASTRAN data set. This program allows systematic model creation by regions, but still

requires considerable user bookkeeping for large models. There is a large family of convenient computer graphic based post-processors, one of these programs (PATRAN-G) was used to simplify modeling of the disk drive.

PATRAN-G is a real-time graphic pre and post-processor. A geometric model is created through a set of interactive commands and graphically displayed for the user. The geometric model has geometric entities which are analogous to the NASTRAN grids and elements: nodes correspond to grids, lines to line elements, patches to surfaces, and hyperpatches to solids. Once the geometry is satisfactorily defined, the geometric entities are transformed into elements. PATRAN also allows the definition of loading cases, SPC cases, element properties, and material properties. Nearly any standard bulk data element may be produced. It is also fairly easy to make after the fact changes to the geometry of the structure.

After the model is completed using PATRAN, a translator program is used to convert the binary PATRAN database into a NASTRAN Bulk Data file. The Bulk Data cards which could not be created by PATRAN may then be manually inserted into the Bulk Data Deck. The Executive and Case Control Decks must also be appended to the Bulk Data.

After the NASTRAN analysis, the NASTRAN results file may be translated into subcase files readable by PATRAN for graphic post-processing. In this manner the results may be easily manipulated for plotting purposes.

3.4 Modal Analysis Using NASTRAN

3.4.1 Reduction Methods.

Eigenvalue extraction is a costly solution procedure due to the large number of required matrix manipulations. Depending on the eigenvalue extraction method, the number of DOFs, and the number of eigenvalues and eigenvectors desired, it may be necessary to reduce the size of the problem. Arbitrary manual elimination of DOFs may adversely effect the solution accuracy, therefore systematic reduction methods have been developed.

3.4.1.1 Guyan Reduction

Guyan reduction, also known as static condensation, reduces the degrees of freedom of the problem such that the static characteristics of the structure are preserved. If $\underset{\sim}{X}_f$ is the displacement vector including all of the DOFs of the original problem, it may be partitioned into two sets: the a-set is the set of DOFs to be used in the solution process, the o-set is the

set of DOFs which are eliminated before the solution step and will be recovered after the solution procedure is completed. The original equations of motion, equation (1), may be partitioned into a and o-sets as follows:

$$\begin{bmatrix} M_{aa} & M_{ao} \\ M_{oa} & M_{oo} \end{bmatrix} \begin{Bmatrix} \ddot{X}_a \\ \ddot{X}_o \end{Bmatrix} + \begin{bmatrix} C_{aa} & C_{ao} \\ C_{oa} & C_{oo} \end{bmatrix} \begin{Bmatrix} \dot{X}_a \\ \dot{X}_o \end{Bmatrix} + \begin{bmatrix} K_{aa} & K_{ao} \\ K_{oa} & K_{oo} \end{bmatrix} \begin{Bmatrix} X_a \\ X_o \end{Bmatrix} = \begin{Bmatrix} F_a \\ F_o \end{Bmatrix} \quad [90]$$

The lower partitioned equation, after rearranging terms, may be written:

$$\underset{\sim}{X}_o = -[K_{oo}]^{-1}[K_{oa}]\ \underset{\sim}{X}_a + \underset{\sim}{\bar{F}} \quad [91]$$

where: $\underset{\sim}{\bar{F}} = \underset{\sim}{F}_o - [M_{oa}]\underset{\sim}{\ddot{X}}_a - [M_{oo}]\underset{\sim}{\ddot{X}}_o - [C_{oa}]\underset{\sim}{\dot{X}}_a - [C_{oo}]\underset{\sim}{\dot{X}}_o$

For static analysis, equation (91) can be substituted directly into equation (90) to eliminate the o-set DOFs because all of the o-set terms on the right hand side of equation (91) drop out. However, for dynamic analysis, the time derivatives of $\underset{\sim}{X}_o$ do not drop out of the right side of equation (91). Therefore, direct substitution does not eliminate the o-set DOFs from equation (90). In order to get around this difficulty, NASTRAN ignores the entire $\underset{\sim}{\bar{F}}$ vector yielding the following simplification of equation (91)[12]:

$$\underset{\sim}{X}_o = [G_{oa}]\underset{\sim}{X}_a \quad [92]$$

where:

$$[G_{oa}] = -[K_{oo}]^{-1}[K_{oa}] \quad [93]$$

In this fashion, the dynamic properties of the o-set are ignored while the static properties are maintained. The transformation that is used to eliminate the o-set is given by:

$$\underset{\sim}{X}_f = \begin{Bmatrix} \underset{\sim}{X}_a \\ \underset{\sim}{X}_o \end{Bmatrix} = \begin{bmatrix} \underset{=}{I} \\ \underset{=}{G}_{oa} \end{bmatrix} \underset{\sim}{X}_a \qquad [94]$$

Equation (94) is substituted into equation (90), reducing the vibration problem to a-set DOFs only. After the solution of the problem is found in terms of the a-set DOFs, the solution for the o-set is recovered using equation (92).

As applied by NASTRAN, the Guyan reduction method requires that the user define the a and o-sets manually. The a-set is defined using the ASET or ASET1 bulk data cards (see A-19,20), the remaining DOFs are put in the o-set. Guyan reduction is automatically invoked with the inclusion of the ASET or ASET1 cards.

The accuracy of the results obtained after using Guyan reduction depends on both the number and distribution of a-set DOFs. The following rules of thumb are suggested for choosing a-set DOFs:[13]

(1) put points with large masses in the a-set, (2) distribute all other a-set points uniformly over the structure. Also, experience has shown that in plate problems it is better to have the a-set consist of all of

the active degrees of freedom (rotations as well as translations) at a few grid points rather than just the translational DOFs at a larger number of grid points.

3.4.1.2 Generalized Dynamic Reduction

Generalized dynamic reduction is a more complex reduction method which includes static condensation. In addition to static condensation, this method uses generalized coordinates to partially account for the inertia effects of the o-set which were ignored in Guyan reduction when the $\underset{\sim}{F}$ vector was neglected. The f-set is again partitioned into the a and o-sets, however the a-set does not consist entirely of physical DOFs. Instead, the a-set consists of a set of generalized coordinates, the q-set, and the remainder of the physical coordinates the t-set. The a-set is partitioned as follows:

$$\underset{\sim}{u}_a = \begin{Bmatrix} u_q \\ \overline{u_t} \end{Bmatrix} \qquad [95]$$

In general, the o-set will be larger for this method than it was for the Guyan reduction method because the generalized coordinates eliminate the need for as many a-set physical DOFs The stiffness matrix for the f-set may also be partitioned:

$$[K_{ff}] = \left[\begin{array}{c|c|c} 0 & 0 & 0 \\ \hline 0 & K_{tt} & K_{to} \\ \hline 0 & K_{ot} & K_{oo} \end{array}\right] \qquad [96]$$

The relation between o-set and a-set DOFs is given by:

$$\underset{\sim}{u}_o = [G_{oa}]\underset{\sim}{u}_a = [G_{oq} \mid G_{ot}] \begin{Bmatrix} u_q \\ u_t \end{Bmatrix} \quad [97]$$

Therefore, the f-set may now be defined:

$$u_f = \begin{Bmatrix} u_a \\ u_o \end{Bmatrix} = \begin{Bmatrix} I \\ [G_{oa}] \end{Bmatrix} = \begin{Bmatrix} u_q \\ u_t \\ u_o \end{Bmatrix} = \begin{bmatrix} I \\ [G_{oq} \mid G_{ot}] \end{bmatrix} \quad [98]$$

The matrix G_{ot} is defined by a static condensation procedure similar to the one used to find G_{oa} in the Guyan reduction method. G_{ot} is given by:

$$[G_{ot}] = -[K_{oo}]^{-1}[K_{ot}] \quad [99]$$

The matrix G_{oq}, however, is determined from an eigenvalue extraction procedure applied to the DOFs in the t and o-sets. The inverse iteration method (see 3.4.2.3) is used to estimate the eigenvectors for the system matrix corresponding to the t and o-set DOFs. These eigenvectors are used to compute G_{oq}, for more detailed information see section 4.1.2 of the NASTRAN Dynamic Handbook.

Once G_{ot} and G_{oq} have been determined, equation 98 is used to reduce the system equations from the f-set to the a-set. The eigenvalues and eigenvectors corresponding to the a-set are determined, and the solution for the o-set DOFs is recovered using the transformation of equation (98) in reverse.

Application of Generalized Dynamic Reduction in NASTRAN requires first, the DYNRED=n card in the Case Control. This identifies the ID of the Bulk Data DYNRED card (see A-21). The most important parameter on the DYNRED card is FMAX (maximum frequency for approximate eigenvalue/eigenvector calculation). FMAX should be chosen such that all of the modes of interest are below it. If it is chosen too low, the modes of higher frequency will have poor accuracy. If it is chosen too high, the reduction procedure will be computationally expensive.

The different DOF sets also must be defined in the Bulk Data Deck. The DOFs in the q-set are scalar points, magnitude only, and therefore must be listed on SPOINT cards (see A-22). In addition the q-set points must be listed on QSET and ASET (or QSET1 and ASET1) cards (see A-19,20 and 23,24). The DOFs in the t-set must also be defined on ASET (ASET1) cards.

NASTRAN gives some guidelines for when to use a reduction method. The cost of reduction methods is not justified for small problems, they should be used only when the cost of eigenvalue extraction is very high (>200 DOFs) [14]. The NASTRAN Dynamic Handbook also provides a chart comparing the two reduction methods (see figure 13).

	Guyan Reduction	Generalized Dynamic Reduction
1. Accuracy of Vibration Modes	Fair	Excellent
2. Relative Cost	Lower if only fair accuracy of vibration modes is required	Lower if good to excellent accuracy is required
3. Skill Required For	Selection of A-set points	Selection of DYNRED parameters
4. Labor Intensive	Yes, if there are many A-set points	No
5. Troubles	Poor selection of A-set points leads to inaccurate modes.	Poor selection of DYNRED parameters leads to missing modes, erratic results, or excessive cost.
6. Diagnostic Aids	None	Sturm sequence indicates number of missing modes
7. Number of good modes	One-fourth to one-half the size of the a-set	Two-thirds the number of q-set variables used.
8. Close roots	No problems	May lose some if NIRV is too small.

Figure 13: Reduction Method Selection Chart [15]

3.4.2 Eigenvalue/Eigenvector Extraction

After the dynamic reduction method is completed, eigenvalue/eigenvector extraction may be performed on the remaining DOFs. The analysis of the disk drive was limited to real modes and therefore this discussion will also be limited to real modes. Any type of system damping, viscous or structural, will yield complex eigenvalues and eigenvectors. Therefore, for real eigenvalue analysis the damping matrix is eliminated. Many structures are lightly damped, and in these cases the real modes provide a good approximation of the structure's behavior.

The homogeneous equations of motion of the undamped system in the Laplace plane may be written from equation (9):

$$\left[[M]s^2 + [K]\right] \underset{\sim}{X}(s) = \underset{\sim}{0} \qquad [100]$$

The solution of equation (100) is non-trivial when the determinate of the system matrix is zero:

$$\left|[M]s^2 + [K]\right| = 0 \qquad [101]$$

The solution of equation (101) is a set of (s) values equal in number to the DOFs of equation (100). If the solution of equation (101) is assumed to be of the form:

$$s^2 = -\lambda_k \qquad [102]$$

The resulting eigenvalue problem (from equation 100) is:

$$\left[[K] - \lambda_k[M]\right] \underset{\sim}{U}_k = \underset{\sim}{0} \qquad [103]$$

where $\underset{\sim}{U}_k$ is the system eigenvector corresponding to the k_{th} eigenvalue. Equation (103) is the equation to be solved by the NASTRAN eigen-extraction methods, for λ_k and $\underset{\sim}{U}_k$.

3.4.2.1 Rigid Body Modes

The set of eigenvectors of a structure may include both elastic and rigid body modes. If a structure is not totally constrained from rigid body motion, the modal vectors obtained from equation (103) will include one or more (zero frequency) rigid body modes. An unconstrained structure has six linearly independent rigid body modes. These six modes could be represented by three mutually orthogonal translational modes, and three mutually orthogonal rotational modes.

The presence of rigid body modes may cause degradation of the elastic eigenvalues and/or eigenvectors which are determined by the eigen-extraction method. If the rigid body modes are determined before extraction of the elastic modes this problem is eliminated. With NASTRAN this is accomplished by use of the SUPORT card (see A-25). If a set of DOFs which are sufficient to constrain rigid body motion are defined on this card, NASTRAN will calculate the rigid body modes before beginning eigenvalue extraction.

Input to the SUPORT card consists of the grid IDs and the corresponding DOFs to be used as rigid body constraints. After calculating the rigid body modes, the SUPORT constraints will be removed from the problem for elastic eigen-extraction. If the SUPORT constraints were insufficient to constrain all of the rigid body modes, those that were unconstrained will remain in the problem and will be extracted by the eigen-extraction method.

3.4.2.2 NASTRAN's Real Eigenvalue Extraction Methods

NASTRAN has three available eigenvalue extraction methods: the Givens method, modified Givens method, and the inverse power method. The Givens and modified Givens methods are known as transformation methods. In a transformation method the dynamic matrix, $\left[[K] - \lambda_k[M]\right]$, is transformed without changing the system eigenvalues/vectors, into a special form from which eigenvalues may be more easily extracted. The inverse power method is a tracking method. This means that eigenvalues are extracted one at a time by iterative procedures applied to the original dynamic matrix.

The Givens and modified Givens methods are very similar with respect to cost and the amount of user input required. One requirement of the Givens method is a positive definite mass matrix. This method will fail if the mass matrix is singular. The modified Givens method overcomes this difficulty and will

solve these types of problems. The Givens method, when it can be used, is quickest for small problems. If the mass matrix is sparse (nearly diagonal) the cost of the Givens method is roughly half that of the modified Givens. However, if a reduction method is used the mass matrix will become dense, and both methods will be of comparable cost.

Both the standard and modified Givens methods will find all of the eigenvalues of a system, it is not possible to skip over any.[16] In addition, rigid body modes which were not removed by a SUPORT card will not affect the eigenvalues of the elastic modes. However, inaccurate rigid body modes will effect the accuracy of the elastic eigenvectors due to the orthogonalization procedure performed on the entire modal matrix.

The standard inverse power method is less reliable than the two transformation methods: it converges slowly, may miss closely spaced roots, and the accuracy deteriorates with higher roots if many roots are required. The shifting procedure employed by the NASTRAN power method minimizes these problems. The shifted inverse power method, however, requires more user input and is more sensitive to the required input parameters than the Givens methods.

The inverse method is best suited to sparse matrices, particularly if only a few eigenvalues are desired. One important application is the refinement of eigenvalues and eigenvectors which have already been determined by one of the

other methods. The inverse method should provide a more accurate result than the other methods once the approximate location of the eigenvalue is determined.

Figure (14) shows an extraction method selection chart based on the analysis of a square plate with 5 DOFs per grid point (N is the number of DOFs in the problem, E is the number of eigenvalues required). For very large problems, the combination of a reduction method and one of the Givens methods is preferable to the inverse power method. However, the inverse power method may be preferable due to better accuracy and lower cost if the number of required eigenvalues is small. For problems with under 100 DOFs, the Givens methods are preferable.

The EIGR card (see A-26) is the Bulk Data card used to select the extraction method. The first field is the EIGR set ID, which must be referenced on the Case Control METHOD card. The second field is the method to be used: INV, GIV, MGIV. For the GIV and MGIV methods, the following input is required: either F1 and F2 or ND, and a scaling option (MASS, MAX, or POINT). ND is the number of eigenvectors to be calculated, while F1 and F2 define a frequency range between which eigenvectors will be calculated. Only one of these two eigenvector range specification methods should be used, if both are specified ND will take precedence. For the inverse method, F1 and F2 indicate the range in which to look for eigenvalues/vectors, and NE the number of eigenvectors that are expected in that range. NE is

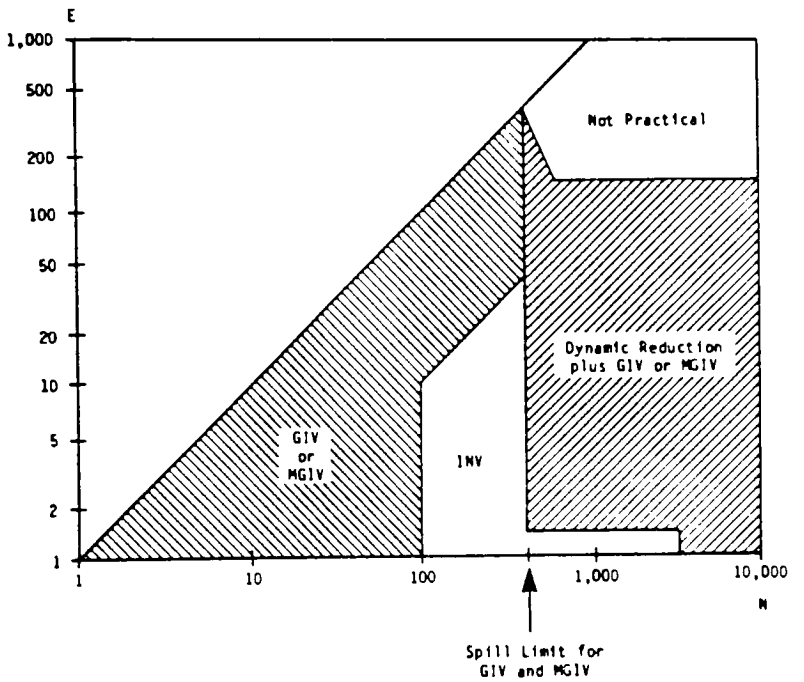

Figure 14: Extraction Method Selection Chart [17]

very important, because it determines the number of shift points to be used (see section 3.5.2.3), 1 shift point per 6 modes. If this estimate is too low, convergence will be very slow. ND is the number of modes to be calculated; the extraction method will stop when it reaches ND modes. The E parameter should be left blank because the default has been found to be sufficient in all cases.[16]

3.4.2.2.1 Givens Method

The first step in the Givens method is determination of the lower triangular matrix [L] through a Cholesky decomposition of the mass matrix:

$$[M] = [L][L]^T \qquad [104]$$

At this point the method will fail if the mass matrix is not positive definite. Equation (105) may be obtained from equation (103) by premultiplying by the inverse of [L], and substituting from equation (104) for [M]:

$$[L]^{-1}[K]\underset{\sim}{u}_k - \lambda_k[L]^{-1}[L][L]^T\underset{\sim}{u}_k = 0 \qquad [105]$$

Equation (105) is of the standard form:

$$\left[[J] - \lambda_k[I]\right] \underset{\sim}{w}_k = \underset{\sim}{0} \qquad [106]$$

where:

$$[J] = [L]^{-1}[K][L]^{-1,T} \quad [107]$$

$$\underset{\sim}{w}_k = [L]^T \underset{\sim}{u}_k \quad [108]$$

The J matrix is converted into a tridiagonal matrix using a procedure developed by Wallace Givens, and the eigenvalues are extracted directly from the tridiagonal matrix. Eigenvectors are determined, within the specified frequency range, by substituting the eigenvalues back into equation (106) and solving for the $\underset{\sim}{w}$ vector. The eigenvector is then determined from the inverse of the transformation defined in equation (108):

$$\underset{\sim}{u}_k = [L]^{T,-1} \underset{\sim}{w}_k \quad [109]$$

3.4.2.2.2 Modified Givens Method

Equation (103) may be alternately written:

$$\left[[K] + \lambda_k[M]\right]\underset{\sim}{u}_k = \left[[K] + \lambda_s[M] - (\lambda+\lambda_s)[M]\right]\underset{\sim}{u}_k = \underset{\sim}{0} \quad [110]$$

where λ_s is a positive number automatically selected by the solution algorithm. The following Cholesky decomposition is performed:

$$\left[[K] + \lambda_s[M]\right] = [L][L]^T \quad [111]$$

Substituting from equation (111) into equation (110) and rearranging terms yields equation (112).

$$\frac{-1}{\lambda_k + \lambda_s}\left[-(\lambda_k-\lambda_s)[M] + [K] + \lambda_s[M]\right]\underset{\sim}{u}_k$$

$$= \left[[M] - \frac{[L][L]^T}{(\lambda_k-\lambda_s)}\right]\underset{\sim}{u}_k = \underset{\sim}{0} \qquad [112]$$

Define $\underset{\sim}{w}$ by equation 113:

$$\underset{\sim}{\bar{w}} = [L]^T\underset{\sim}{u}_k \qquad [113]$$

Equation (114) results from substituting equation (113) into equation (112), and premultiplying by $[L]^{-1}$:

$$\left[[\bar{J}] - \bar{\lambda}_k[I]\right]\underset{\sim}{\bar{w}}_k = \underset{\sim}{0} \qquad [114]$$

Where:

$$[\bar{J}] = [L]^{-1}[M][L]^{-1,T} \qquad [115]$$

$$\bar{\lambda}_k = \frac{1}{(\lambda_k+\lambda_s)} \qquad [116]$$

Equation (114) is of the same form as equation (106), and the rest of the solution procedure is analogous to the Givens method described in the previous section.

3.4.2.2.3 Inverse Power Method with Shifting

Given the eigenvalue problem of equation (103), let:

$$\lambda_k = \lambda_0 + \Lambda_k \qquad [117]$$

where λ_0 is called the shift point. The iteration algorithm is given by equation (118):

$$\left[[K] - \lambda_0[M]\right] \underset{\sim}{w}_n = [M] \underset{\sim}{u}_{n-1} \qquad [118]$$

A starting vector for $\underset{\sim}{u}_{n-1}$ and the shift point λ_0 are chosen automatically. The shift points are selected so that only a few nearby eigenvalues (nominally 6) are extracted from each shift point, otherwise the convergence rate becomes very slow. Substituting the shift point and starting vector into equation (118) yields an initial estimate for the vector $\underset{\sim}{w}_n$. Equation (118) performs max element scaling on $\underset{\sim}{w}_n$ (C_n=largest element of $\underset{\sim}{w}_n$).

$$\underset{\sim}{u}_n = \frac{1}{C_n} \underset{\sim}{w}_n \qquad [119]$$

The eigenvector estimate (u_n) is substituted into equation (116) as u_{n-1}, and the iteration procedure continues.

The scale factor of equation (119), $1/C_n$, converges to Λ_1 from which the eigenvalue λ_1 may be defined. The vector $\underset{\sim}{u}_n$ converges to the corresponding eigenvector. After λ_1 and the associated eigenvector is determined, the effect of the first mode is eliminated from the system of equations through modification of the dynamic matrix. The iteration then continues until all of the eigenvalues and eigenvectors (nominally six sets) are found for the given shift point. A new shift point is then chosen by the program and another set of eigenvalues determined for that shift point.

4. Winchester Disk Drive Analysis

4.1 Disk Drive Vibration Problem Background

The disk drive which was analyzed is a Winchester type hard disk drive. This type of drive could be used as the primary hard drive for a personal computer, or for add on memory in an external unit. Figure (15) shows a top view of the assembled unit and figure (16) shows a bottom view with the bottom cover removed. The major components are labeled in the two figures: main housing, bottom cover, drive motor, read head support arms and magnet. The disks were not included in the study.

In operation these drives are subject to two families of vibration inputs. One type of input is shock loading due to sharply moving or dropping the host unit. The second type of input is continuous vibration transmitted from nearby sources. System printers, the processing unit cooling fan, and the disk drive motors are a few of the many sources of continuous vibration. Hard drives offer much better performance than floppy drives with respect to storage volume and retrieval speed. However, they are much more sensitive to vibration than floppy drives.[19] Impacting between the read heads and disk may cause loss of stored information, failure of a read/write procedure, or in extreme cases permanent head or media damage.

The shock problem may be addressed by mounting the drive

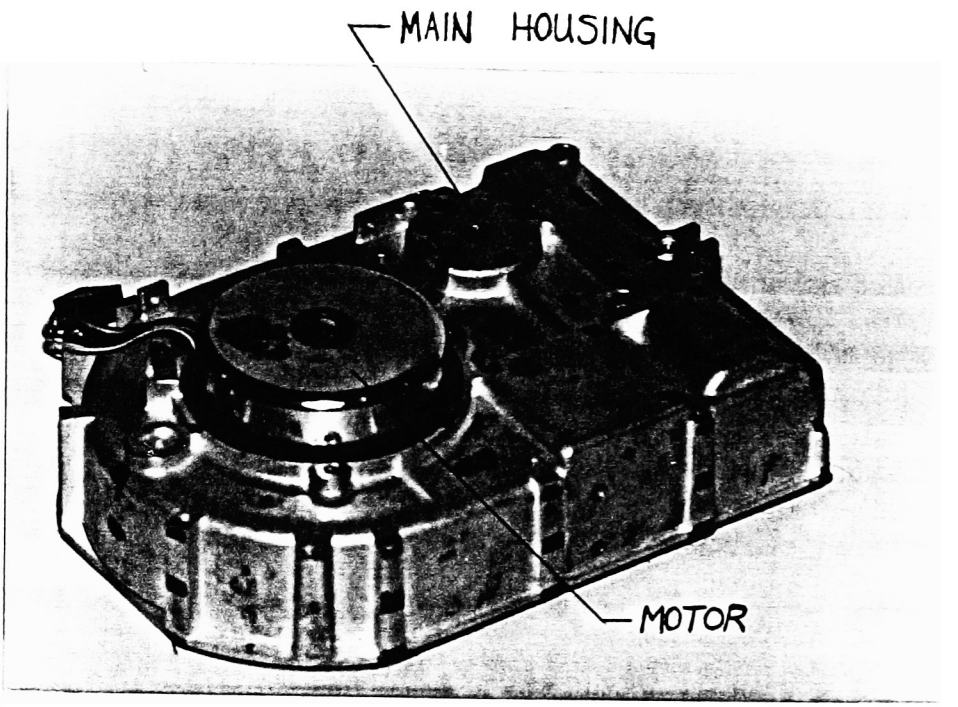

Figure 15: Assembled Disk Drive

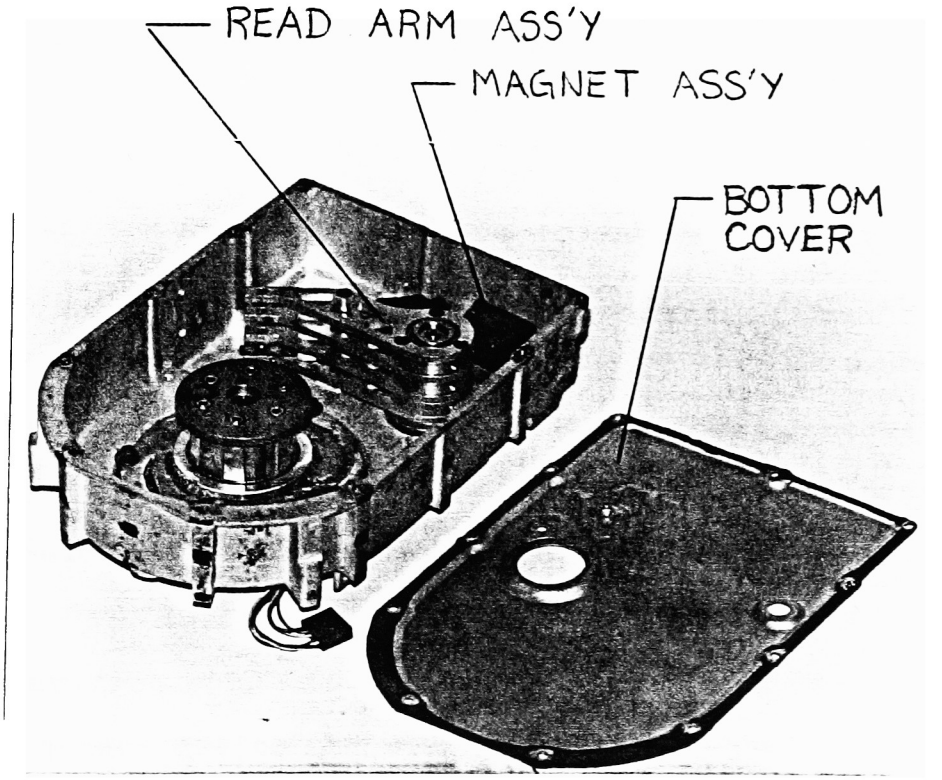

Figure 16: Bottom View of Disk Drive with Bottom Cover Removed

such that shock pulses are not fully transmitted to the drive. Shock mounts may also be useful for isolating the drive from continuous vibration. It is this continuous vibration, often harmonic in nature, which may excite a structural resonance of the disk drive assembly. Any motor operational frequencies (hard drive motor, floppy drive motors, fan motors) will have some first order (operating frequency) vibration due to unbalance. The first order excitation frequency is defined by equation (120):

$$freq_{(1^{st}\ Order)} = \frac{(rpm)}{60} \quad (hz) \qquad [120]$$

In addition, the following higher orders of vibration (operating speed harmonics) may be transmitted from the vibration sources:

$$freq_{(n^{th}\ Order)} = \frac{n(rpm)}{60} \quad (hz) \qquad [121]$$

In general, the vibration amplitude will decrease significantly with the order, assuming a similar level of power input at each frequency. Some possible sources of higher frequency vibration are fan blades, and bad bearings. Rotational speeds for Winchester type drives may be as high as 36000rpm, this operating speed would yield the following harmonics:

$$f_n = 600, 1200, 1800, 2400, 3000, \ldots \ (hz) \qquad [122]$$

The first order frequency (600hz) would probably be the primary excitation frequency due to the disk drive motor unbalance.

Ideally, the vibration signature of the rotating components

would be known early in the design process. If this was the case, the disk drive could be designed from the start such that there are no structural resonances in the range of the strong sources of excitation. In addition, the mounting configuration could be chosen such that vibration transmission through the mounting points is minimized.

Minimizing the relative motion between the read heads and the disk hub is critical from a performance standpoint. Vibration of the rest of the disk drive structure may cause high transmitted noise levels and therefore should also be minimized.

4.2 Component Models

The disk drive was broken down into components for modeling and model validation convenience. Item 1 is the main housing, item 2 the bottom plate, item 3 the read arms, item 4 the motor assembly, and item 5 is the magnet and backing plate.

4.2.1 NASTRAN Component Modeling Assumptions

The NASTRAN model for item 1 (figure 17) is composed entirely of QUAD4 and a few TRIA3 elements. Once the part dimensions were measured, the modeling was straightforward (see appendix B for the bulk data). Likewise, the item 2 model (figure 18) is composed entirely of QUAD4 and TRIA3 elements.

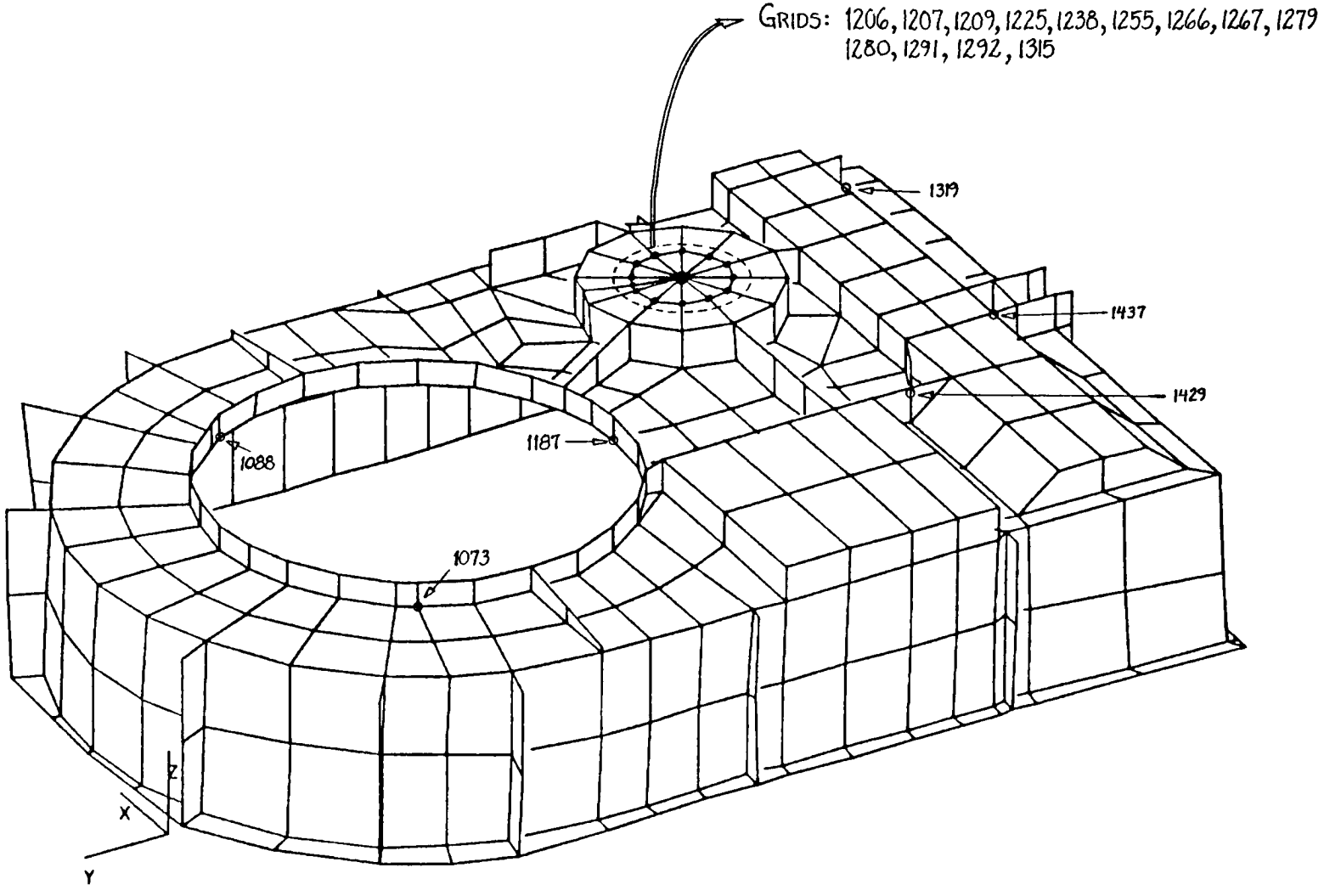

Figure 17: Item 1 NASTRAN Model

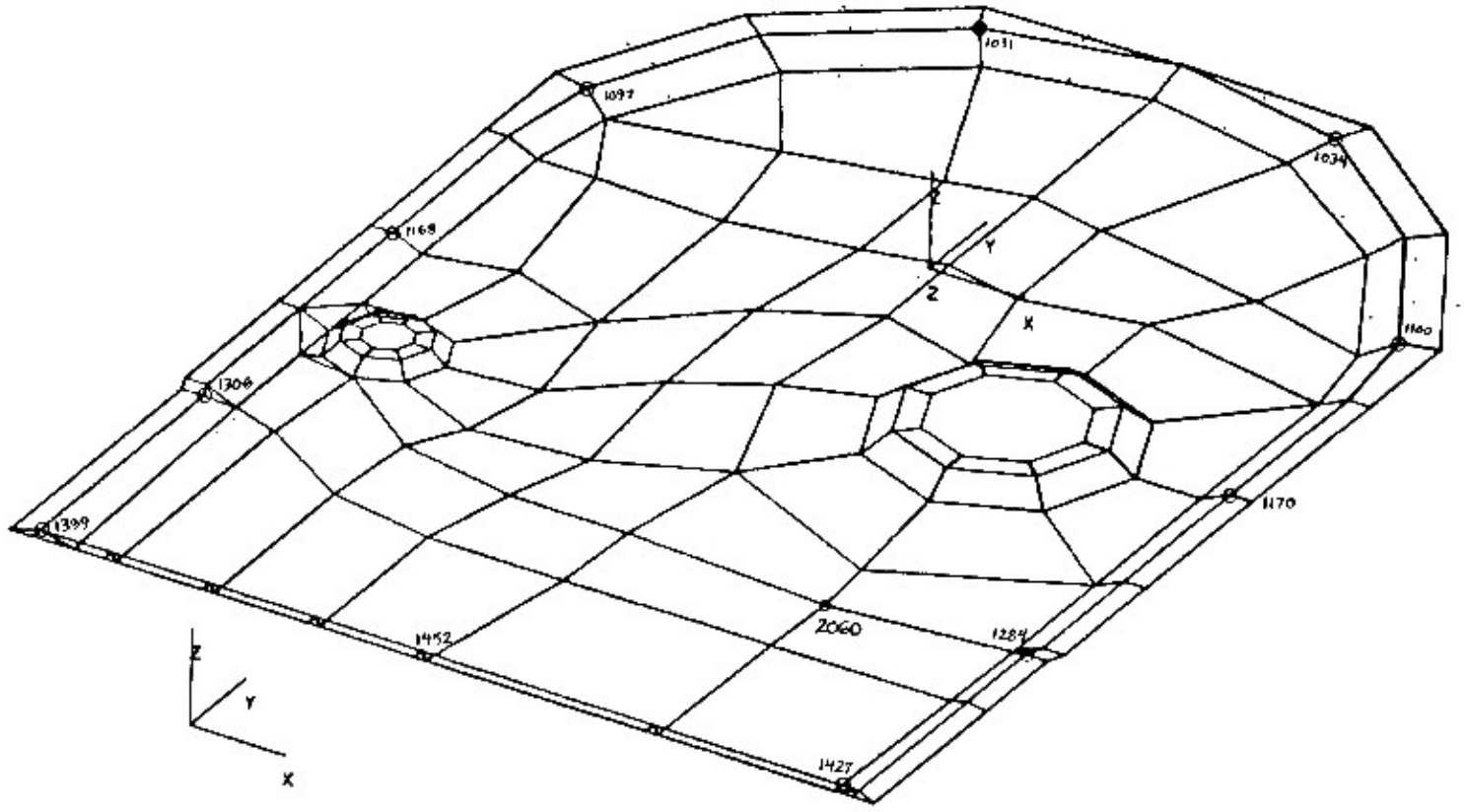

Figure 18: Item 2 NASTRAN Model

Although the models for items 3 and 4 required fewer grids and elements, the modeling was not as straightforward. Special purpose elements were required to represent rigid body mass and inertia properties, and to join flexible and rigid parts.

Figure (19) gives a closer view of item 3, the read arms and hub, and figure (20) shows a schematic of the final NASTRAN model. The read arms are modeled with QUAD4 elements which proved to be superior to BAR elements. The BAR element model was investigated in an attempt to reduce the number of DOFs required to model the arm. Section 4.2.2 explains the experimental comparison which led to the selection of the QUAD4 model over the BAR model. The hub, which is assumed to be very rigid, is modeled with stiff bar elements. Each read arm is rigidly supported by the hub assembly at several boundary points. This connection is modeled by an RBE2 element, which attaches the boundary grids of the read arm to a single grid on the hub. Due to the characteristics of the RBE2 element the motion of the boundary grids of the arm is computed directly from the motion of the single hub grid.

Item 4 consists of the disk drive motor, the disk hub, and a mounting plate (figure 21). The motor and disk hub are assumed to be rigid, therefore their elastic deflections are ignored. The corresponding mass, however, is a significant fraction of the entire disk drive mass and cannot be ignored. A CONM2 element was used to apply the mass and inertia of the two parts to grid

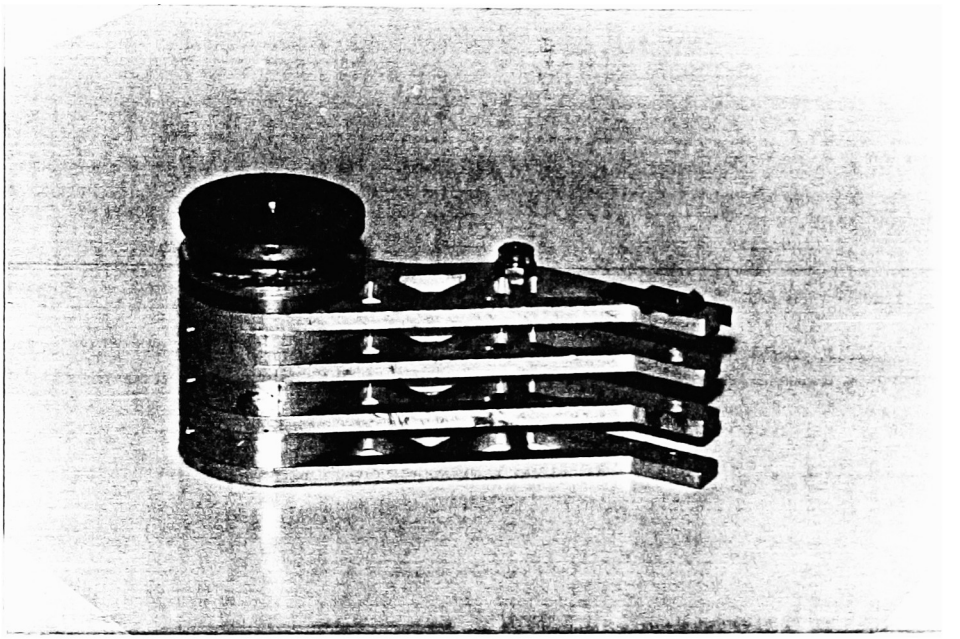

Figure 19: Item 3 (Read Arm Assembly)

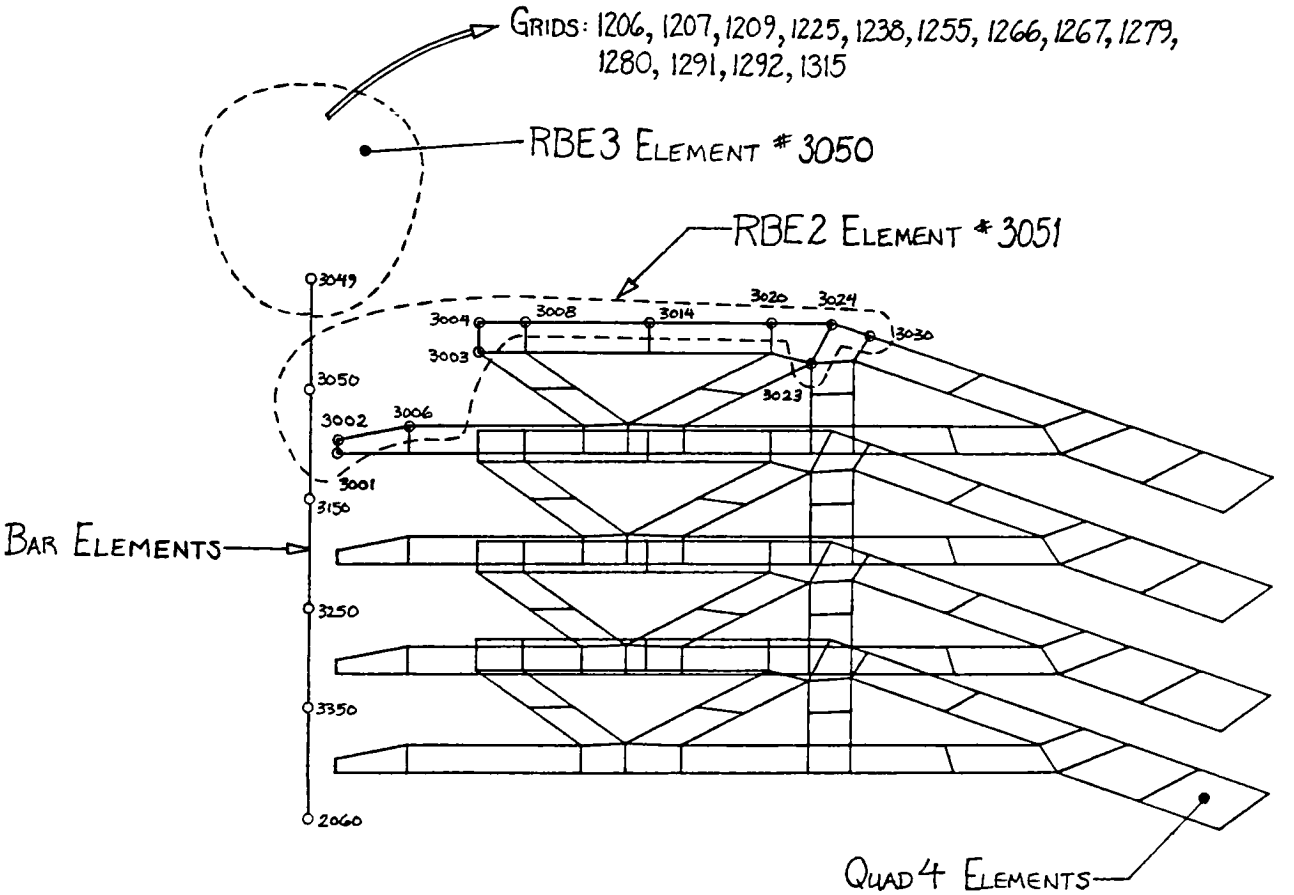

Figure 20: Item 3 NASTRAN Model

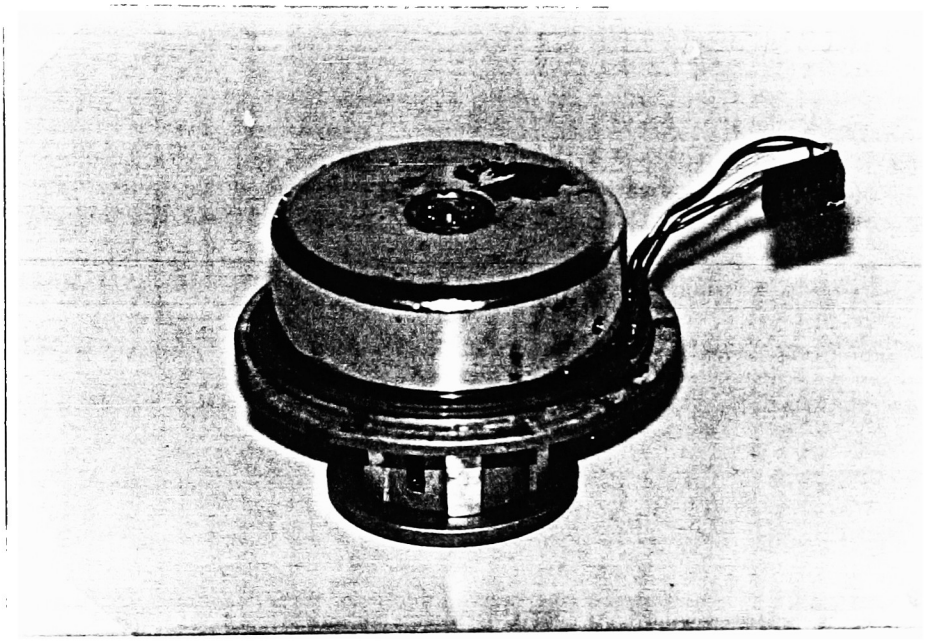

Figure 21: Item 4 (Drive Motor)

point 4100. The mounting plate adds stiffness to the main housing, and the motor and disk hub mount to it. The plate is modeled with QUAD4 elements as shown in figure (22). Grid 4100 and the CONM2 element representing the motor and hub mass are attached to the plate using an RBE3 element. Due to the characteristics of the RBE3 element, the motion at grid point 4100 is determined as an average of the motion of grid points 4009, 4012, 4015, and 4017. An alternate method of attaching the CONM2 element was also investigated; a framework of four rigid bars (RBAR elements) was used to attach the CONM2 element. The attachment method using the RBE3 element proved to be superior to the set of RBAR elements as explained in the following section.

The magnet and backing plate (item 5) are shown in figure (23). The mass of the magnets was modeled using a concentrated mass element, CONM2, located at their center of gravity. The backing plate was modeled using offset bar elements (figure 24).

4.2.2 Comparison of Component Natural Frequency Results

Component model validation was performed by comparison of the NASTRAN component natural frequency results with experimentally determined natural frequencies. This comparison, of course, requires that identical boundary conditions be used for both analytical and experimental analyses. The alternate modeling concepts discussed in the last section for items 3 and 4

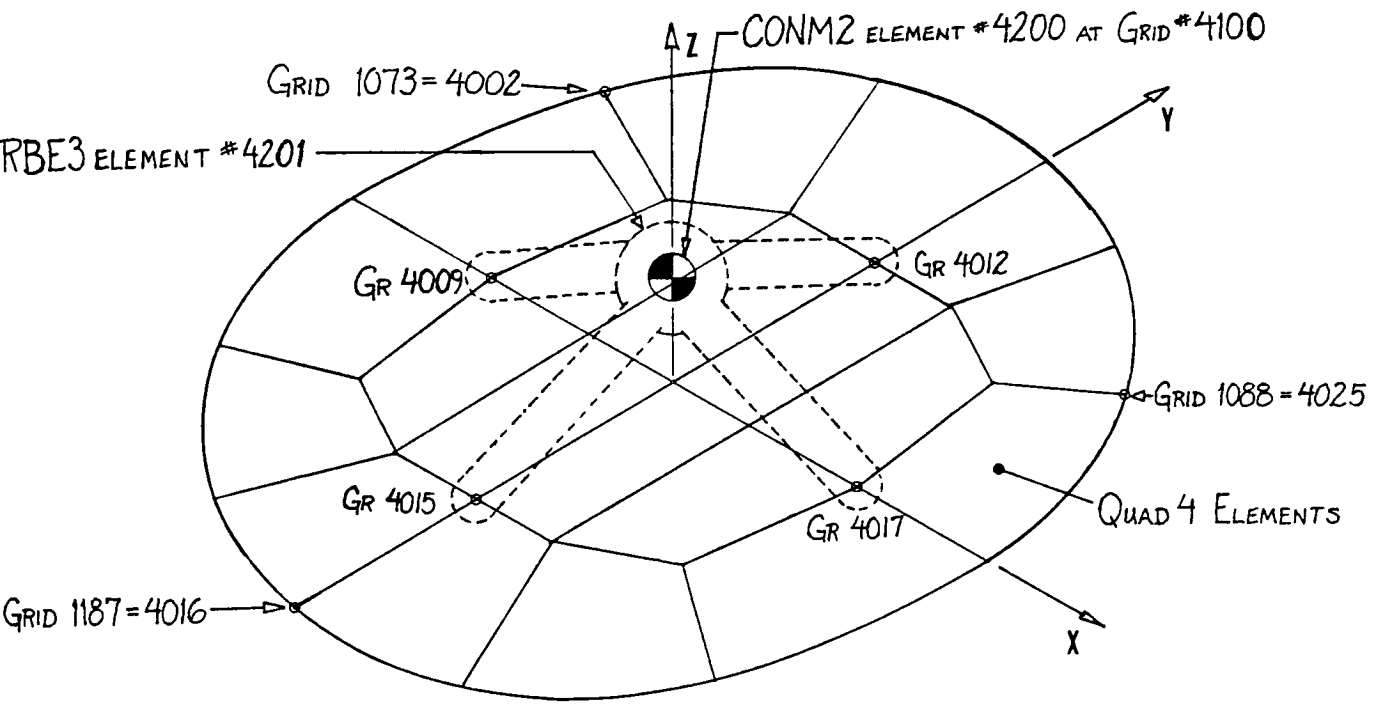

Figure 22: Item 4 NASTRAN Model

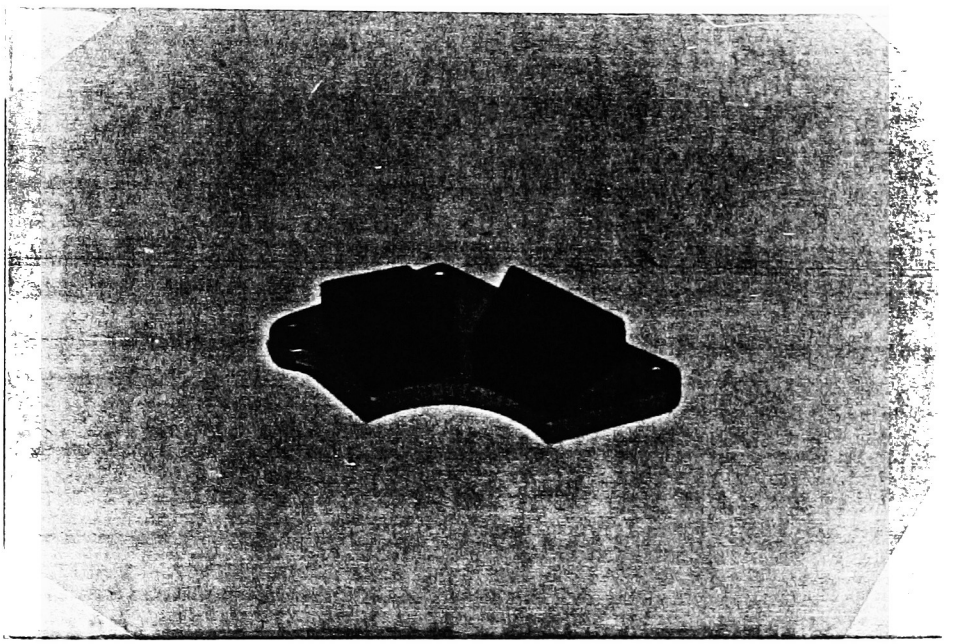

Figure 23: Item 5 (Magnet and Backing Plate)

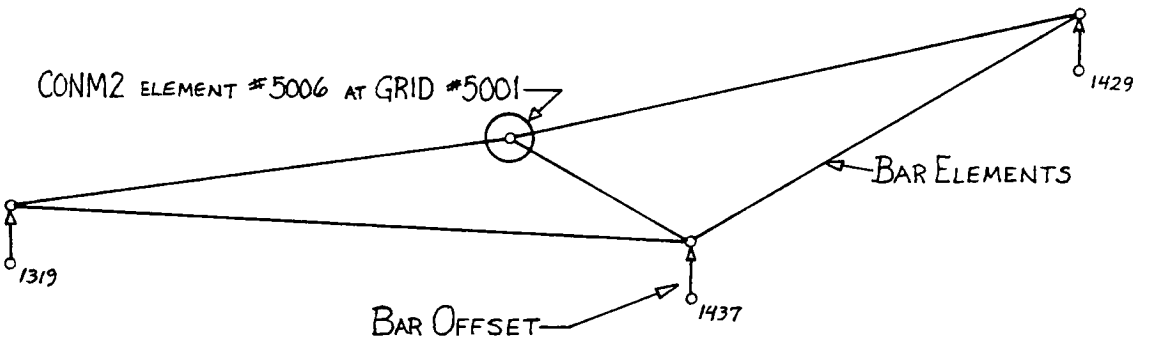

Figure 24: Item 5 NASTRAN Model

were also evaluated in this manner.

Natural frequency surveys were made on the items using an impact hammer and response accelerometer to generate frequency response functions. The natural frequencies of the structures were manually picked from the FRFs for comparison with the natural frequencies determined from the NASTRAN component models. For each survey, at least seven response accelerometer DOFs were used to insure that no modes were missed. Also, for each response DOF, a large number of input DOFs were investigated to yield a complete survey.

The correlation of frequencies for item 1 is shown in table (1). The NASTRAN results are from the SOL 3 solution sequence, using: the coupled mass option, generalized dynamic reduction, and the modified Givens extraction method. The NASTRAN model was unconstrained, except for the rigid body SUPORT which is applied only during rigid body mode generation. The experimental structure was therefore free mounted on a light string to approximate the same free-free boundary condition. The seven separate experimental surveys corresponding to the different response accelerometer locations are indicated by T1, T2, ... T7. The frequency correlation is good up to 2000hz except for the first two modes; NASTRAN results for these two modes are significantly lower (20%) than the experimentally determined natural frequencies. Correlation above 2000hz is difficult due to the large number of closely spaced modes.

TABLE 1: Correlation of Natural Frequencies of Item 1

T1	T2	T3	T4	T5	T6	T7	Tavr	NASTRAN	%DEV
470	450	450	470	460	470	460	461	371	-19.5
1205	1210	1210	1210	1210	1210	1210	1209	917	-24.2
xxxx	1455	1470	1450	xxxx	1440	1460	1455	1461	+0.4
xxxx	xxxx	xxxx	xxxx	1650	xxxx	xxxx	1650	1775	+7.6
xxxx	1730	xxxx	xxxx	xxxx	xxxx	xxxx	1730	1804	+4.3
1790	xxxx	1810	1780	xxxx	1800	1770	1790	1846	+3.1
xxxx	1860	xxxx	1860	1860	1870	1870	1864	1989	+6.7

The first two mode shapes of item 1 consisted primarily of deflection in the motor mounting flange and the rest of the upper surface of the housing. The large frequency deviation indicates that the item 1 NASTRAN model is not stiff enough in this area. This is probably due to one of three factors: insufficient mesh density, inaccurate connection between the upper surface and side walls of the housing, or insufficient stiffness of the motor mounting ring. The effect of mesh density could have been investigated on a simple model by running several models of a rectangular box with differing densities. The second possibility is that the connection between the upper surface and side walls yielded a low stiffness. This connection was simply modeled as a "sharp" corner, while in actuality there is a radius at the intersection. By the nature of the QUAD4 element the corner is not actually "sharp", there is some small radius built in due to the element shape functions. The effect of modeling the actual radius could be compared with the "sharp" corner approach through the use of a simple rectangular box model. The third possibility is that the motor mounting ring, modeled with thick QUAD4 elements, was insufficiently stiff. A model using 8 grid solid HEXA elements might have provided increased ring stiffness in bending and torsion. This theory could also be investigated with a simple model. Comparative analysis of a washer with QUAD4 and alternately HEXA elements forming a ring around its inner periphery would indicate whether the QUAD4 element was

sufficiently accurate in this application.

At this point, refinement of the item 1 model should have been performed using the methods indicated above. Because the model inaccuracies were not corrected, the errors were carried through into the rest of the component model comparisons and ultimately into the final assembled FEA model.

The results for the assembly of item 1 and item 5 are given in table (2). The first two modes still show about 20 percent deviation between the NASTRAN and experimental results. The remaining modes show good frequency correlation and also better one to one correspondence of modes above 2000 hz.

The results of the item 1 and 2 assembly are given in table (3). In addition to the modeling inaccuracies carried through from item 1, two other modeling inaccuracies may contribute to the deviations in table (3). The bolted connections between the parts are modeled by totally rigid single point connections. This is the simplest and quickest method of modeling this connection, but clearly it does not exactly represent the true physical situation. In addition, the non-linear boundary conditions between adjacent surfaces are not accurately modeled. Although these two factors will contribute to modeling inaccuracies, it is not within the scope of this thesis to account for them in the FEA model. These modeling difficulties will be further discussed in section 4.3.2.

The mode shapes associated with modes 2, 3, 6, and 7 consist

TABLE 2: Correlation of Natural Frequencies for Item 1 and 5 Assembly

T1	T2	T3	T4	T5	T6	T7	Tavr	NASTRAN	%DEV
520	500	490	520	500	510	510	507	402	-20.7
1210	1210	1210	1210	1210	1210	1210	1210	899	-17.4
1360	xxxx	xxxx	xxxx	1320	xxxx	xxxx	1340	1452	+8.4
xxxx	1450	1460	1430	1480	1400	1410	1438	1494	+3.9
xxxx	1650	1670	xxxx	xxxx	xxxx	1680	1667	1697	+1.8
1830	1820	1800	1830	1840	1830	1830	1826	1869	+2.4
xxxx	2040	xxxx	xxxx	xxxx	xxxx	xxxx	2040	2014	-1.3
2130	xxxx	2120	2130	xxxx	2140	2130	2130	2133	+0.1
xxxx	xxxx	xxxx	xxxx	xxxx	xxxx	xxxx	"	2153	+1.1
xxxx	2345	xxxx	2350	xxxx	2360	xxxx	2352	2231	-5.1
2400	xxxx	2410	2430	2420	2430	xxxx	2418	2378	-1.7
2660	xxxx	xxxx	xxxx	2690	2690	2680	2680	2572	-4.0
2840	2840	2850	xxxx	2870	2850	2860	2852	2799	-1.9

TABLE 3: Correlation of Natural Frequencies for Item 1 and 2 Assembly

T1	T2	T3	T4	T5	T6	T7	Tavr	NASTRAN	%DEV
350	350	340	350	350	350	350	349	308	-11.7
xxxx	580	xxxx	580	580	580	580	580	532	-8.3
900	900	900	900	900	900	900	900	815	-9.4
985	985	990	990	990	990	990	989	1014	+2.5
1060	1060	xxxx	1070	1060	xxxx	1070	1064	1147	+7.8
1380	1390	1380	1390	1390	1380	1390	1386	1216	-12.3
1440	1450	1450	1450	1450	1470	1440	1450	1326	-8.6
1490	1490	1570	1500	1510	1510	1500	1510	1594	+5.6
xxxx	1685	1690	1640	1680	1650	1680	1671	1689	+1.1
1790	1820	1810	1810	1810	1820	1830	1813	1760	-2.9
1855	1860	1860	1855	1860	1850	1850	1856	1783	-3.9
1910	1900	1900	1910	1895	xxxx	1900	1903	1796	-5.6

primarily of deflection of the motor mounting ring and upper surface of item 1. It is therefore probable that the inaccuracy of the item 1 model is responsible for the large negative frequency deviations associated with these modes. The first mode is primarily an item 2 "breathing" mode. The low NASTRAN frequency for this mode is probably indicative of the two problems in modeling the item 1 to item 2 connection which were mentioned above. The remaining mode shapes are composed of significant deflection in both items 1 and 2 and show varying frequency deviations.

The results of the item 1 and 4 assembly are given in table (4). Modes 1 and 2 of the assembly exhibit similar deflection patterns to mode 1 of item 1 alone. Mode 3 of the assembly exhibits a deflection pattern similar to mode 2 of item 1 alone. In both cases, the experimental frequencies of the assembly are lower, while the NASTRAN frequencies are higher than the corresponding item 1 frequencies. This phenomenon is difficult to explain, especially in light of the item 1 inaccuracy. Apparently, the FEA model of item 1 was stiffened significantly by the motor mounting plate, offsetting the increase in mass and raising the resonant frequency. In the experimental test, the increase in mass dominated the increase in stiffness causing a reduction in the resonant frequencies associated with the first two modes of item 1. The remaining modes show good frequency correlation.

TABLE 4: Correlation of Natural Frequencies for Item 1 and 4 Assembly

T1	T2	T3	T4	T5	T6	T7	T8	Tavr	NASTRAN (RBE3)	%DEV	NASTRAN (RBAR)
xxxx	xxxx	380	xxxx	xxxx	xxxx	xxxx	420	400	423	+5.8	382
490	470	480	490	480	490	480	490	484	493	+1.9	494
xxxx	xxxx	xxxx	xxxx	xxxx	xxxx	xxxx	990	990	933	-5.8	1082
xxxx	xxxx	xxxx	xxxx	xxxx	xxxx	xxxx	1140	1140	1122	-1.6	1207
xxxx	xxxx	xxxx	xxxx	xxxx	xxxx	xxxx	1190	1190	1177	-1.1	xxxx
1300	1300	1290	1300	1250	1300	1300	1290	1291	1359	+5.3	1426
xxxx	xxxx	xxxx	xxxx	1460	xxxx	xxxx	1450	1455	1573	+8.1	1580
1665	1680	1670	1670	xxxx	1660	1640	1680	1666	1590	-4.6	1586
1890	1810	1840	1890	1880	1870	1880	1870	1866	1795	-3.8	xxxx
xxxx	1940	1980	1990	1980	2000	xxxx	xxxx	1978	2036	+2.9	xxxx

Table (4) also shows a comparison of the two methods used for distributing the mass of the disk drive motor. The experimental correlation of the frequencies obtained from the RBAR model is comparable to the correlation of the RBE3 model frequencies. However, the RBAR model missed some of the closely spaced modes in the 0-2000hz frequency range which showed up in the RBE3 model and in the experimental analysis.

Comparison of the two methods of read arm modeling is shown in table (5). The NASTRAN results are from the SOL 3 solution sequence using: no reduction method, and the modified Givens extraction method. The NASTRAN QUAD4 model was rigidly constrained with SPCs at the eleven DOFs which attach to the RBE2 element (see figure 20). In order to simulate the same arm mounting physically for testing purposes, a single arm was clamped between two shaped aluminum plates. The first natural frequency of the QUAD4 model was within 2 percent of the experimentally determined value, while the BAR element model showed 24 percent deviation. The higher modes of the arm were above the frequency range of interest and were not checked experimentally.

TABLE 5: Correlation of Natural Frequencies for Read Arm

T1	T2	T3	T4	Tavr	NASTRAN (BARS)	%DEV	NASTRAN (QUAD4s)	%DEV
2080	2085	2080	2082	2082	1574	-24.4	2053	-1.4

4.3 Modeling of Assembled Disk Drive

4.3.1 Experimental Model

The disk drive motor, and read arm assembly are free to rotate during disk drive operation. The modes of the structure cannot be uniquely defined, however, until the read arm unit is locked into a fixed position. It was decided to lock the arms such that the length of the arm is fixed in the direction of the X axis of the main housing. The motor, being symmetric, does not create the same problems as the read arm assembly. It was, however, fixed from rotating in order to prevent any type of noise interference in the FRFs. Figure (25) shows the DOFs of the experimental model. Two coordinate systems were used to define the structure: a cylindrical coordinate system, A, was used for modeling the front part of the housing, and a rectangular coordinate system, B, was used for modeling the remainder of the structure. DOFs 1A-6A represent the motor mounting ring, and DOFs 22A-27A are located on the upper surface of the motor. DOFs 5,6,9, and 10 B represent the square bossed section, while 18B-26B and 68B represent the rectangular raised section. Finally, DOFs 11B-15B represent the upper cylindrical raised section that the read arm hub mounts into, and 55B-58B are DOFs located on the bottom cover, located around where the read arm hub connects.

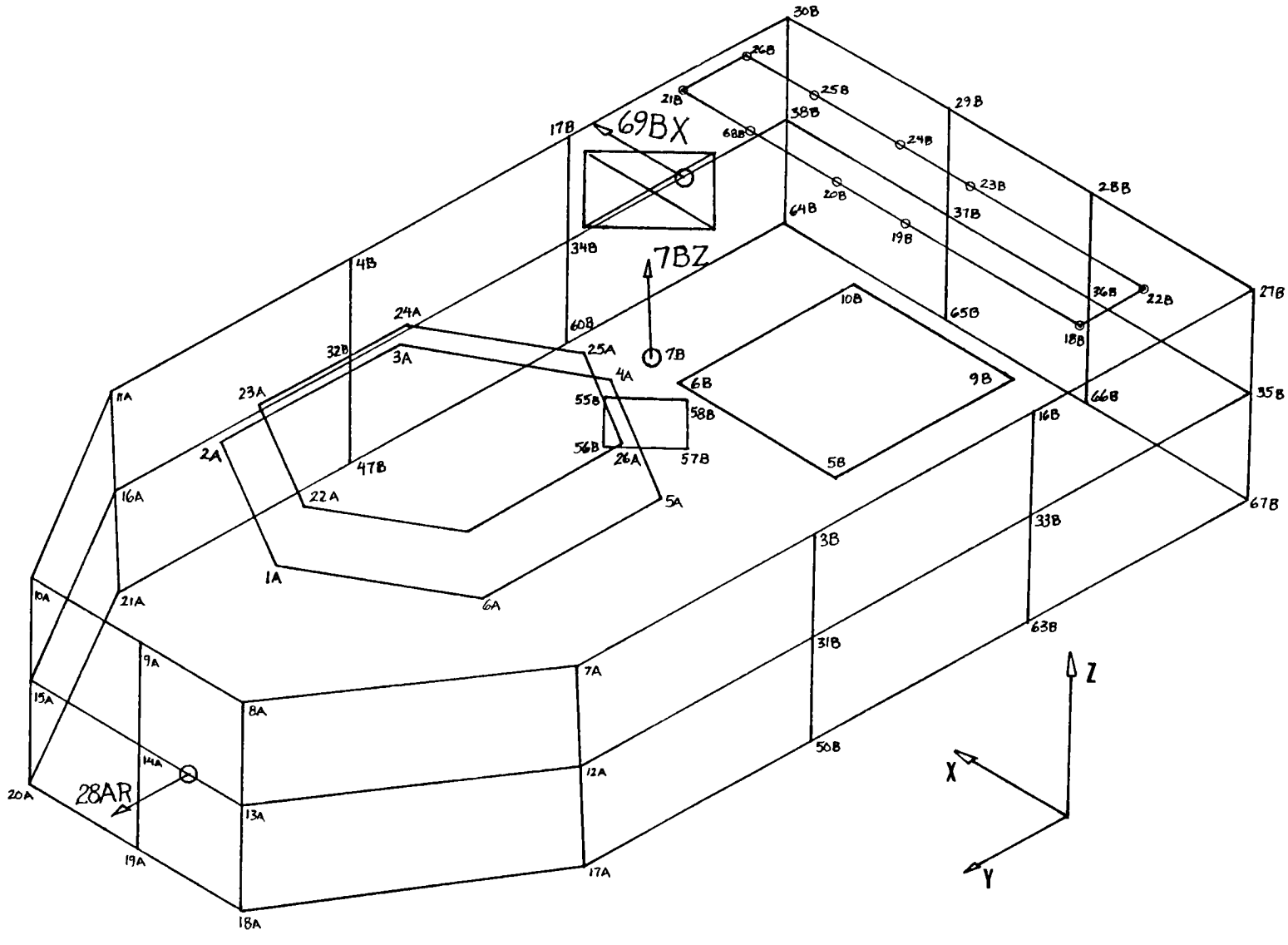

Figure 25: Experimental Test DOFs

It was impossible to instrument the read arm due to its inaccessibility, this was a major limitation of the experimental model. In addition, the low stiffness of the bottom cover made it impossible to obtain clean, repeatable FRFs there with the impact testing method. The rough motion of the read arm assembly can be estimated by the motion of its top and bottom mounts. The first elastic mode of the arm is toward the higher end of the frequency range of interest, therefore the arm motion is primarily rigid body and may be extrapolated for all but the highest test frequencies.

4.3.2 Assembly of the NASTRAN Model

The following is a summary of the components of the NASTRAN model: 867 grid points, 778 quad4 and tria3 elements, 10 bar elements, 2 CONM2 elements, 2 RBE3 rigid elements, and 4 RBE2 rigid elements. The model of the assembled disk drive was formed by joining the individual component models together at grid DOFs. Figures (17, 18, 20,22, and 24) show the grid points that were used for connecting the components.

The connection points all correspond to bolted joints. For modeling purposes it was assumed that these bolted connections could be modeled as totally rigid connections of the adjacent grid points of the components being joined. This assumption creates varying degrees of inaccuracy in the NASTRAN model; a

non-rigid, distributed connection is being modeled as a rigid, point constraint. In actuality, the bolted joint has stiffness and the constraint is distributed over an area. Another factor which should not be ignored is the constraint of the mating surfaces between the bolted joints. There is no constraint on the motion of these two surfaces, therefore physically impossible displacements, such as the two surfaces passing through each other, are possible within the model.

The distributed, non-rigid bolted constraint could be more accurately modeled within the SOL 3 rigid solution format, however it would require a great deal of time and model complexity to do so. In this case the displacement in the immediate neighborhood of the joint is unimportant and therefore as long as the errors don't extend to the remainder of the structure this approximation is acceptable.

In order to accurately model the constraint between the two adjacent mating surfaces a nonlinear (one way) constraint would be required. Within the NASTRAN nonlinear solution sequences it would be possible to model this, however, the cost in terms of solution convenience and solution time would be significant. As with the bolted joint, the motion in the neighborhood of the adjacent surfaces is not of interest, and therefore if the remainder of the structure is not significantly influenced, the model is acceptable.

4.3.2.1 Static Check Run on Assembled NASTRAN Model

As a final check before the modal solution sequence is run, a static check run was made to verify the assembled model. The model was constrained at its actual mounting locations with single point constraints and a gravity loading case was run. In addition the grid point weight generator was invoked in order to check the mass and mass distribution of the structure.

The static solution sequence is much less costly than the modal solution, and therefore it is often used to find problems in a model prior to dynamic analyses. The following are a few of the model problems that could be found using this technique: incorrect mass units, incorrect mass distribution, missing or incomplete SPCs, incorrectly connected elements, and even missing elements.

The initial gravity loading run found a problem with the attachment of the read arms to the read arm hub, and the read arm hub to the main housing. Through an oversight, the read arms were not correctly attached to constrain rotation about the hub, therefore the AUTOSPC function dropped these DOFs out of the problem and issued a warning message. In addition, the bar elements used to model the hub were rigidly fixed to the main housing and bottom cover at single grid points (top and bottom) at all DOFs. The QUAD and TRIA elements do not have rotational stiffness about the surface normal, and therefore the AUTOSPC

function also dropped out these DOFs. The arms were then correctly connected to the hub, solving the first problem. The hub was attached to the main housing at a set of grids using a RBE3 element, and the hub was attached to the bottom cover at a single axial DOF.

The displacement results of the gravity loading are shown in figures (26) and (27). The deformed shape is reasonable based on the applied constraints. The grid point weight generator output is summarized in table (6) along with the measured values obtained by experimentally balancing the assembled structure. The mass and two of the C.G. values agree closely; the X_{cg} value was difficult to measure accurately and had a small absolute value yielding a high percent deviation.

4.4 Determination of the Disk Drive Modes

The assembled disk drive was analyzed in an unmounted state to eliminate the problems associated with matching physical and analytical boundary conditions. The assembled NASTRAN model was therefore run with no mounting constraints and had six rigid body modes. A SUPORT card with six DOFs indicated on it was used to support the structure for rigid body mode calculation. The free-free boundary condition was simulated experimentally by supporting the structure from a light string.

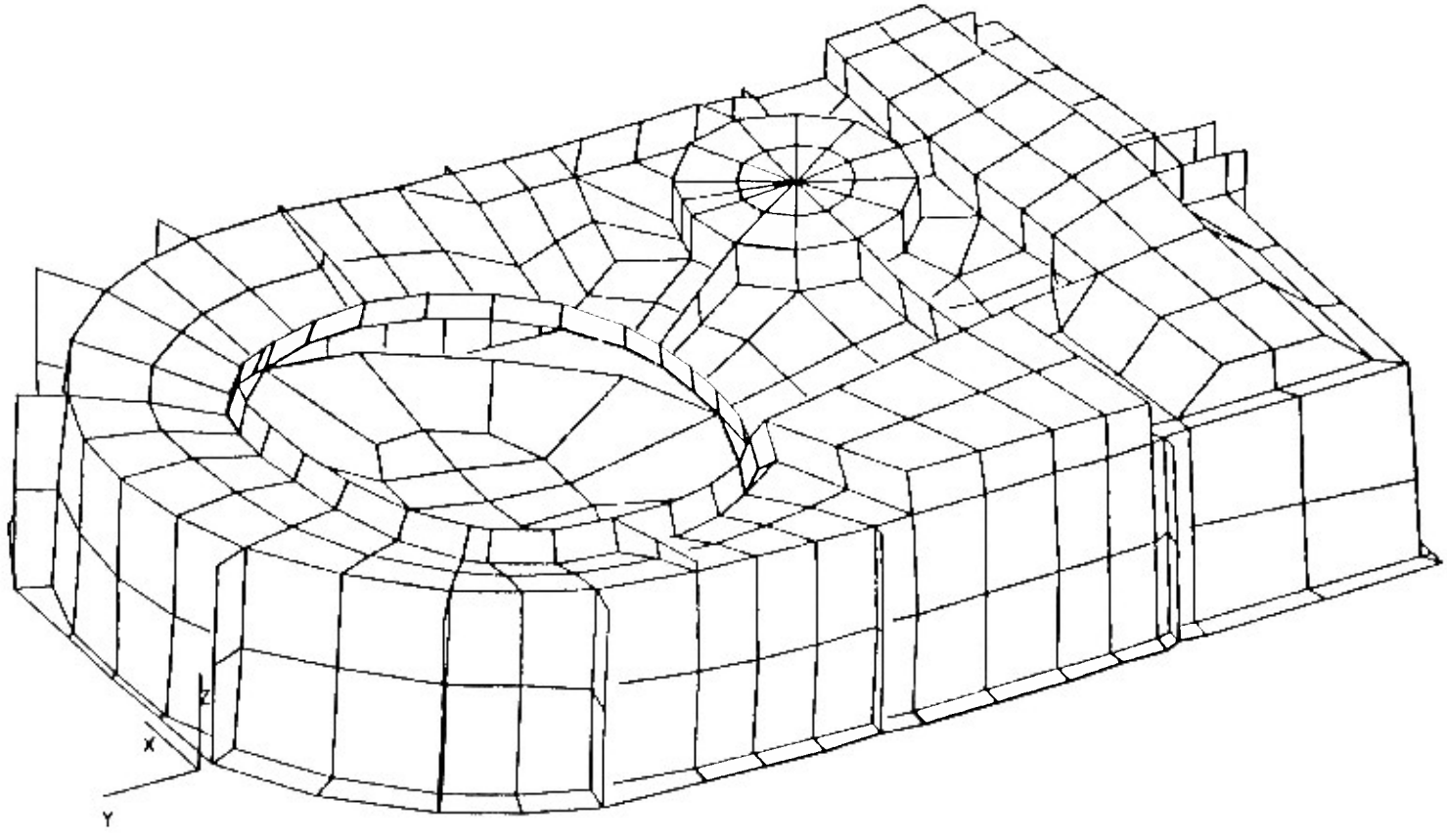

Figure 26: Gravity Loading (top view)

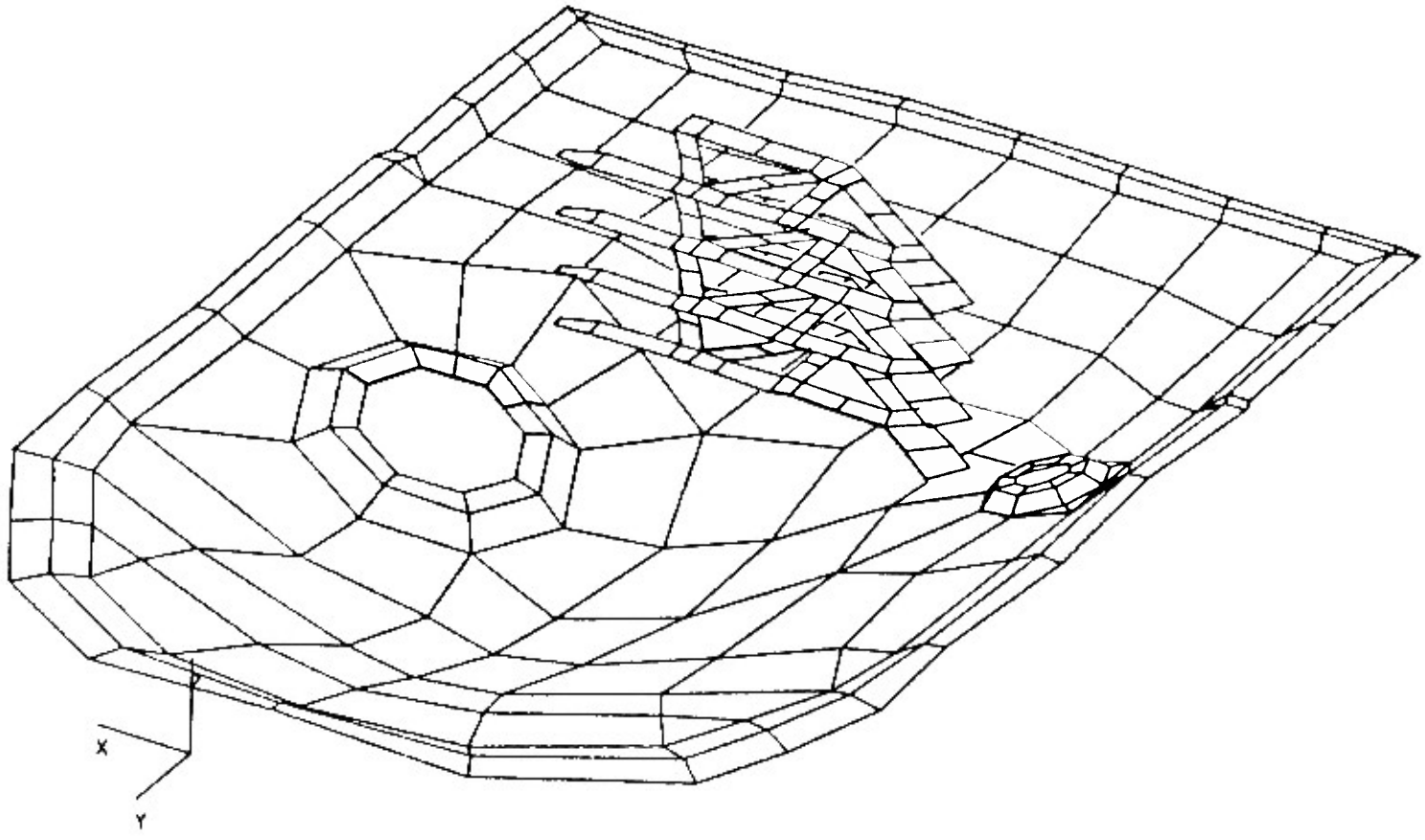

Figure 27: Gravity Loading (bottom cover and read arms)

TABLE 6: Grid Point Weight Generator Output

	Measured	NASTRAN	%DEV
Mass(lbf-sec/in^2)	8.165×10^{-3}	8.273×10^{-3}	+1.3
X_{cg} (in)	0.20	0.308	+54.1
Y_{cg} (in)	-1.39	-1.509	-8.6
Z_{cg} (in)	-0.24	-0.234	+2.5

4.4.1 Experimental Modal Test Results

Three complete impact modal tests were performed with three different response accelerometer locations. The three response DOFs were (see figure 25): 7BZ for test DDRIVE1, 69BX for test DDRIVE2, and 28AR for test DDRIVE3. The three locations were chosen in order to take into account as many types of elastic modes as possible. For a particular mode, at least one of the response accelerometer locations must not coincide with a structural anti node. If the response location does coincide with, or lie close to an anti node, the mode will not show up or it will yield a very poor mode shape estimate due to the weak contribution of that particular mode to the FRF.

Single and Multi degree of freedom polynomial curvefits were used for modal parameter estimation leading to the mode shapes. These single reference, non-global methods, were the most accurate methods available with the software version that was used.

The modal parameters determined in the three tests are given in table (7). These results show the importance of response DOF selection; each of the tests missed several of the modes in the frequency range of interest. The slight shift in the modal frequencies between tests is probably due to structural nonlinearities; nonlinear stiffness and damping are two possible causes.

TABLE 7: Results of Three Independent Modal Tests

	DDRIVE1		DDRIVE2		DDRIVE3		Tavr	
MODE #	Freq	Damp	Freq	Damp	Freq	Damp	Freq	Damp
1	334	1.36	xxxx	xxxx	xxxx	xxxx	334	1.36
2	596	1.30	592	2.78	595	1.51	594	1.86
3	647	1.62	656	1.16	656	1.37	653	1.38
4	683	1.19	686	0.52	687	1.10	685	0.94
5	xxxx	xxxx	929	3.58	923	2.42	926	3.00
6	1011	0.80	xxxx	xxxx	1013	0.90	1012	0.85
7	xxxx	xxxx	1021	1.88	1026	0.93	1024	1.41
8	1380	0.61	1370	0.86	1380	0.97	1377	0.81
9	xxxx	xxxx	1413	0.69	xxxx	xxxx	1413	0.69
10	xxxx	xxxx	1452	1.19	1460	0.13	1456	0.66
11	xxxx	xxxx	1479	0.98	1478	1.30	1479	1.14
12	1842	1.22	1838	1.37	1830	1.05	1837	1.21
13	1899	0.62	1900	0.52	1898	0.76	1899	0.63
14	1940	0.60	1944	0.58	xxxx	xxxx	1942	0.59
15	2077	0.30	2072	0.52	xxxx	xxxx	2075	0.41

The mode shapes corresponding to the modal frequencies are given in appendix C. Each page of appendix C shows plots of a single mode shape. The first column consists of different views of the mode shape from test DDRIVE1. Likewise, the second and third columns correspond to DDRIVE2, and DDRIVE3 respectively. A large number of the mode shapes show obviously erratic deflections at certain DOFs. These erratic deflections are generally due to one of three causes: The FRF is poorly defined in the particular frequency range, a curvefit procedure was incorrectly applied, or the structure exhibits nonlinear behavior which is not accurately treated by non-global curve fitting methods. Nonlinearity may be evidenced by the modal frequency shifting that occurred with several of the modes. For most of the modes, however, the frequency shifting was negligible.

The frequencies of the three different tests compare closely, however, the damping ratios vary widely. The damping estimation method used by the non-global polyfit routines is not generally very accurate. More advanced curvefit methods will, however, provide repeatable damping estimates. The mode shapes that do not have many erratic DOFs show good cross correlation.

4.4.2 NASTRAN Results

The modes of the assembled model were determined for the frequency range 0-2200hz using the data set listed in appendix B.

The structure was unconstrained, however, a SUPORT card was used to support the rigid body modes of the structure. The AUTOSPC and COUPMASS parameter options were invoked, the generalized dynamic reduction method was used to reduce the problem, and the modified Givens method was used to extract the eigenvalues and eigenvectors. The generalized dynamic reduction method reduced the problem to only 30 generalized coordinates. The number of generalized coordinates was chosen automatically be the reduction method in order to accurately determine the 18 modes in the 0-2200hz frequency range. The natural frequencies are given in table (8), as output by NASTRAN.

The mode shapes corresponding to the modal frequencies are displayed graphically in appendix D. These plots include the deformed shape of the main housing for comparison with the experimental mode shape. Also included are the deflected shapes of the read arms and motor mounting plate. Because the disk drive motor and disk hub are attached to the mounting plate the relative motion between the read head and disk can be extrapolated.

4.4.3 Comparison of NASTRAN and Experimental Results

Table (9) shows a comparison of the modal frequencies determined by each of the methods. For each of the modes, the percent deviation of the NASTRAN frequency from the experimental

TABLE 8: Results of NASTRAN Analysis (Free-Free B.C.)

MODE NO.	EXTRACTION ORDER	REAL EIGENVALUES EIGENVALUE	RADIANS	CYCLES	GENERALIZED MASS	GENERALIZED STIFFNESS
1	7	5.490220E+06	2.343122E+03	3.729194E+02	1.000000E+00	5.490220E+06
2	8	1.194348E+07	3.455934E+03	5.500289E+02	1.000000E+00	1.194348E+07
3	9	1.389602E+07	3.727737E+03	5.932877E+02	1.000000E+00	1.389602E+07
4	10	1.533668E+07	3.916208E+03	6.232838E+02	1.000000E+00	1.533668E+07
5	11	2.060399E+07	4.539162E+03	7.224301E+02	1.000000E+00	2.060399E+07
6	12	3.433387E+07	5.859511E+03	9.325701E+02	1.000000E+00	3.433387E+07
7	13	3.755647E+07	6.128333E+03	9.753546E+02	1.000000E+00	3.755647E+07
8	14	5.714938E+07	7.559721E+03	1.203167E+03	0.0	0.0
9	15	6.327503E+07	7.954560E+03	1.266008E+03	0.0	0.0
10	16	8.084636E+07	8.991460E+03	1.431035E+03	0.0	0.0
11	17	8.367379E+07	9.147338E+03	1.455844E+03	0.0	0.0
12	18	1.063517E+08	1.031270E+04	1.641317E+03	0.0	0.0
13	24	1.464002E+08	1.209960E+04	1.925710E+03	0.0	0.0
14	30	1.509448E+08	1.228596E+04	1.955371E+03	0.0	0.0
15	27	1.651711E+08	1.285189E+04	2.045442E+03	0.0	0.0
16	29	1.680131E+08	1.296199E+04	2.062964E+03	0.0	0.0
17	28	1.741388E+08	1.319617E+04	2.100235E+03	0.0	0.0
18	26	1.892193E+08	1.375570E+04	2.189288E+03	0.0	0.0
19	25	2.013552E+08	1.418997E+04	2.258404E+03	0.0	0.0
20	22	2.507572E+08	1.583532E+04	2.520269E+03	0.0	0.0
21	23	2.613140E+08	1.616521E+04	2.572773E+03	0.0	0.0
22	21	3.266761E+08	1.807418E+04	2.876596E+03	0.0	0.0
23	19	3.561639E+08	1.887231E+04	3.003621E+03	0.0	0.0
24	20	3.811623E+08	1.952338E+04	3.107242E+03	0.0	0.0
25	6	0.0	0.0	0.0	0.0	0.0
26	5	0.0	0.0	0.0	0.0	0.0
27	4	0.0	0.0	0.0	0.0	0.0
28	3	0.0	0.0	0.0	0.0	0.0
29	2	0.0	0.0	0.0	0.0	0.0
30	1	0.0	0.0	0.0	0.0	0.0

TABLE 9: Comparison of Disk Drive Natural Frequencies

MODE #	DDRIVE1	DDRIVE2	DDRIVE3	Tavr	NASTRAN	%DEV
1	334	xxxx	xxxx	334	373	+11.7
2	596	592	595	594	550	-7.4
3	647	656	656	653	593	-9.2
4	683	686	687	685	623	-9.1
5	xxxx	929	923	926	722	-22.0
6	1011	xxxx	1013	1012	932	-7.9
7	xxxx	1021	1026	1024	975	-4.8
8	1380	1370	1380	1377	1203	-12.6
9	xxxx	1413	xxxx	1413	1266	-10.4
10	xxxx	1452	1460	1456	1431	-1.7
11	xxxx	1479	1478	1479	1456	-1.6
12	1842	1838	1830	1837	1641	-10.7
13	1899	1900	1898	1899	1926	+1.4
14	1940	1944	xxxx	1942	1955	+0.7
15	2077	2072	xxxx	2075	2045	-1.4

average frequency is calculated. Several of the modes show large percent deviation magnitudes, in excess of 10%. Mode 1 (+11.7%) is primarily a "breathing" mode of the bottom cover with a slight vertical bounce mode of the motor on the housing. The motor bounce is shown by both NASTRAN (D-1) and modal (C-1) results. Mode 5 shows the highest percent deviation magnitude (-22%). The NASTRAN mode shape (D-5) shows that most of the deflection is in the motor and the motor mount area of the main housing. Both experimental mode shapes (C-5) are very noisy and provide poor verification of the mode shape, although they do seem to show the same motion in the area of the motor mount. Mode 8 has a deviation of (-12.6%); the NASTRAN mode shape (D-8) shows torsional twisting of the main housing about the Y axis. The experimental mode shapes (C-8) show some indication of the same type of twisting, but again are noisy. The NASTRAN (D-9) and experimental mode shapes (C-9) for mode 9 (-10.4%) correlate. Although the experimental shape is noisy, it shows the same type of motion in the region behind the motor. Both NASTRAN (D-12) and experimental mode shapes (C-12) for mode 12 (-10.7%) show a very similar main housing deflection pattern to mode 9. Modes 3 and 4 also show deviation magnitudes close to ten percent. The NASTRAN shape for mode 3 (D-3) shows housing torsion about the Y axis; the experimental plots (C-3) show the same housing torsion as well as significant motor rocking about the Y axis. The mode shapes for the fourth mode are very similar to the third mode and

show good correlation between NASTRAN and experimental results. The other mode shapes all show good correlation, and the modal frequency deviation magnitudes are all below 7.9%.

4.4.4 Discussion of Modal Frequency Deviations

For twelve of the fifteen modes in the frequency range of interest the frequency modal determined by NASTRAN was lower than the experimentally determined frequency. The NASTRAN frequency was significantly higher (11.7%) than the experimental average for the first mode only.

The low FEA frequencies indicate that the model stiffness associated with the particular modal deflection pattern is too low, or that the associated mass/inertia is too low. Mode shape comparison shows that, in general, the modes with the higher percent deviation magnitudes show significant main housing torsion, or bending or torsion in the area of the motor mounting ring. Conversely, the modes with smaller magnitude deviations show less main housing deflection, and less deflection in the area of the motor mounting ring.

These observations point to previously mentioned FEA model inaccuracies as the cause of poor frequency correlation between the FEA and experimental models. The consistently low NASTRAN values indicate a lack of stiffness in the FEA model. The major inaccuracy in the assembled FEA model is probably the modeling

inaccuracy in item 1 which was carried through into the assembled model. As previously discussed, the item 1 component model exhibited insufficient stiffness of the upper surface of the main housing, particularly in the motor mounting ring. The method of connecting items 1 and 2 and the failure to model the boundary between the two parts may also contribute to low stiffness of certain deflection patterns. Gross bending or torsion of the main housing would probably not be adequately stiffened by the bottom cover. Also, higher order deflections of the bottom cover would probably be incorrectly constrained due to the failure to model the nonlinear boundary between the two parts.

4.5 Conclusions

The frequencies and mode shapes showed good correlation in general. Although most of the frequency deviations were in excess of 5 percent, there was a one to one correspondence of modes and the mode shapes corresponded in form. If the necessary improvements had been made to the finite element model, the frequency and mode shape correlation would certainly have improved. Although the inaccuracy of the item 1 component FEA model confuses the investigation of other potential FEA modeling inaccuracies, it does appear that the assumption of rigid single point connection at bolted joints, as well as the failure to model the nonlinear boundary conditions, results in noticeable

deviations between experimental and finite element models.

Assuming that this disk drive was to operate at a motor frequency of 600hz, there are several modes of the unconstrained structure which might cause performance problems or high operational noise levels. Modes 2, 3, and 4 are close to the first order frequency of the motor (600 hz), and all of these modes show relative motion between the disk drive motor and read arms as well as significant housing deflection. Modes 12, and 13 are near the third order frequency of the motor (1800hz) and also show relative motion between the read arms and drive motor. This information could lead the disk drive designer to make design changes to shift these frequencies, or to mount the main housing such that it is stiffened and the frequencies are thereby shifted.

4.6 Suggestions for Advanced Analysis

There are several advanced analysis techniques that could be applied to this structure to improve the analysis results, or simplify the analysis: substructuring in both FEA and experimental modal analysis, poly-reference and/or global curve fitting, and direct numerical mode shape comparison.

Substructuring could be very usefully applied to the disk drive problem. Substructuring is a technique by which: the components of a structure may be modeled and solved separately

and the solution of the global structure may be retrieved from the results of the individual component problems. NASTRAN has both static and dynamic substructuring capabilities. In the Literature, modal substructuring is also called component mode synthesis. A set of modes for each component is used to model the dynamic characteristics of that component. The modes of the assembled structure are calculated directly from the component modes. The component modes may include: normal modes, rigid body modes, and constraint and/or attachment modes.[20] The normal and rigid body modes of the component carry: elastic behavior information, and the inertia properties of the component. The constraint and attachment modes define the attachment of the component to other components.

Modal 3.0 also has optional substructuring software which can now be added to the standard Modal 3.0 analysis software. This procedure is especially applicable to the disk drive problem. If substructuring had been available, the read arm assembly could have been separately tested and substructured into the problem.

Other capabilities which SMS has recently made available with the Modal 3.0 system are poly-reference curvefitting, and single reference global curvefitting. Global curvefitting looks at a set of measurements when it curve fits each mode. This means that true global frequency and damping can be defined, as well as averaging out the effects of a single bad measurement.

Missing Page

numerical comparison procedure may then be used. KIT-MAS uses the Modal Assurance Criterion (MAC) to numerically correlate the mode shapes. The MAC calculates a value from 1.000-0.000 which defines the degree of dependence/independence of the two modal vectors using an orthogonality check.

References

[1] Richard L. Burden and J. Douglas Faires, Numerical Analysis. (Boston: Prindle, Weber & Schmidt), p. 417.

[2] SMS Modal 3.0 Manual. (San Jose: Structural Measurement Systems), p. 12-24.

[3] Haines, Charles W. Analysis for Engineers. (New York: West Publishing Co.), p. 241.

[4] Ibid.

[5] The Fundamentals of Modal Testing; Application Note 243-3. (Palo Alto: Hewlett-Packard Co.), p. 9.

[6] Kennedy, C. C., and Pancu, C. D. P. "Use of Vectors in Vibration Measurement and Analysis," J. Aero. Sci., V 14, 1947, pp. 603-625.

[7] MacNeal, Richard H. MSC/NASTRAN Handbook for Linear Static Analysis. MSC/NASTRAN Version 61. (Los Angeles: MacNeal Schwendler Corporation), p. 7-4.

[8] Ibid., p. 7-18.

[9] Ibid., p. 2.3-12.

[10] Ibid., p. 7-19.

[11] Ibid., p. 12-121.

[12] Gockel, M.A., ed. MSC/Nastran Handbook for Dynamic Analysis. MSC/NASTRAN Version 63. (Los Angeles: MacNeal Schwendler Corporation), p. 4.1-3.

[13] Ibid., p. 4.1-5.

[14] Ibid., p. 5.1-1.

[15] Ibid., p. 5.1-2.

[16] Ibid., p. 5.2-1.

[17] Ibid., p. 5.2-3.

[18] Ibid., p. 4.2-11.

[19] Rahimi, Alireza. "Designing Hard Drives to Take Abuse." Computer Design, Oct. 1, 1984, p. 141.

[20] Craig, Roy R. Structural Dynamics. (New York: John Wiley & Sons), pp. 469-470.

APPENDIX A

NASTRAN Bulk Data Card Description

Input Data Card GRID Grid Point

Description: Defines the location of a geometric grid point of the structural model, the directions of its displacement, and its permanent single-point constraints.

Format and Example:

1	2	3	4	5	6	7	8	9	10
GRID	ID	CP	X1	X2	X3	CD	PS		
GRID	2	3	1.0	-2.0	3.0		316		

Field	Contents
ID	Grid point identification number (1,000,000 > Integer > 0)
CP	Identification number of coordinate system in which the location of the grid point is defined (Integer ≥ 0 or blank*)
X1,X2,X3	Location of the grid point in coordinate system CP (Real)
CD	Identification number of coordinate system in which displacements, degrees of freedom, constraints, and solution vectors are defined at the grid point (Integer ≥ 0 or blank*)
PS	Permanent single-point constraints associated with grid point (any of the digits 1-6 with no imbedded blanks) (Integer ≥ 0 or blank*)

Remarks:

1. All grid point identification numbers must be unique with respect to all other structural, scalar and fluid points.
2. The meaning of X1, X2 and X3 depend on the type of coordinate system, CP, as follows: (see CØRDi card descriptions)

Type	X1	X2	X3
Rectangular	X	Y	Z
Cylindrical	R	θ(degrees)	Z
Spherical	R	θ(degrees)	φ(degrees)

3. The collection of all CD coordinate systems defined on all GRID cards is called the Global Coordinate System. All degrees-of-freedom, constraints, and solution vectors are expressed in the Global Coordinate System.

*See the GRDSET card for default options for fields 3, 7 and 8.

Input Data Card SPC Single-Point Constraint

Description: Defines sets of single-point constraints and enforced displacements.

Format and Examole:

1	2	3	4	5	6	7	8	9	10
SPC	SID	G	C	D	G	C	D		
SPC	2	32	436	-2.6	5		+2.9		

Field	Contents
SID	Identification number of single-point constraint set (Integer > 0).
G	Grid or scalar point identification number (Integer > 0).
C	Component number (6 ≥ Integer ≥ 0; up to six unique digits may be placed in the field with no imbedded blanks).
D	Value of enforced displacement for all coordinates designated by G and C (Real).

Remarks:

1. Coordinates specified on this card form members of a mutually exclusive set. They may not be specified on other cards that define mutually exclusive sets.
2. Single-point forces of constraint are recovered during stress data recovery.
3. Single-point constraint sets must be selected in the Case Control Deck (SPC=SID) to be used by NASTRAN.
4. From one to twelve single-point constraints may be defined on a single card.
5. SPC degrees of freedom may be redundantly specified as permanent constraints on the GRID card.
6. Continuation cards are not allowed.

Input Data Card SPC1 Single-Point Constraint, Alternate Form

Description: Defines sets of single-point constraints.

Format and Example:

1	2	3	4	5	6	7	8	9	10
SPC1	SID	C	G1	G2	G3	G4	G5	G6	
SPC1	3	2	1	3	10	9	6	5	ABC
	G7	G8	G9	-etc-					
+8C	2	8							

Alternate Form

SPC1	SID	C	GID1	"THRU"	GID2				
SPC1	313	12456	6	THRU	32				

Field	Contents
SID	Identification number of single-point constraint set (Integer > 0).
C	Component number (any unique combination of the digits 1-6 (with no imbedded blanks) when point identification numbers are grid points; must be null if point identification numbers are scalar points).
Gi,GIDi	Grid or scalar point identification numbers (Integer > 0).

Remarks:

1. Note that enforced displacements are not available via this card. As many continuation cards as desired may appear when "THRU" is not used.
2. Coordinates specified on this card form members of a mutually exclusive set. They may not be specified on other cards that define mutually exclusive sets.
3. Single-point constraint sets must be selected in the Case Control Deck (SPC=SID) to be used by NASTRAN.
4. SPC degrees of freedom may be redundantly specified as permanent constraints on the GRID card.
5. If the alternate form is used, points in the sequence GID1 thru GID2 are not required to exist. Points which do not exist will collectively produce a warning message but will otherwise be ignored.

Input Data Card CBAR Simple Beam Element Connection

Description: Defines a simple beam element (BAR) of the structural model.

Format and Example:

1	2	3	4	5	6	7	8	9	10
CBAR	EID	PID	GA	GB	X1,GO	X2	X3		
CBAR	2	39	7	3	13				123
	PA	PB	W1A	W2A	W3A	W1B	W2B	W3B	
+23		513							

Field	Contents
EID	Unique element identification number (Integer > 0).
PID	Identification number of a PBAR property card (Default is EID unless BARØR card has nonzero entry in field 3)(Integer > 0 or blank *).
GA,GB	Grid point identification numbers of connection points (Integer > 0; GA ≠ GB).
X1,X2,X3	Components of vector $\vec{v}$, at end A, (Figure 1(a) in Section 1.3) measured at end A, parallel to the components of the displacement coordinate system for GA, to determine (with the vector from end A to end B) the orientation of the element coordinate system for the BAR element (Real, 0 or blank;* see Remark 5).
GO	Grid point identification number to optionally supply X1, X2, X3 (Integer > 0 or blank;* see Remark 5).
PA,PB	Pin flags for bar ends A and B, respectively. (Up to 5 of the unique digits 1 - 6 anywhere in the field with no imbedded blanks; Integer > 0.) Used to remove connections between the grid point and selected degrees of freedom of the bar. The degrees of freedom are defined in the element's coordinate system (see Figure 1(a), Section 1.3). The bar must have stiffness associated with the pin flag. For example, if PA=4 is specified, the PBAR card must have a value for J, the torsional stiffness.
W1A,W2A,W3A W1B,W2B,W3B	Components of offset vectors $\vec{w}_a$ and $\vec{w}_b$, respectively, (see Figure 3, p. 7.1-4) in displacement coordinate systems at points GA and GB, respectively (Real or blank).

*See the BARØR card for default options for fields 3 and 6 - 8.

Remarks: 1. Element identification numbers must be unique with respect to all other element identification numbers.

2. For an explanation of BAR element geometry, see Figure 3, p. 7.1-4.

3. If there are no pin flags or offsets, the continuation card may be omitted.

(Continued)

4. The old CBAR card used field 9 for a flag, F, which was used to specify the nature of fields 6 - 8 as follows:

FIELD	6	7	8
F=1	X1	X2	X3
F=2	G0	Blank or 0	Blank or 0
F=blank	Provided by BARØR card.		

This data item is no longer required but may continue to be used if desired (See Remark 5). If F=1 in field 9, a zero (0) in field 6, 7, or 8 will override entries on the BARØR card, but a blank will not.

5. For the case where field 9 is blank and not provided by the BARØR card, if X1,G0 is integer, then G0 is used; if X1,G0 is blank or real, then X1, X2, X3 is used.

Input Data Card PBAR Simple Beam Property

Description: Defines the properties of a simple beam (bar) which is used to create bar elements via the CBAR card.

Format and Example:

1	2	3	4	5	6	7	8	9	10
PBAR	PID	MID	A	I1	I2	J	NSM		
PBAR	39	6	2.3		5.97				123
	C1	C2	D1	D2	E1	E2	F1	F2	
+23			2.0	4.0					
	K1	K2	I12						

Field	Contents
PID	Property identification number (Integer > 0)
MID	Material identification number (Integer > 0)
A	Area of bar cross-section (Real)
I1, I2, I12	Area moments of inertia (Real) ($I_1 \geq 0.$, $I_2 \geq 0.$, $I_1 I_2 > I_{12}^2$)
J	Torsional constant (Real)
NSM	Nonstructural mass per unit length (Real)
K1, K2	Area factor for shear (Real)
Ci,Di,Ei,Fi	Stress recovery coefficients (Real)

Remarks:

1. For structural problems, PBAR cards may only reference MAT1 material cards.
2. See Figure 3, p. 7.1-4 for a discussion of bar element geometry.
3. For heat transfer problems, PBAR cards may only reference MAT4 or MAT5 material cards.
4. The transverse shear stiffnesses in planes 1 and 2 are (K1)AG and (K2)AG, respectively. The default values for K1 and K2 are infinite; in other words, the transverse shear flexibilities are set equal to zero. K1 and K2 are ignored if I12 ≠ 0.
5. The stress recovery coefficients C1 and C2, etc., are the y and z coordinates in the BAR element coordinate system of a point at which stresses are computed. Stresses are computed at both ends of the BAR.

Input Data Card CQUAD4 Quadrilateral Element Connection

Description: Defines a quadrilateral plate element (QUAD4) of the structural model. This is an isoparametric membrane-bending element.

Format and Example:

1	2	3	4	5	6	7	8	9	10
CQUAD4	EID	PID	G1	G2	G3	G4	θ		
CQUAD4	111	203	31	74	75	32	2.6		ABC
			T1	T2	T3	T4			
+BC			1.77	2.04	2.09	1.80			

Field	Contents
EID	Element identification number (Unique integer > 0)
PID	Identification number of a PSHELL or PCØMP property card (Integer > 0 or blank, default is EID)
G1,G2, G3,G4	Grid point identification numbers of connection points (Integers > 0, all unique)
θ	Material property orientation angle in degrees (Real). The sketch below gives the sign convention for TH.
T1,T2, T3,T4	Membrane thickness of element at grid points G1 through G4 (Real or blank, see PSHELL for default)

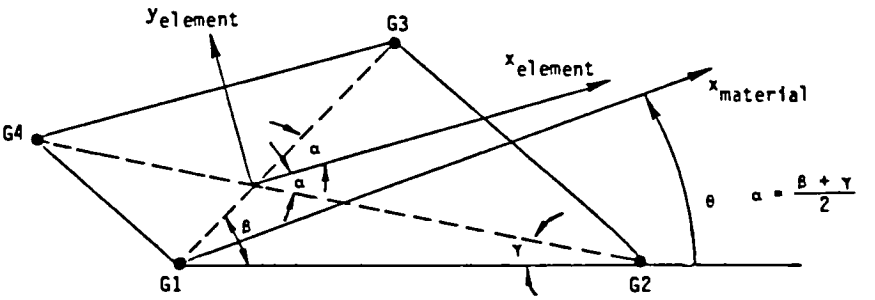

Remarks:
1. Element identification numbers must be unique with respect to all other element identification numbers.
2. Grid points G1 through G4 must be ordered consecutively around the perimeter of the element.
3. All the interior angles must be less than 180°.

(Continued)

4. The continuation card is optional. If it is not supplied, then T1 through T4 will be set equal to the value of T on the PSHELL data card.

5. Stresses are output in the element coordinate system.

Input Data Card PSHELL Shell Element Property

Description: Defines the membrane, bending, transverse shear, and coupling properties of thin shell elements.

Format and Example:

1	2	3	4	5	6	7	8	9	10
PSHELL	PID	MID1	T	MID2	$12I/T^3$	MID3	TS/T	NSM	
PSHELL	203	204	1.90	205	1.2	206	0.8	6.32	BCD
	Z1	Z2	MID4						
+CD	+.95	-.95							

Field	Contents
PID	Property identification number (Integer > 0)
MID1	Material identification number for membrane (Integer > 0 or blank)
T	Default value for membrane thickness (Real)
MID2	Material identification number for bending (Integer > 0 or blank)
$12I/T^3$	Bending stiffness parameter (Real or blank, default = 1.0)
MID3	Material identification number for transverse shear (Integer > 0 or blank)
TS/T	Transverse shear thickness divided by membrane thickness (Real or blank, default = .833333)
NSM	Nonstructural mass per unit area (Real)
Z1,Z2	Fiber distances for stress computation. The positive direction is determined by the righthand rule and the order in which the grid points are listed on the connection card. (Real or blank, defaults are -1/2 T for Z1 and 1/2 T for Z2.)
MID4	Material identification number for membrane-bending coupling (Integer > 0 or blank).

Remarks: 1. All PSHELL property cards must have unique identification numbers.

2. The structural mass is computed from the density using the membrane thickness and membrane material properties.

3. The results of leaving an MID field blank are:

   MID1 No membrane or coupling stiffness.
   MID2 No bending, coupling, or transverse shear stiffness.
   MID3 No transverse shear flexibility.
   MID4 No bending-membrane coupling.

(Continued)

4. The continuation card is not required.

5. The structural damping (for dynamics rigid formats) uses the values defined for the MID1 material.

6. The MID4 field should be left blank if the material properties are symmetric with respect to the middle surface of the shell.

7. This card is used in connection with the CTRIA3, CQUAD4 and CQUAD8 cards.

Input Data Card CTRIA3 Triangular Element Connection

Description: Defines a triangular plate element (TRIA3) of the structural model. This is an isoparametric membrane-bending element.

Format and Example:

1	2	3	4	5	6	7	8	9	10
CTRIA3	EID	PID	G1	G2	G3	θ			
CTRIA3	111	2D3	31	74	75	3.D			ABC
			T1	T2	T3				
+BC			1.77	2.04	2.09				

Field	Contents
EID	Element identification number (Unique integer > 0)
PID	Identification number of a PSHELL or PCØMP property card (Integer > 0 or blank, default is EID)
G1,G2,G3	Grid point identification numbers of connection points (Integers > 0, all unique)
θ	Material property orientation angle in degrees (Real). The sketch below gives the sign convention for TH.
T1,T2,T3	Membrane thickness of element at grid points G1, G2, and G3 (Real or blank, see PSHELL for default)

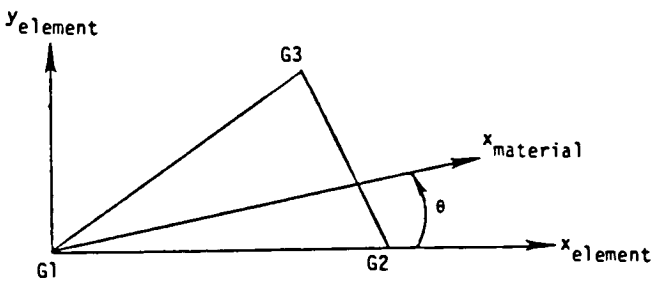

Remarks: 1. Element identification numbers must be unique with respect to all other element identification numbers.

2. The continuation card is optional. If it is not supplied, then T1 through T3 will be set equal to the value of T on the PSHELL or PCØMP data card.

Input Data Card CØNM2 Concentrated Mass Element Connection, Rigid Body Form

Description: Defines a concentrated mass at a grid point of the structural model.

Format and Example:

1	2	3	4	5	6	7	8	9	10
CØNM2	EID	G	CID	M	X1	X2	X3		
CØNM2	2	15	6	49.7					123
	I11	I21	I22	I31	I32	I33			
+23	16.2		16.2			7.8			

Field	Contents
EID	Element identification number (Integer > 0)
G	Grid point identification number (Integer > 0)
CID	Coordinate system identification number (Integer ≥ 0). A CID of -1 (integer) allows the user to input X1, X2, X3 as the center of gravity location in the basic coordinate system.
M	Mass value (Real)
X1,X2,X3	Offset distances from the grid point to the center of gravity of the mass in the coordinate system defined in field 4, unless CID = -1, in which case X1, X2, X3 are the coordinates of the center of gravity of the mass in the basic coordinate system (Real).
Iij	Mass moments of inertia measured at the mass c.g. in coordinate system defined by field 4·(Real). If CID = -1, the basic coordinate system is implied.

Remarks:

1. Element identification numbers must be unique with respect to all other element identification numbers.
2. For a more general means of defining concentrated mass at grid points, see CØNM1.
3. The continuation card may be omitted.
4. If CID = -1, offsets are internally computed as the difference between the grid point location and X1, X2, X3. The grid point locations may be defined in a nonbasic coordinate system. In this case, the values of Iij must be in a coordinate system that parallels the basic coordinate system.
5. The form of the inertia matrix about its c.g. is taken as:

$$\begin{bmatrix} M & & & & & \\ & M & & & \text{SYM.} & \\ & & M & & & \\ & & & I11 & & \\ & & & -I21 & I22 & \\ & & & -I31 & -I32 & I33 \end{bmatrix}$$

(Continued)

where $M = \int \rho dV$

$I11 = \int \rho (x_2^2 + x_3^2) dV$

$I22 = \int \rho (x_1^2 + x_3^2) dV$

$I33 = \int \rho (x_1^2 + x_2^2) dV$

$I21 = \int \rho x_1 x_2 dV$

$I31 = \int \rho x_1 x_3 dV$

$I32 = \int \rho x_2 x_3 dV$

and x_1, x_2, x_3 are components of distance from the c.g. in the coordinate system defined in Field 4. The negative signs for the off-diagonal terms are supplied by the program. A warning message is issued if the inertia matrix is non-positive definite, as this may cause fatal errors in dynamic analysis modules.

Input Data Card RBE3 Rigid Body Element, Form 3

Description: Defines the motion at a "reference" grid point as the weighted average of the motions at a set of other grid points.

Format and Example:

1	2	3	4	5	6	7	8	9	10
RBE3	EID		REFGRID	REFC	WT1	C1	G1,1	G1,2	
RBE3	14		100	1234	1.0	123	1	3	AE
	G1,3	WT2	C2	G2,1	G2,2	---	WT3	C3	
+E	5	4.7	1	2	4	6	5.2	2	AE
	G3,1	---		WT4	C4	G4,1	G4,2	---	
+F	7	8	...	5.1	1	15	16		AG
	"UM"	GM1	CM1	GM2	CM2	GM3	CM3		
+G	UM	100	14	5	3	7	2		
		GM4	CM4	GM5	CM5	GM6	CM6		

Field	Contents
EID	Identification number. Unique with respect to other rigid elements (integer > 0)
REFGRID	Reference grid point (integer > 0)
REFC	Global Components of motion whose values will be computed at the reference grid point. Any of the digits 1, 2, ..., 6 with no imbedded blanks (integer > 0).
WT_i	Weighting factor for components of motion on the following card at grid points $G_{i,j}$. (Real)
C_i	Global components of motion which have weighting factor WT_i at grid points $G_{i,j}$. Any of the digits 1, 2, ..., 6 with no imbedded blanks (integer > 0).
$G_{i,j}$	Grid point whose components C_i have weighting factor WT_i in the averaging equations (integer > 0)
UM	(Optional) BCD data word which indicates the start of the data set belonging to $\{u_m\}$. The DEFAULT is that all of the components in REFC at the reference grid point, and no others, will be placed in $\{u_m\}$.
GM_i	Grid points with components in $\{u_m\}$ (integer > 0).
CM_i	Components of motion at GM_i in $\{u_m\}$. Any of the digits 1, 2, ..., 6 with no imbedded blanks (integer > 0).

Remarks:

1. Blank spaces may be left at the end of a $G_{i,j}$ sequence.

(Continued)

2. The default for UM should be used except in cases where the user wishes to include some or all REFC components in displacement sets exclusive from the $\{u_m\}$ set. If the default is not used for UM:

   a. The total number of components in $\{u_m\}$ (i.e., the total number of dependent degrees of freedom defined by the element) must be equal to the number of components in REFC (four components in the example).

   b. The components in UM must be a subset of the components mentioned in REFC and $(G_{i,j}; C_i)$.

   c. The coefficient matrix $[R_m]$ in the constraints equation $[R_m]\{u_m\} + [R_n]\{u_n\} = 0$ must be nonsingular.

3. Dependent degrees of freedom assigned by one rigid element may not also be assigned dependent by another rigid element or by a multi-point constraint.

4. Rigid elements unlike MPC's are <u>not</u> selected through Case Control Deck.

5. Forces of constraint are not recovered.

6. Rigid elements are ignored in heat transfer problems.

7. The m-set coordinates specified on this card may not be specified on other cards that define mutually exclusive sets.

8. All element identification numbers must be unique.

Input Data Card R8E2 Rigid Body Element , Form 2

Description: Defines a rigid body whose independent degrees of freedom are specified at a single grid point and whose dependent degrees of freedom are specified at an arbitrary number of grid points.

Format and Example:

1	2	3	4	5	6	7	8	9	10
R8E2	EID	GN	CM	GM1	GM2	GM3	GM4	GM5	
R8E2	9	8	12	10	12	14	15	16	AE
	GM6	GM7	GM8	etc.					
+E	20								

Field	Contents
EID	Identification number of rigid element.
GN	The grid point to which all six independent degrees of freedom for the element are assigned (integer > 0).
CM	Component number of the dependent degrees of freedom in the global coordinate system at grid points GM1, GM2, etc. The components are indicated by any of the digits 1 - 6 with no imbedded blanks (integer > 0).
GM1, GM2, etc.	Grid points at which dependent degrees of freedom are assigned.

Remarks:

1. The components indicated by CM are made dependent (members of the $\{u_m\}$ set) at all grid points, GMi.
2. Dependent degrees of freedom assigned by one rigid element may not also be assigned dependent by another rigid element or by a multipoint constraint.
3. Element identification numbers must be unique.
4. Rigid elements, unlike MPC's, are not selected through the Case Control Deck.
5. Forces of constraint are not recovered.
6. Rigid elements are ignored in heat transfer problems.
7. See Section 2.5.4 for a discussion of rigid elements.
8. The m-set coordinates specified on this card may not be specified on other cards that define mutually exclusive sets.

Input Data Card MAT1 Material Property Definition, Form 1

Description: Defines the material properties for linear, temperature-independent, isotropic materials.

Format and Example:

1	2	3	4	5	6	7	8	9	10
MAT1	MID	E	G	NU	RHØ	A	TREF	GE	
MAT1	17	3.+7	1.9+7		4.28	6.5-6	5.37+2	0.23	ABC
	ST	SC	SS	MCSID					
+BC	20.+4	15.+4	12.+4	1003					

Field	Contents
MID	Material identification number (Integer > 0)
E	Young's modulus (Real or blank)
G	Shear modulus (Real or blank)
NU	Poisson's ratio (-1.0 < Real $\leq$ 0.5 or blank)
RHØ	Mass density (Real)
A	Thermal expansion coefficient (Real)
TREF	Thermal expansion reference temperature (Real)
GE	Structural element damping coefficient (Real)
ST,SC,SS	Stress limits for tension, compression, and shear (Real). (Used only to compute margins of safety in certain elements; they have no effect on the computational procedures.)
MCSID	Material Coordinate System identification number (Integer $\geq$ 0 or blank)

Remarks: 1. Either E or G must be specified (i.e., nonblank).

2. If any one of E, G, or NU is blank, it will be computed to satisfy the identity E = 2(1+NU)G; otherwise, values supplied by the user will be used. This calculation is only made for initial values of E, G, and NU.

3. The material identification number must be unique for all MAT1, MAT2, MAT3 and MAT9 cards.

4. MAT1 materials may be made temperature dependent by use of the MATT1 card.

5. The mass density, RHØ, will be used to automatically compute mass for all structural elements.

6. If E and NU or G and NU are both blank, they will both be given the value 0.0.

(Continued)

7. Weight density may be used in field 6 if the value 1/g is entered on the PARAM card WTMASS, where g is the acceleration of gravity (see p. 11-7).

8. MCSID must be nonzero if the CURV module is used to calculate stresses or strains at grid points.

9. To obtain the damping coefficient, GE, multiply the critical damping ratio C/C_0, by 2.0.

Input Data Card ASET Selected Coordinates for the a-set

Description: Defines coordinates (degrees of freedom) that the user desires to place in the analysis set. Used to define the number of independent degrees of freedom.

Format and Example:

1	2	3	4	5	6	7	8	9	10
ASET	ID	C	ID	C	ID	C	ID	C	
ASET	16	2	23	3516			1	4	

Field	Contents
ID	Grid or scalar point identification number (Integer > 0).
C	Component number, zero or blank for scalar points, any unique combinations of the digits 1-6 for grid points.

Remarks:

1. Coordinates specified on this card form members of a mutually exclusive set. They may not be specified on other cards that define mutually exclusive sets.
2. As many as 24 coordinates may be placed in the analysis set by a single card.
3. When ASET and/or ASET1 cards are present, all degrees of freedom not otherwise constrained will be placed in the o-set.
4. Continuation cards are not allowed.

Input Data Card ASET1 Selected Coordinates for the a-set, Alternate Form

Description: Defines coordinates (degrees of freedom) that the user desires to place in the analysis set. Used to define the number of independent degrees of freedom.

Format and Example:

1	2	3	4	5	6	7	8	9	10
ASET1	C	G	G	G	G	G	G	G	abc
ASET1	345	2	1	3	10	9	6	5	ABC
+bc	G	G	G	--etc--					
+8C	7	8		--etc--					

Alternate Form

1	2	3	4	5	6	7	8	9	10
ASET1	C	ID1	"THRU"	ID2					
ASET1	123456	7	THRU	109					

Field	Contents
C	Component number (any unique combination of the digits 1-6 (with no imbedded blanks) when point identification numbers are grid points; must be null or zero if point identification numbers are scalar points).
G,ID1,ID2	Grid or scalar point identification numbers (Integer > 0, ID1 < ID2).

Remarks:

1. Coordinates specified on this card form members of a set that is exclusive from other sets defined by bulk data cards.
2. When ASET and/or ASET1 cards are present, all degrees of freedom not otherwise constrained will be placed in the o-set.
3. If the alternate form is used, all points in the sequence ID1 thru ID2 are not required to exist, but there must be at least one degree of freedom in the a-set for the model, or a fatal error will result. Any points implied in the THRU that do not exist will collectively produce a warning message but will otherwise be ignored.

Input Data Card DYNRED Dynamic Reduction Data

Description: Defines data needed to perform dynamic reduction

Format and Example:

1	2	3	4	5	6	7	8	9	10
DYNRED	SID	FMAX	NIRV	NIT	IDIR	NQDES			
DYNRED	2	20.0							

Field	Contents
SID	Set identification number (Unique Integer > 0)
FMAX	Highest frequency of interest (cycles per unit time)(Real > 0.)
NIRV	Number of initial random vectors (Integer ≥ 0 or blank) Default 6
NIT	Number of iterations (100 ≥ Integer > or blank) Default = 10
IDIR	Integer used to select starting point to generate initial random vectors (any of the integers 0 thru 9 or blank)
NQDES	Number of generalized coordinates to be used on present computation (Integer ≥ 0 or blank). If 0 (zero) or blank, the autoselection feature of Remark 4 is used.

Remarks:

1. Dynamic reduction uses generalized coordinates to approximate the v-set ("free to vibrate") degrees of freedom. This set is the combination of the o-, c-, and r-sets. The generalized functions are approximate eigenvectors, with the b-set fixed. The strengths of the generalized functions are contained in the q-set. The user must define scalar points (SPOINT bulk data card) for these generalized coordinates, and must place them in the q-set and the a-set. After the approximate eigenvectors are found, their generalized coordinates are combined with the b-set to determine the exact eigensolution or direct forced response solution of the global system. See Section 3.3.24 for the equations used.

2. Dynamic reduction data must be selected in the Case Control Deck (DYNRED=SID) to be used by MSC/NASTRAN.

3. FMAX is needed to assist the program in selecting a good set of vectors for the generalized coordinates. The intention is to represent all modes below FMAX accurately. Do not select FMAX larger than necessary.

4. It is recommended that the number of generalized coordinates be 1.5 times the number of vibration modes whose natural frequency is below FMAX. Two methods of selecting this number are provided.

   If NQDES > 0, the number is set by NQDES. NQDES must be equal to or less than N_q, the number of degrees of freedom in the q-set. The remaining degrees of freedom, (N_q-NQDES) in number, are removed prior to eigensolutions, and given null displacements in the eigenvector matrix. In the direct forced response rigid formats, uncoupled unit spring coefficients are placed on the unused degrees of freedom.

(Continued)

If NØDES is 0 or blank ("autoselection") the number of generalized coordinates required is determined by the program from FMAX, using a Sturm sequence technique. If the number required is greater than N_g, a fatal error results. If it is equal to or less than N_g, any unused degrees of freedom are disposed of as described above. This is the recommended method.

Approximate natural frequencies, eigenvectors, and the scalar identification number of the generalized coordinates are output if requested by PARAM, PRPHIVZ.

5. The user may also include physical degrees of freedom in the a-set by use of the following cards. See Section 1.4 for a description of these sets, and default actions if they are not used.

Card Names		Function
Non-superelement or residual structure	Superelement	
BSETi	SEBSETi	Fixed in approximate eigenvectors
CSETi	SECSETi	Free in approximate eigenvectors
SUPØRT	SESUP	Reference points for rigid-body modes. Free in approximate eigenvectors.

6. (Superelements) Dynamic reduction may be applied to both superelements and the residual structure. Generalized coordinates are defined on SPØINT bulk data cards, and attached to superelements with SEQSETi bulk data cards. They are automatically members of the residual structure, also.

7. (Nonsuperelements or residual structure) Generalized coordinates must be defined on SPØINT bulk data cards, and be placed on ASETi and QSETi bulk data cards.

   Generalized coordinates of the superelements may be processed in two different ways in the residual structure. If placed on ASETi cards they are regarded as dynamic variables. If placed on selected SPCi cards they are in effect removed from the model. This is useful for eliminating generalized coordinates with implausibly high natural frequencies whose eigenvectors tend to be numerical noise, or for non-essential modes.

8. If the default for IDIR is taken (0 or blank), the initial random vectors will be identical for solutions with the same number of generalized coordinates and the same values of NIRV and NIT. Other values of IDIR may be used to check the sensitivity of the solution to the random selection of initial vectors.

9. Field 9 was used to request autoselection prior to MSC/61. For reasons of upward compatibility, data may be placed in this field, but it is ignored.

Input Data Card QSET Generalized Coordinate for Dynamic Reduction and Component Modal Synthesis

Description: Places generalized coordinates to be used for dynamic reduction in the q-set

Format and Example:

1	2	3	4	5	6	7	8	9	10
QSET	ID	C	ID	C	ID	C	ID	C	
QSET	15	123456	1	7	9	2	105	6	

Field	Contents
ID	Identification number for superelement (Integer > 0)
C	Component number (any unique combination of the digits 1-6 (with no imbedded blanks) when point identification numbers are grid points; must be null if point identification numbers are scalar points).

Remarks:

1. Coordinates specified on this card form members of a mutually exclusive set. They may not be specified on other cards that define mutually exclusive sets. See Section 1.4.1 for a list of these cards.
2. Continuation cards are not allowed.
3. If a q-set exists, the o-set must also exist. Except for the residual structure, the o-set is always present in superelement analysis. In the residual structure, an o-set can be created by placing some degrees of freedom in the a-set using ASETi cards. The remainder of the f-set will go to the o-set. If no physical a-set points are desired, a disjoint grid point can be added and placed in the a-set. This disjoint point will be eliminated by the auto-omit feature.
4. For use with component modal synthesis, these degrees of freedom will represent the generalized displacements of the user-supplied modes. The size of this set must equal the number of the user-supplied modes.
5. Modal masses, stiffness, damping and loads may be defined directly on these coordinates via CELASi, etc. data cards.

Input Data Card QSET1 Generalized Coordinate for Dynamic Reduction and Component Modal Synthesis

Description: Places generalized coordinates to be used for dynamic reduction in the q-set

Format and Example:

1	2	3	4	5	6	7	8	9	10
QSET1	C	G1	G2	G3	G4	G5	G6	G7	
QSET1	123456	1	7	9	22	105	6	22	+ABC
	G8	G9	-etc.-						
+ABC	52	53							

Alternate Form

QSET1	C	GID1	"THRU"	GID2					
QSET1	0	101	THRU	110					

Field	Contents
C	Component number (any unique combination of the digits 1-6 (with no imbedded blanks) when point identification numbers are grid points; must be null if point identification numbers are scalar points).
G_i,GID_i	Grid or scalar point identification number (Integer > 0)

Remarks:

1. Coordinates specified on this card form members of a mutually exclusive set. They may not be specified on other cards that define mutually exclusive sets. See Section 1.4.1 for a list of these cards.
2. If a q-set exists, the o-set must also exist. Except for the residual structure, the o-set is always present in superelement analysis. In the residual structure, an o-set can be created by placing some degrees of freedom in the a-set using ASETi cards. The remainder of the f-set will go to the o-set. If no physical a-set points are desired, a disjoint grid point can be added and placed in the a-set. This disjoint point will be eliminated by the auto-omit feature.
3. For use with component modal synthesis, these degrees of freedom will represent the generalized displacements of the user supplied modes. The size of this set must equal the number of the user-supplied modes.
4. Modal masses, stiffnesses, damping and loads may be defined directly on these coordinates via CELASi, etc. data cards.

Input Data Card SUPØRT Fictitious Support

Description: Defines coordinates at which the user desires determinate reactions to be applied to a free body during analysis

Format and Example:

1	2	3	4	5	6	7	8	9	10
SUPØRT	ID	C	ID	C	ID	C	ID	C	
SUPØRT	16	215							

Field	Contents
ID	Grid or scalar point identification number (Integer > 0)
C	Component number (zero or blank for scalar points; any unique combination of the digits 1-6 for grid points)

Remarks:

1. Coordinates specified on this card form members of a mutually exclusive set. They may not be specified on other cards that define mutually exclusive sets. See Section 1.4.1 for a list of these cards.
2. From one to twenty-four support coordinates may be defined on a single card.
3. See Section 3.5.3 of The NASTRAN Theoretical Manual for a discussion of supported coordinates (members of the r-set).
4. Continuation cards are not allowed.

Input Data Card EIGR Real Eigenvalue Extraction Data

Description: Defines data needed to perform real eigenvalue analysis

Format and Example:

1	2	3	4	5	6	7	8	9	10
EIGR	SID	METHØD	F1	F2	NE	ND		E	
EIGR	13	INV	1.9	15.6	10	12		1.-6	ABC
	NØRM	G	C						
+BC	PØINT	32	4						

Field	Contents
SID	Set identification number (Unique integer > 0)
METHØD	Method of eigenvalue extraction, one of the BCD values, "INV," "GIV," or "MGIV"
	INV - Inverse power method, symmetric matrix operations
	GIV - Givens' method of tridiagonalization
	MGIV - Modified Givens' method
F1,F2	Frequency range of interest (Real $\geq$ 0.0; F1 < F2). (Required for METHØD = "INV"). For GIV and MGIV, frequency range in which eigenvectors will be computed, except if ND > 0, in which case the eigenvectors for the first ND positive roots are computed).
NE	Estimate of number of roots in range (Required for METHØD = "INV"). (Integer > 0).
ND	Desired number of roots (eigenvalues and eigenvectors) for METHØD = "INV" (Integer > 0). Desired number of eigenvectors for METHØD = "GIV" and "MGIV" (Default is 3 NE) (Integer $\geq$ 0).
E	Mass orthogonality test parameter (Default is 1.E-10) (Real > 0.0). Nonzero values are also used for convergence in "INV". Inverse power limits this value to $10^{-4} \leq E \leq 10^{-6}$.
NØRM	Method for normalizing eigenvectors, one of the BCD values, "MASS," "MAX" or "PØINT"
	MASS - Normalize to unit value of the generalized mass
	MAX - Normalize to unit value of the largest component in the analysis set
	PØINT - Normalize to unit value of the component defined in fields 3 and 4 (defaults to "MAX" if defined component is zero)

(Continued)

G — Grid or scalar point identification number (Required if and only if NØRM = "PØINT") (Integer $\geq$ 0)

C — Component number (One of the integers 1-6) (Required if and only if NØRM = "PØINT") and G is a geometric grid point)

Remarks:

1. See Section 10.1 of the Theoretical Manual for a discussion of method selection.
2. Real eigenvalue extraction data sets must be selected in the Case Control Deck (METHØD = SIO) to be used by MSC/NASTRAN.
3. The units of F1 and F2 are cycles per unit time.
4. The continuation card is required.
5. If METHØD = "GIV" or "MGIV," all eigenvalues are found.
6. If METHØD = "GIV," the mass matrix for the analysis set must be positive definite. This means that all degrees of freedom, including rotations, must have mass properties. ØMIT cards may be used to remove massless degrees of freedom.
7. A nonzero value of E in field 9 also modifies the convergence criteria. See Sections 10.3.6 and 10.4.2.2 of the Theoretical Manual for a discussion of convergence criteria.
8. If NØRM = MAX, components that are not in the analysis set may have values larger than unity.
9. If NØRM = PØINT, the selected component must be in the analysis set.
10. The desired number of roots (NO) includes all roots previously found, such as rigid body modes determined with the use of the SUPØRT card, or the number of roots found on the previous run when restarting and APPENDing the eigenvector file.
11. MGIV is a modified form of the Givens' method that allows a non-positive definite mass matrix for the analysis set (i.e., massless degrees of freedom may exist in the analysis set). The MGIV method should give improved accuracy for the lowest frequency solutions.

APPENDIX B

NASTRAN Data Set for Disk Drive

```
ID    THURSTON, MG
TIME 300
SOL 3    $NORMAL MODES ANALYSIS
ALTER 450 $
OUTPUT2 OUGV1,//C,N,-1/C,N,11/V,N,Z $
OUTPUT2 ,,,,//C,N,-9/C,N,11/V,N,Z $
ENDALTER $
CEND
 TLE=DISK DRIVE (ITEM1&2&3(1ARM))
  BTITLE=GEN/RED & COUPMASS OPTION
 LABEL=
 SP= ALL
 SPC=
 NRED=20
 THOD = 30

 AKE OUT PATRAN BEGIN BULK CARD

 GIN BULK
 PARAM,GRDPNT,0
 RAM,AUTOSPC,YES
 RAM,COUPMASS,1
 $$$$DYNRED,20,7500.0
 NRED,20,2200.0
 GR,30,MGIV,1000.,2200.,,,,,,+EI1
 I1,MASS
SPOINT,10001,THRU,10075
ASET1,0,10001,THRU,10075
QSET1,0,10001,THRU,10075
SUPORT,1031,123,1399,13,1170,3
$$
$$
$DISK DRIVE (ITEM1&2)
$--BULK DATA CARDS PRODUCED BY "PATNAS" VERSION 1.7 :     2-JUL-86   13:31:34
CORD2R          1          0.       0.       0.       0.       0.       1.00000 CF     1
+CF     1 1.00000 0.       1.00000
CORD2R          2          0.       0.      -1.38750 0.       0.      -0.38750 CF     2
+CF     2 1.00000 0.      -0.38750
GRID         1001        1 0.       2.71250-1.38750        1
GRID         1002        1 0.       2.66250-1.38750        1
GRID         1003        1 0.       2.65475-0.69375        1
GRID         1004        1 0.       2.62200 0.             1
GRID         1005        1 0.       2.12100 0.             1
GRID         1006        1 0.       1.62000 0.             1
GRID         1007        1 0.       1.62000 0.20000        1
GRID         1008        1-0.35063  1.58160 0.20000        1
GRID         1009        1-0.35063  1.58160 0.             1
GRID         1010        1-0.45907  2.07072 0.             1
GRID         1011        1-0.56750  2.55985 0.             1
GRID         1012        1-1.23619  2.65090 0.             1
GRID         1013        1-0.57459  2.59182-0.69375        1
GRID         1014        1-0.58168  2.62380-1.38750        1
GRID         1015        1-0.58168  2.68750-1.38750        1
GRID         1016        1-1.23619  2.65090-0.69375        1
GRID         1017        1 0.58168  2.68750-1.38750        1
GRID         1018        1 0.58168  2.62380-1.38750        1
GRID         1019        1 0.57459  2.59182-0.69375        1
GRID         1020        1 1.23619  2.65090-0.69375        1
GRID         1021        1 1.23619  2.65090 0.             1
GRID         1022        1 0.56750  2.55985 0.             1
```

```
GRID          1024          1 0.35063 1.58160 0.                    1
GRID          1025          1 0.35063 1.58160 0.20000               1
GRID          1026          1-0.68464 1.46822 0.20000               1
GRID          1027          1-0.68464 1.46822 0.                    1
GRID          1028          1-0.89637 1.92228 0.                    1
GRID          1029          1-1.10811 2.37634 0.                    1
GRID          1030          1-1.12195 2.40602-0.69374               1
GRID          1031          1-1.13579 2.43570-1.38750               1
GRID          1032          1-1.23619 2.65090-1.38750               1
GRID          1033          1 1.23619 2.65090-1.38750               1
GRID          1034          1 1.13579 2.43570-1.38750               1
GRID          1035          1 1.12195 2.40602-0.69375               1
GRID          1036          1 1.10810 2.37634 0.                    1
GRID          1037          1 0.89637 1.92228 0.                    1
GRID          1038          1 0.68464 1.46822 0.                    1
GRID          1039          1 0.68464 1.46822 0.20000               1
GRID          1040          1-1.04132 1.24099 0.20000               1
GRID          1041          1-1.04132 1.24099 0.                    1
GRID          1042          1-1.36335 1.62478 0.                    1
GRID          1043          1-1.68539 2.00857 0.                    1
GRID          1044          1-2.53110 1.77231 0.                    1
GRID          1045          1-1.70474 2.03162-0.63756               1
GRID          1046          1-1.72749 2.05874-1.38750               1
GRID          1047          1-1.88019 2.24054-1.38750               1
GRID          1048          1-2.46900 1.72882-0.63756               1
GRID          1049          1 1.88019 2.24064-1.38750               1
GRID          1050          1 1.72749 2.05874-1.38750               1
GRID          1051          1 1.70474 2.03162-0.63757               1
GRID          1052          1 2.46900 1.72882-0.63756               1
GRID          1053          1 2.53110 1.77231 0.                    1
GRID          1054          1 1.68539 2.00857 0.                    1
GRID          1055          1 1.36335 1.62478 0.                    1
GRID          1056          1 1.04132 1.24099 0.                    1
GRID          1057          1 1.04132 1.24099 0.20000               1
GRID          1058          1-1.32703 0.92919 0.20000               1
GRID          1059          1-1.32703 0.92919 0.                    1
GRID          1060          1-1.73742 1.21656 0.                    1
GRID          1061          1-2.14782 1.50392 0.                    1
GRID          1062          1-2.17247 1.52118-0.63756               1
GRID          1063          1-2.20147 1.54149-1.38750               1
GRID          1064          1-2.39597 1.67769-1.38750               1
GRID          1065          1 2.39597 1.67769-1.38750               1
GRID          1066          1 2.20147 1.54149-1.38750               1
GRID          1067          1 2.17247 1.52118-0.63756               1
GRID          1068          1 2.14782 1.50392 0.                    1
GRID          1069          1 1.73742 1.21656 0.                    1
GRID          1070          1 1.32703 0.92919 0.                    1
GRID          1071          1 1.32703 0.92919 0.20000               1
GRID          1072          1-1.40296 0.81000 0.20000               1
GRID          1073          1-1.40296 0.81000 0.                    1
GRID          1074          1-1.88965 0.95905 0.                    1
GRID          1075          1-2.37634 1.10810 0.                    1
GRID          1076          1-2.82533 0.75708 0.                    1
GRID          1077          1-2.40360 1.12082-0.63716               1
GRID          1078          1-2.43570 1.13579-1.38750               1
GRID          1079          1-2.65090 1.23619-1.38750               1
GRID          1080          1-2.82533 0.75708-0.69375               1
GRID          1081          1 2.65090 1.23619-1.38750               1
GRID          1082          1 2.43570 1.13579-1.33750               1

GRID          1202          1 1.51250-2.23724 0.                    1
```

```
GRID        1143        1-2.63750-0.83230-1.38750       1
GRID        1144        1-2.82750-0.83230-1.38750       1
GRID        1145        1-2.74475-1.24850-0.69375       1
GRID        1146        1 2.82750-0.83230-1.38750       1
GRID        1147        1 2.63750-0.83230-1.38750       1
GRID        1148        1 1.40296-0.81000 0.20000       1
GRID        1149        1 2.65475-0.83230-0.69375       1
GRID        1150        1 2.74475-1.24850-0.69375       1
  ID        1151        1 2.71200-1.24850 0.            1
  ID        1152        1 1.40296-0.81000 0.            1
  ID        1153        1 2.62200-0.83230 0.            1
  ID        1154        1 2.01248-0.82115 0.            1
  ID        1155        1 2.82750-1.24850-1.38750       1
  ID        1156        1 1.14551-1.14551 0.20000       1
  ID        1157        1 0.81000-1.40296 0.20000       1
  ID        1158        1 0.28131-1.59539 0.20000       1
  ID        1159        1 0.      -1.62000 0.20000      1
  ID        1160        1-0.41929-1.56480 0.20000       1
  ID        1161        1-1.14551-1.14551 0.            1
  ID        1162        1-0.81000-1.40296 0.20000       1
  ID        1163        1-0.81000-1.40296 0.            1
  ID        1164        1-1.88376-1.19701 0.            1
  ID        1165        1-1.72700-1.53600 0.            1
  ID        1166        1-2.62200-1.24850 0.            1
  ID        1167        1-2.65475-1.24850-0.69375       1
GRID        1168        1-2.68750-1.24850-1.38750       1
GRID        1169        1-2.82750-1.24850-1.38750       1
GRID        1170        1 2.68750-1.24850-1.38750       1
GRID        1171        1 2.65475-1.24850-0.69375       1
GRID        1172        1 1.14551-1.14551 0.            1
GRID        1173        1 2.62200-1.24850 0.            1
GRID        1174        1 1.73276-1.19701 0.            1
GRID        1175        1 2.32000-1.24850 0.            1
GRID        1176        1 1.33526-1.45086 0.            1
GRID        1177        1 1.52500-1.75620 0.            1
GRID        1178        1 2.68750-1.60235-1.38750       1
GRID        1179        1 2.82750-1.60235-1.38750       1
GRID        1180        1 0.81000-1.40296 0.            1
GRID        1181        1 0.55407-1.52230 0.20000       1
GRID        1182        1 1.32500-2.18700 0.            1
GRID        1183        1 1.06750-1.79498 0.            1
GRID        1184        1 0.75204-1.90489 0.25600       1
GRID        1185        1 0.55407-1.52230 0.            1
GRID        1186        1 0.28131-1.59539 0.            1
GRID        1187        1 0.      -1.62000 0.            1
GRID        1188        1-0.41929-1.56480 0.            1
GRID        1189        1-0.83200-1.53600 0.            1
GRID        1190        1-0.83200-1.53600 0.28000       1
GRID        1191        1-1.72700-1.53600 0.28000       1
GRID        1192        1-2.62200-1.53600 0.28000       1
GRID        1193        1-2.62200-1.53600 0.            1
GRID        1194        1-2.65475-1.53600-0.69375       1
GRID        1195        1-2.68750-1.53600-1.38750       1
GRID        1196        1-2.82750-1.53600-1.38750       1
GRID        1197        1 2.65475-1.60235-0.69375       1
GRID        1198        1 2.62200-1.60235 0.            1
GRID        1199        1 1.82763-1.52660 0.            1
GRID        1200        1 2.32000-1.60235 0.            1
GRID        1201        1 1.92250-1.85620 0.            1
GRID        1202        1 1.51250-2.23724 0.            1
```

```
GRID    1203          1 2.65475-1.95620-0.69375        1
GRID    1204          1 2.68750-1.95620-1.38750        1
GRID    1205          1 2.82750-1.95620-1.38750        1
GRID    1206          1 1.32500-2.18700 0.31200        1
GRID    1207          1 1.51250-2.23724 0.31200        1
GRID    1208          1 0.75204-1.90489 0.             1
GRID    1209          1 0.95000-2.28748 0.31200        1
GRID    1210          1 0.95000-2.28748 0.             1
GRID    1211          1 0.47840-2.07869 0.             1
GRID    1212          1 0.      -2.09100 0.            1
GRID    1213          1-0.41929-2.06340 0.             1
GRID    1214          1-0.83200-2.04900 0.             1
GRID    1215          1-0.83200-2.04900 0.28000        1
GRID    1216          1-1.72700-2.04900 0.28000        1
GRID    1217          1-2.62200-2.04900 0.28000        1
GRID    1218          1-2.62200-2.04900 0.             1
GRID    1219          1-2.65475-2.04900-0.69375        1
GRID    1220          1-2.68750-2.04900-1.38750        1
GRID    1221          1-2.82750-2.04900-1.38750        1
GRID    1222          1 2.62200-1.95620 0.             1
GRID    1223          1 2.32000-1.95620 0.31200        1
GRID    1224          1 2.32000-1.95620 0.             1
GRID    1225          1 1.70000-2.28748 0.31200        1
GRID    1226          1 1.70000-2.28748 0.             1
GRID    1227          1 2.32000-2.38510 0.31200        1
GRID    1228          1 2.62200-2.38510 0.             1
GRID    1229          1 2.65475-2.38510-0.69375        1
GRID    1230          1 2.68750-2.38510-1.38750        1
GRID    1231          1 2.82750-2.38510-1.38750        1
GRID    1232          1 1.41875-2.58712 0.31200        1
GRID    1233          1 1.32500-2.56200 0.31200        1
GRID    1234          1 1.13750-2.61224 0.31200        1
GRID    1235          1 1.51250-2.61224 0.31200        1
GRID    1236          1 1.00024-2.74950 0.31200        1
GRID    1237          1 0.95000-2.93700 0.31200        1
GRID    1238          1 0.67548-2.56200 0.31200        1
GRID    1239          1 0.67548-2.56200 0.             1
GRID    1240          1 0.      -2.56200 0.            1
GRID    1241          1 0.      -2.93700 0.30662       1
GRID    1242          1-0.41929-2.56200 0.             1
GRID    1243          1-0.83200-2.56200 0.             1
GRID    1244          1-0.41929-2.93700 0.29321        1
GRID    1245          1-0.83200-2.56200 0.28000        1
GRID    1246          1-1.72700-2.56200 0.28000        1
GRID    1247          1-2.62200-2.56200 0.28000        1
GRID    1248          1-2.62200-2.56200 0.             1
GRID    1249          1-2.65475-2.56200-0.69375        1
GRID    1250          1-2.68750-2.56200-1.38750        1
GRID    1251          1-2.82750-2.56200-1.38750        1
GRID    1252          1 1.64976-2.74950 0.31200        1
GRID    1253          1 1.70000-2.93700 0.31200        1
GRID    1254          1 2.32000-2.38510 0.             1
GRID    1255          1 1.97452-2.56200 0.31200        1
GRID    1256          1 1.97452-2.56200 0.             1
GRID    1257          1 2.32000-2.81400 0.31200        1
GRID    1258          1 2.32000-2.81400 0.             1
GRID    1259          1 2.65475-2.81400-0.69375        1
GRID    1260          1 2.62200-2.81400 0.             1
GRID    1261          1 2.68750-2.81400-1.38750        1
GRID    1262          1 2.82750-2.81400-1.38750        1
```

```
GRID    1324        1 0.75180-3.89100 0.                    1
GRID    1325        1 0.19060-3.89100 0.                    1
GRID    1326        1-0.83200-3.56100 0.                    1
GRID    1327        1-1.61100-3.26100 0.                    1
GRID    1328        1-1.61100-3.56100 0.                    1
GRID    1329        1-2.56000-3.37350 0.                    1
GRID    1330        1-2.39000-3.26100 0.                    1
GRID    1331        1-2.60087-3.37350-0.69375               1
GRID    1332        1-2.64175-3.37350-1.38750               1
GRID    1333        1-2.78175-3.37350-1.38750               1
GRID    1334        1 2.78175-3.89100-1.38750               1
GRID    1335        1 1.81430-3.89100 0.28000               1
GRID    1336        1 2.64175-3.89100-1.38750               1
GRID    1337        1 2.31560-3.89100 0.28000               1
GRID    1338        1 2.56000-3.89100 0.                    1
GRID    1339        1 2.60087-3.89100-0.69375               1
GRID    1340        1 2.56000-3.89100 0.28000               1
GRID    1341        1 1.31300-3.89100 0.28000               1
GRID    1342        1-0.83200-3.89100 0.28000               1
GRID    1343        1-0.19060-3.89100 0.28000               1
GRID    1344        1 0.75180-3.89100 0.28000               1
GRID    1345        1 0.19060-3.89100 0.28000               1
GRID    1346        1 1.31300-4.24850 0.28000               1
GRID    1347        1-1.61100-3.89100 0.28000               1
GRID    1348        1-2.39000-3.56100 0.                    1
GRID    1349        1-2.39000-3.89100 0.28000               1
GRID    1350        1-2.60087-3.56100-0.69375               1
GRID    1351        1-2.56000-3.56100 0.                    1
GRID    1352        1-2.64175-3.56100-1.38750               1
GRID    1353        1-2.78175-3.56100-1.38750               1
GRID    1354        1 2.78175-4.24850-1.38750               1
GRID    1355        1 2.64175-4.24850-1.38750               1
GRID    1356        1 1.81430-4.24850 0.28000               1
GRID    1357        1 2.31560-4.24850 0.28000               1
GRID    1358        1 2.60472-4.24850-0.75909               1
GRID    1359        1 2.56000-4.24850 0.28000               1
GRID    1360        1 2.56000-4.24850 0.                    1
GRID    1361        1-1.62550-4.24850 0.28000               1
GRID    1362        1-0.86100-4.24850 0.28000               1
GRID    1363        1 2.56000-4.60600 0.28000               1
GRID    1364        1 0.75180-4.24850 0.28000               1
GRID    1365        1-0.19060-4.24850 0.28000               1
GRID    1366        1 0.19060-4.24850 0.28000               1
GRID    1367        1 0.75180-4.60600 0.28000               1
GRID    1368        1 1.31300-4.60600 0.28000               1
GRID    1369        1 1.81430-4.60600 0.28000               1
GRID    1370        1-2.39000-4.24850 0.28000               1
GRID    1371        1-2.56000-4.33350 0.                    1
GRID    1372        1-2.39000-4.24850 0.                    1
GRID    1373        1-2.64175-4.35850-1.38750               1
GRID    1374        1-2.60473-4.34718-0.75921               1
GRID    1375        1-2.78175-4.39850-1.38750               1
GRID    1376        1-2.60862-5.13574-0.82520               1
GRID    1377        1-2.78175-5.23600-1.38750               1
GRID    1378        1 2.64175-4.60600-1.38750               1
GRID    1379        1 2.78175-4.60600-1.38750               1
GRID    1380        1 2.60861-4.60600-0.82501               1
GRID    1381        1 2.31560-4.60600 0.28000               1
GRID    1382        1 2.56000-4.60600 0.                    1
```

```
GRID        1384        1-0.89000-4.60600 0.28000        1
GRID        1385        1-1.64000-4.60600 0.28000        1
GRID        1386        1-2.39000-4.60600 0.28000        1
GRID        1387        1-0.19060-4.60600 0.28000        1
GRID        1388        1-0.89000-4.60600 0.             1
GRID        1389        1 2.31560-4.60600 0.             1
GRID        1390        1 0.19060-4.60600 0.28000        1
GRID        1391        1-0.19060-4.60600 0.             1
GRID        1392        1 0.19060-4.60600 0.             1
GRID        1393        1 0.75180-4.60600 0.             1
GRID        1394        1 1.31300-4.60600 0.             1
GRID        1395        1 1.81430-4.60600 0.             1
GRID        1396        1-2.39000-4.93600 0.             1
GRID        1397        1-2.56000-5.10600 0.             1
GRID        1398        1-2.60699-5.13474-0.79756        1
GRID        1399        1-2.64175-5.15600-1.38750        1
GRID        1400        1-2.64175-5.23600-1.38750        1
GRID        1401        1 2.64175-4.81250-1.38750        1
GRID        1402        1 2.60861-4.81250-0.82501        1
GRID        1403        1 2.78175-4.81250-1.38750        1
GRID        1404        1 2.60861-5.13573-0.82501        1
GRID        1405        1 2.78175-5.23600-1.38750        1
GRID        1406        1 2.56000-4.81250 0.             1
GRID        1407        1 2.31560-4.81250 0.             1
GRID        1408        1-0.19060-4.81250 0.28000        1
GRID        1409        1-0.89000-4.93600 0.             1
GRID        1410        1-1.64000-4.93600 0.             1
GRID        1411        1-0.19060-5.10600 0.28000        1
GRID        1412        1-0.19060-5.24400 0.28000        1
GRID        1413        1-0.19060-4.81250 0.             1
GRID        1414        1 0.19060-4.81250 0.28000        1
GRID        1415        1 0.19060-5.10600 0.28000        1
GRID        1416        1 0.19060-5.24400 0.28000        1
GRID        1417        1 1.81430-4.81250 0.             1
GRID        1418        1 0.19060-4.81250 0.             1
GRID        1419        1 0.75130-4.81250 0.             1
GRID        1420        1 1.31300-4.81250 0.             1
GRID        1421        1-1.72500-5.10600 0.             1
GRID        1422        1-1.74645-5.13225-0.72834        1
GRID        1423        1-1.76587-5.15600-1.38750        1
GRID        1424        1-1.76587-5.23600-1.38750        1
GRID        1425        1 2.56000-5.10600 0.             1
GRID        1426        1 2.60696-5.13472-0.79698        1
GRID        1427        1 2.64175-5.15600-1.38750        1
GRID        1428        1 2.64175-5.23600-1.38750        1
GRID        1429        1 2.31560-5.10600 0.             1
GRID        1430        1 1.81430-5.10600 0.             1
GRID        1431        1 0.19060-5.24400 0.             1
GRID        1432        1-0.19060-5.10600 0.             1
GRID        1433        1-0.89000-5.10600 0.             1
GRID        1434        1 0.19060-5.26775-0.65906        1
GRID        1435        1-0.19060-5.24400 0.             1
GRID        1436        1-0.19060-5.26775-0.65906        1
GRID        1437        1 0.19060-5.10600 0.             1
GRID        1438        1 1.31300-5.10600 0.             1
GRID        1439        1 0.75130-5.10600 0.             1
GRID        1440        1-0.89000-5.12975-0.65906        1
GRID        1441        1-0.89000-5.15600-1.38750        1
GRID        1442        1-0.89000-5.23600-1.38750        1
```

```
GRID     2047        2 1.71315-0.78535 0.04000        2
GRID     2048        2 1.42413-1.66888 0.04000        2
GRID     2049        2 1.59825-0.90025 0.04000        2
GRID     2050        2 1.25000-1.74100 0.04000        2
GRID     2051        2 1.25000-0.75600 0.04000        2
GRID     2052        2 1.07587-1.66888 0.04000        2
GRID     2053        2 0.90175-0.90025 0.04000        2
GRID     2054        2 0.90175-1.59675 0.04000        2
GRID     2055        2 0.75750-1.24850 0.04000        2
GRID     2056        2 1.31300-5.23600 0.             2
GRID     2057        2 1.31300-5.15600 0.             2
GRID     2058        2 1.31300-5.10600-0.08500        2
GRID     2059        2 1.32412-4.51620-0.08500        2
GRID     2060        2 1.32500-2.93700-0.08500        2
GRID     2061        2 1.35746-3.38437-0.08500        2
GRID     2062        2 1.33523-3.92641-0.08500        2
GRID     2063        2 1.25000-2.08100-0.08500        2
GRID     2064        2 1.25000-1.90350 0.04000        2
GRID     2065        2 1.62239 0.79438-0.08500        2
GRID     2066        2 1.25000 0.25000-0.08500        2
GRID     2067        2 1.25000-0.41600-0.08500        2
GRID     2068        2 1.25000-0.59350 0.04000        2
GRID     2069        2 1.74739 1.17234-0.08500        2
GRID     2070        2 2.13576 1.87022 0.             2
GRID     2071        2 2.01384 1.71754 0.             2
GRID     2072        2 1.87239 1.55030-0.08500        2
GRID     2073        2 1.01842-1.80758 0.04000        2
GRID     2074        2 0.78685-0.78535 0.04000        2
GRID     2075        2 0.78685-1.71165 0.04000        2
GRID     2076        2 0.59500-1.24850 0.04000        2
GRID     2077        2 1.23619 2.65090 0.             2
GRID     2078        2 0.       2.73750 0.            2
GRID     2079        2 0.56120-5.23600 0.             2
GRID     2080        2 0.56120-5.15600 0.             2
GRID     2081        2 0.56120-5.10600-0.08500        2
GRID     2082        2 0.61441-4.51620-0.08500        2
GRID     2083        2 0.66762-3.92641-0.08500        2
GRID     2084        2 0.75625-2.66105-0.08500        2
GRID     2085        2 0.95567-1.95908-0.08500        2
GRID     2086        2 0.69654-3.33627-0.08500        2
GRID     2087        2 0.50000 1.00000-0.08500        2
GRID     2088        2 0.50000 0.10000-0.08500        2
GRID     2089        2 0.73841 1.59751-0.08500        2
GRID     2090        2 0.66133-0.65983-0.08500        2
GRID     2091        2 0.97683 2.19501-0.08500        2
GRID     2093        2 0.66133-1.83717-0.08500        2
GRID     2094        2 0.41750-1.24850-0.08500        2
GRID     2095        2 0.       2.63750 0.            2
GRID     2096       2-1.23619 2.65090 0.             2
GRID     2098       2-0.19060-5.23600 0.             2
GRID     2100       2-0.19060-5.10600-0.08500        2
GRID     2101       2-0.09530-4.51620-0.08500        2
GRID     2102        2 0.      -3.92641-0.08500        2
GRID     2103        2 0.03562-3.28817-0.08500        2
GRID     2104        2 0.18750-2.38510-0.08500        2
GRID     2105        2 0.       1.11800-0.08500        2
GRID     2106        2 0.       0.21800-0.08500        2
GRID     2107        2 0.       1.75587-0.08500        2
GRID     2108        2 0.      -0.45000-0.08500        2
GRID     2109        2 0.       2.39375-0.08500        2
```

```
GRID     2111    2-0.97683 2.19501-0.08500       2
GRID     2112    2-2.28559 1.87014 0.            2
GRID     2113    2-2.10365 1.71754 0.            2
GRID     2114    2-1.87239 1.55030-0.08500       2
GRID     2115    2-0.87626-5.23600 0.            2
GRID     2116    2-0.87626-5.15600 0.            2
GRID     2117    2-0.87626-5.10600-0.08500       2
GRID     2118    2-0.87626-4.51621-0.08500       2
GRID     2119    2-0.87626-3.92642-0.08500       2
GRID     2120    2-0.73219-3.28093-0.08500       2
GRID     2121    2-0.55575-2.70505-0.08500       2
GRID     2122    2-0.64980-1.73600-0.08500       2
GRID     2123    2-0.73841 1.59751-0.08500       2
GRID     2124    2-0.50000 1.00000-0.08500       2
GRID     2125    2-0.50000 0.10000-0.08500       2
GRID     2126    2-0.64967-0.78017-0.08500       2
GRID     2127    2-1.64739 1.17234-0.08500       2
GRID     2128    2-2.55546 1.31361 0.            2
GRID     2129    2-2.34979 1.20656 0.            2
GRID     2130    2-2.13777 1.06657-0.08500       2
GRID     2131    2-1.17460-2.18600-0.08500       2
GRID     2132    2-1.75000-2.24850-0.08500       2
GRID     2133    2-1.85000-2.24850 0.            2
GRID     2134    2-1.96550-2.24850 0.            2
GRID     2135    2-2.01222-2.13572 0.            2
GRID     2136    2-2.01222-2.36128 0.            2
GRID     2137    2-1.55307-5.23600 0.            2
GRID     2138    2-1.55307-5.15600 0.            2
GRID     2139    2-1.55307-5.10600-0.08500       2
GRID     2140    2-1.55308-4.45371-0.08500       2
GRID     2141    2-1.55308-3.80141-0.08500       2
GRID     2142    2-1.50000-3.12350-0.08500       2
GRID     2143    2-1.23900-2.77500-0.08500       2
GRID     2144    2-1.29934-1.36034-0.08500       2
GRID     2145    2-1.42239 0.79438-0.08500       2
GRID     2146    2-1.29739-0.03062-0.08500       2
GRID     2147    2-2.40315 0.58284-0.08500       2
GRID     2148    2-2.82533 0.75708 0.            2
GRID     2150    2-1.85984-1.98334-0.08500       2
GRID     2151    2-1.85984-2.51366-0.08500       2
GRID     2152    2-1.93055-2.05405 0.            2
GRID     2153    2-1.93055-2.44295 0.            2
GRID     2154    2-2.12500-2.08900 0.            2
GRID     2155    2-2.12500-1.97350 0.            2
GRID     2156    2-2.12500-2.40800 0.            2
GRID     2157    2-2.12500-2.52350 0.            2
GRID     2158    2-2.23778-2.13572 0.            2
GRID     2159    2-2.23778-2.36128 0.            2
GRID     2160    2-2.28450-2.24850 0.            2
GRID     2161    2-2.18750-5.23600 0.            2
GRID     2162    2-2.18750-5.15600 0.            2
GRID     2163    2-2.18750-5.10600-0.08500       2
GRID     2164    2-2.18750-4.24050-0.08500       2
GRID     2165    2-2.18750-3.37500-0.08500       2
GRID     2166    2-2.12500-2.62350-0.08500       2
GRID     2167    2-2.12500 0.      -0.08500       2
GRID     2168    2-1.96000-1.12500-0.08500       2
GRID     2169    2-2.12500-1.87350-0.08500       2
GRID     2170    2-2.50000 0.      -0.08500       2
```

```
GRID    2172          2-2.82750 0.        0.                  2
GRID    2173          2-2.31945-2.05405 0.                    2
GRID    2174          2-2.39016-1.98334-0.08500               2
GRID    2175          2-2.31945-2.44295 0.                    2
GRID    2176          2-2.39016-2.51366-0.08500               2
GRID    2177          2-2.40000-2.24850 0.                    2
GRID    2178          2-2.64175-5.23600 0.                    2
GRID    2180          2-2.45425-5.10600-0.08500               2
GRID    2181          2-2.47712-4.18350-0.08500               2
GRID    2182          2-2.50000-3.26100-0.08500               2
GRID    2183          2-2.50000-2.56200-0.08500               2
GRID    2184          2-2.50000-1.24850-0.08500               2
GRID    2185          2-2.50000-1.89000-0.08500               2
GRID    2187          2-2.82750-1.24850 0.                    2
GRID    2188          2-2.50000-2.24850-0.08500               2
GRID    2189          2-2.78175-5.23600 0.                    2
GRID    2190          2-2.78175-4.30475 0.                    2
GRID    2191          2-2.64175-4.26475 0.                    2
GRID    2192          2-2.64175-3.37350 0.                    2
GRID    2194          2-2.68750-2.24850 0.                    2
GRID    2195          2-2.82750-2.24850 0.                    2
GRID    2196          2-2.78175-3.37350 0.                    2
GRID    2197          2-2.82750-3.26100 0.                    2
CQUAD4  1164    110     1109    1123    1122    1108    0.000
CQUAD4  1165    110     1123    1138    1136    1122    0.000
CQUAD4  1166    110     1138    1161    1137    1136    0.000
CQUAD4  1167    110     1161    1163    1162    1137    0.000
CQUAD4  1168    110     1163    1188    1160    1162    0.000
CQUAD4  1169    110     1188    1187    1159    1160    0.000
CQUAD4  1170    110     1137    1186    1158    1159    0.000
CQUAD4  1171    110     1186    1185    1181    1158    0.000
CQUAD4  1172    110     1185    1180    1157    1181    0.000
CQUAD4  1173    110     1180    1172    1156    1157    0.000
CQUAD4  1174    110     1172    1152    1148    1156    0.000
CQUAD4  1175    110     1152    1135    1131    1148    0.000
CQUAD4  1176    110     1135    1120    1121    1131    0.000
CQUAD4  1177    110     1120    1105    1107    1121    0.000
CQUAD4  1178    110     1107    1089    1088    1105    0.000
CQUAD4  1179    110     1089    1071    1070    1088    0.000
CQUAD4  1180    110     1071    1057    1056    1070    0.000
CQUAD4  1181    110     1056    1038    1039    1057    0.000
CQUAD4  1182    110     1038    1024    1025    1039    0.000
CQUAD4  1183    110     1024    1006    1007    1025    0.000
CQUAD4  1184    110     1006    1009    1008    1007    0.000
CQUAD4  1185    110     1009    1027    1026    1008    0.000
CQUAD4  1186    110     1027    1041    1040    1026    0.000
CQUAD4  1187    110     1041    1059    1058    1040    0.000
CQUAD4  1188    110     1059    1073    1072    1058    0.000
CQUAD4  1189    110     1073    1091    1090    1072    0.000
CQUAD4  1190    110     1091    1109    1108    1090    0.000
CQUAD4  1200    110     1190    1191    1165    1189    0.000
CQUAD4  1201    110     1191    1192    1193    1165    0.000
CQUAD4  1202    110     1243    1245    1215    1214    0.000
CQUAD4  1203    110     1214    1215    1190    1189    0.000
CQUAD4  1204    110     1247    1248    1218    1217    0.000
CQUAD4  1205    110     1217    1218    1193    1192    0.000
CQUAD4  1206    110     1300    1299    1301    1327    0.000
CQUAD4  1207    110     1327    1301    1302    1330    0.000
CQUAD4  1208    110     1384    1409    1410    1385    0.000
```

CQUAD4	1210	110	1346	1396	1372	1370	0.000
CQUAD4	1211	110	1370	1372	1348	1349	0.000
CQUAD4	1212	110	1349	1348	1328	1347	0.000
CQUAD4	1213	110	1347	1328	1326	1342	0.000
CQUAD4	1214	110	1363	1382	1360	1359	0.000
CQUAD4	1215	110	1359	1360	1338	1340	0.000
CQUAD4	1230	110	1271	1272	1245	1243	0.000
CQUAD4	1231	110	1274	1275	1248	1247	0.000
CQUAD4	1232	110	1300	1299	1272	1271	0.000
CQUAD4	1233	110	1302	1303	1275	1274	0.000
CTRIA3	1234	110	1388	1384	1409	0.000	
CTRIA3	1235	110	1321	1342	1326	0.000	
CQUAD4	1244	110	1343	1323	1321	1342	0.000
CQUAD4	1245	110	1345	1325	1323	1343	0.000
CQUAD4	1246	110	1344	1324	1325	1345	0.000
CQUAD4	1247	110	1341	1322	1324	1344	0.000
CQUAD4	1248	110	1335	1317	1322	1341	0.000
CQUAD4	1249	110	1314	1337	1335	1317	0.000
CQUAD4	1250	110	1340	1338	1314	1337	0.000
CTRIA3	1251	110	1330	1302	1303	0.000	
CQUAD4	1252	110	1391	1387	1384	1388	0.000
CQUAD4	1253	110	1392	1390	1387	1391	0.000
CQUAD4	1254	110	1393	1367	1390	1392	0.000
CQUAD4	1255	110	1368	1394	1393	1367	0.000
CQUAD4	1256	110	1395	1369	1368	1394	0.000
CQUAD4	1257	110	1389	1381	1369	1395	0.000
CQUAD4	1258	110	1363	1382	1389	1381	0.000
CQUAD4	1267	111	1433	1409	1410	1421	0.000
CQUAD4	1268	111	1421	1410	1396	1397	0.000
CQUAD4	1269	111	1300	1326	1328	1327	0.000
CQUAD4	1270	111	1327	1328	1348	1330	0.000
CQUAD4	1271	111	1397	1396	1372	1371	0.000
CQUAD4	1272	111	1371	1372	1348	1351	0.000
CQUAD4	1273	111	1120	1119	1104	1105	0.000
CQUAD4	1274	111	1119	1118	1102	1104	0.000
CQUAD4	1275	111	1105	1104	1087	1088	0.000
CQUAD4	1276	111	1104	1102	1086	1087	0.000
CQUAD4	1277	111	1086	1087	1069	1068	0.000
CQUAD4	1278	111	1037	1088	1070	1069	0.000
CQUAD4	1279	111	1068	1069	1055	1054	0.000
CQUAD4	1280	111	1069	1070	1056	1055	0.000
CQUAD4	1281	111	1056	1055	1037	1038	0.000
CQUAD4	1282	111	1055	1054	1036	1037	0.000
CQUAD4	1283	111	1038	1037	1023	1024	0.000
CQUAD4	1284	111	1037	1036	1022	1023	0.000
CQUAD4	1285	111	1024	1023	1005	1006	0.000
CQUAD4	1286	111	1023	1022	1004	1005	0.000
CQUAD4	1287	111	1006	1005	1010	1009	0.000
CQUAD4	1288	111	1005	1004	1011	1010	0.000
CQUAD4	1289	111	1009	1010	1028	1027	0.000
CQUAD4	1290	111	1010	1011	1029	1028	0.000
CQUAD4	1291	111	1027	1028	1042	1041	0.000
CQUAD4	1292	111	1028	1029	1043	1042	0.000
CQUAD4	1293	111	1041	1042	1060	1059	0.000
CQUAD4	1294	111	1042	1043	1061	1060	0.000
CQUAD4	1295	111	1059	1060	1074	1073	0.000
CQUAD4	1296	111	1060	1061	1075	1074	0.000
CQUAD4	1297	111	1073	1074	1092	1091	0.000
CQUAD4	1298	111	1074	1075	1095	1092	0.000

CQUAD4	1300	111	1092	1095	1111	1110	0.000
CQUAD4	1301	111	1109	1123	1124	1110	0.000
CQUAD4	1302	111	1110	1124	1125	1111	0.000
CQUAD4	1303	111	1123	1138	1139	1124	0.000
CQUAD4	1304	111	1124	1139	1140	1125	0.000
CQUAD4	1305	111	1138	1161	1164	1139	0.000
CQUAD4	1306	111	1139	1164	1166	1140	0.000
CQUAD4	1307	111	1189	1161	1164	1165	0.000
CQUAD4	1308	111	1165	1164	1166	1193	0.000
CQUAD4	1309	111	1135	1120	1119	1134	0.000
CQUAD4	1310	111	1134	1119	1118	1133	0.000
CQUAD4	1311	111	1152	1135	1134	1154	0.000
CQUA04	1312	111	1154	1134	1133	1153	0.000
CQUAD4	1313	111	1172	1152	1154	1174	0.000
CQUAD4	1314	111	1174	1154	1153	1175	0.000
CQUAD4	1315	111	1224	1226	1202	1201	0.000
CQUAD4	1316	111	1201	1202	1182	1177	0.000
CQUAD4	1317	111	1177	1201	1199	1176	0.000
CQUAD4	1318	111	1201	1224	1200	1199	0.000
CQUAD4	1319	111	1176	1199	1174	1172	0.000
CQUAD4	1320	111	1199	1200	1175	1174	0.000
CQUAD4	1321	111	1243	1242	1213	1214	0.000
CQUAD4	1322	111	1214	1213	1188	1189	0.000
CQUAD4	1323	111	1188	1187	1212	1213	0.000
CQUAD4	1324	111	1213	1212	1240	1242	0.000
CQUAD4	1325	111	1187	1186	1211	1212	0.000
CQUAD4	1326	111	1212	1211	1239	1240	0.000
CQUAD4	1327	111	1239	1211	1208	1210	0.000
CQUAD4	1328	111	1211	1186	1185	1208	0.000
CQUAD4	1329	111	1180	1183	1208	1185	0.000
CQUAD4	1330	111	1183	1182	1210	1208	0.000
CQUAD4	1331	111	1180	1183	1176	1172	0.000
CQUAD4	1332	111	1183	1182	1177	1176	0.000
CQUAD4	1333	111	1224	1222	1198	1200	0.000
CQUAD4	1334	111	1200	1198	1173	1175	0.000
CQUAD4	1335	111	1348	1330	1329	1351	0.000
CTRIA3	1336	111	1303	1329	1330	0.000	
CTRIA3	1337	111	1175	1153	1173	0.000	
CQUAD4	1338	111	1243	1242	1270	1271	0.000
CQUAD4	1339	111	1242	1240	1269	1270	0.000
CQUAD4	1340	111	1240	1239	1268	1269	0.000
CQUAD4	1341	111	1254	1228	1222	1224	0.000
CQUAD4	1342	111	1256	1254	1224	1226	0.000
CQUAD4	1343	111	1256	1254	1258	1281	0.000
CQUAD4	1344	111	1254	1228	1260	1258	0.000
CQUAD4	1345	111	1258	1260	1282	1281	0.000
CQUAD4	1346	111	1281	1282	1312	1310	0.000
CQUAD4	1347	111	1338	1312	1310	1314	0.000
CQUAD4	1348	111	1310	1314	1317	1293	0.000
CQUAD4	1349	111	1293	1317	1322	1316	0.000
CTRIA3	1350	111	1321	1319	1326	0.000	
CTRIA3	1351	111	1321	1319	1323	0.000	
CQUAD4	1352	111	1319	1326	1300	1298	0.000
CQUAD4	1353	111	1319	1323	1297	1298	0.000
CQUAD4	1354	111	1300	1298	1270	1271	0.000
CQUAD4	1355	111	1298	1297	1269	1270	0.000
CQUAD4	1356	111	1325	1296	1297	1323	0.000
CTRIA3	1357	111	1297	1269	1296	0.000	
CQUAD4	1358	111	1296	1295	1268	1269	0.000

CQUAD4	1360	111	1296	1295	1294	1324	0.000
CQUAD4	1361	111	1324	1294	1316	1322	0.000
CTRIA3	1362	111	1161	1163	1189	0.000	
CTRIA3	1363	111	1189	1188	1163	0.000	
CQUAD4	1364	111	1425	1406	1407	1429	0.000
CQUAD4	1365	111	1406	1382	1389	1407	0.000
CQUAD4	1366	111	1429	1407	1417	1430	0.000
CQUAD4	1367	111	1430	1417	1420	1438	0.000
CQUAD4	1368	111	1417	1395	1394	1420	0.000
CQUAD4	1369	111	1438	1420	1419	1439	0.000
CQUAD4	1370	111	1420	1394	1393	1419	0.000
CQUAD4	1371	111	1439	1419	1418	1437	0.000
CQUAD4	1372	111	1419	1393	1392	1418	0.000
CQUAD4	1373	111	1407	1389	1395	1417	0.000
CQUAD4	1374	111	1418	1437	1432	1413	0.000
CQUAD4	1375	111	1418	1392	1391	1413	0.000
CQUAD4	1376	111	1413	1432	1433	1409	0.000
CQUAD4	1377	111	1391	1413	1409	1388	0.000
CQUAD4	1378	109	1245	1246	1216	1215	0.000
CQUAD4	1379	109	1246	1247	1217	1216	0.000
CQUAD4	1380	109	1215	1216	1191	1190	0.000
CQUAD4	1381	109	1216	1217	1192	1191	0.000
CQUAD4	1382	109	1272	1273	1246	1245	0.000
CQUAD4	1383	109	1273	1274	1247	1246	0.000
CQUAD4	1384	109	1299	1301	1273	1272	0.000
CQUAD4	1385	109	1301	1302	1274	1273	0.000
CQUAD4	1386	109	1386	1370	1361	1385	0.000
CQUAD4	1387	109	1370	1349	1347	1361	0.000
CQUAD4	1388	109	1385	1361	1362	1384	0.000
CQUAD4	1389	109	1361	1347	1342	1362	0.000
CQUAD4	1390	109	1387	1365	1362	1384	0.000
CQUAD4	1391	109	1365	1343	1342	1362	0.000
CQUAD4	1392	109	1390	1366	1365	1387	0.000
CQUAD4	1393	109	1366	1345	1343	1365	0.000
CQUAD4	1394	109	1367	1364	1366	1390	0.000
CQUAD4	1395	109	1364	1344	1345	1366	0.000
CQUAD4	1396	109	1368	1346	1364	1367	0.000
CQUAD4	1397	109	1346	1341	1344	1364	0.000
CQUAD4	1398	109	1369	1356	1346	1368	0.000
CQUAD4	1399	109	1356	1335	1341	1346	0.000
CQUAD4	1400	109	1337	1357	1356	1335	0.000
CQUAD4	1401	109	1357	1381	1369	1356	0.000
CQUAD4	1402	109	1363	1359	1357	1381	0.000
CQUAD4	1403	109	1359	1340	1337	1357	0.000
CTRIA3	1404	113	1252	1263	1253	0.000	
CQUAD4	1405	113	1253	1279	1255	1252	0.000
CTRIA3	1406	113	1235	1263	1252	0.000	
CQUAD4	1407	113	1252	1255	1225	1235	0.000
CTRIA3	1410	113	1234	1263	1233	0.000	
CQUAD4	1411	113	1233	1206	1209	1234	0.000
CTRIA3	1412	113	1236	1263	1234	0.000	
CQUAD4	1413	113	1234	1209	1238	1236	0.000
CTRIA3	1414	113	1237	1263	1236	0.000	
CQUAD4	1415	113	1236	1238	1266	1237	0.000
CTRIA3	1416	113	1265	1263	1237	0.000	
CQUAD4	1417	113	1237	1266	1267	1265	0.000
CTRIA3	1418	113	1290	1263	1265	0.000	
CQUAD4	1419	113	1265	1267	1292	1290	0.000
CTRIA3	1420	113	1289	1263	1290	0.000	

CTRIA3	1422	113	1288	1263	1289	0.000	
CQUAD4	1423	113	1289	1315	1291	1288	0.000
CTRIA3	1424	113	1264	1263	1288	0.000	
CQUAD4	1425	113	1288	1291	1280	1264	0.000
CTRIA3	1426	113	1253	1263	1264	0.000	
CQUAD4	1427	113	1264	1280	1279	1253	0.000
CQUAD4	1428	113	1189	1163	1162	1190	0.000
CQUAD4	1429	111	1121	1106	1119	1120	0.000
CQUAD4	1430	111	1106	1103	1118	1119	0.000
CQUAD4	1431	111	1108	1093	1110	1109	0.000
CQUAD4	1432	111	1093	1094	1111	1110	0.000
CQUAD4	1433	111	1210	1208	1184	1209	0.000
CQUAD4	1434	111	1208	1185	1181	1184	0.000
CQUAD4	1435	112	1258	1254	1227	1257	0.000
CQUAD4	1436	112	1254	1224	1223	1227	0.000
CQUAD4	1437	111	1279	1281	1256	1255	0.000
CQUAD4	1438	111	1255	1256	1226	1225	0.000
CQUAD4	1439	111	1225	1226	1202	1207	0.000
CQUAD4	1440	111	1207	1202	1182	1206	0.000
CQUAD4	1441	111	1206	1182	1210	1209	0.000
CQUAD4	1442	111	1209	1210	1239	1238	0.000
CQUAD4	1443	111	1238	1239	1268	1266	0.000
CQUAD4	1444	111	1266	1268	1295	1267	0.000
CQUAD4	1445	111	1267	1295	1294	1292	0.000
CQUAD4	1446	111	1292	1294	1316	1315	0.000
CQUAD4	1447	111	1315	1316	1293	1291	0.000
CQUAD4	1448	111	1291	1293	1310	1280	0.000
CQUAD4	1449	111	1280	1310	1281	1279	0.000
CQUAD4	1450	115	1281	1258	1257	1279	0.000
CQUAD4	1451	111	1300	1326	1318	1299	0.000
CTRIA3	1452	111	1318	1342	1326	0.000	
CQUAD4	1453	113	1319	1323	1343	1320	0.000
CQUAD4	1454	113	1319	1326	1318	1320	0.000
CQUAD4	1455	111	1266	1241	1269	1268	0.000
CQUAD4	1456	111	1241	1244	1270	1269	0.000
CQUAD4	1457	111	1244	1272	1271	1270	0.000
CQUAD4	1458	117	1315	1316	1322	1341	0.000
CQUAD4	1459	117	1389	1381	1383	1407	0.000
CQUAD4	1460	111	1414	1415	1437	1418	0.000
CQUAD4	1461	111	1408	1411	1432	1413	0.000
CQUAD4	1462	111	1437	1415	1416	1431	0.000
CQUAD4	1463	111	1432	1411	1412	1435	0.000
CQUAD4	1464	114	1391	1387	1408	1413	0.000
CQUAD4	1465	114	1413	1408	1414	1418	0.000
CQUAD4	1466	114	1418	1414	1390	1392	0.000
CTRIA3	1467	113	1232	1263	1235	0.000	
CQUAD4	1468	113	1235	1225	1207	1232	0.000
CTRIA3	1469	113	1233	1263	1232	0.000	
CQUAD4	1470	113	1232	1207	1206	1233	0.000
CQUAD4	1472	110	1350	1351	1329	1331	0.000
CQUAD4	1473	110	1331	1329	1303	1305	0.000
CQUAD4	1474	110	1305	1303	1275	1276	0.000
CQUAD4	1475	110	1276	1275	1248	1249	0.000
CQUAD4	1477	110	1194	1193	1166	1167	0.000
CQUAD4	1478	110	1167	1166	1140	1142	0.000
CQUAD4	1479	110	1142	1140	1125	1126	0.000
CQUAD4	1480	110	1126	1125	1111	1112	0.000
CQUAD4	1481	110	1112	1111	1095	1096	0.000
CQUAD4	1482	110	1095	1096	1077	1075	0.000

CQUAD4	1483	110	1075	1077	1062	1061	0.000
CQUAD4	1484	110	1061	1062	1045	1043	0.000
CQUAD4	1485	110	1043	1045	1030	1029	0.000
CQUAD4	1486	110	1029	1030	1013	1011	0.000
CQUAD4	1487	110	1011	1013	1003	1004	0.000
CQUAD4	1488	110	1004	1003	1019	1022	0.000
CQUAD4	1489	110	1019	1022	1036	1035	0.000
CQUAD4	1490	110	1035	1036	1054	1051	0.000
CQUAD4	1491	110	1051	1054	1068	1067	0.000
CQUAD4	1492	110	1067	1068	1086	1083	0.000
CQUAD4	1493	110	1083	1086	1102	1101	0.000
CQUAD4	1494	110	1101	1102	1118	1117	0.000
CQUAD4	1495	110	1404	1425	1406	1402	0.000
CQUAD4	1496	110	1402	1406	1382	1380	0.000
CQUAD4	1498	110	1339	1338	1312	1311	0.000
CQUAD4	1499	110	1311	1312	1282	1285	0.000
CQUAD4	1500	110	1285	1282	1260	1259	0.000
CQUAD4	1501	110	1259	1260	1228	1229	0.000
CQUAD4	1502	110	1228	1229	1203	1222	0.000
CQUAD4	1504	110	1173	1171	1149	1153	0.000
CQUAD4	1505	110	1153	1149	1132	1133	0.000
CQUAD4	1506	110	1133	1132	1117	1118	0.000
CQUAD4	1508	110	1440	1433	1432	1450	0.000
CQUAD4	1509	110	1450	1432	1437	1449	0.000
CQUAD4	1510	110	1449	1437	1439	1451	0.000
CQUAD4	1511	110	1451	1439	1438	1448	0.000
CQUAD4	1512	110	1448	1438	1430	1447	0.000
CQUAD4	1513	110	1447	1430	1429	1444	0.000
CQUAD4	1514	110	1444	1429	1425	1426	0.000
CQUAD4	1515	110	1249	1248	1218	1219	0.000
CQUAD4	1516	110	1219	1218	1193	1194	0.000
CQUAD4	1517	110	1222	1203	1197	1198	0.000
CQUAD4	1518	110	1198	1197	1171	1173	0.000
CQUAD4	1519	110	1376	1397	1371	1374	0.000
CQUAD4	1520	110	1374	1371	1351	1350	0.000
CQUAD4	1521	110	1380	1382	1360	1358	0.000
CQUAD4	1522	110	1358	1360	1338	1339	0.000
CQUAD4	1523	110	1398	1397	1421	1422	0.000
CQUAD4	1524	110	1422	1421	1433	1440	0.000
CQUAD4	1525	111	1437	1449	1434	1431	0.000
CQUAD4	1526	111	1432	1450	1436	1435	0.000
CQUAD4	1527	114	1434	1436	1450	1449	0.000
CQUAD4	1528	115	1312	1311	1287	1283	0.000
CQUAD4	1529	115	1329	1304	1308	1331	0.000
CQUAD4	1530	115	1173	1171	1150	1151	0.000
CQUAD4	1531	115	1166	1141	1145	1167	0.000
CQUAD4	1532	115	1101	1102	1085	1084	0.000
CQUAD4	1533	115	1096	1080	1076	1095	0.000
CQUAD4	1534	115	1036	1035	1020	1021	0.000
CQUAD4	1535	115	1029	1012	1016	1030	0.000
CQUAD4	1536	116	1068	1067	1052	1053	0.000
CQUAD4	1537	116	1061	1044	1048	1062	0.000
CQUAD4	1538	110	1336	1339	1311	1313	0.000
CQUAD4	1539	110	1313	1311	1285	1284	0.000
CQUAD4	1540	110	1284	1285	1259	1261	0.000
CQUAD4	1541	110	1261	1259	1229	1230	0.000
CQUAD4	1542	110	1066	1067	1083	1082	0.000
CQUAD4	1543	110	1050	1051	1067	1066	0.000
CQUAD4	1544	110	1034	1035	1051	1050	0.000
CQUAD4	1545	110	1082	1083	1101	1100	0.000

CQUAD4	1546	110	1077	1078	1063	1062	0.000
CQUAD4	1547	110	1062	1063	1046	1045	0.000
CQUAD4	1548	110	1096	1097	1078	1077	0.000
CQUAD4	1549	110	1045	1046	1031	1030	0.000
CQUAD4	1550	110	1399	1376	1374	1373	0.000
CQUAD4	1551	110	1373	1374	1350	1352	0.000
CQUAD4	1552	110	1352	1350	1331	1332	0.000
CQUAD4	1553	110	1332	1331	1305	1306	0.000
CQUAD4	1554	110	1306	1305	1276	1277	0.000
CQUAD4	1555	110	1277	1276	1249	1250	0.000
CQUAD4	1556	110	1250	1249	1219	1220	0.000
CQUAD4	1557	110	1220	1219	1194	1195	0.000
CQUAD4	1558	110	1195	1194	1167	1168	0.000
CQUAD4	1559	110	1168	1167	1142	1143	0.000
CQUAD4	1560	110	1143	1142	1126	1127	0.000
CQUAD4	1561	110	1127	1126	1112	1113	0.000
CQUAD4	1562	110	1113	1112	1096	1097	0.000
CQUAD4	1563	110	1030	1031	1014	1013	0.000
CQUAD4	1564	110	1013	1014	1002	1003	0.000
CQUAD4	1565	110	1427	1404	1402	1401	0.000
CQUAD4	1566	110	1401	1402	1380	1378	0.000
CQUAD4	1567	110	1378	1380	1358	1355	0.000
CQUAD4	1568	110	1355	1358	1339	1336	0.000
CQUAD4	1569	110	1229	1230	1204	1203	0.000
CQUAD4	1570	110	1203	1204	1178	1197	0.000
CQUAD4	1571	110	1197	1178	1170	1171	0.000
CQUAD4	1572	110	1171	1170	1147	1149	0.000
CQUAD4	1573	110	1149	1147	1130	1132	0.000
CQUAD4	1574	110	1132	1130	1116	1117	0.000
CQUAD4	1575	110	1100	1101	1117	1116	0.000
CQUAD4	1576	110	1003	1002	1018	1019	0.000
CQUAD4	1577	110	1018	1019	1035	1034	0.000
CQUAD4	1578	110	1399	1398	1422	1423	0.000
CQUAD4	1579	110	1423	1422	1440	1441	0.000
CQUAD4	1580	110	1441	1440	1450	1452	0.000
CQUAD4	1581	110	1452	1450	1449	1457	0.000
CQUAD4	1582	110	1457	1449	1451	1455	0.000
CQUAD4	1583	110	1455	1451	1448	1456	0.000
CQUAD4	1584	110	1456	1448	1447	1453	0.000
CQUAD4	1585	110	1453	1447	1444	1445	0.000
CQUAD4	1586	110	1445	1444	1426	1427	0.000
CQUAD4	1587	115	1311	1313	1309	1287	0.000
CQUAD4	1588	115	1331	1308	1333	1332	0.000
CQUAD4	1589	115	1171	1170	1155	1150	0.000
CQUAD4	1590	115	1167	1145	1169	1168	0.000
CQUAD4	1591	115	1100	1101	1084	1099	0.000
CQUAD4	1592	115	1097	1098	1080	1096	0.000
CQUAD4	1593	115	1035	1034	1033	1020	0.000
CQUAD4	1594	115	1030	1016	1032	1031	0.000
CQUAD4	1595	117	1067	1066	1065	1052	0.000
CQUAD4	1596	117	1062	1048	1064	1063	0.000
CQUAD4	1597	110	1116	1130	1129	1115	0.000
CQUAD4	1598	110	1130	1147	1146	1129	0.000
CQUAD4	1599	110	1147	1170	1155	1146	0.000
CQUAD4	1600	110	1170	1178	1179	1155	0.000
CQUAD4	1601	110	1178	1204	1205	1179	0.000
CQUAD4	1602	110	1204	1230	1231	1205	0.000
CQUAD4	1603	110	1230	1261	1262	1231	0.000
CQUAD4	1604	110	1261	1284	1286	1262	0.000
CQUAD4	1605	110	1284	1313	1309	1286	0.000

```
CQUAD4    1606     110     1313     1336     1334     1309    0.000
CQUAD4    1607     110     1336     1355     1354     1334    0.000
CQUAD4    1608     110     1355     1378     1379     1354    0.000
CQUAD4    1609     110     1378     1401     1403     1379    0.000
CQUAD4    1610     110     1401     1427     1405     1403    0.000
CTRIA3    1611     110     1427     1428     1405    0.000
CQUAD4    1612     110     1445     1427     1428     1446    0.000
CQUAD4    1613     110     1445     1453     1454     1446    0.000
CQUAD4    1614     110     1453     1456     1458     1454    0.000
CQUAD4    1615     110     1456     1455     1460     1458    0.000
CQUAD4    1616     110     1455     1457     1459     1460    0.000
CQUAD4    1617     110     1452     1441     1442     1443    0.000
CQUAD4    1618     110     1441     1442     1424     1423    0.000
CQUAD4    1619     110     1423     1424     1400     1399    0.000
CTRIA3    1620     110     1400     1399     1377    0.000
CQUAD4    1621     110     1113     1127     1128     1114    0.000
CQUAD4    1622     110     1127     1143     1144     1128    0.000
CQUAD4    1623     110     1143     1168     1169     1144    0.000
CQUAD4    1624     110     1168     1195     1196     1169    0.000
CQUAD4    1625     110     1195     1220     1221     1196    0.000
CQUAD4    1626     110     1220     1250     1251     1221    0.000
CQUAD4    1627     110     1250     1277     1278     1251    0.000
CQUAD4    1628     110     1277     1306     1307     1278    0.000
CQUAD4    1629     110     1306     1332     1333     1307    0.000
CQUAD4    1630     110     1332     1352     1353     1333    0.000
CQUAD4    1631     110     1352     1353     1375     1373    0.000
CQUAD4    1632     110     1373     1375     1377     1399    0.000
CQUAD4    1633     110     1116     1115     1099     1100    0.000
CQUAD4    1634     110     1100     1099     1081     1082    0.000
CQUAD4    1635     110     1032     1081     1065     1066    0.000
CQUAD4    1636     110     1066     1065     1049     1050    0.000
CQUAD4    1637     110     1050     1049     1033     1034    0.000
CQUAD4    1638     110     1034     1033     1017     1018    0.000
CQUAD4    1639     110     1002     1018     1017     1001    0.000
CQUAD4    1640     110     1014     1002     1001     1015    0.000
CQUAD4    1641     110     1014     1031     1032     1015    0.000
CQUAD4    1642     110     1031     1046     1047     1032    0.000
CQUAD4    1643     110     1046     1063     1064     1047    0.000
CQUAD4    1644     110     1063     1078     1079     1064    0.000
CQUAD4    1645     110     1078     1097     1098     1079    0.000
CQUAD4    1646     110     1097     1113     1114     1098    0.000
CQUAD4    2001     210     2023     1100     2024     2013    0.000
CQUAD4    2002     210     1100     2044     2043     2024    0.000
CQUAD4    2003     210     2044     2071     2070     2043    0.000
CQUAD4    2004     210     2071     1034     2077     2070    0.000
CQUAD4    2005     210     2077     2078     2095     1034    0.000
CQUAD4    2006     210     2078     2096     1031     2095    0.000
CQUAD4    2007     210     1031     2113     2112     2096    0.000
CQUAD4    2008     210     2113     2129     2128     2112    0.000
CQUAD4    2009     210     2129     1097     2148     2128    0.000
CQUAD4    2010     210     1097     2171     2172     2148    0.000
CQUAD4    2011     210     2040     2042     1100     2023    0.000
CQUAD4    2012     210     2042     2045     2044     1100    0.000
CQUAD4    2013     210     2045     2072     2071     2044    0.000
CQUAD4    2014     210     2072     2091     1034     2071    0.000
CQUAD4    2015     210     1034     2095     2109     2091    0.000
CQUAD4    2016     210     2095     1031     2111     2109    0.000
CQUAD4    2017     210     2111     2114     2113     1031    0.000
CQUAD4    2018     210     2114     2130     2129     2113    0.000
CQUAD4    2019     210     2130     2147     1097     2129    0.000
```

CQUAD4	2020	210	2170	2147	1097	2171	0.000
CQUAD4	2021	210	2040	2042	2065	2066	0.000
CQUAD4	2022	210	2056	2065	2097	2088	0.000
CQUAD4	2023	210	2088	2087	2105	2106	0.000
CQUAD4	2024	210	2042	2045	2069	2065	0.000
CTRIA3	2025	210	2045	2072	2069	0.000	
CQUAD4	2026	210	2065	2069	2099	2087	0.000
CQUAD4	2027	210	2069	2072	2091	2089	0.000
CQUAD4	2028	210	2087	2089	2107	2105	0.000
CQUAD4	2029	210	2089	2091	2109	2107	0.000
CTRIA3	2030	210	2170	2147	2167	0.000	
CTRIA3	2031	210	2127	2114	2130	0.000	
CQUAD4	2032	210	2130	2147	2145	2127	0.000
CQUAD4	2033	210	2114	2127	2123	2111	0.000
CQUAD4	2034	210	2127	2145	2124	2123	0.000
CQUAD4	2035	210	2111	2123	2107	2109	0.000
CQUAD4	2036	210	2123	2124	2105	2107	0.000
CQUAD4	2037	210	2147	2167	2146	2145	0.000
CQUAD4	2038	210	2145	2146	2125	2124	0.000
CQUAD4	2039	210	2124	2125	2106	2105	0.000
CQUAD4	2040	210	2031	2029	2047	2049	0.000
CQUAD4	2041	210	2049	2047	2068	2051	0.000
CQUAD4	2042	210	2051	2068	2074	2053	0.000
CQUAD4	2043	210	2053	2074	2076	2055	0.000
CQUAD4	2044	210	2055	2076	2075	2054	0.000
CQUAD4	2045	210	2054	2075	2073	2052	0.000
CQUAD4	2046	210	2052	2073	2064	2050	0.000
CQUAD4	2047	210	2050	2064	2046	2048	0.000
CQUAD4	2048	210	2048	2046	2028	2030	0.000
CQUAD4	2049	210	2030	2028	2029	2031	0.000
CQUAD4	2050	210	2029	2027	2041	2047	0.000
CQUAD4	2051	210	2047	2041	2067	2068	0.000
CQUAD4	2052	210	2068	2067	2090	2074	0.000
CQUAD4	2053	210	2074	2090	2094	2076	0.000
CQUAD4	2054	210	2076	2094	2093	2075	0.000
CQUAD4	2055	210	2075	2093	2085	2073	0.000
CQUAD4	2056	210	2073	2085	2063	2064	0.000
CQUAD4	2057	210	2064	2063	2039	2046	0.000
CQUAD4	2058	210	2046	2039	2026	2028	0.000
CQUAD4	2059	210	2028	2026	2027	2029	0.000
CQUAD4	2060	210	2021	2040	2023	1170	0.000
CQUAD4	2061	210	1170	2010	2019	2021	0.000
CQUAD4	2062	210	2013	2012	1170	2023	0.000
CQUAD4	2063	210	2012	2009	2010	1170	0.000
CQUAD4	2064	210	2041	2040	2066	2067	0.000
CQUAD4	2065	210	2067	2066	2088	2090	0.000
CQUAD4	2066	210	2088	2106	2108	2090	0.000
CQUAD4	2067	210	2146	2144	2126	2125	0.000
CQUAD4	2068	210	2125	2106	2108	2126	0.000
CQUAD4	2069	210	2108	2090	2094	2110	0.000
CQUAD4	2070	210	2110	2094	2093	2104	0.000
CQUAD4	2071	210	2104	2093	2085	2084	0.000
CQUAD4	2072	210	2084	2085	2063	2060	0.000
CQUAD4	2073	210	2063	2060	2038	2039	0.000
CQUAD4	2074	210	2039	2038	2019	2026	0.000
CQUAD4	2075	210	2026	2019	2021	2027	0.000
CQUAD4	2076	210	2027	2021	2040	2041	0.000
CQUAD4	2077	210	2126	2108	2110	2122	0.000
CQUAD4	2078	210	2122	2110	2104	2121	0.000
CQUAD4	2079	210	2144	2126	2122	2131	0.000

CQUAD4	2081	210	2134	2133	2152	2135	0.000
CQUAD4	2082	210	2135	2152	2155	2154	0.000
CQUAD4	2083	210	2154	2155	2173	2158	0.000
CQUAD4	2084	210	2158	2173	2177	2160	0.000
CQUAD4	2085	210	2160	2177	2175	2159	0.000
CQUAD4	2086	210	2159	2175	2157	2156	0.000
CQUAD4	2087	210	2156	2157	2153	2136	0.000
CQUAD4	2088	210	2136	2153	2133	2134	0.000
CQUAD4	2089	210	2133	2132	2150	2152	0.000
CQUAD4	2090	210	2152	2150	2169	2155	0.000
CQUAD4	2091	210	2155	2169	2174	2173	0.000
CQUAD4	2092	210	2173	2174	2188	2177	0.000
CQUAD4	2093	210	2177	2188	2176	2175	0.000
CQUAD4	2094	210	2175	2176	2166	2157	0.000
CQUAD4	2095	210	2157	2166	2151	2153	0.000
CQUAD4	2096	210	2153	2151	2132	2133	0.000
CTRIA3	2097	210	2182	1306	2192	0.000	
CQUAD4	2098	210	2172	2187	1168	2171	0.000
CQUAD4	2099	210	2197	2196	2192	1306	0.000
CTRIA3	2100	210	2138	2183	2176	0.000	
CTRIA3	2101	210	2176	2183	2166	0.000	
CQUAD4	2102	210	2183	2182	1306	2194	0.000
CTRIA3	2103	210	2194	2188	2183	0.000	
CTRIA3	2104	210	2194	2188	2185	0.000	
CQUAD4	2105	210	2185	2184	1168	2194	0.000
CQUAD4	2106	210	1306	2194	2195	2197	0.000
CQUAD4	2107	210	2194	1168	2187	2195	0.000
CQUAD4	2108	210	2171	1168	2184	2170	0.000
CTRIA3	2109	210	2188	2185	2174	0.000	
CTRIA3	2110	210	2174	2185	2169	0.000	
CQUAD4	2111	210	2184	2170	2167	2168	0.000
CQUAD4	2112	210	2167	2168	2144	2146	0.000
CQUAD4	2113	210	2185	2184	2168	2169	0.000
CQUAD4	2114	210	2168	2169	2150	2144	0.000
CQUAD4	2115	210	2150	2144	2131	2132	0.000
CQUAD4	2116	210	2132	2131	2143	2151	0.000
CQUAD4	2117	210	2151	2143	2142	2166	0.000
CQUAD4	2118	210	2166	2142	2141	2165	0.000
CQUAD4	2119	210	2165	2166	2183	2182	0.000
CQUAD4	2120	210	2196	2190	2191	2192	0.000
CQUAD4	2121	210	2190	2189	1399	2191	0.000
CQUAD4	2122	210	2192	2191	2181	2182	0.000
CQUAD4	2123	210	2191	1399	2180	2181	0.000
CQUAD4	2124	210	2009	2003	1284	2010	0.000
CQUAD4	2125	210	2003	2002	2005	1284	0.000
CQUAD4	2126	210	2005	2006	2001	2002	0.000
CQUAD4	2127	210	2010	1284	2016	2019	0.000
CQUAD4	2128	210	2016	2015	2006	2005	0.000
CTRIA3	2129	210	1284	2005	2016	0.000	
CTRIA3	2130	210	1427	2022	2011	0.000	
CTRIA3	2131	210	1399	2178	2189	0.000	
CQUAD4	2132	210	2163	2139	2138	2162	0.000
CQUAD4	2133	210	2162	2138	2137	2161	0.000
CQUAD4	2134	210	2116	1452	2098	2115	0.000
CQUAD4	2135	210	1452	2080	2091	2100	0.000
CQUAD4	2136	210	2080	2057	2058	2081	0.000
CQUAD4	2137	210	2056	2032	2033	2057	0.000
CQUAD4	2138	210	2032	2022	1427	2033	0.000
CQUAD4	2139	210	2057	2033	2034	2058	0.000

```
CQUAD4          2140      210      2033      1427      2018      2034    0.000
CQUAD4          2141      210      1452      2080      2079      2098    0.000
CQUAD4          2142      210      2080      2057      2056      2079    0.000
CQUAD4          2143      210      2117      2100      1452      2116    0.000
CQUAD4          2144      210      2180      2163      2162      1399    0.000
CQUAD4          2145      210      1399      2162      2161      2178    0.000
CQUAD4          2146      210      2015      2017      2007      2006    0.000
CQUAD4          2147      210      2017      2018      1427      2007    0.000
CQUAD4          2148      210      2006      2007      2004      2001    0.000
CQUAD4          2149      210      2007      1427      2011      2004    0.000
CQUAD4          2150      210      2139      2117      2116      2138    0.000
CQUAD4          2151      210      2138      2116      2115      2137    0.000
CQUAD4          2152      210      2121      2104      2103      2120    0.000
CQUAD4          2153      210      2104      2103      2086      2084    0.000
CQUAD4          2154      210      2084      2086      2061      2060    0.000
CQUAD4          2155      210      2060      2061      2035      2038    0.000
CQUAD4          2156      210      2038      2035      2016      2019    0.000
CQUAD4          2157      210      2143      2121      2120      2142    0.000
CQUAD4          2158      210      2142      2120      2119      2141    0.000
CQUAD4          2159      210      2120      2103      2102      2119    0.000
CQUAD4          2160      210      2103      2086      2083      2102    0.000
CQUAD4          2161      210      2086      2061      2062      2083    0.000
CQUAD4          2162      210      2061      2035      2036      2062    0.000
CQUAD4          2163      210      2035      2016      2015      2036    0.000
CQUAD4          2164      210      2182      2165      2164      2181    0.000
CQUAD4          2165      210      2181      2164      2163      2180    0.000
CQUAD4          2166      210      2165      2141      2140      2164    0.000
CQUAD4          2167      210      2164      2140      2139      2163    0.000
CQUAD4          2168      210      2141      2119      2118      2140    0.000
CQUAD4          2169      210      2140      2118      2117      2139    0.000
CQUAD4          2170      210      2119      2102      2101      2118    0.000
CQUAD4          2171      210      2118      2101      2100      2117    0.000
CQUAD4          2172      210      2102      2083      2082      2101    0.000
CQUAD4          2173      210      2083      2062      2059      2082    0.000
CQUAD4          2174      210      2101      2082      2081      2100    0.000
CQUAD4          2175      210      2082      2059      2058      2081    0.000
CQUAD4          2176      210      2062      2036      2037      2059    0.000
CQUAD4          2177      210      2036      2015      2017      2037    0.000
CQUAD4          2178      210      2059      2037      2034      2058    0.000
CQUAD4          2179      210      2037      2017      2018      2034    0.000
PSHELL           109      120 0.07500       120                 120
PSHELL           110      120 0.10000       120                 120
PSHELL           111      120 0.12500       120                 120
PSHELL           112      120 0.14000       120                 120
PSHELL           113      120 0.15000       120                 120
PSHELL           114      120 0.20000       120                 120
PSHELL           115      120 0.30000       120                 120
PSHELL           116      120 0.37500       120                 120
PSHELL           117      120 0.40000       120                 120
PSHELL           210      220 0.03200       220                 220
MAT1             120 1.060+7 3.985+6 0.33000 2.590-4 0.        0.        0.        M     1
+M     1  0.        0.        0.
MAT1             220 1.060+7 3.985+6 0.33000 2.590-4 0.        0.        0.        M     2
+M     2  0.        0.        0.
$$$$$
$DISK DRIVE  ITEM3 (4 ARMs) QUAD4 ELEMs
$$$$$
GRID,3049,31,0.,0.,0.5625,31
GRID,3050,31,0.,0.,0.,31  $ARM ATTACHMENT POINT
GRID,3150,32,0.,0.,0.,32
```

```
GRID,3350,34,0.,0.,0.,34
$CBAR,3054,3010,1263,2060,1.,0.,0.
$CBAR,3054,3010,1263,3050,1.,0.,0. $8
CBAR,3054,3011,3049,3050,1.,0.,0.
R8E3,3049,,3049,123456,1.0,123456,1206,1207,+R8A
+R8A,1209,1225,1238,1255,1266,1267,1279,1280,+R88
+R88,1291,1292,1315
CBAR,3055,3010,3050,3150,1.,0.,0.
CBAR,3056,3010,3150,3250,1.,0.,0.
CBAR,3057,3010,3250,3350,1.,0.,0.
CBAR,3058,3010,3350,2060,1.,0.,0.,,+CB3054
+CB3054,,4
$PBAR,3010,3020,0.442,.0155,.0155
PBAR,3010,3020,1.2272,0.11984,0.11984
PBAR,3011,3020,0.4708,0.0477,0.0477
MAT1,3020,3.+7,,.3,7.51-4
$R8E3,3050,,3050,123456,1.0,123456,1263,2060  $ATTACHMENT FOR ARM
$$$$$R8E3,3053,,3051,123456,1.0,123456,1263,2060  $ATTACHMENT FOR C.G.
R8E2,3051,3050,123456,3001,3002,3003,3004,3006,+R83051
+R83051,3008,3020,3023,3024,3029,3030,3014
R8E2,3151,3150,123456,3101,3102,3103,3104,3106,+R83151
+R83151,3108,3120,3123,3124,3129,3130,3114
R8E2,3251,3250,123456,3201,3202,3203,3204,3206,+R83251
+R83251,3208,3220,3223,3224,3229,3230,3214
R8E2,3351,3350,123456,3301,3302,3303,3304,3306,+R83351
+R83351,3308,3320,3323,3324,3329,3330,3314
CORD2R,31,,1.325,-2.937,-0.3255,1.325,-2.937,1.0,+CR31
+CR31,2.325,-2.937,1.
CORD2R,32,,1.325,-2.937,-0.7005,1.325,-2.937,1.0,+CR32
+CR32,2.325,-2.937,1.
CORD2R,33,,1.325,-2.937,-1.0755,1.325,-2.937,1.0,+CR33
+CR33,2.325,-2.937,1.
CORD2R,34,,1.325,-2.937,-1.4505,1.325,-2.937,1.0,+CR34
+CR34,2.325,-2.937,1.
$DISK DRIVE ITEM3 (4 ARMS - QUAD 4)
$--BULK DATA CARDS PRODUCED BY "PATNAS" VERSION 1.7 :   13-JUL-86   19:12:00
GRID          3001      31-0.20991 0.62500 0.           31
GRID          3002      31-0.20991 0.54400 0.           31
GRID          3003      31-0.62120-0.16000 0.           31
GRID          3004      31-0.62120 0.02300 0.           31
GRID          3005      31-0.41983 0.62500 0.           31
GRID          3006      31-0.41983 0.46300 0.           31
GRID          3007      31-0.75746 0.02296 0.           31
GRID          3008      31-0.75746-0.16004 0.           31
GRID          3009      31-0.77662 0.24282 0.           31
GRID          3010      31-0.91001 0.23772 0.           31
GRID          3011      31-0.93205 0.46264 0.           31
GRID          3012      31-0.93205 0.62464 0.           31
GRID          3013      31-1.12151 0.02360 0.           31
GRID          3014      31-1.12151-0.16002 0.           31
GRID          3015      31-1.06255 0.45248 0.           31
GRID          3016      31-1.06255 0.62534 0.           31
GRID          3017      31-1.41590 0.27371 0.           31
GRID          3018      31-1.27406 0.23836 0.           31
GRID          3019      31-1.48556 0.02423 0.           31
GRID          3020      31-1.43556-0.16000 0.           31
GRID          3021      31-1.22930 0.46300 0.           31
GRID          3022      31-1.22930 0.62500 0.           31
GRID          3023      31-1.60250 0.08442 0.           31
```

```
GRID     3024          31-1.66500-0.16000 0.          31
GRID     3025          31-1.60250 0.27353 0.          31
GRID     3026          31-1.72750 0.26602 0.          31
GRID     3027          31-1.60250 0.46265 0.          31
GRID     3028          31-1.60250 0.62465 0.          31
GRID     3029          31-1.72750 0.06870 0.          31
GRID     3030          31-1.77594-0.08212 0.          31
GRID     3031          31-1.72750 0.46334 0.          31
GRID     3032          31-1.72750 0.62534 0.          31
GRID     3033          31-2.00771 0.26585 0.          31
GRID     3034          31-2.10876 0.15154 0.          31
GRID     3035          31-2.03488 0.62506 0.          31
GRID     3036          31-2.00771 0.46317 0.          31
GRID     3037          31-2.28792 0.46300 0.          31
GRID     3038          31-2.41938 0.36961 0.          31
GRID     3039          31-2.34226 0.62477 0.          31
GRID     3040          31-2.55251 0.46307 0.          31
GRID     3041          31-2.58474 0.79549 0.          31
GRID     3042          31-2.76413 0.60916 0.          31
GRID     3043          31-2.97575 0.75524 0.          31
GRID     3044          31-2.82723 0.96620 0.          31
GRID     3101          32-0.20991 0.62500 0.          32
GRID     3102          32-0.20991 0.54400 0.          32
GRID     3103          32-0.62120-0.16000 0.          32
GRID     3104          32-0.62120 0.02300 0.          32
GRID     3105          32-0.41983 0.62500 0.          32
GRID     3106          32-0.41983 0.46300 0.          32
GRID     3107          32-0.75746 0.02296 0.          32
GRID     3108          32-0.75746-0.16004 0.          32
GRID     3109          32-0.77662 0.24282 0.          32
GRID     3110          32-0.91001 0.23772 0.          32
GRID     3111          32-0.93205 0.46264 0.          32
GRID     3112          32-0.93205 0.62464 0.          32
GRID     3113          32-1.12151 0.02360 0.          32
GRID     3114          32-1.12151-0.16002 0.          32
GRID     3115          32-1.06255 0.45248 0.          32
GRID     3116          32-1.06255 0.62534 0.          32
GRID     3117          32-1.41590 0.27371 0.          32
GRID     3118          32-1.27406 0.23836 0.          32
GRID     3119          32-1.48556 0.02423 0.          32
GRID     3120          32-1.48556-0.16000 0.          32
GRID     3121          32-1.22930 0.46300 0.          32
GRID     3122          32-1.22930 0.62500 0.          32
GRID     3123          32-1.60250 0.08442 0.          32
GRID     3124          32-1.66500-0.16000 0.          32
GRID     3125          32-1.60250 0.27353 0.          32
GRID     3126          32-1.72750 0.26602 0.          32
GRID     3127          32-1.60250 0.46265 0.          32
GRID     3128          32-1.60250 0.62465 0.          32
GRID     3129          32-1.72750 0.06870 0.          32
GRID     3130          32-1.77594-0.08212 0.          32
GRID     3131          32-1.72750 0.46334 0.          32
GRID     3132          32-1.72750 0.62534 0.          32
GRID     3133          32-2.00771 0.26585 0.          32
GRID     3134          32-2.10876 0.15154 0.          32
GRID     3135          32-2.03488 0.62506 0.          32
GRID     3136          32-2.00771 0.46317 0.          32
GRID     3137          32-2.28792 0.46300 0.          32
GRID     3138          32-2.41938 0.36961 0.          32
GRID     3139          32-2.34226 0.62477 0.          32
```

```
GRID    3140          32-2.55251 0.46307 0.                  32
GRID    3141          32-2.58474 0.79549 0.                  32
GRID    3142          32-2.76413 0.60916 0.                  32
GRID    3143          32-2.97575 0.75524 0.                  32
GRID    3144          32-2.82723 0.96620 0.                  32
GRID    3201          33-0.20991 0.62500 0.                  33
GRID    3202          33-0.20991 0.54400 0.                  33
GRID    3203          33-0.62120-0.16000 0.                  33
GRID    3204          33-0.62120 0.02300 0.                  33
GRID    3205          33-0.41983 0.62500 0.                  33
GRID    3206          33-0.41983 0.46300 0.                  33
GRID    3207          33-0.75746 0.02296 0.                  33
GRID    3208          33-0.75746-0.16004 0.                  33
GRID    3209          33-0.77662 0.24282 0.                  33
GRID    3210          33-0.91001 0.23772 0.                  33
GRID    3211          33-0.93205 0.46264 0.                  33
GRID    3212          33-0.93205 0.62464 0.                  33
GRID    3213          33-1.12151 0.02360 0.                  33
GRID    3214          33-1.12151-0.16002 0.                  33
GRID    3215          33-1.06255 0.45248 0.                  33
GRID    3216          33-1.06255 0.62534 0.                  33
GRID    3217          33-1.41590 0.27371 0.                  33
GRID    3218          33-1.27406 0.23836 0.                  33
GRID    3219          33-1.48556 0.02423 0.                  33
GRID    3220          33-1.48556-0.16000 0.                  33
GRID    3221          33-1.22930 0.46300 0.                  33
GRID    3222          33-1.22930 0.62500 0.                  33
GRID    3223          33-1.60250 0.08442 0.                  33
GRID    3224          33-1.66500-0.16000 0.                  33
GRID    3225          33-1.60250 0.27353 0.                  33
GRID    3226          33-1.72750 0.26602 0.                  33
GRID    3227          33-1.60250 0.46265 0.                  33
GRID    3228          33-1.60250 0.62465 0.                  33
GRID    3229          33-1.72750 0.06870 0.                  33
GRID    3230          33-1.77594-0.08212 0.                  33
GRID    3231          33-1.72750 0.46334 0.                  33
GRID    3232          33-1.72750 0.62534 0.                  33
GRID    3233          33-2.00771 0.26585 0.                  33
GRID    3234          33-2.10876 0.15154 0.                  33
GRID    3235          33-2.03488 0.62506 0.                  33
GRID    3236          33-2.00771 0.46317 0.                  33
GRID    3237          33-2.28792 0.46300 0.                  33
GRID    3238          33-2.41938 0.36961 0.                  33
GRID    3239          33-2.34226 0.62477 0.                  33
GRID    3240          33-2.55251 0.46307 0.                  33
GRID    3241          33-2.58474 0.79549 0.                  33
GRID    3242          33-2.76413 0.60916 0.                  33
GRID    3243          33-2.97575 0.75524 0.                  33
GRID    3244          33-2.82723 0.96620 0.                  33
GRID    3301          34-0.20991 0.62500 0.                  34
GRID    3302          34-0.20991 0.54400 0.                  34
GRID    3303          34-0.62120-0.16000 0.                  34
GRID    3304          34-0.62120 0.02300 0.                  34
GRID    3305          34-0.41983 0.62500 0.                  34
GRID    3306          34-0.41983 0.46300 0.                  34
GRID    3307          34-0.75746 0.02296 0.                  34
GRID    3308          34-0.75746-0.16004 0.                  34
GRID    3309          34-0.77662 0.24282 0.                  34
GRID    3310          34-0.91001 0.23772 0.                  34
GRID    3311          34-0.93205 0.46264 0.                  34
```

```
GRID           3312          34-0.93205 0.62464 0.                34
GRID           3313          34-1.12151 0.02360 0.                34
GRID           3314          34-1.12151-0.16002 0.                34
GRID           3315          34-1.06255 0.45248 0.                34
GRID           3316          34-1.06255 0.62534 0.                34
GRID           3317          34-1.41590 0.27371 0.                34
GRID           3318          34-1.27406 0.23836 0.                34
GRID           3319          34-1.48556 0.02423 0.                34
GRID           3320          34-1.48556-0.16000 0.                34
GRID           3321          34-1.22930 0.46300 0.                34
GRID           3322          34-1.22930 0.62500 0.                34
GRID           3323          34-1.60250 0.08442 0.                34
GRID           3324          34-1.66500-0.16000 0.                34
GRID           3325          34-1.60250 0.27353 0.                34
GRID           3326          34-1.72750 0.26602 0.                34
GRID           3327          34-1.60250 0.46265 0.                34
GRID           3328          34-1.60250 0.62465 0.                34
GRID           3329          34-1.72750 0.06870 0.                34
GRID           3330          34-1.77594-0.08212 0.                34
GRID           3331          34-1.72750 0.46334 0.                34
GRID           3332          34-1.72750 0.62534 0.                34
GRID           3333          34-2.00771 0.26585 0.                34
GRID           3334          34-2.10876 0.15154 0.                34
GRID           3335          34-2.03488 0.62506 0.                34
GRID           3336          34-2.00771 0.46317 0.                34
GRID           3337          34-2.28792 0.46300 0.                34
GRID           3338          34-2.41938 0.36961 0.                34
GRID           3339          34-2.34226 0.62477 0.                34
GRID           3340          34-2.55251 0.46307 0.                34
GRID           3341          34-2.58474 0.79549 0.                34
GRID           3342          34-2.76413 0.60916 0.                34
GRID           3343          34-2.97575 0.75524 0.                34
GRID           3344          34-2.82723 0.96620 0.                34
CQUAD4         3001      310     3002     3001     3005     3006    0.000
CQUAD4         3002      310     3006     3005     3012     3011    0.000
CQUAD4         3003      310     3011     3012     3016     3015    0.000
CQUAD4         3004      310     3015     3016     3022     3021    0.000
CQUAD4         3005      310     3021     3022     3028     3027    0.000
CQUAD4         3006      310     3027     3028     3032     3031    0.000
CQUAD4         3007      310     3031     3032     3035     3036    0.000
CQUAD4         3008      310     3036     3035     3039     3037    0.000
CQUAD4         3009      310     3038     3037     3039     3040    0.000
CQUAD4         3010      310     3040     3039     3041     3042    0.000
CQUAD4         3011      310     3042     3041     3044     3043    0.000
CQUAD4         3012      310     3007     3004     3009     3010    0.000
CQUAD4         3013      310     3010     3009     3011     3015    0.000
CQUAD4         3014      310     3023     3019     3018     3017    0.000
CQUAD4         3015      310     3017     3018     3015     3021    0.000
CQUAD4         3016      310     3029     3023     3025     3026    0.000
CQUAD4         3017      310     3026     3025     3027     3031    0.000
CQUAD4         3018      310     3003     3004     3007     3008    0.000
CQUAD4         3019      310     3008     3007     3013     3014    0.000
CQUAD4         3020      310     3014     3013     3019     3020    0.000
CQUAD4         3021      310     3020     3019     3023     3024    0.000
CQUAD4         3022      310     3024     3023     3029     3030    0.000
CQUAD4         3023      310     3030     3029     3033     3034    0.000
CQUAD4         3024      310     3034     3033     3037     3038    0.000
CQUAD4         3101      310     3102     3101     3105     3106    0.000
CQUAD4         3102      310     3106     3105     3112     3111    0.000
CQUAD4         3103      310     3111     3112     3116     3115    0.000
```

CQUAD4	3104	310	3115	3116	3122	3121	0.000
CQUAD4	3105	310	3121	3122	3128	3127	0.000
CQUAD4	3106	310	3127	3128	3132	3131	0.000
CQUAD4	3107	310	3131	3132	3135	3136	0.000
CQUAD4	3108	310	3136	3135	3139	3137	0.000
CQUAD4	3109	310	3138	3137	3139	3140	0.000
CQUAD4	3110	310	3140	3139	3141	3142	0.000
CQUAD4	3111	310	3142	3141	3144	3143	0.000
CQUAD4	3112	310	3107	3104	3109	3110	0.000
CQUAD4	3113	310	3110	3109	3111	3115	0.000
CQUAD4	3114	310	3123	3119	3118	3117	0.000
CQUAD4	3115	310	3117	3118	3115	3121	0.000
CQUAD4	3116	310	3129	3123	3125	3126	0.000
CQUAD4	3117	310	3126	3125	3127	3131	0.000
CQUAD4	3118	310	3103	3104	3107	3108	0.000
CQUAD4	3119	310	3108	3107	3113	3114	0.000
CQUAD4	3120	310	3114	3113	3119	3120	0.000
CQUAD4	3121	310	3120	3119	3123	3124	0.000
CQUAD4	3122	310	3124	3123	3129	3130	0.000
CQUAD4	3123	310	3130	3129	3133	3134	0.000
CQUAD4	3124	310	3134	3133	3137	3138	0.000
CQUA04	3201	310	3202	3201	3205	3206	0.000
CQUAD4	3202	310	3206	3205	3212	3211	0.000
CQUAD4	3203	310	3211	3212	3216	3215	0.000
CQUAD4	3204	310	3215	3216	3222	3221	0.000
CQUAD4	3205	310	3221	3222	3228	3227	0.000
CQUAD4	3206	310	3227	3228	3232	3231	0.000
CQUAD4	3207	310	3231	3232	3235	3236	0.000
CQUAD4	3208	310	3236	3235	3239	3237	0.000
CQUAD4	3209	310	3238	3237	3239	3240	0.000
CQUAD4	3210	310	3240	3239	3241	3242	0.000
CQUAD4	3211	310	3242	3241	3244	3243	0.000
CQUAD4	3212	310	3207	3204	3209	3210	0.000
CQUAD4	3213	310	3210	3209	3211	3215	0.000
CQUAD4	3214	310	3223	3219	3218	3217	0.000
CQUAD4	3215	310	3217	3218	3215	3221	0.000
CQUAD4	3216	310	3229	3223	3225	3226	0.000
CQUAD4	3217	310	3226	3225	3227	3231	0.000
CQUAD4	3218	310	3203	3204	3207	3208	0.000
CQUAD4	3219	310	3208	3207	3213	3214	0.000
CQUAD4	3220	310	3214	3213	3219	3220	0.000
CQUAD4	3221	310	3220	3219	3223	3224	0.000
CQUAD4	3222	310	3224	3223	3229	3230	0.000
CQUAD4	3223	310	3230	3229	3233	3234	0.000
CQUAD4	3224	310	3234	3233	3237	3238	0.000
CQUAD4	3301	310	3302	3301	3305	3306	0.000
CQUAD4	3302	310	3306	3305	3312	3311	0.000
CQUAD4	3303	310	3311	3312	3316	3315	0.000
CQUAD4	3304	310	3315	3316	3322	3321	0.000
CQUAD4	3305	310	3321	3322	3328	3327	0.000
CQUAD4	3306	310	3327	3328	3332	3331	0.000
CQUAD4	3307	310	3331	3332	3335	3336	0.000
CQUAD4	3308	310	3336	3335	3339	3337	0.000
CQUAD4	3309	310	3338	3337	3339	3340	0.000
CQUAD4	3310	310	3340	3339	3341	3342	0.000
CQUAD4	3311	310	3342	3341	3344	3343	0.000
CQUAD4	3312	310	3307	3304	3309	3310	0.000
CQUAD4	3313	310	3310	3309	3311	3315	0.000
CQUAD4	3314	310	3323	3319	3318	3317	0.000
CQUAD4	3315	310	3317	3318	3315	3321	0.000

```
CQUAD4       3320      310     3314     3313     3319     3320    0.000
CQUAD4       3321      310     3320     3319     3323     3324    0.000
CQUAD4       3322      310     3324     3323     3329     3330    0.000
CQUAD4       3323      310     3330     3329     3333     3334    0.000
CQUAD4       3324      310     3334     3333     3337     3338    0.000
PSHELL        310      320 0.12500      320              320
MAT1          320 1.060+7 3.985+6 0.33000 2.590-4 0.       0.       0.       M  320
+M  320  0.       0.       0.
$$$$$$$$$$$$$$$$$$
$DISK DRIVE (ITEM5)
$$$$$$$$$$$$$$$$$$
$$
$ disk drive item5
GRID,5001,1,0.82663,-4.38615,-0.25,1
CBAR,5001,5010,1437,1319,0.,1.,0.,,+CB5001
CBAR,5002,5010,1319,5001,0.,1.,0.,,+CB5002
CBAR,5003,5010,1437,5001,0.,1.,0.,,+CB5003
CBAR,5004,5010,1429,5001,0.,1.,0.,,+CB5004
CBAR,5005,5010,1429,1437,0.,1.,0.,,+CB5005
+CB5001,,,0.,0.,-0.1875,0.,0.,-0.1875
+CB5002,,,0.,0.,-0.1875,0.,0.,0.0625
+CB5003,,,0.,0.,-0.1875,0.,0.,0.0625
+CB5004,,,0.,0.,-0.1875,0.,0.,0.0625
+CB5005,,,0.,0.,-0.1875,0.,0.,-0.1875
PBAR,5010,5020,0.09375,1.0986-3,4.883-4
MAT1,5020,28.+6,10.6+6,,7.40-7
CONM2,5006,5001,1,9.519-4
$$
$$$$$$$$$$$$$$$$$$
$DISK DRIVE (ITEM4)
$$$$$$$$$$$$$$$$$$
GRID,4100,4,0.,0.,.25,
CONM2,4200,4100,,2.801-3,,,,,+CM1
+CM1,2.6-3,,2.6-3
RBE3,4201,,4100,123456,1.,123456,4017,4012,+RB1
+RB1,4009,4015
$$$$$
$$
$DISK DRIVE ITEM4
$--BULK DATA CARDS PRODUCED BY "PATNAS" VERSION 1.7 :    7-JUL-86   21:52:46
GRID         4001       4-1.62500 0.       0.             4
$$$$$GRID         4002       4-1.40729 0.81250 0.             4
GRID         4003       4-0.70365 0.40625 0.             4
GRID         4004       4-0.81250 0.       0.             4
GRID         4005       4-0.70365-0.40625 0.             4
GRID         4006       4-1.40729-0.81250 0.             4
GRID         4007       4-0.81250 1.40729 0.             4
GRID         4008       4-0.32906 0.56995 0.             4
GRID         4009       4-0.40625 0.       0.             4
GRID         4010       4-0.32906-0.56995 0.             4
GRID         4011       4-0.81250-1.40729 0.             4
GRID         4012       4 0.       0.56995 0.             4
GRID         4013       4 0.       1.62500 0.             4
GRID         4014       4 0.       0.       0.             4
GRID         4015       4 0.      -0.56995 0.             4
$$$$$GRID         4016       4 0.      -1.62500 0.             4
```

```
GRID           4017          4 0.40625 0.        0.                4
GRID           4018          4 0.32906 0.56995 0.                4
GRID           4019          4 0.81250 1.40729 0.                4
GRID           4020          4 0.32906-0.56995 0.                4
GRID           4021          4 0.81250-1.40729 0.                4
GRID           4022          4 0.81250 0.        0.                4
GRID           4023          4 0.70365 0.40625 0.                4
GRID           4024          4 0.70365-0.40625 0.                4
 $$$$GRID             4025          4 1.40729 0.81250 0.                     4
 RID           4026          4 1.40729-0.81250 0.                4
 RID           4027          4 1.62500 0.        0.                4
 QUAD4         4001        410      1187      4015      4020      4021    0.000
 QUAD4         4002        410      4021      4020      4024      4026    0.000
 QUAD4         4003        410      4026      4024      4022      4027    0.000
 QUAD4         4004        410      4027      4022      4023      1088    0.000
 QUAD4         4005        410      1088      4023      4018      4019    0.000
 QUAD4         4006        410      4019      4018      4012      4013    0.000
 QUAD4         4007        410      4012      4013      4007      4008    0.000
 QUAD4         4008        410      4007      4008      4003      1073    0.000
 QUAD4         4009        410      1073      4003      4004      4001    0.000
 QUAD4         4010        410      4001      4004      4005      4006    0.000
 QUAD4         4011        410      4006      4005      4010      4011    0.000
 QUAD4         4012        410      4011      4010      4015      1187    0.000
 QUAD4         4013        410      4024      4022      4017      4020    0.000
 QUAD4         4014        410      4022      4023      4018      4017    0.000
CQUAD4         4015        410      4020      4017      4014      4015    0.000
CQUAD4         4016        410      4017      4018      4012      4014    0.000
CQUAD4         4017        410      4015      4014      4009      4010    0.000
CQUAD4         4018        410      4014      4012      4008      4009    0.000
CQUAD4         4019        410      4010      4009      4004      4005    0.000
CQUAD4         4020        410      4009      4008      4003      4004    0.000
PSHELL          410        420 0.18750       420                 420
MAT1            420 1.060+7 3.985+6 0.33000 2.590-4 0.        0.        0.       M     4
+M     4  0.        0.        0.
CORD2R           4          0.        0.        0.        0.        0.       1.00000 CF    4
+CF     4 1.00000 0.        1.00000
ENDDATA
```

APPENDIX C

Experimental Mode Shapes

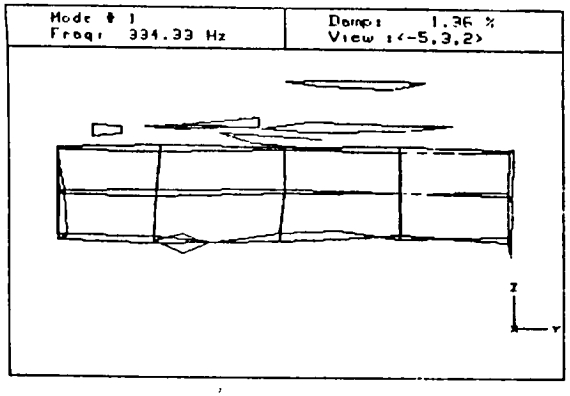

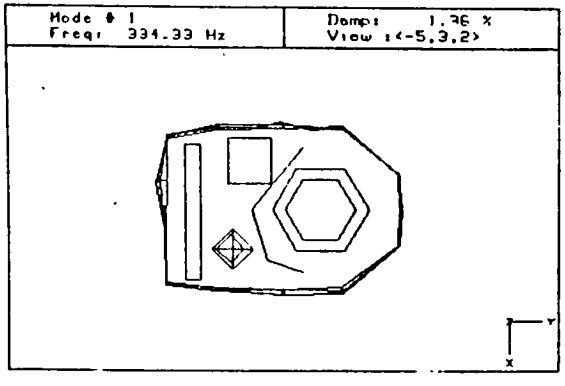

Experimental Mode 1 (334hz)

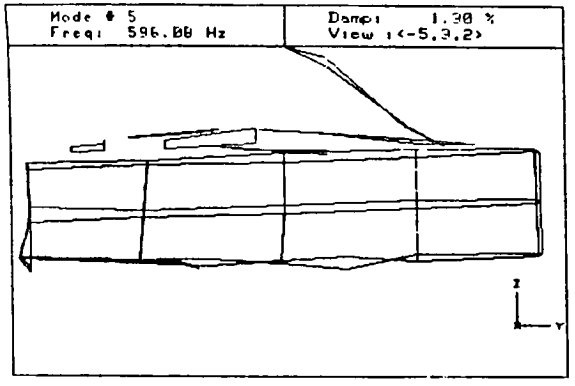

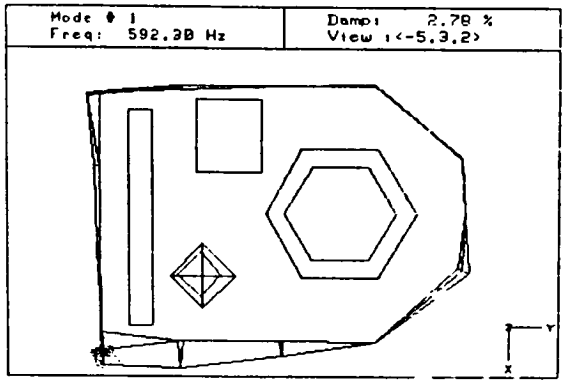

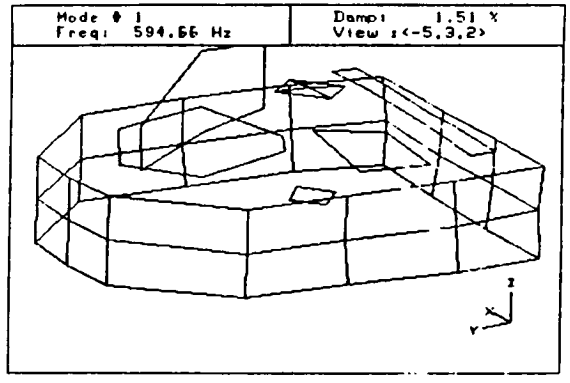

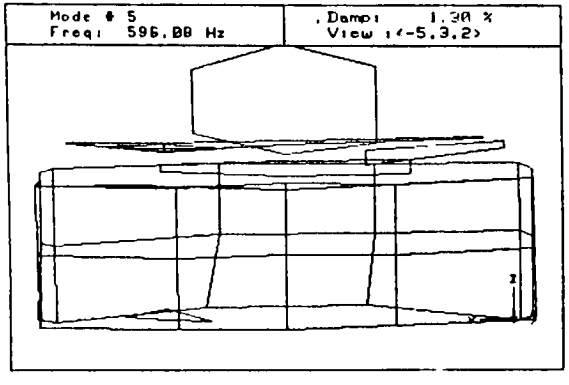

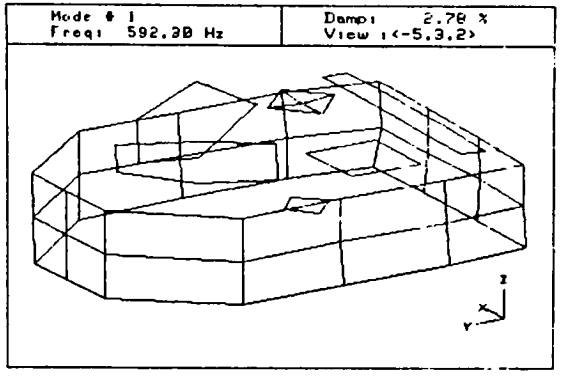

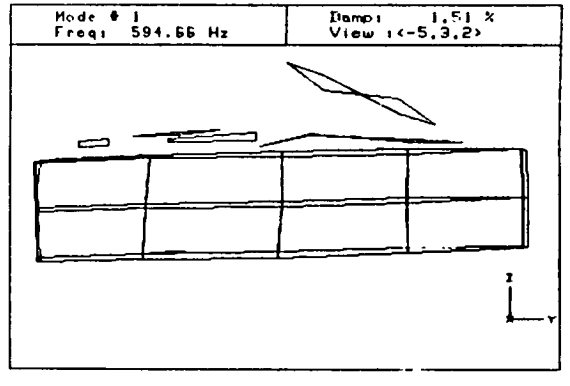

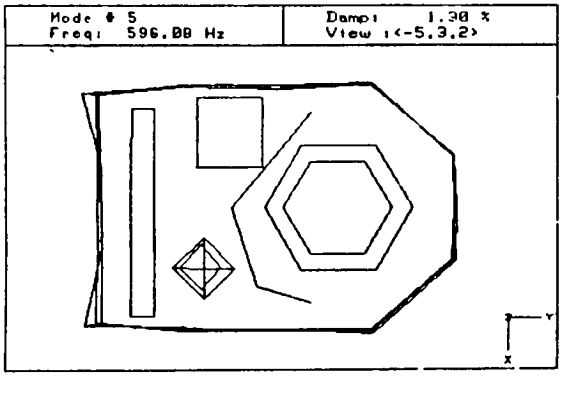

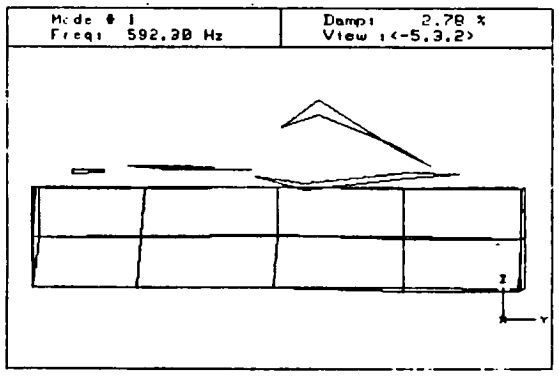

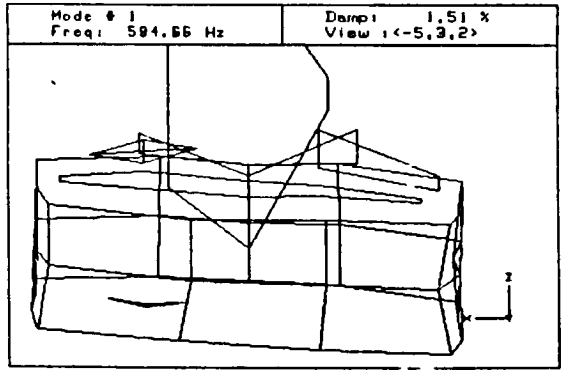

Experimental Mode 2 (594hz avr)

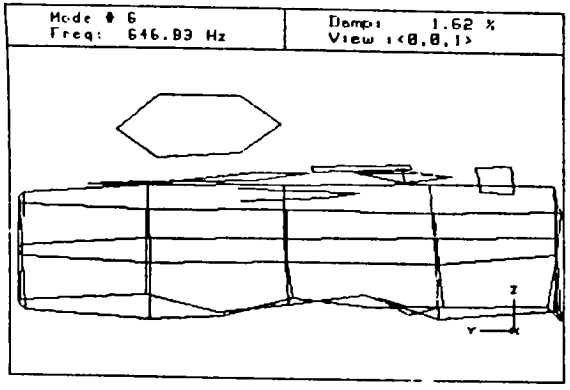

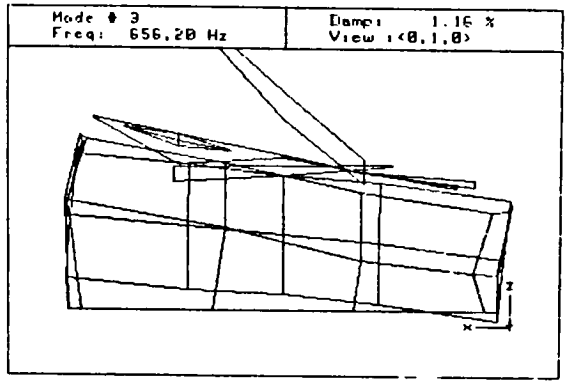

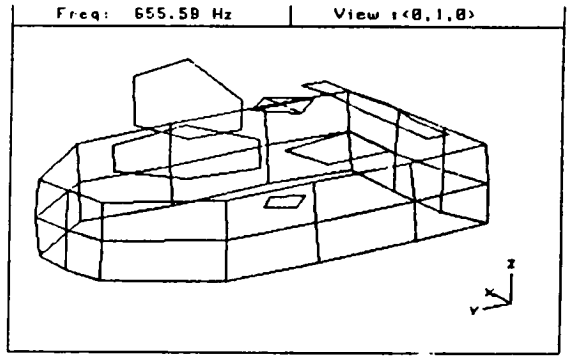

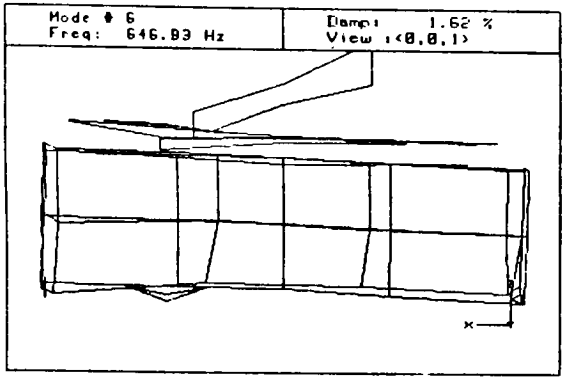

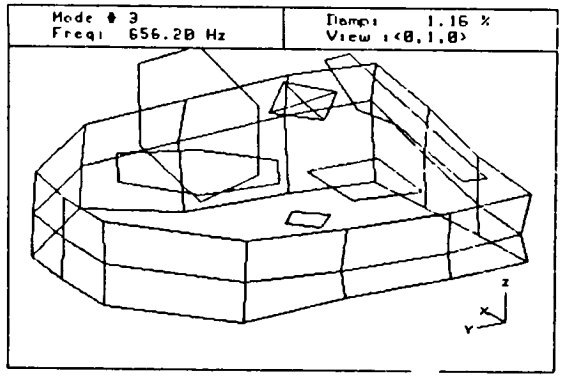

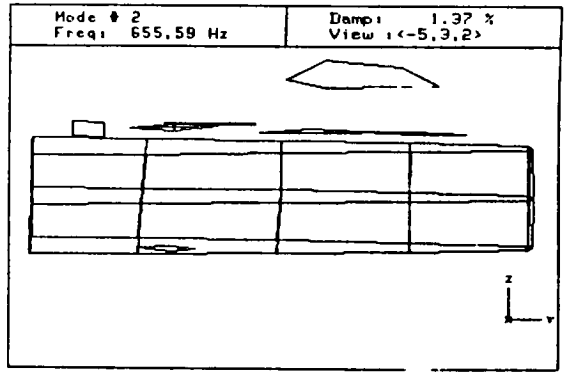

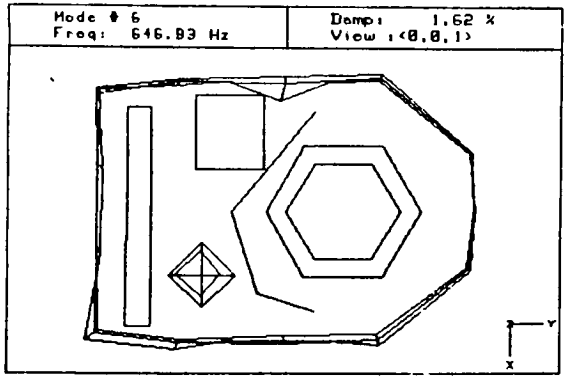

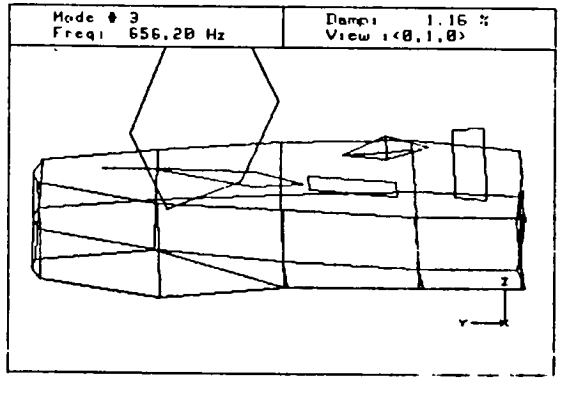

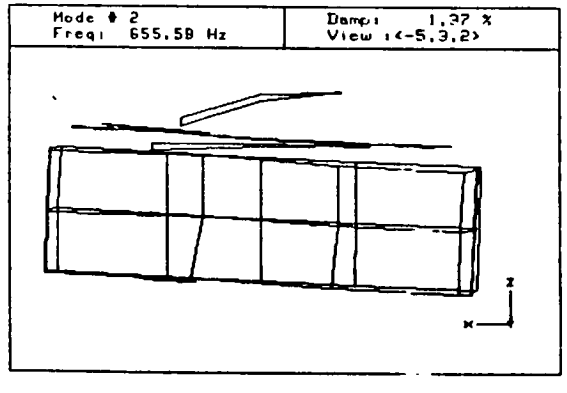

Experimental Mode 3 (653hz avr)

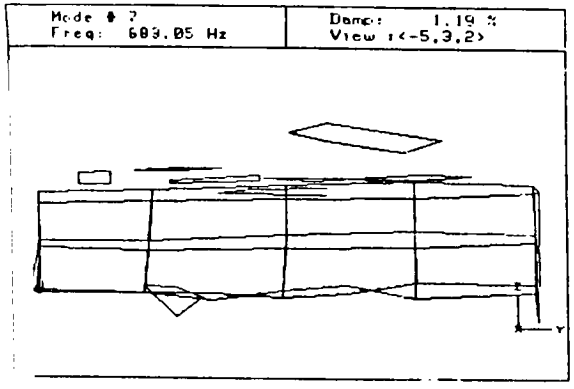

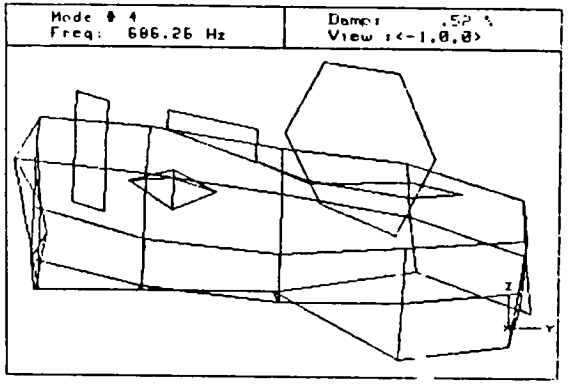

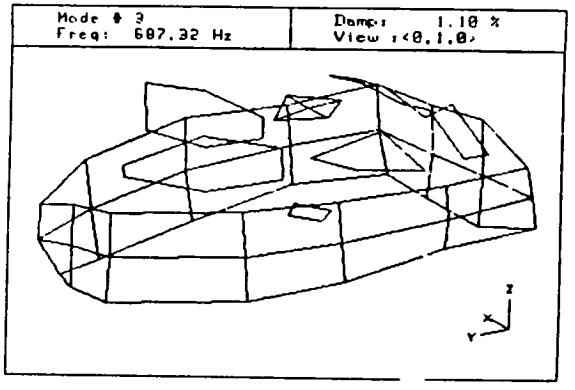

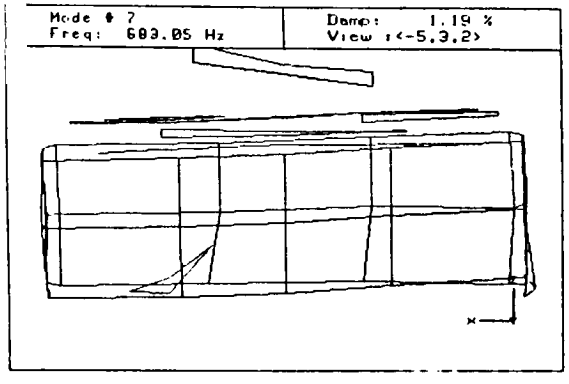

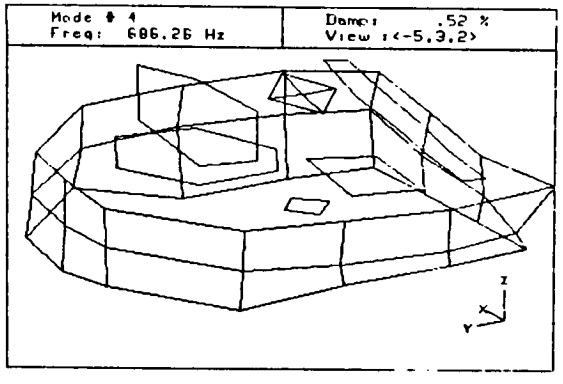

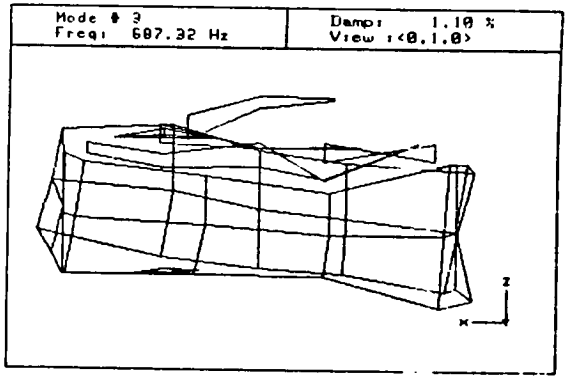

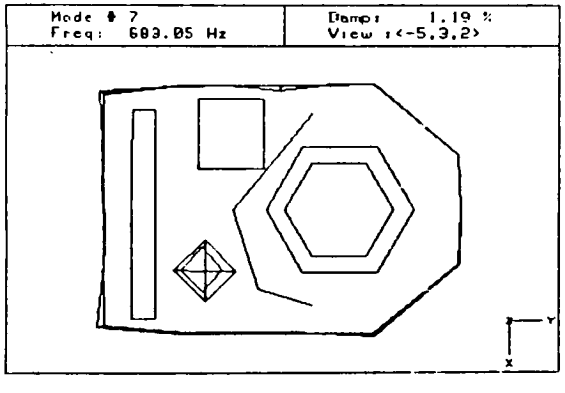

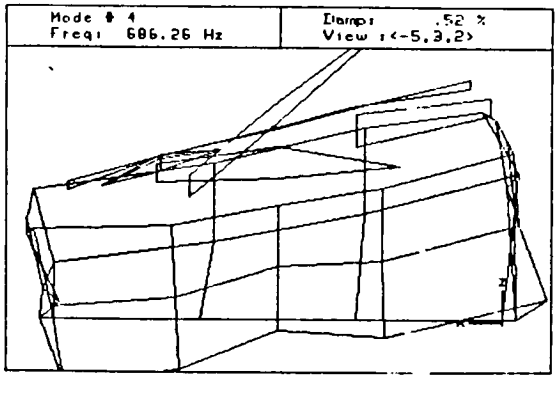

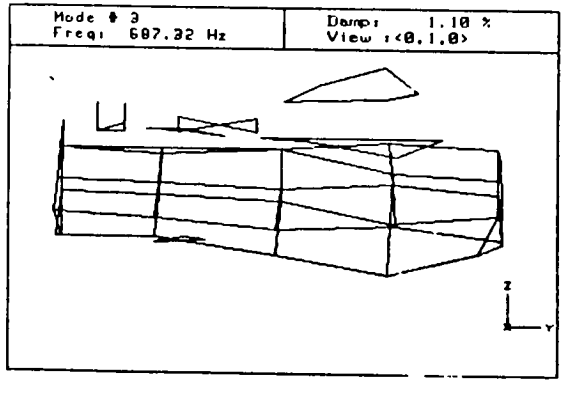

Experimental Mode 4 (685hz avr)

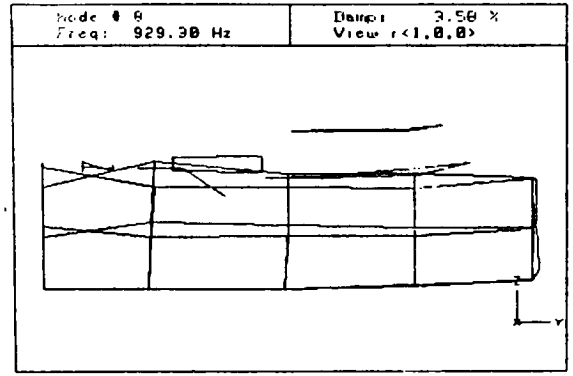

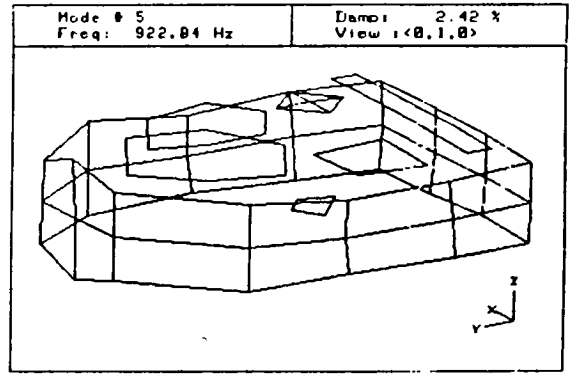

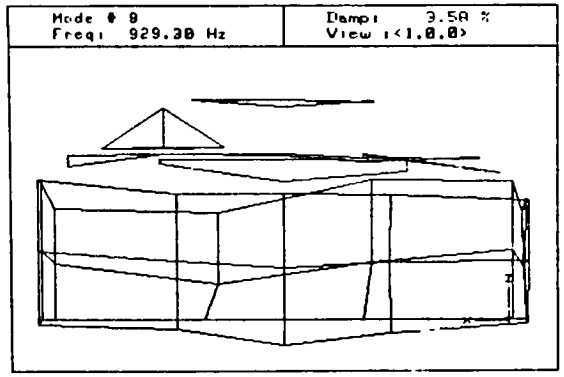

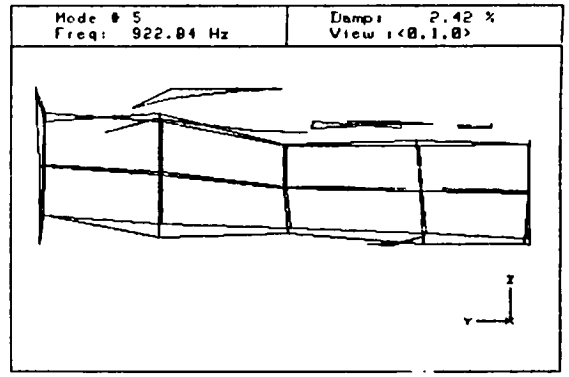

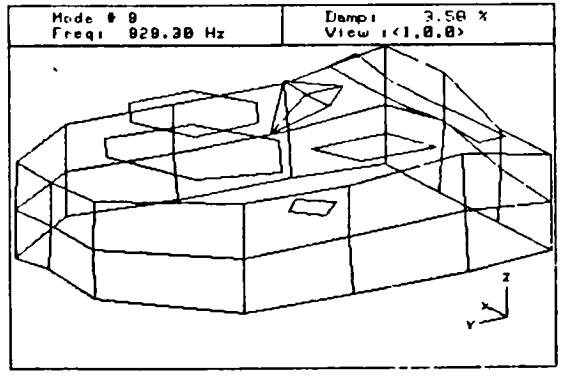

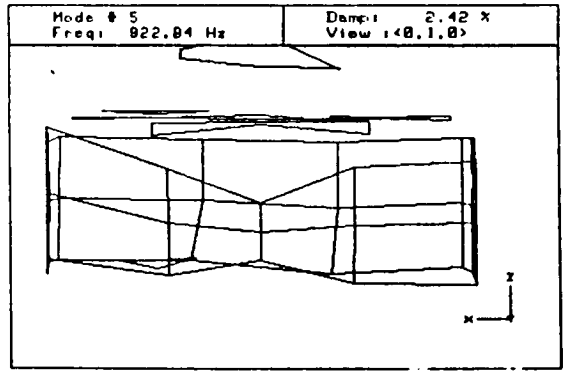

Experimental Mode 5 (926hz avr)

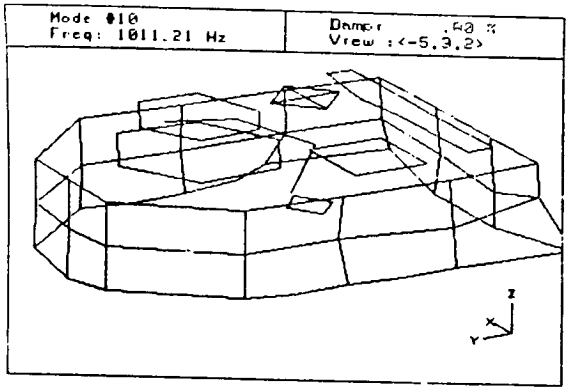

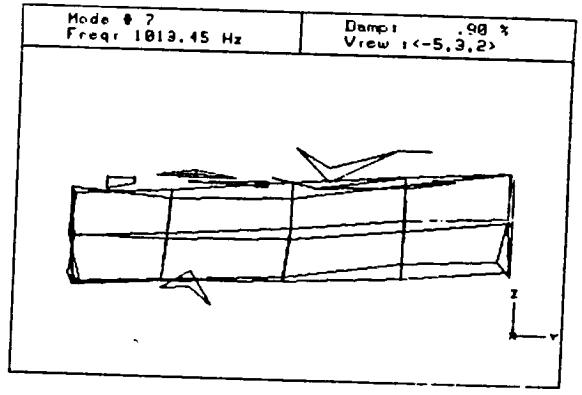

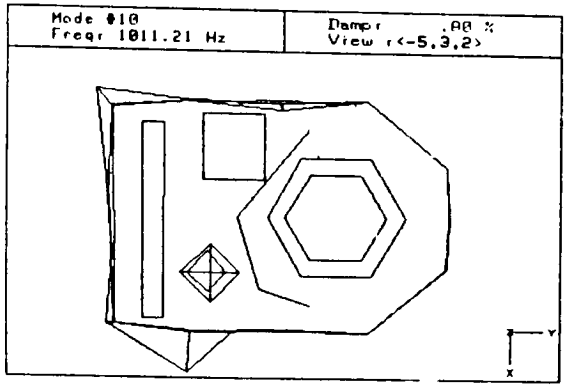

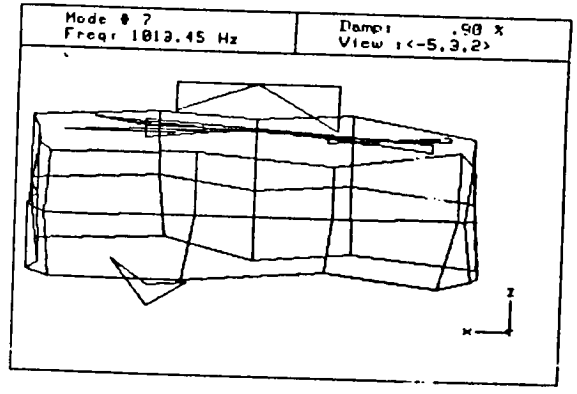

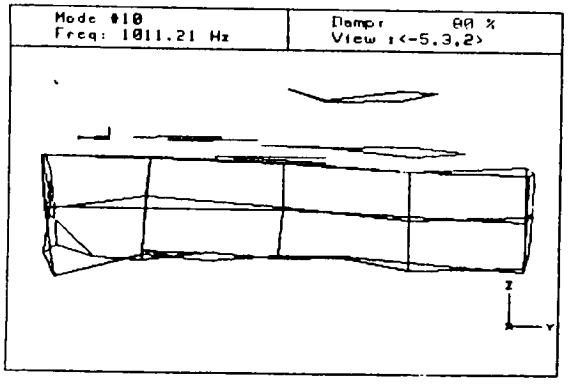

Experimental Mode 6 (1012hz avr)

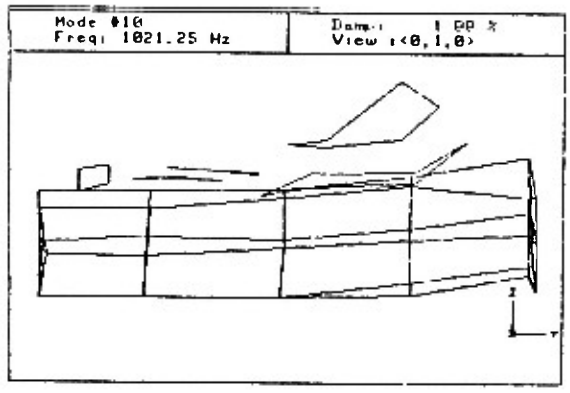

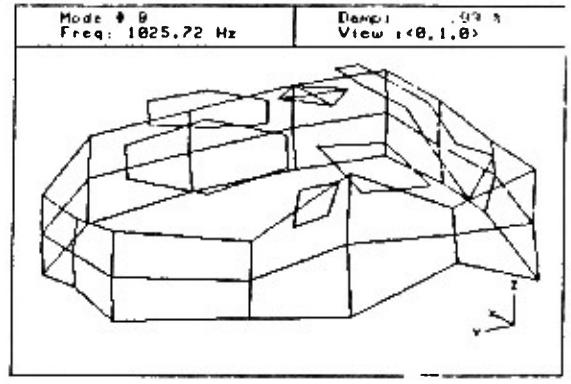

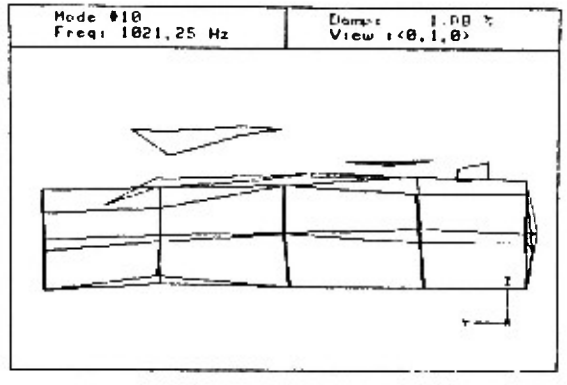

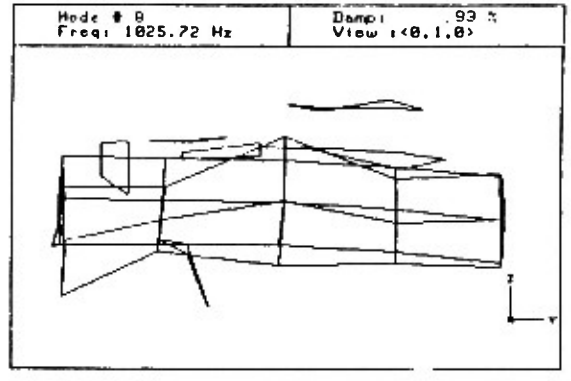

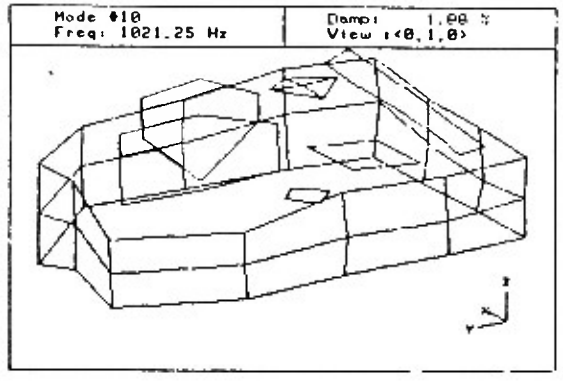

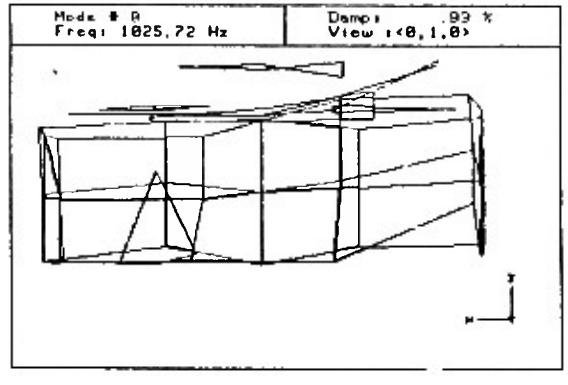

Experimental Mode 7 (1024hz avr)

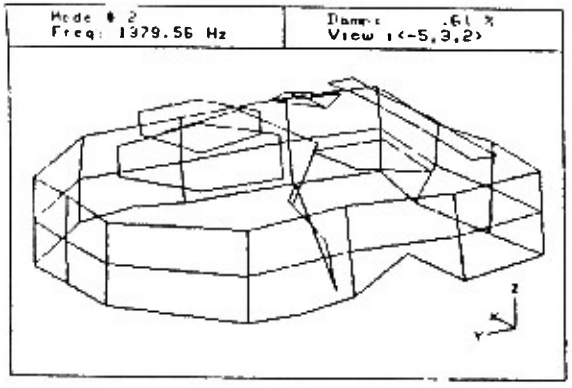

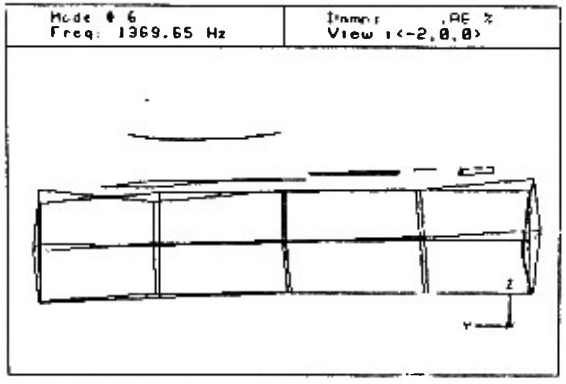

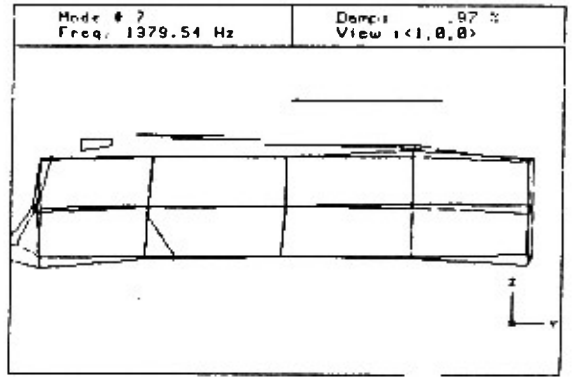

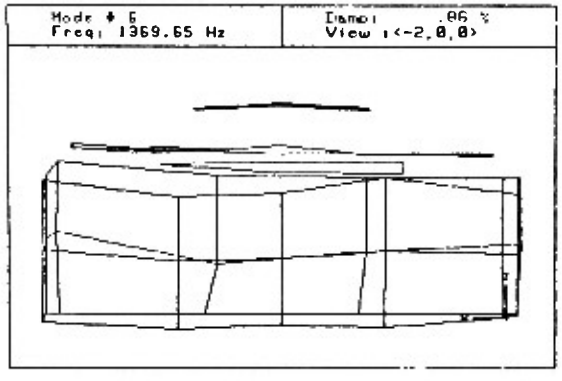

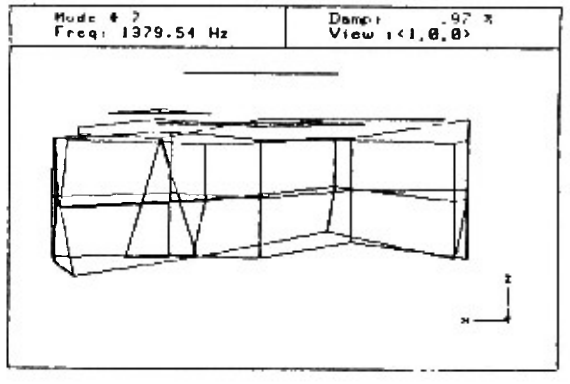

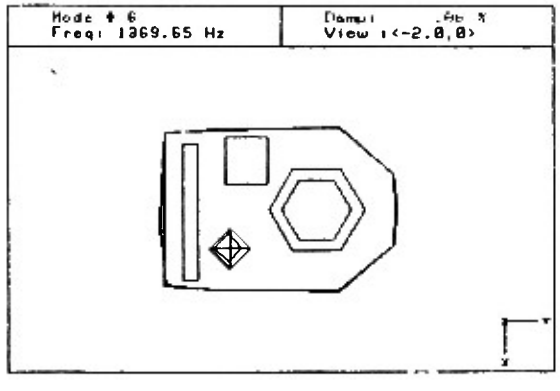

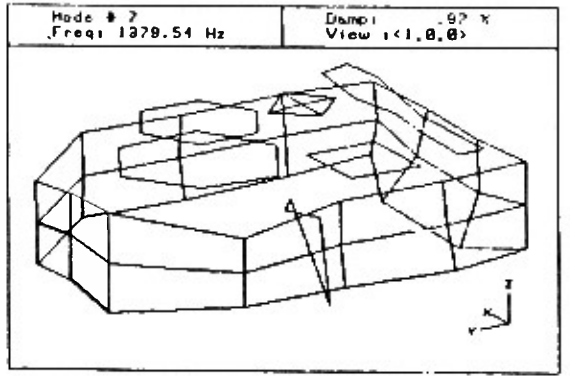

Experimental Mode 8 (1377hz avr)

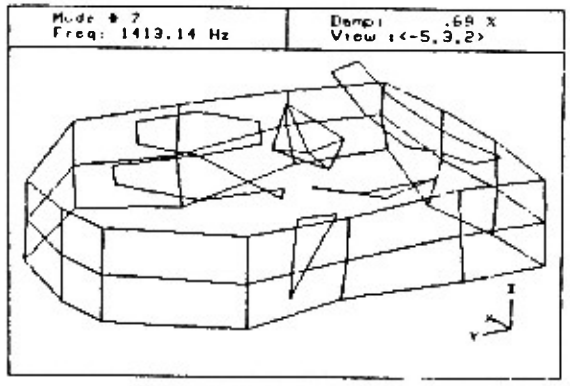

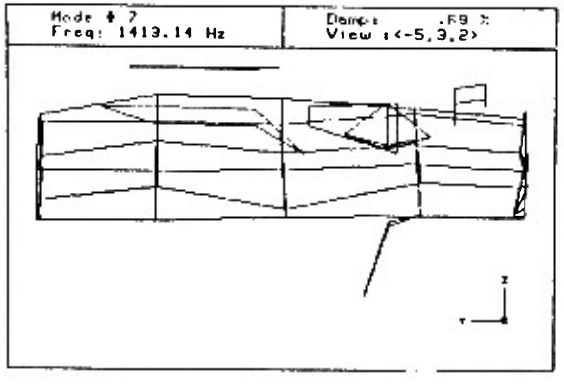

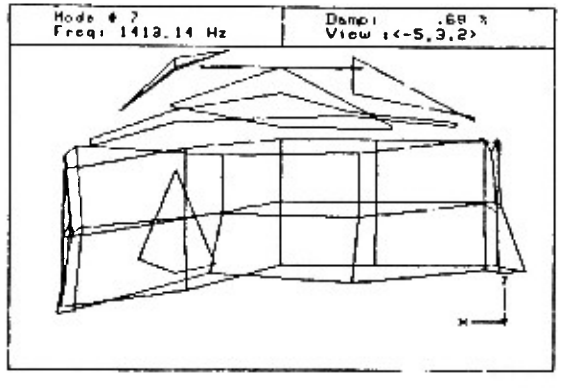

Experimental Mode 9 (1413hz)

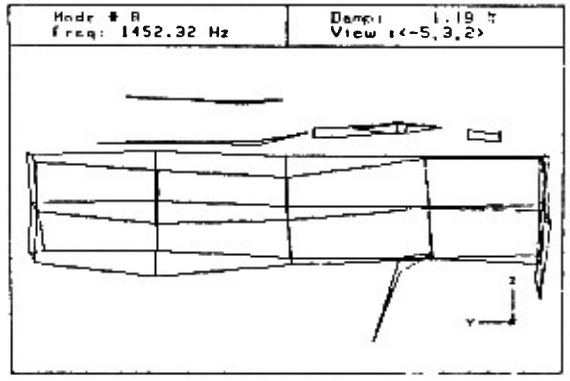

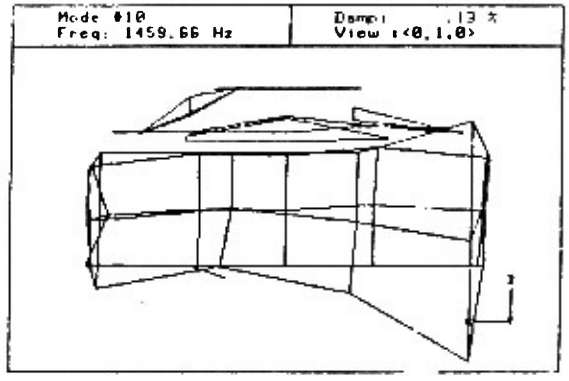

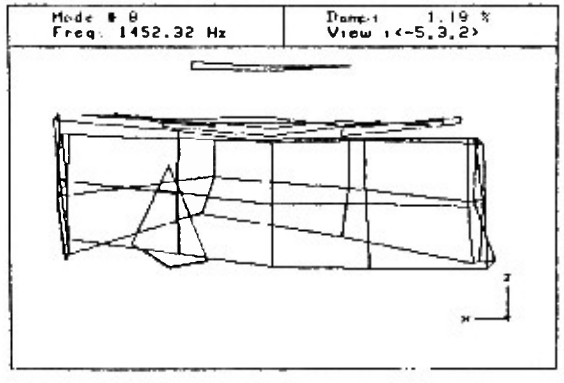

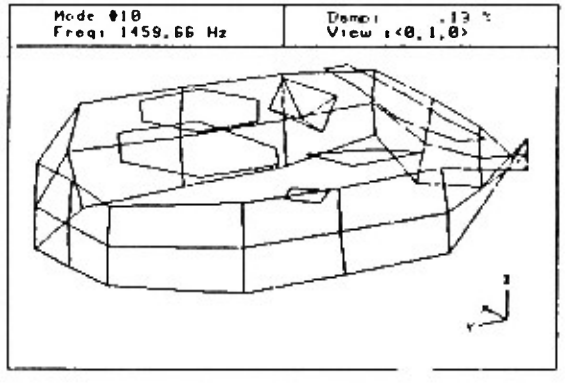

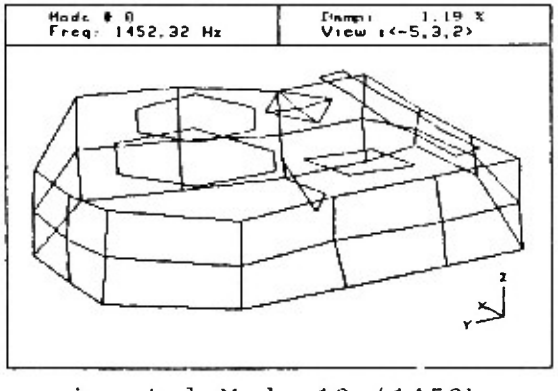

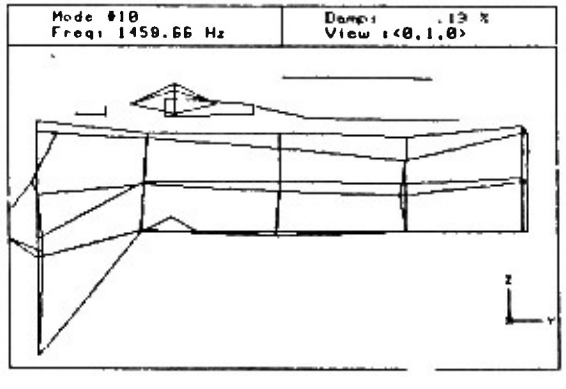

Experimental Mode 10 (1456hz avr)

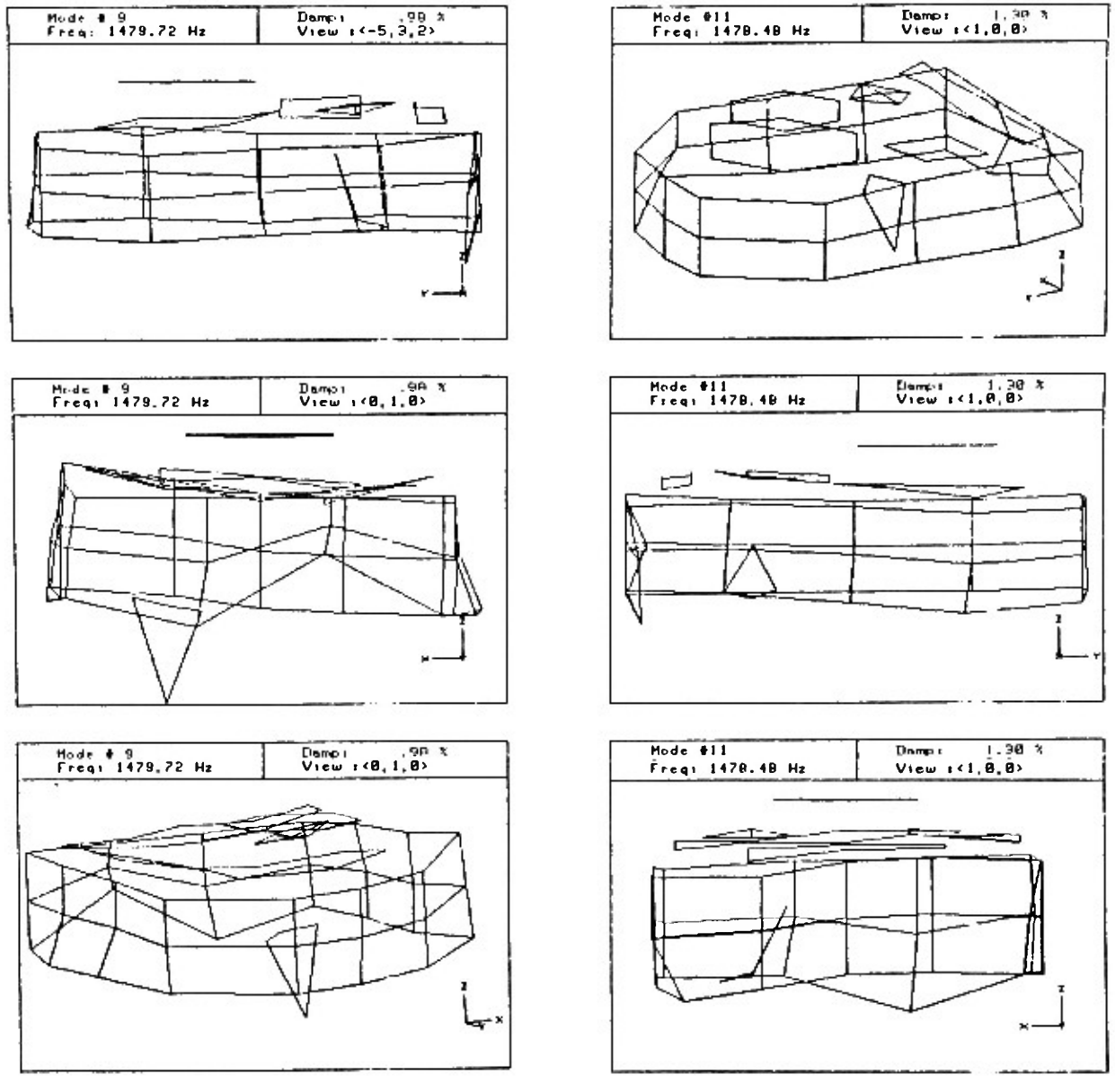

Experimental Mode 11 (1479hz avr)

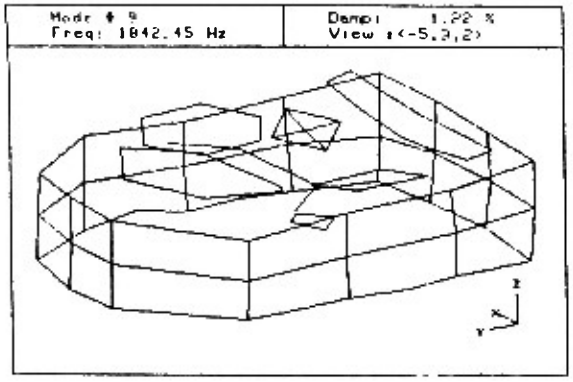

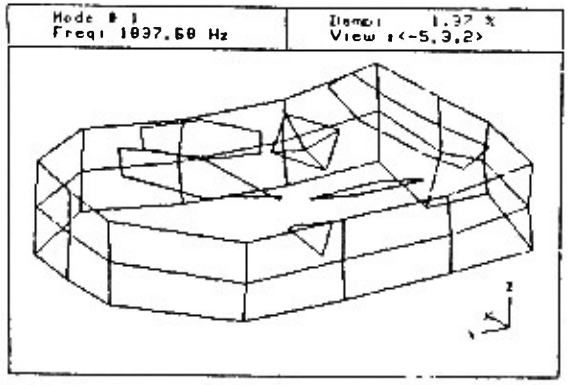

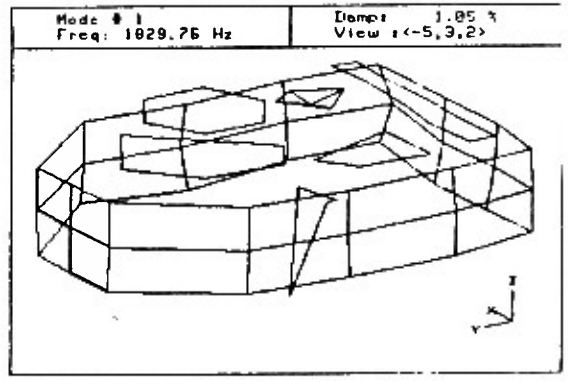

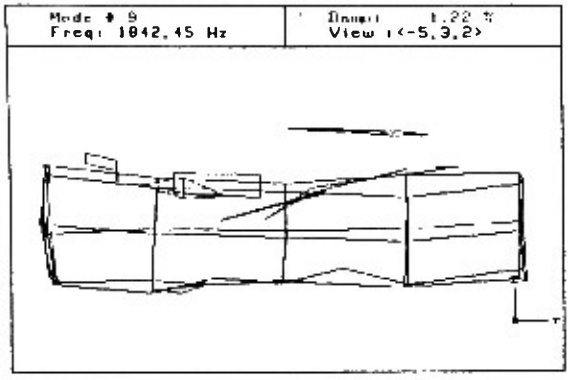

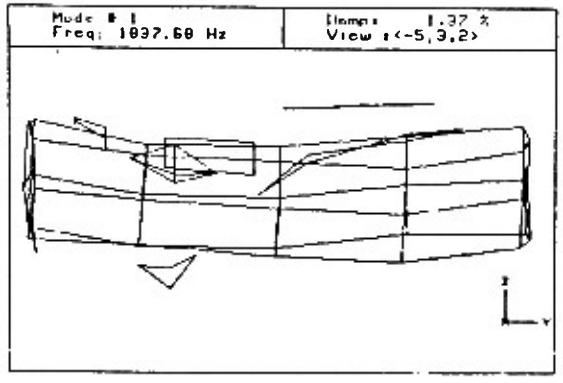

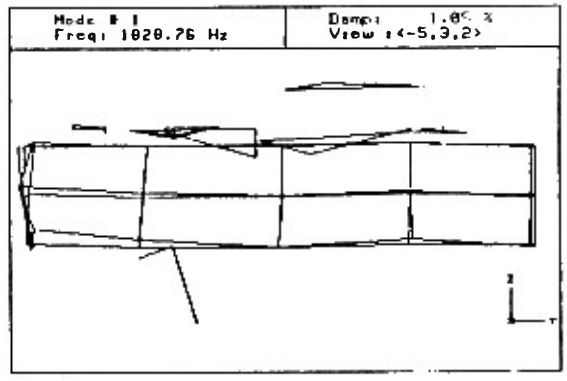

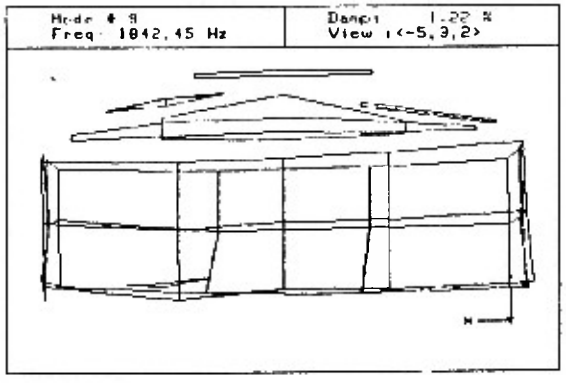

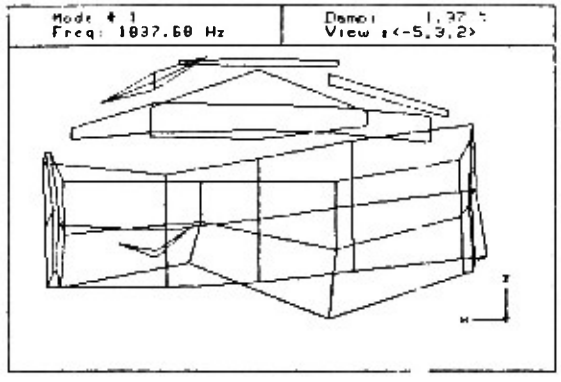

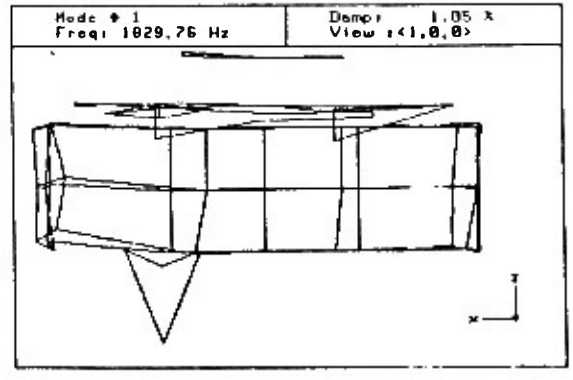

Experimental Mode 12 (1837hz avr)

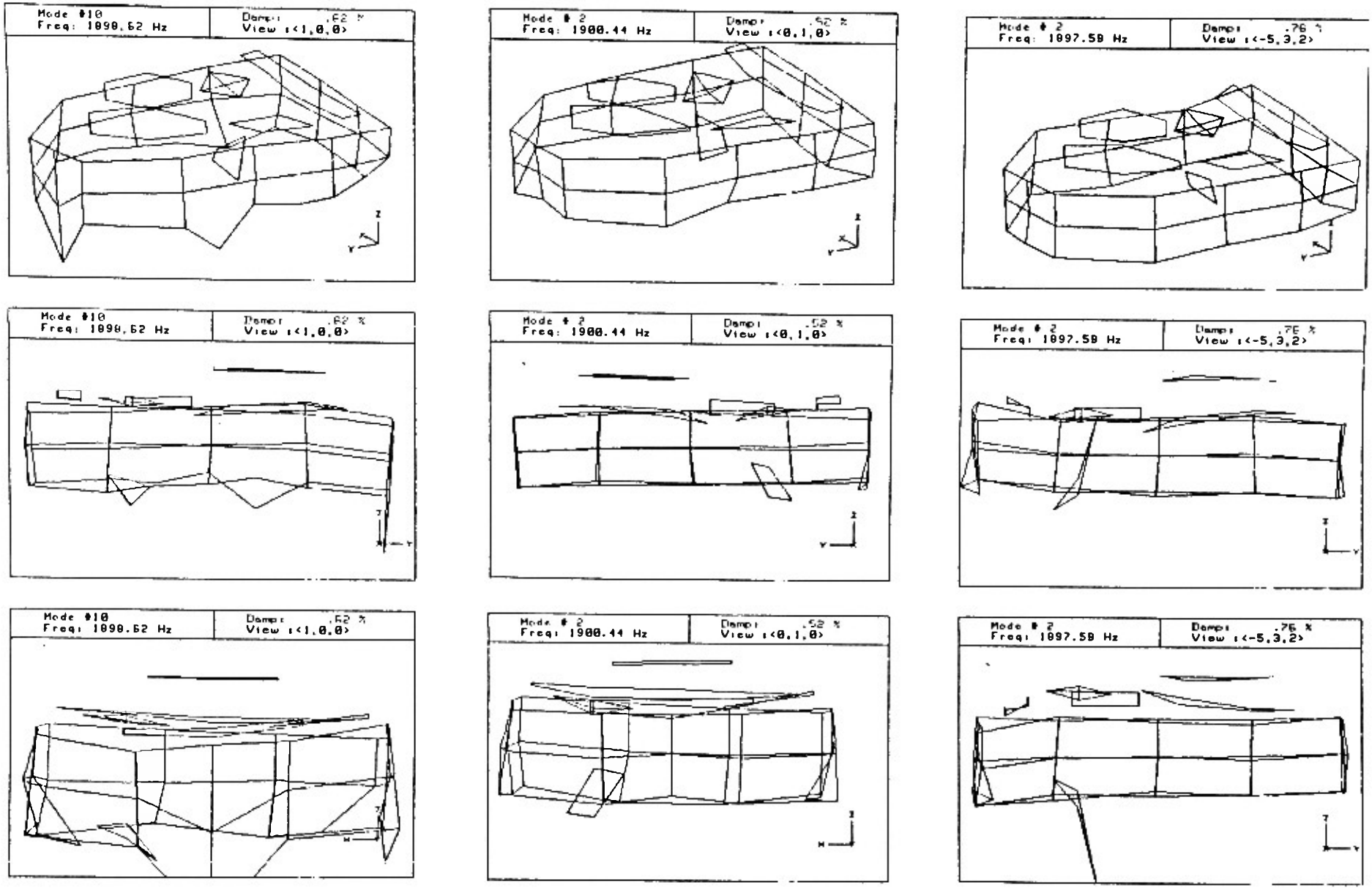

Experimental Mode 13 (1899hz)

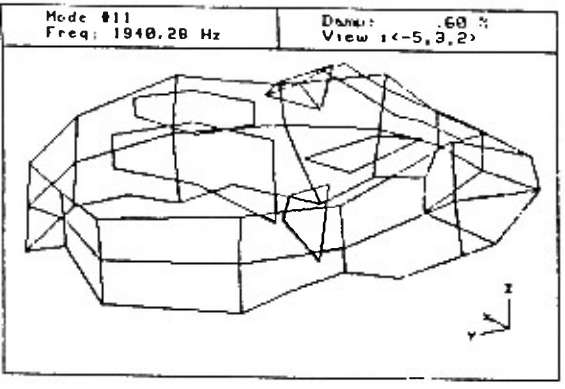

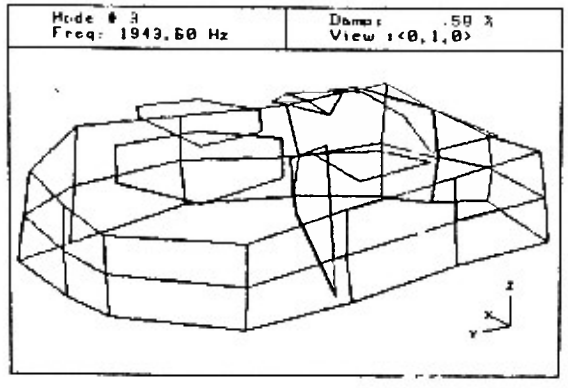

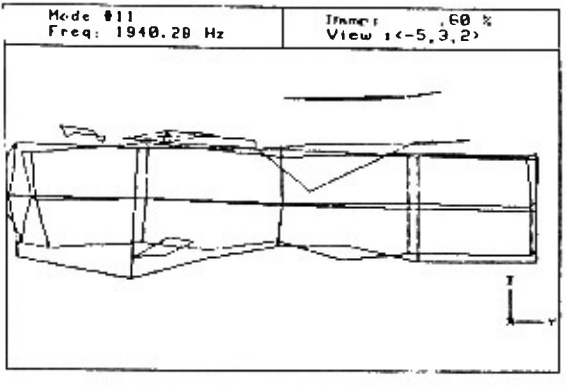

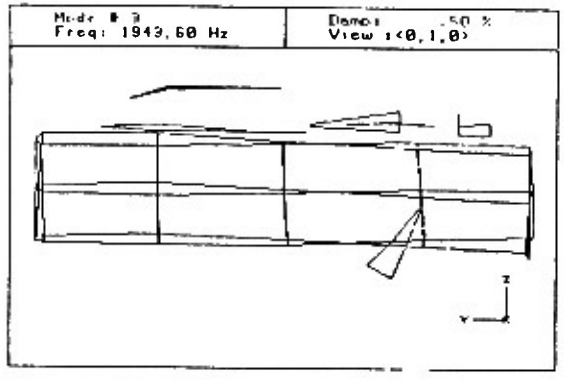

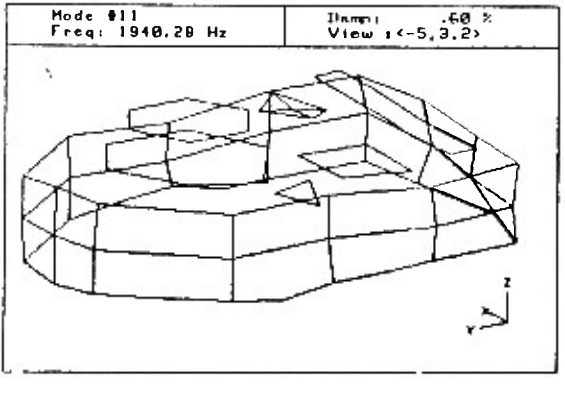

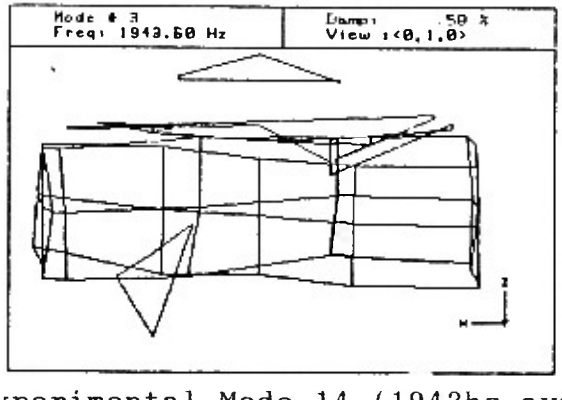

Experimental Mode 14 (1942hz avr)

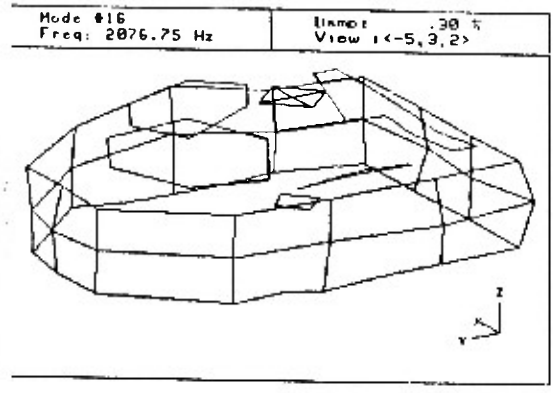

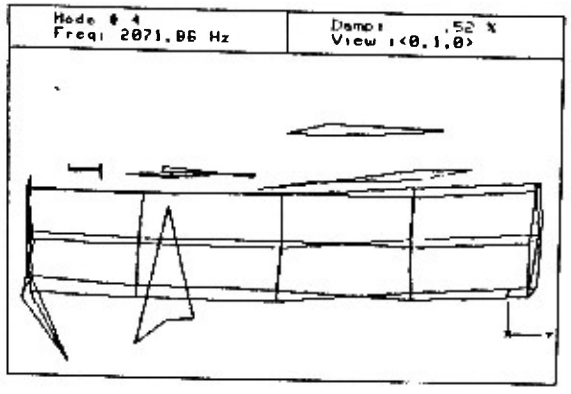

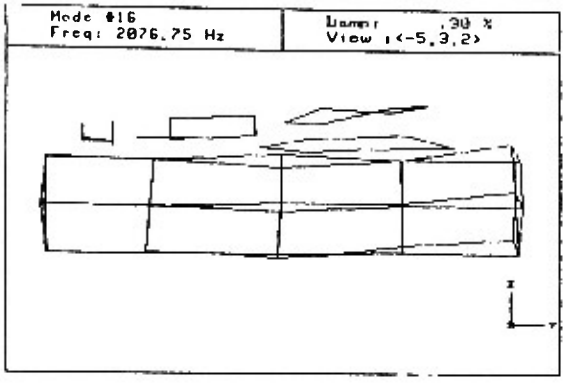

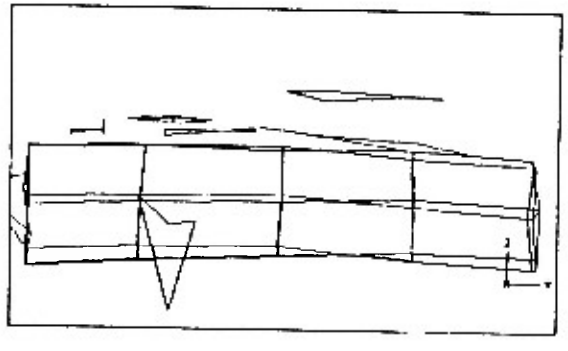

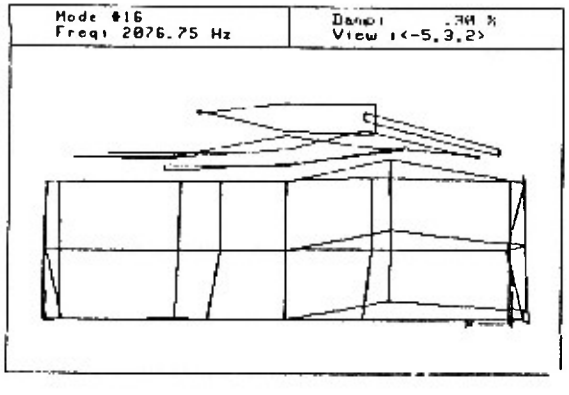

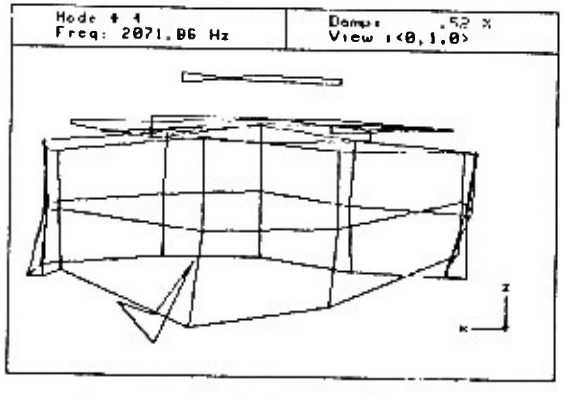

Experimental Mode 15 (2075hz avr)

APPENDIX D

NASTRAN Mode Shapes

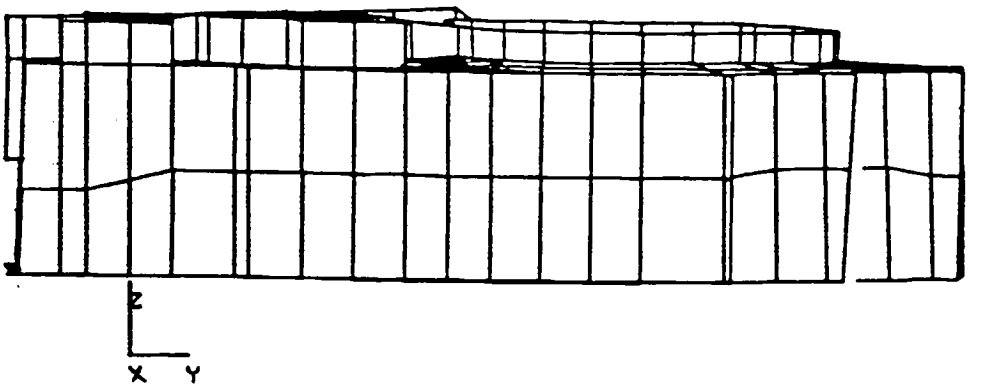

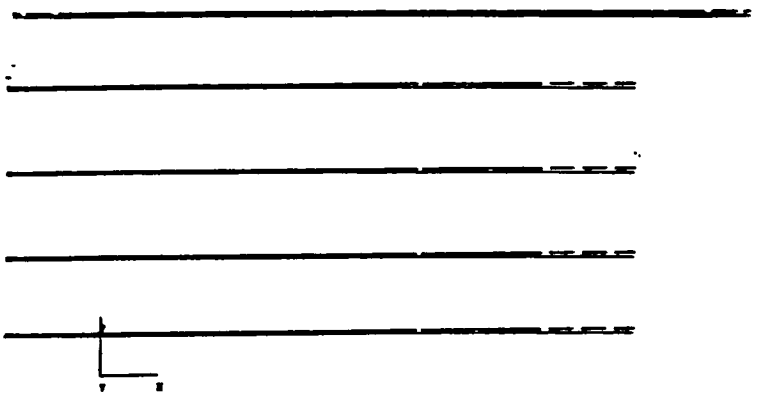

NASTRAN Mode 1 (373hz)

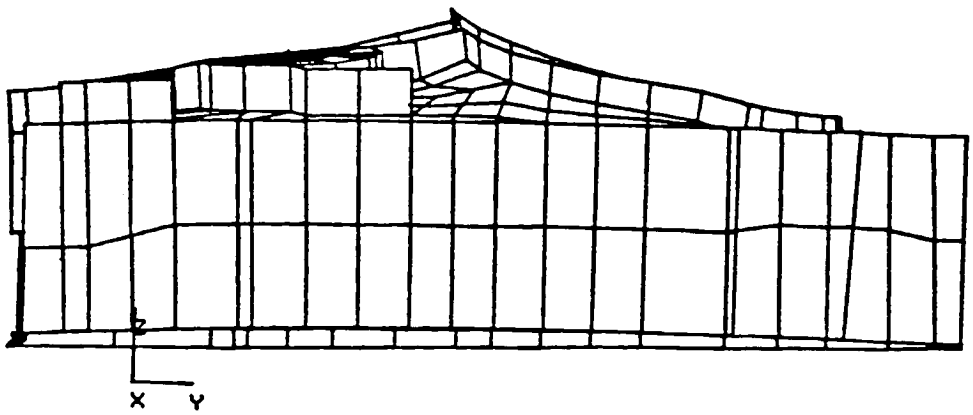

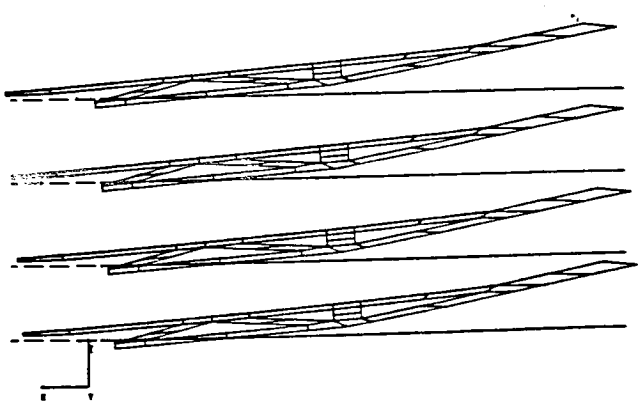

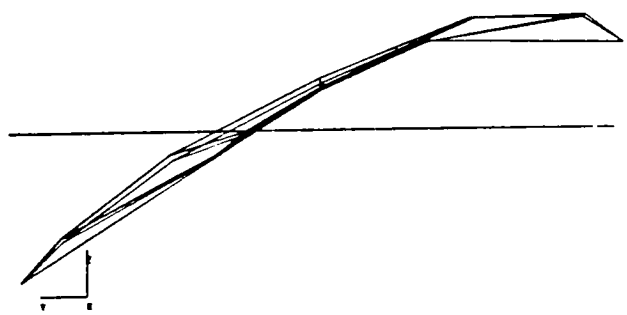

NASTRAN Mode 2 (550hz)

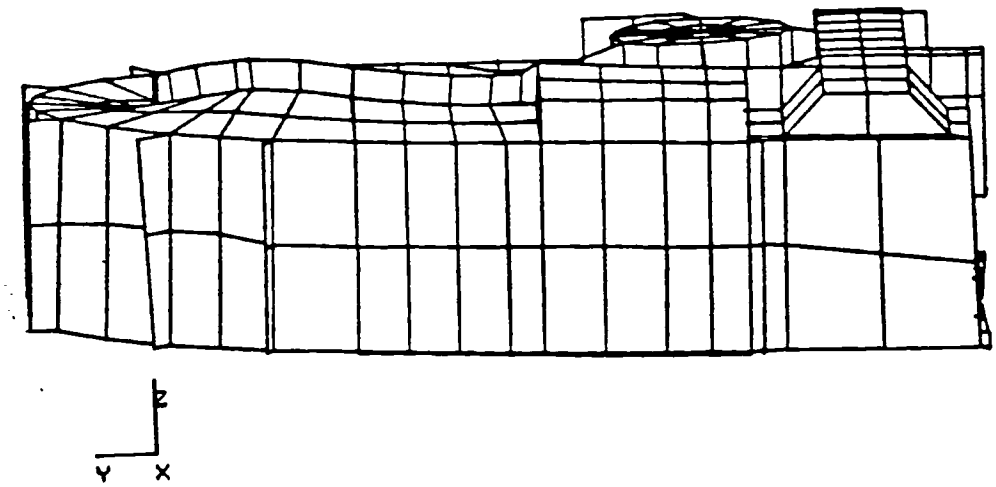

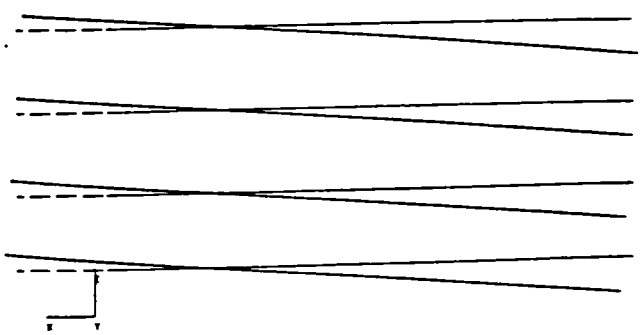

NASTRAN Mode 3 (593hz)

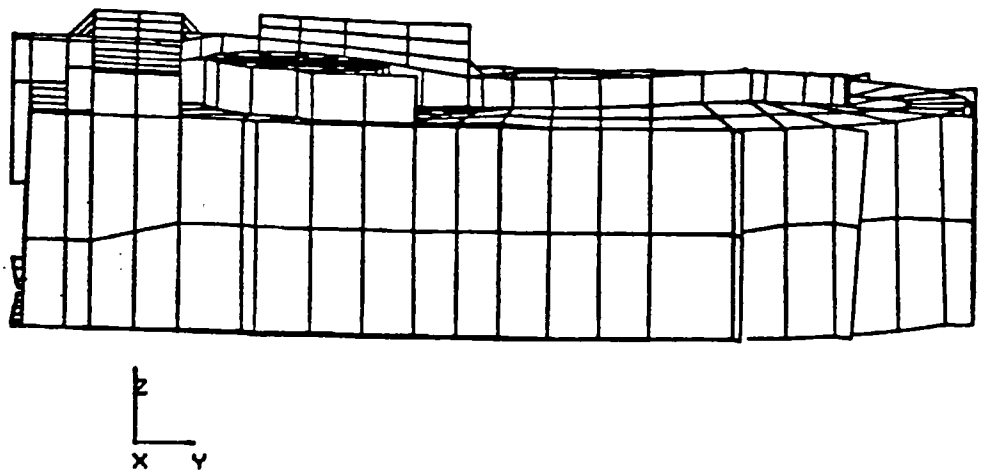

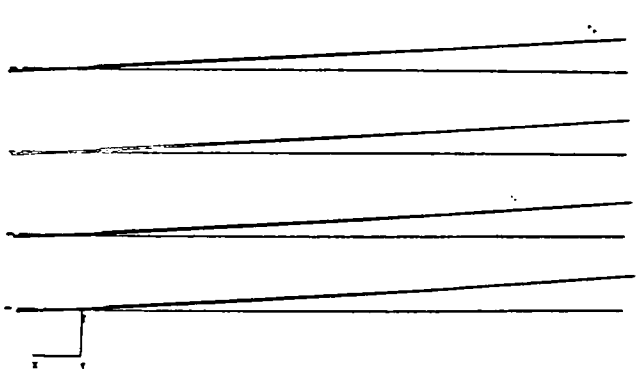

NASTRAN Mode 4 (623hz)

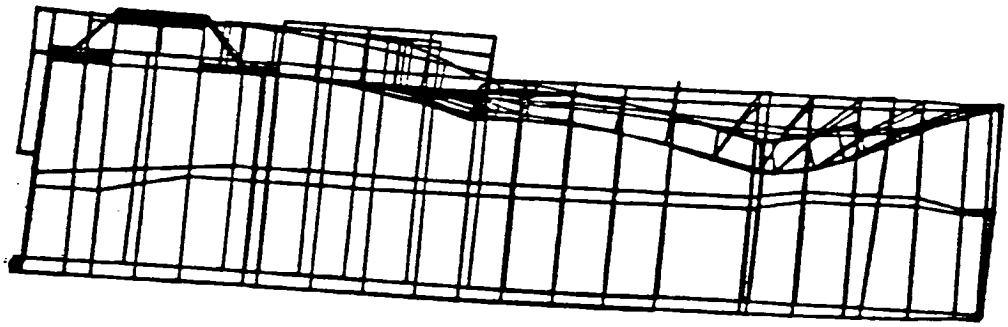

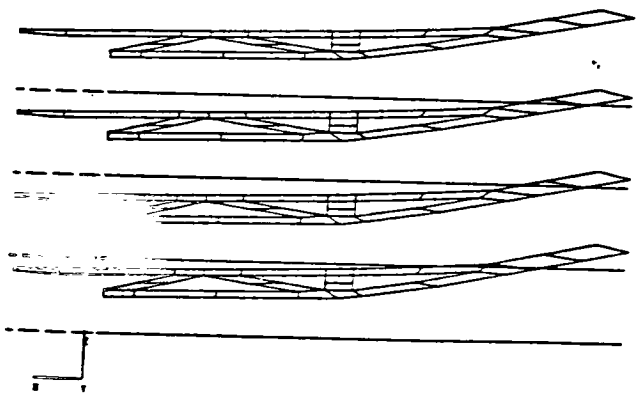

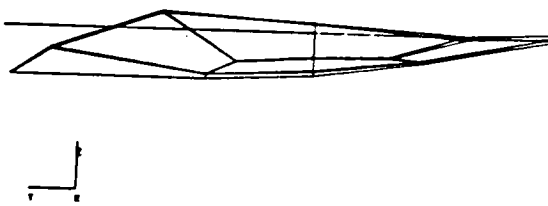

NASTRAN Mode 5 (722hz)

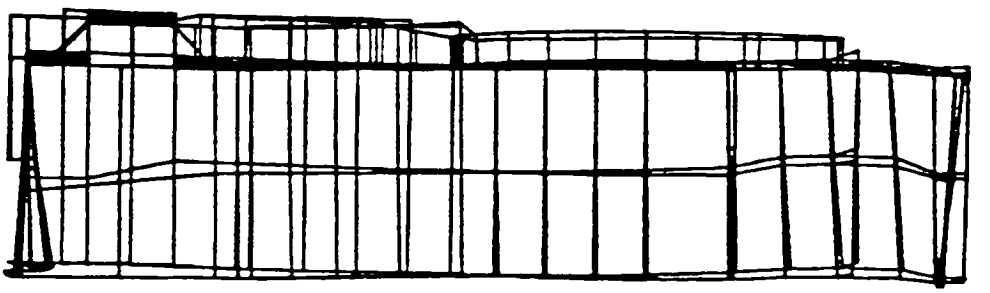

NASTRAN Mode 6 (932hz)

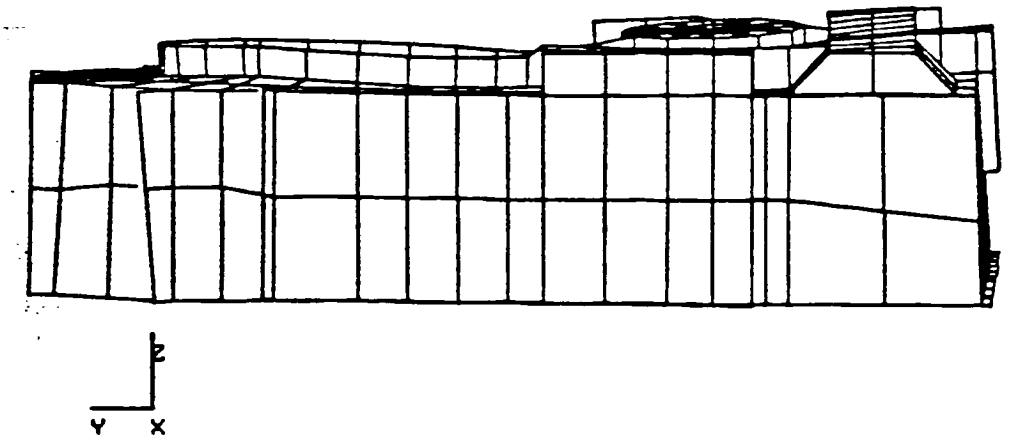

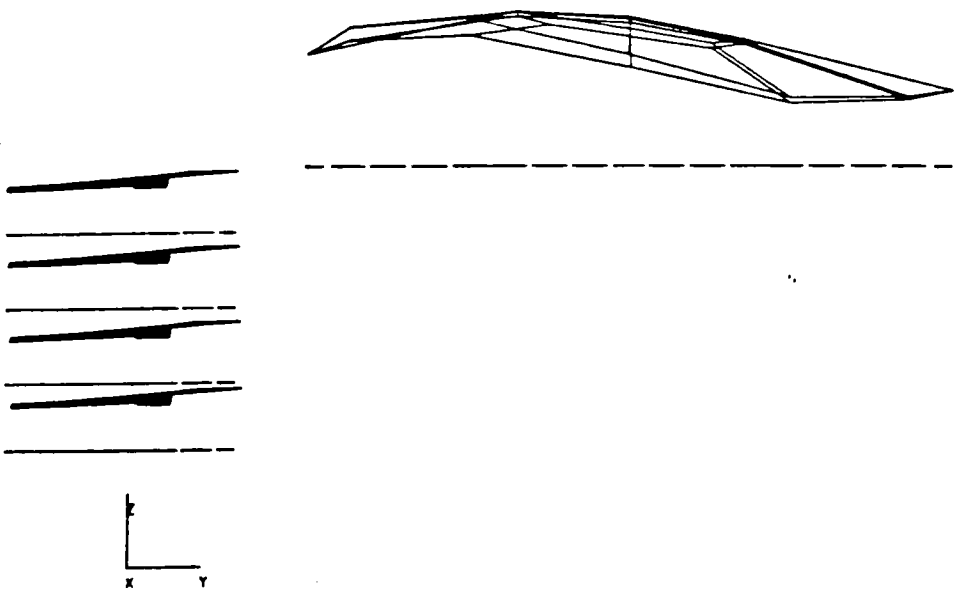

NASTRAN Mode 7 (975hz)

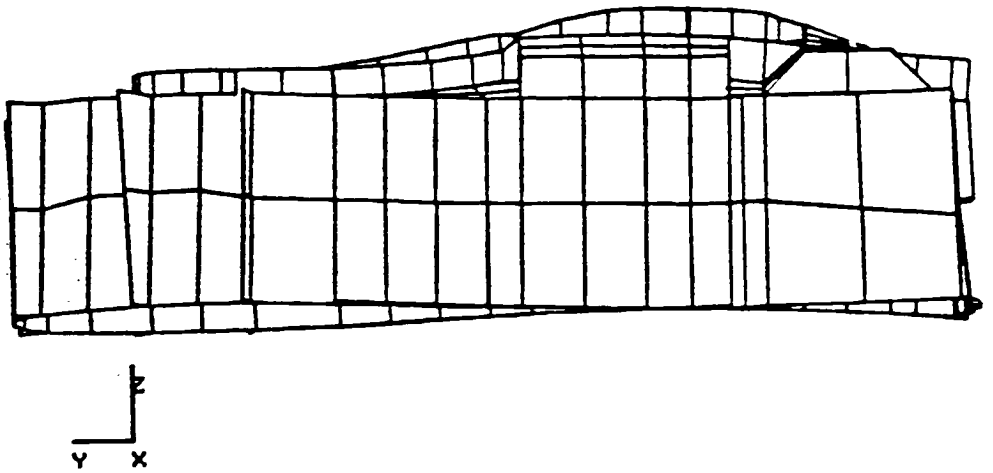

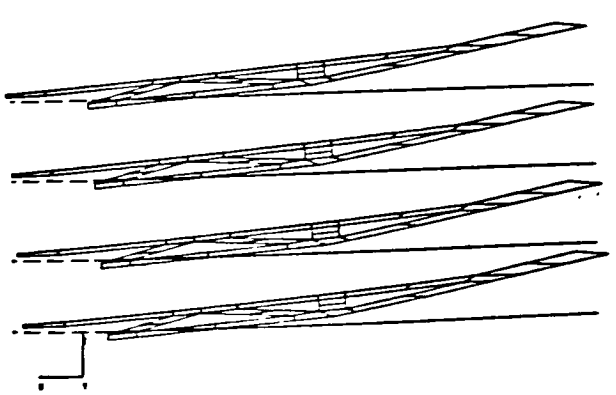

NASTRAN Mode 8 (1203hz)

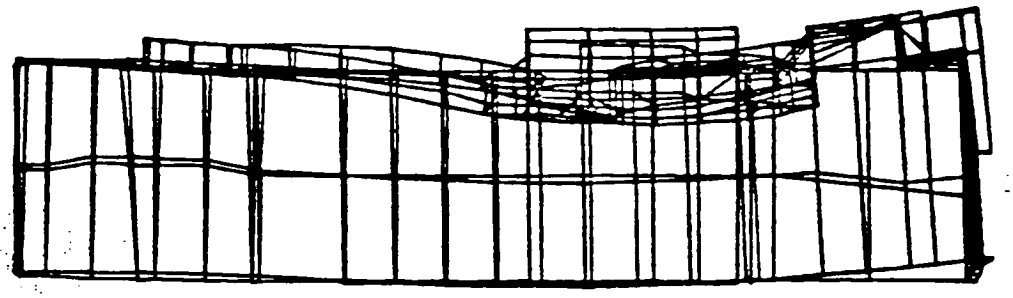

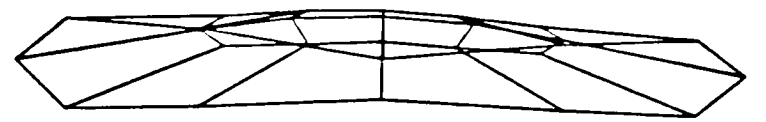

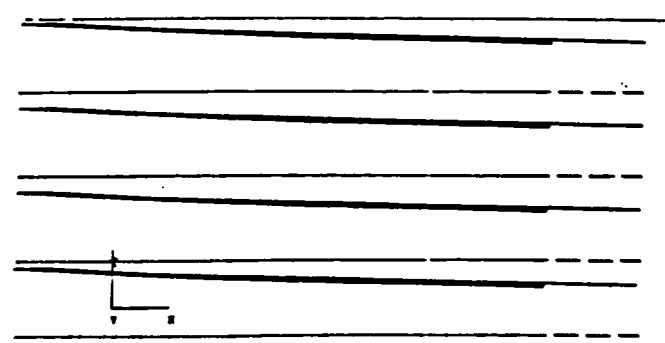

NASTRAN Mode 9 (1266hz)

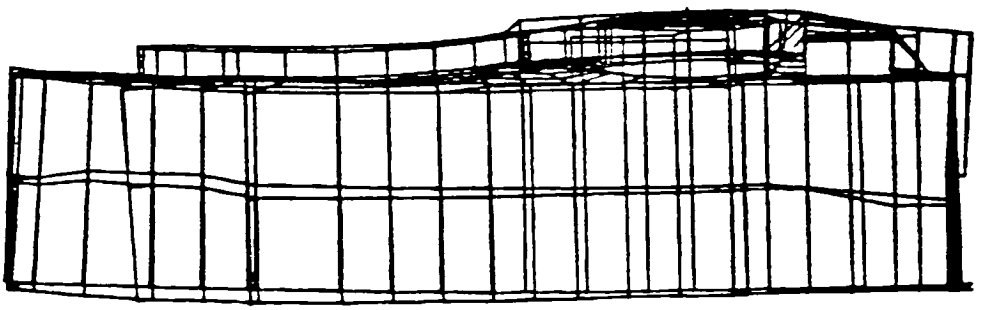

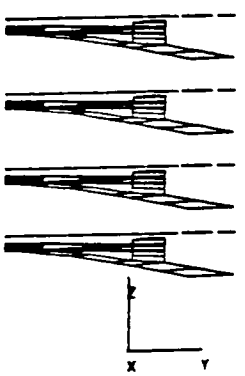

NASTRAN Mode 10 (1431hz)
D-10

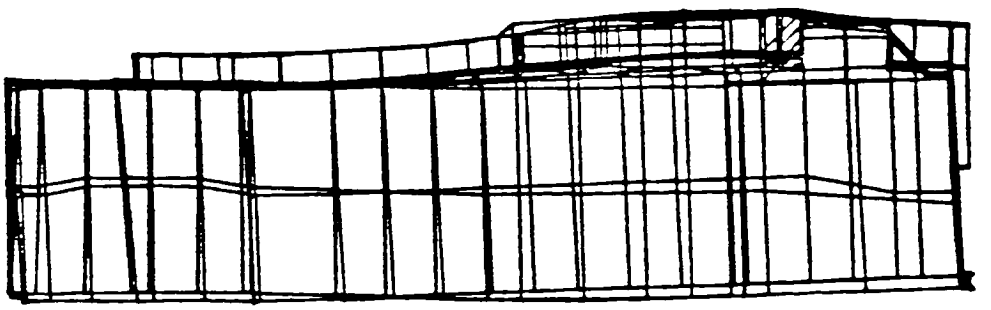

NASTRAN Mode 11 (1456hz)

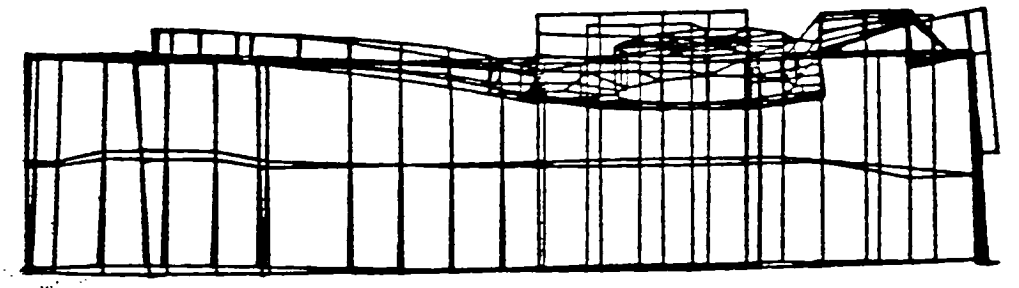

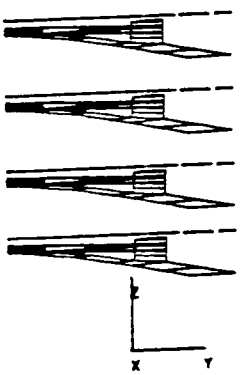

NASTRAN Mode 12 (1641hz)

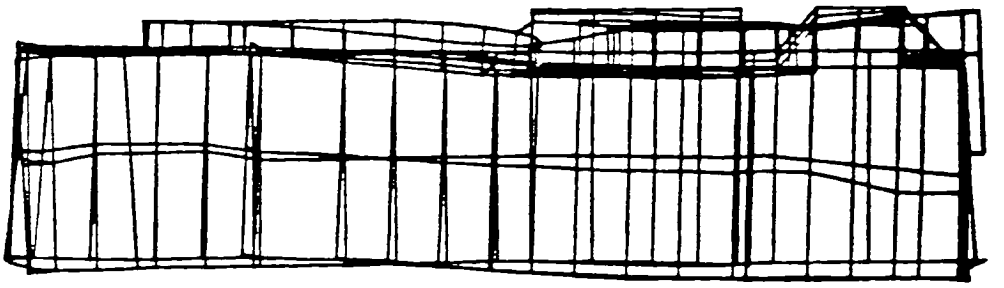

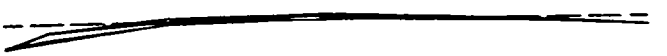

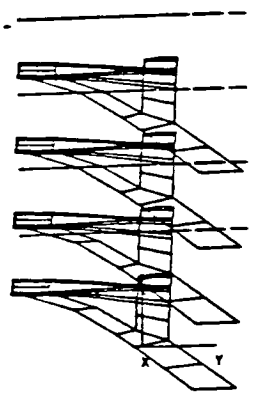

NASTRAN Mode 13 (1926hz)

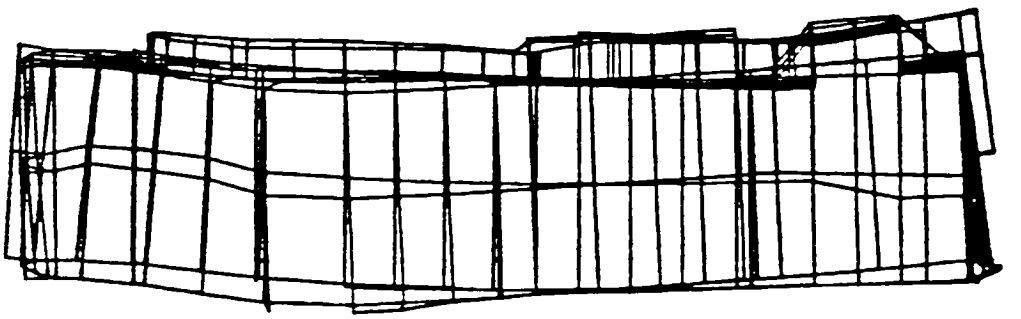

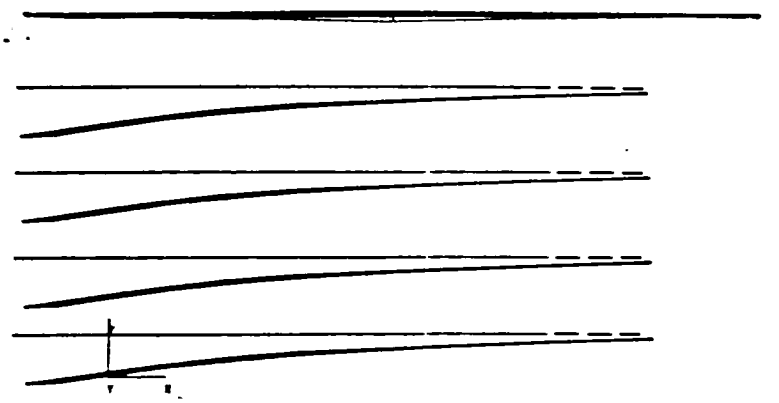

NASTRAN Mode 14 (1955hz)
D-14

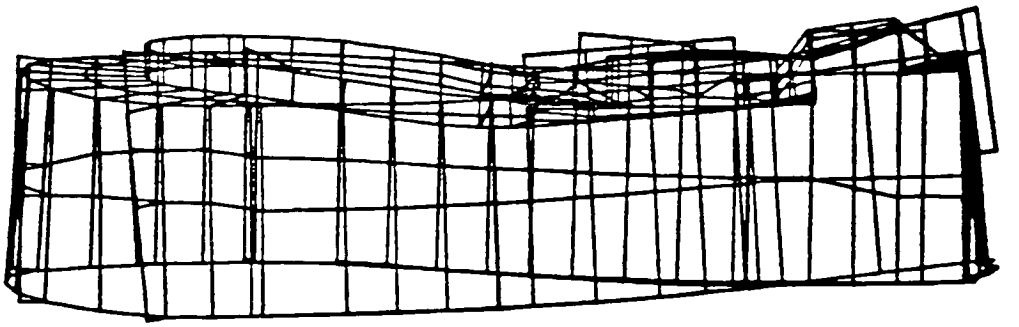

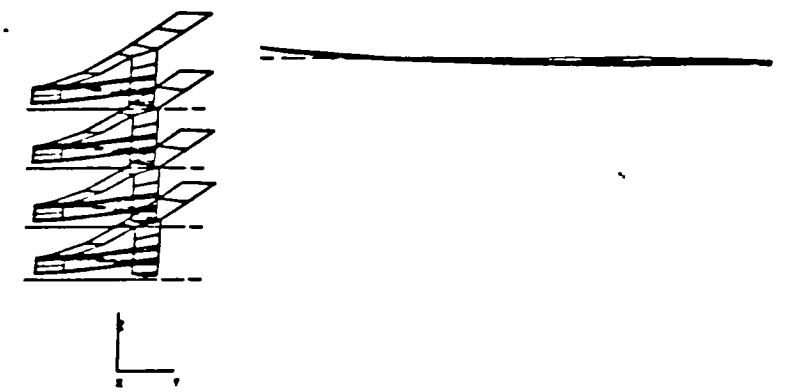

NASTRAN Mode 15 (2045hz)

BIBLIOGRAPHY

Blakely, Ken, et. al. "Finite Element Analysis in the Test Lab." Sound and Vibration, April 1986, pp. 14-19.

Brown, D., Carbon, G., and Ramsey, K. "Survey of Excitation Techniques Applicable to the Testing of Automotive Structures." Society of Automotive Engineers, #770029, 1977.

Carelli, D., Brown, D.L. "Impact Testing Considerations," International Modal Analysis Conference Proceedings, 1984, pp. 735-742.

Craig, Roy R. Structural Dynamics. New York: John Wiley & Sons, 1981.

Gockel, M.A., ed. MSC/Nastran Handbook for Dynamic Analysis. MSC/NASTRAN Version 63. Los Angeles: MacNeal Schwendler Corporation, 1983.

Guyan, Robert J. "Reduction of Stiffness and Mass Matrices." AIAA Journal, Vol. 3, No. 2, 1965.

Haines, Charles W. Analysis for Engineers. New York: West Publishing Co. 1974.

Klosterman, Albert and Zimmerman, Raymond. "Modal Survey Activity via Frequency Response Functions." Society of Automotive Engineers, #751068, 1975.

MacNeal, Richard H., ed. MSC/NASTRAN Handbook for Linear Static Analysis. MSC/NASTRAN Version 61, Los Angeles: MacNeal Schwendler Corporation, 1981.

Peterson, Edward L. and Klosterman, Albert L. "Obtaining Good Results from an Experimental Modal Survey." Journal of the Society of Environmental Engineers, March 1978.

Petrick, LeRoy, Benz, Alan D., and Kensinger, Steven G. "A Case Study in the Correlation of Analytical and Experimental Analysis." Sound and Vibration, April 1986, pp. 24-31.

Rahimi, Alireza. "Designing Hard Drives to Take Abuse." Computer Design, Oct. 1, 1984, pp. 141-148.

Rieger, Neville F. "The Relationship Between Finite Element Analysis and Modal Analysis." Sound and Vibration, January 1986, pp. 16-31.

Schmidtberg, Rupert, and Pal, Thomas. "Solving Vibration Problems Using Modal Analysis." Sound and Vibration, March 1986, pp. 16-21.

Sloane, E., and McKelver, Bruce. "Modal Survey Techniques and Theory." Society of Automotive Engineers, #751067, 1975.

SMS Modal 3.0 Manual. San Jose: Structural Measurement Systems.

BIBLIOGRAPHY (cont)

"The Fundamentals of Modal Testing." Hewlett Packard Application Note 243-3, May 1986.

Tomlinson, G.R. "Detection, Identification and Quantification of Nonlinearity in Modal Analysis -- A Review." Simon Engineering Laboratories.

Wilkinson, J.H., The Algebraic Eigenvalue Problem, (Oxford: Clarendon Press, 1965).